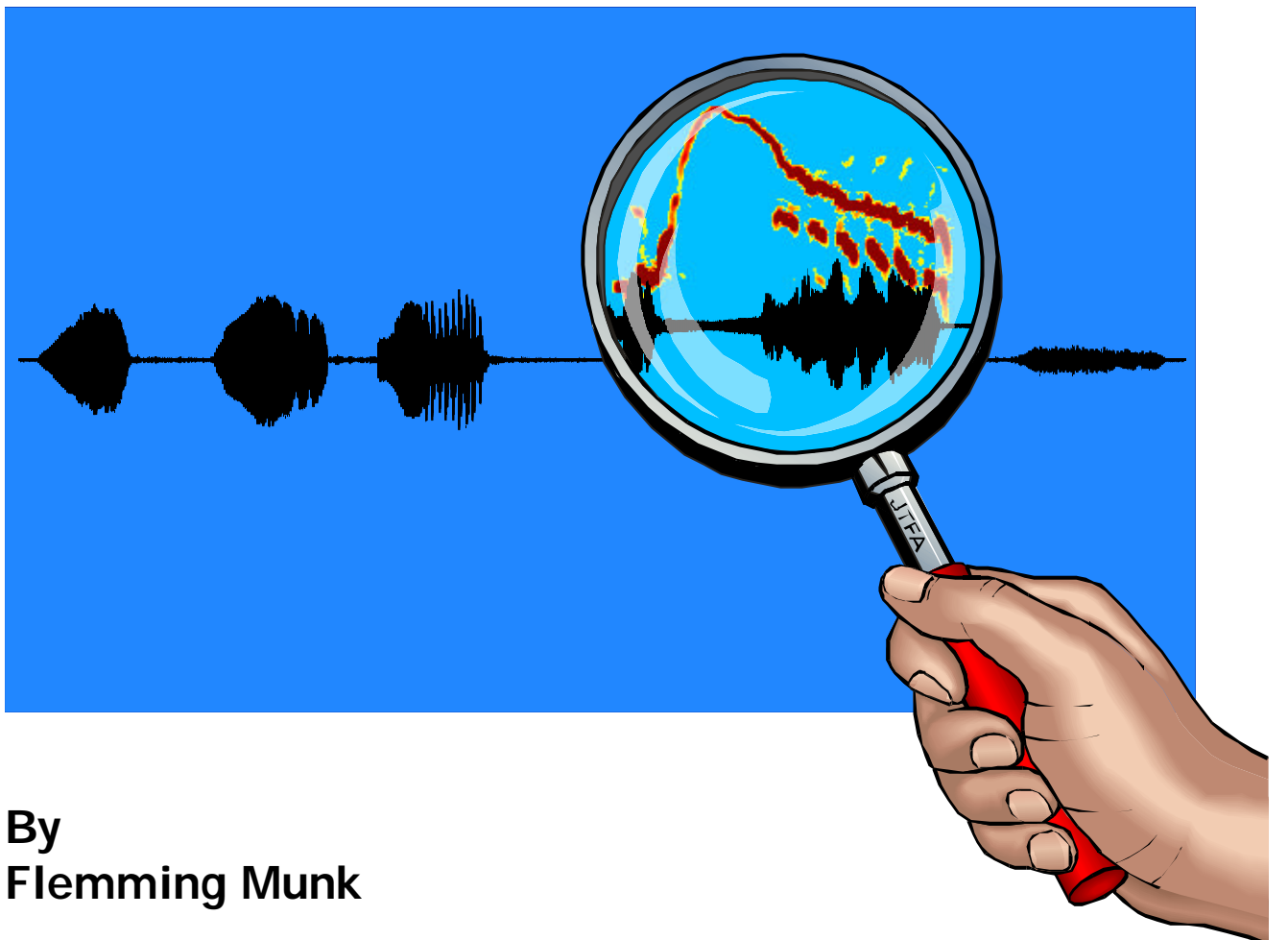


Introduction to

Joint Time Frequency Analysis



**By
Flemming Munk**

**Department of Communication Technology
Institute of Electronic Systems
Aalborg University
Denmark
2001**

Introduction to Joint Time Frequency Analysis

Flemming Munk

IR 99-1001
Version 1.03

Aalborg University
Department of Communication Technology
Fredrik Bajers Vej 7, A3-202
DK-9220 Aalborg East
Denmark

Phone: +45 96 35 86 88
Fax: +45 98 15 37 68
E-mail: fm@kom.auc.dk
URL: <http://www.kom.auc.dk/~fm>

The following software tools have been used for this compendium:

Desktop : Adobe FrameMaker 5.5
Drawing : CorelDraw 4.0 or FrameMaker
Simulation : Matlab 4.5

The front page and appendix illustrations are made by Johnna Nonboe using CorelDraw 7.0

Preface

The present compendium has been written to students following the course *Joint Time Frequency Analysis* (SB8-2) on the Signal Processing line - SB8 at Aalborg University. The topic of JTFA can be treated in two ways - as a mathematical topic or as a signal processing tool. The compendium has been placed between these two disciplines. Whenever a mathematical derivation or understanding is necessary, an appendix has been added. For further information on JTFA, see [Qian 96] and [Cohen 95] for general introduction and see [Hlawatsch 97] and [Feichtinger 98] for a deeper examination of the Wigner-Ville Distribution and the Gabor expansion.

The main goal of the course is to show the student, that their well-known Fourier transformation has certain limitations, and that these limitations can be removed using a Gabor expansion and a Wigner-Ville distribution. The course contains the following 5 lectures:

1 mm - Fourier spectrogram. The lecture will revive the students experience with the Fourier transformation, show how to construct a Fourier spectrogram using FFT and illustrate the window distortion in the spectrogram. The Heisenberg relation and Wavelets are discussed.

The lecture is based on chapters 1 and section 2.1

2 mm - Wigner Ville Distribution. This lecture introduces the students to a new transformation - the Wigner-Ville distribution. The students will learn the advantages and disadvantages of this distribution during matlab exercises. The disadvantages can be removed using the Gabor expansion from 3-4 mm. The lecture is based on section 2.2 and appendix 1.2+1.3. Appendices 1.1 is optional.

3+4 mm - Gabor Expansion. The lecture examines how a signal can be reconstructed from the coefficients from Short-Time Fourier Transformation. The results are known as the Gabor Expansion. The expansion is made discrete and prepared for matlab. The Students determine analysis and synthesis functions in matlab. The lecture is based on appendix 2.

5.mm - Time Frequency Distribution Series. This last lecture is the moment of truth. The limitations of the Fourier spectrogram, which were observed in 1 mm can now be removed using the Wigner-Ville from 2. mm and the Gabor expansion from 3.+4. mm. The resulting frequency transformation is called a *Time Frequency Distribution Series* or *Gabor spektrogram*. The well-known window distortion will disappear, and the signals real time frequency structure will become visible. The lecture is based on section 2.3, chapter 3 and appendix 3.

Flemming Munk

June 2001

Information about errors and inaccuracy in the compendium and suggestions to modification and improvements are highly appreciated by the author.

Table of contents

Preface	iii
Table of contents	v
1. Joint Time Frequency Analysis	1
1.1 Introduction and motivation	1
2. Second-Order Distributions	7
2.1 Fourier Spectrogram	7
2.2 Wigner-Ville distribution	13
2.3 The Gabor spectrogram	21
3. Application of JTFA in Signal Processing	29
3.1 Bat Echolocation	29
3.2 Blackbird	35
3.3 In-bore Doppler Radar System	38
Appendix 1. The Wigner-Ville Distribution	43
1.1 Derivation of the Wigner-Ville distribution	43
1.2 Properties of the Wigner Ville Distribution	48
1.3 Discrete Wigner-Ville distribution	55
Appendix 2. Gabor Expansion	69
2.1 Prologue: The Delta functions	69
2.2 Continuous Gabor Expansion - CGE	71
2.3 Periodic Discrete Gabor Expansion - PDGE	78
2.4 Discrete Gabor Expansion - DGE	85
Appendix 3. Gabor spectrogram	97
Exercises	109
References	113
Abbreviation	115
Notation	117

Chapter 1

Joint Time Frequency Analysis

In this chapter we motivate the idea and need of *Joint Time Frequency Analysis*.

1.1 Introduction and motivation

Many areas of signal processing are concerned with extraction of information from a signal. This information may be directly available from a signal $x(t)$, or may be obtained after transformation of the signal to a more advantageous domain. A very important piece of information is how the signal energy is distributed. This information has traditionally been divided into three categories: *Time Analysis*, *Frequency Analysis* and *Joint Time Frequency Analysis*.

Time Analysis consists of finding the energy distribution of the signal $x(t)$ as a function of the time index t . This distribution is given by $|x(t)|^2$, and is a density function indicating the signal energy per unit time (Joule/s) at the time t . It is often referred to as the *Instantaneous Power (IP)*. The energy in a small time interval Δt around the time t_0 can be found to be $|x(t_0)|^2 \cdot \Delta t$ (Joule). Because the IP has accumulated all contributions in the spectra for a specific time, the frequency dependency is unknown. The transformation of a signal containing two Gaussian functions to its IP representation is illustrated in Figure 1.1

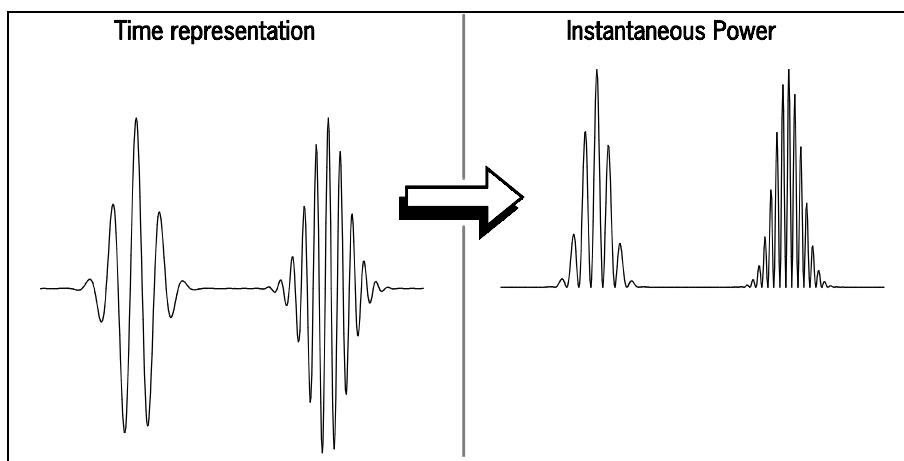


Figure 1.1 The signal $x(t)$, and its corresponding IP $|x(t)|^2$.

It is clear from the figure, that signals containing negative or even complex components are all transferred into a positive value in the Power domain. All zero passages are preserved. This makes them easier to deal with. However, as the transformation (a surjective projection) is quadratic and therefore irreversible, the original signal cannot be obtained again from a power domain.

Frequency Analysis consists of finding the energy distribution as a function of the frequency index ω . Therefore, it is necessary to transform the signal into the frequency domain by means of the Fourier transformation¹:

$$X(\omega) = \int x(t) e^{-j\omega t} dt \quad (1.1)$$

This representation of the signal is complete in the sense that it contains all information about the signal. It is therefore always possible to return to the time representation by an inverse Fourier transformation. The corresponding energy distribution can likewise be obtained by squaring the modulus of the Fourier transformed signal $X(\omega)$, which it indicates the signal energy per unit frequency (Joule/Hz) at the frequency ω , and is referred to at the *Power Spectrum (PS)*. The transformation of the signal from Figure 1.1 into its PS representation is illustrated in Figure 1.2

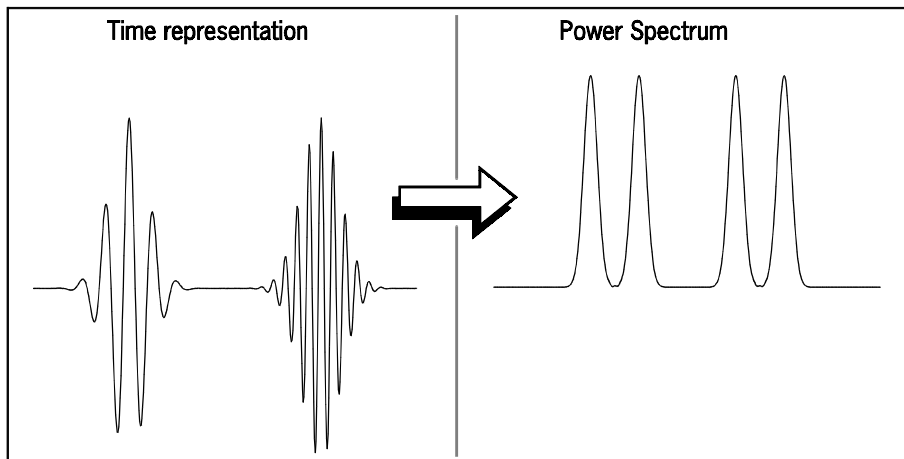


Figure 1.2 The signal $x(t)$, and its corresponding PS $|X(\omega)|^2$.

As the PS has accumulated all contributions in the signal for a specific frequency, the time dependency is unknown. By inspecting the PS in Figure 1.2, it is evident that the signal contains two different frequency components. However, it is not possible to determine from the PS whether they appeared simultaneously or one after the other. This problem arises when analysing a non-stationary signal with a changing spectral content. A more appropriate representation of this kind of signals is a spectral representation which also contains information about the time dependency of the spectral content. A pseudo-solution to the PS in Figure 1.2 could be obtained if the signal was cut in half, and a Fourier transformation was performed on each half. This will decouple the two signal components, and illustrate that the low frequency component appeared first, followed by the high frequency component. This example illustrates the need for a Joint Time Frequency Analysis technique. A pure time or frequency analysis is inadequate to describe how the spectral content is evolving during time.

1. When the limits of the integral are missing, it is assumed to be from minus infinity to infinity as defined in the Notation chapter.

Joint Time Frequency Analysis (JTFA) combines information given by the IP and PS to one single energy distribution. The purpose of JTFA is to map a one-dimensional function of time or frequency into a two-dimensional function of time **and** frequency. The signal is now represented in a two-dimensional domain, where the frequency content to each instant of time is marked by a shading or color. The representation indicates energy only when the signal is non-zero, and only for the frequencies present in the signal. These are the fundamental ideas of JTFA and are illustrated in Figure 1.3.

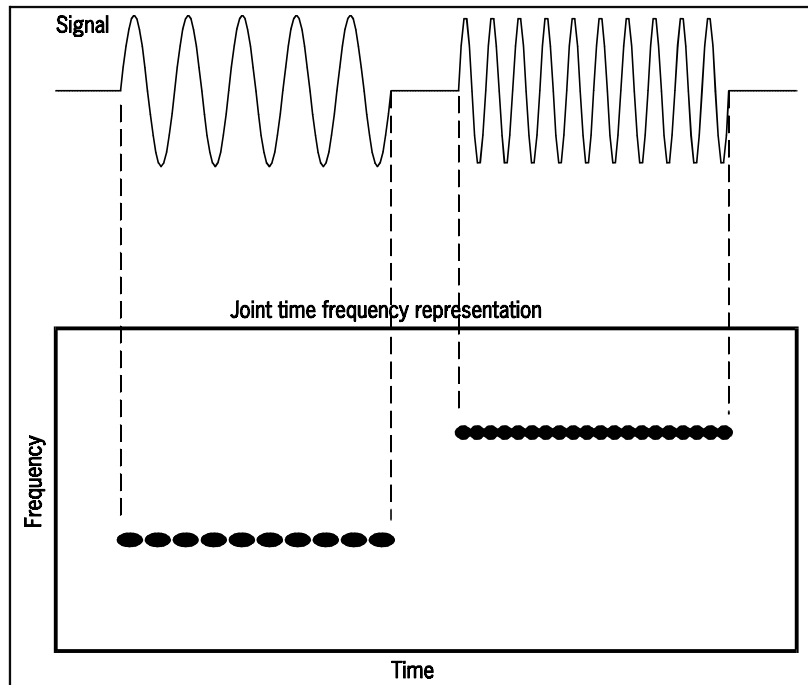


Figure 1.3 The core of Joint Time Frequency Analysis

The result of JTFA of the signal from Figure 1.1 is illustrated in Figure 1.4. From the joint time frequency representation, the time dependence of the two frequency components can now be determined by inspection. This dependence is not visible from the PS neither in the IP.

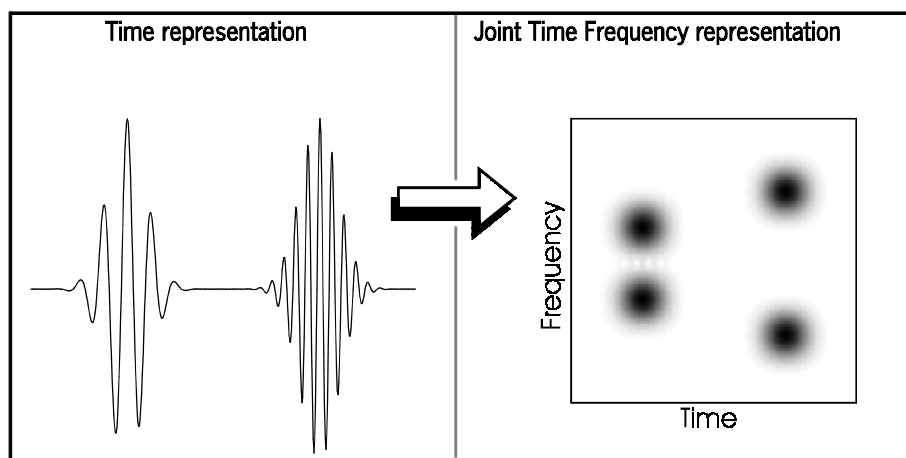


Figure 1.4 The signal $x(t)$, and a corresponding JTFA representation

JTFA representations have in fact been used for centuries by music composers. The music notes are a time frequency descriptive language used to compose music, where the music is often composed by compounding small sound segments. A classic example of a piece of music is illustrated in Figure 1.5

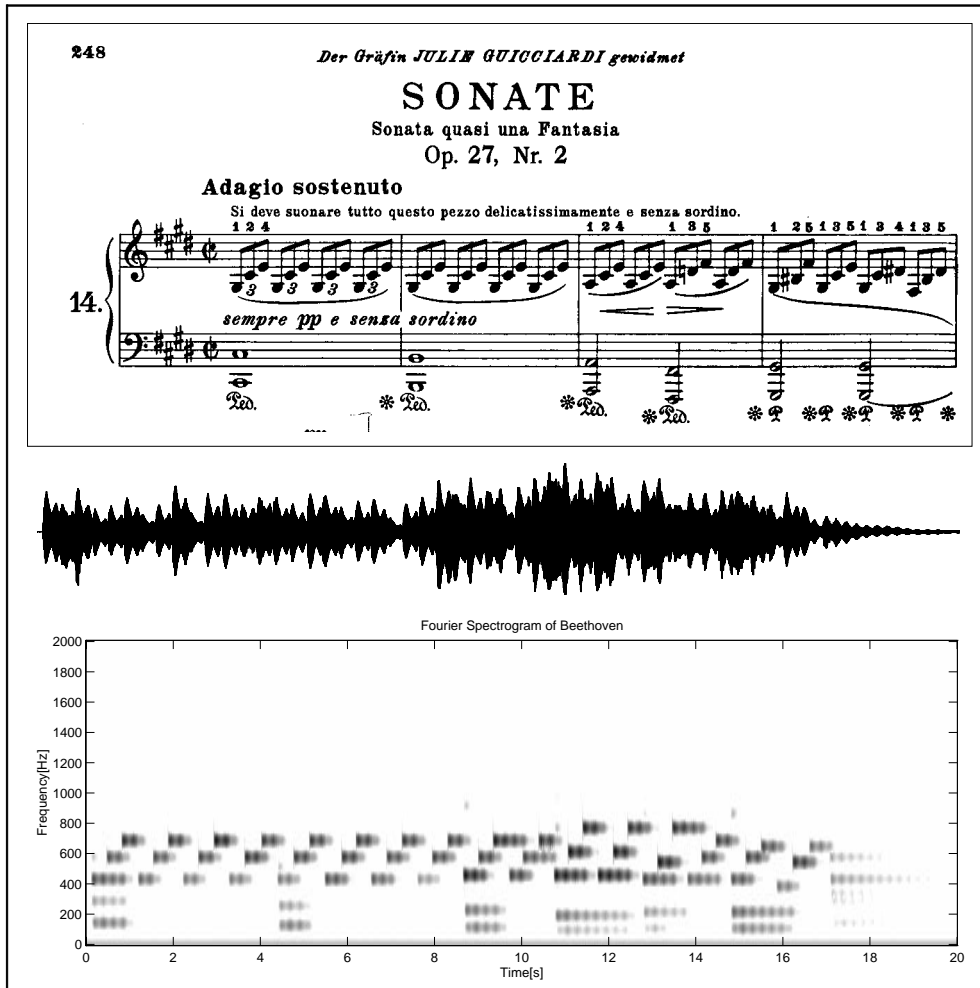


Figure 1.5 Three different representations of the music *Moonlight Sonata*.

These notes describe the Moonlight Sonate (Beethoven Sonate Op. 27, nr. 2)[Hansen]. The corresponding music has been played on a Yamaha clavinova CLP123 (Vibes) and sampled at 4kHz and is illustrated below the notes. From the waveform it is impossible to recognize the music, but if the signal is played through a sound device on a computer, we would immediately recognize the music. If we instead made a JTFA of the signal, we would see the illustration shown below the waveform. This illustration tells us much more about the signal than the waveform, and it is clear that there is a strong coincidence between the musical notes and the JTFA illustration. However, the applications of notes are limited to music, and would be inadequate to describe complex sounds like speech or EEG (ElectroEncephaloGram). For this kind of signal, more general tools like JTFA have to be used.

The first attempt to perform a JTFA was obtained by means of the *Short Time Fourier Transformation (STFT)*. When only a frame of the signal is Fourier transformed, it is possible to obtain time dependent spectral information because the frame only contains information about the signal in a short time interval. The corresponding energy distribution, named the *Fourier Spectrogram (FS)*, is given by the following formula:

$$FS(t, \omega) = \left| \int x(\tau) h^*(t - \tau) e^{-j\tau\omega} d\tau \right|^2 \quad (1.2)$$

The result obtained from the FS is highly dependent of the window function $h(t)$, because this function is used to emphasize part of the signal (the frame). Both the length and shape must be chosen with care. Especially the window length is involved in a phenomenon known as the *Heisenberg Uncertainty Relation*. The implications of this relation are that it is not possible to obtain high resolution in both the time and frequency domain. A long window length gives a high spectral resolution, but poor time resolution. Good time resolution is obtained using a short window length, but this will give a poor frequency resolution. This case is illustrated for two Gaussian functions in Figure 1.6.

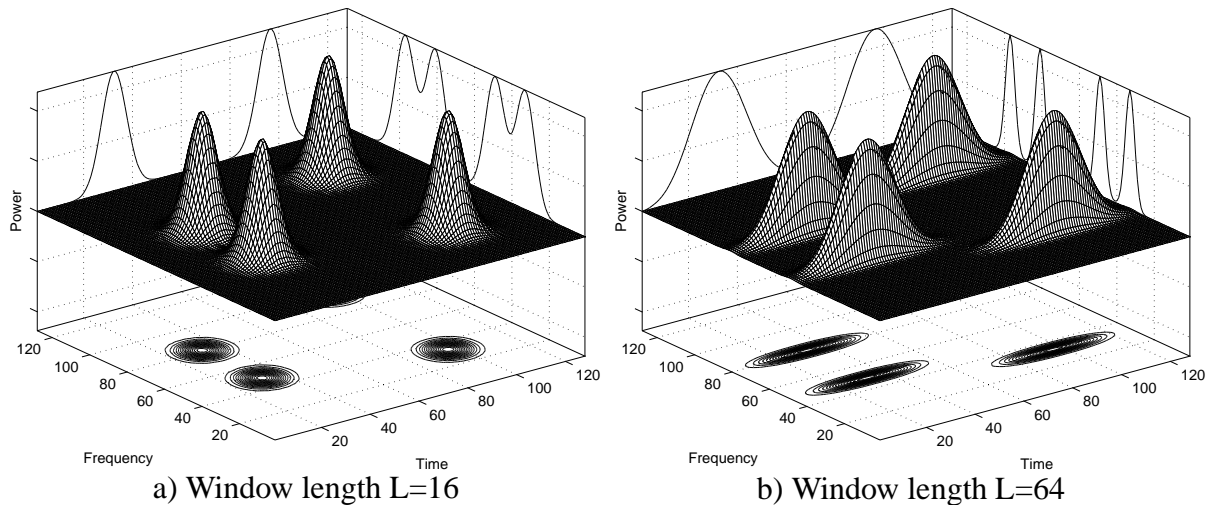


Figure 1.6 Fourier Spectrogram with different window lengths.

The two distributions illustrate different information about the same signal. This phenomenon has been the challenge and the seed to the research area of JTFA. In more than thirty years, researchers have tried to overcome the resolution limitations of the FS, and many new energy distributions have been proposed. However, the lack of a single distribution being best for all applications has resulted in a proliferation of distributions, each corresponding to a different, fixed mapping from the signal to the time-frequency plan. A major drawback of all fixed mappings is that for each mapping the resulting distribution is satisfactory only for a limited class of signals.

The most prominent distribution besides the FS is the *Wigner-Ville Distribution (WVD)*. This distribution was developed in quantum mechanics by Eugene Paul Wigner in 1932 [Wigner 32], and was first introduced in signal processing by J. Ville in 1948 [Ville 48]. The formula for the WVD is given by:

$$WVD(t, \omega) = \int x(t + \tau/2) x^*(t - \tau/2) e^{-j\omega\tau} d\tau \quad (1.3)$$

Derivation of the WVD can be found in appendix 1.1 and some fundamental properties are

given in appendix 1.2. The main difference between the FS and WVD is that the latter contains what is commonly known as *Cross-Terms (CT)*. This phenomenon is illustrated in Figure 1.7, where the WVD is shown for the same two Gaussian functions, introduced in Figure 1.1.

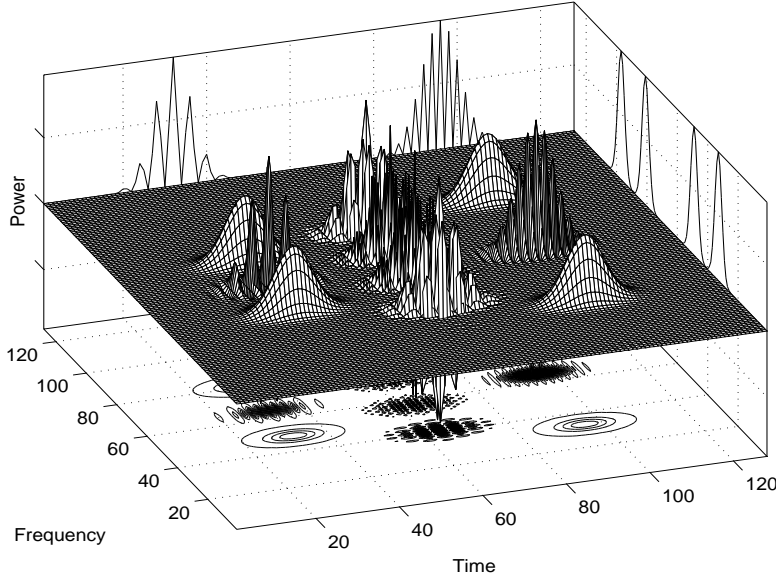


Figure 1.7 The Wigner-Ville distribution.

The CT appears between every two sets of components, and are oscillation negative! It is clear that the CT limit any practical use of a WVD. The nature of the CT does not agree with our intuitive expectation of the signals spectral contentl. But an important property of the WVD is that the marginal distributions are equal to the IP and PS. This can also be seen from Figure 1.7, where the marginals are illustrated on the surface of the box. They correspond to the directly calculated IP and PS in Figure 1.1 and Figure 1.2 .

The FS and WVD are interesting because each of them has properties that are desirable: positivity and correct marginals respectively. Our interest in these properties is based on the fact that JTFA representations are very simular to two-dimensional probability distributions. The probability distribution indicates the probability of a certain two-dimensional outcome, and the total probability is always one. A JTFA representation can be viewed as a probability distribution, which indicates the probability of the existence of a signal component in the time frequency plan. The total energy is normalized to one. The marginal distributions for a two-dimensional probability distribution must correspond to the IP and PS. But where a probability distribution by definition is positive, the JTFA representations used nowadays might go negative.

Chapter 2

Second-Order Distributions

This chapter first introduces two very important distributions in JTFA - the Fourier Spectrogram in section 2.1 and the Wigner-Ville in section 2.2 . An efficient algorithm to remove the cross-terms in the Wigner-Ville distribution is presented in section 2.3 - the Gabor spectrogram.

2.1 Fourier Spectrogram

The traditional Fourier transformation contains no information about the time dependence of the frequency. The frequency content for the whole signal is obtained by projection of the signal onto a complex sinusoidal basis function.

$$F(\omega) = \int x(t) e^{-j\omega t} dt = \langle x, e^{j\omega t} \rangle \quad (2.1)$$

This transformation is sufficient, when the signal is stationary. But when the signal is quasi-stationary or non-stationary, the frequency content is time dependent. In order to obtain a time indication, the signal is limited by a window function, and the extracted frame is then Fourier transformed. This technique was used for the first time by Dennis Gabor [Gabor 46] in 1946. This version of the Fourier transformation is called the *Short Time Fourier Transformation (STFT)*, and can be expressed by inner-product notation as a projection of the signal onto a *Time Frequency (TF)* shifted window function (a basis):

$$STFT(t, \omega) = \int x(\tau) h^*(t - \tau) e^{-j\omega\tau} d\tau = \langle x, h_{t, \omega} \rangle \quad (2.2)$$

The inner-product measures the similarity between the signal and a basis function - one can say that $\langle x, h_{t, \omega} \rangle$ measures the amount of $h_{t, \omega}$ in x . The characteristics we would like to measure are therefore placed in the basis. Different areas of the signals TF plan are analysed by a corresponding TF shift of the basis function before calculating the inner-product. As the result of the inner-product is dependent on the choice of basis, many different bases are used. The four main categories are given in equation (2.3).

Dirac basis	$b_t(\tau) = \delta(t - \tau)$
Fourier basis	$b_\omega(\tau) = e^{j\omega\tau}$
Windowed Fourier basis	$b_{t, \omega}(\tau) = g(t - \tau) e^{j\omega\tau}$
Wavelet basis	$b_{a, b}(\tau) = a ^{-0.5} \cdot w\left(\frac{\tau - b}{a}\right), a \neq 0$

$$(2.3)$$

The resolution properties of the inner-product are limited by the time frequency extension of the basis function. This extension can be evaluated using the *Heisenberg uncertainty relation*. It expresses a physical and fundamental relationship between the standard deviation of two density functions $|x(t)|^2$ and $|X(\omega)|^2$. The functions $x(t)$ and $X(\omega)$ are not arbitrary functions, but

Fourier pairs! These deviations can be calculated by:

$$\sigma_t^2 = \int t^2 \frac{|x(t)|^2}{\int |x(t')|^2 dt'} dt \quad \sigma_\omega^2 = \frac{1}{2\pi} \int \omega^2 \frac{|X(\omega)|^2}{\int |X(\omega')|^2 d\omega'} d\omega \quad (2.4)$$

The usual statistic variance is calculated by $\sigma_t^2 = \int t^2 f(t) dt$, where $f(t)$ is a statistical distribution. Therefore, we have to square the modulus of $x(t)$ to obtain a density function, and normalize it to unity energy. The Heisenberg relation expresses the fact that the product of the deviations are bounded by:

$$\sigma_t \cdot \sigma_\omega \geq \frac{1}{2} \quad \sigma_t \cdot \sigma_f \geq \frac{1}{4\pi} \quad (2.5)$$

This means that given a function of time or frequency, the corresponding density functions can not be optimally concentrated in both time and frequency. The name *uncertainty* comes from quantum mechanics which it is a pure probabilistic science. In signal analysis it is therefore a little misleading because there is nothing uncertain about a signal. The only function which reaches the bound of the Heisenberg uncertainty is the Gaussian function. This is illustrated by the following example:

Example 2.1 : Calculate the Heisenberg product for a Gaussian function

Time deviation:

$$g(t) = (\pi\sigma^2)^{-0.25} \exp\left(-\frac{t^2}{2\sigma^2}\right) \Rightarrow \sigma_t^2 = \int t^2 \frac{|g(t)|^2}{\int |g(t')|^2 dt'} dt = \frac{\sigma^2}{2} \quad (2.6)$$

Frequency deviation:

$$G(\omega) = (4\pi\sigma^2)^{0.25} \exp\left(-\frac{\omega^2\sigma^2}{2}\right) \Rightarrow \sigma_\omega^2 = \frac{1}{2\pi} \int \omega^2 \frac{|G(\omega)|^2}{\int |G(\omega')|^2 d\omega'} d\omega = \frac{1}{2\sigma^2} \quad (2.7)$$

Heisenberg product:

$$\sigma_t \cdot \sigma_\omega = \frac{\sigma}{\sqrt{2}} \cdot \frac{1}{\sqrt{2}\sigma} = \frac{1}{2} \quad (2.8)$$

The following application of Heisenberg uncertainty may be a little inconsistent, because we will need to argue that the TF extension of a function is limited, because its densities are limited. But Heisenberg's uncertainty only deals with the densities. A graphical way to illustrate the Heisenberg relation is the so-called *Heisenberg ellipse*, which is illustrated in Figure 2.1.

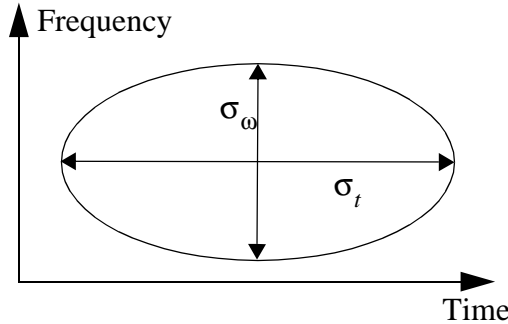


Figure 2.1 Heisenberg ellipse

No density function can have an ellipse with an area smaller than $\pi/8$ ¹. The center of the ellipse is the TF offset of the corresponding function. The ellipses for the four bases in equation (2.3) are illustrated in Figure 2.2.

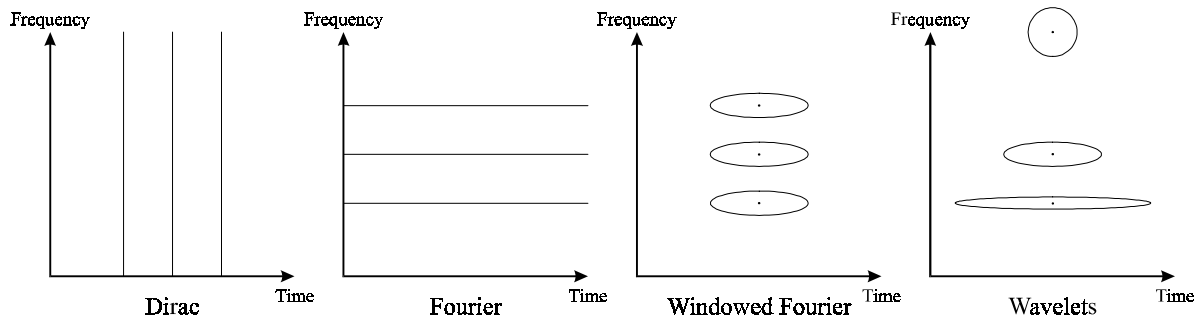


Figure 2.2 The Heisenberg ellipses for the four basis functions.

It is clear that the Dirac basis has a very well-defined time location but infinity frequency extension. The corresponding representation $STFT(t, \omega)$ is proportional to the signal $x(t)$, and is reduced to a pure time representation of the signal. The Fourier basis, on the other hand, has a very well-defined frequency, but infinity time extension. The representation $STFT(t, \omega)$ is now proportional to the Fourier transformation, and the representation is reduced to a pure frequency representation of the signal. These two bases are of course extremes, and the following two bases are something in between. The Windowed Fourier basis is limited in both the time and frequency domain. Therefore, the corresponding representation will illustrate the time-frequency structure of the signal. However, since the ellipses are fixed, it will only be satisfactory for a signal with the same shape. If the signal is a multi-component signal with both a transient and a harmonic structure, the window Fourier basis will do a poor job. A compromise has been made with the Wavelet basis, because it uses a frequency dependent shape of the Heisenberg ellipse. Wavelet has good temporary resolution for high frequencies and a good frequency res-

1. The area of an ellipse is $A = \pi ab$, where a and b are the semi-axis

$$A = \pi \cdot \frac{\sigma_t}{2} \cdot \frac{\sigma_\omega}{2} = \frac{\pi}{4} \cdot \sigma_t \cdot \sigma_\omega \geq \frac{\pi}{8}, \text{ as } \sigma_t \cdot \sigma_\omega \geq \frac{1}{2}.$$

solution for low frequencies. But the total resolution (area of the ellipse) of the Wavelets is not better than the Window Fourier basis.

The Heisenberg relation is sometimes abused to argue that *the negative energies are not just a strange phenomenon but are due to a violation of the uncertainty principle* [Gram 89, pp93] or *the uncertainty principle does not allow the notation of energy at a specific time and frequency* [Hlawatsch 92]. But the Heisenberg relation has only the following two influences on JTFA:

- The spectral/temporal resolution of TF-distributions based on the inner-product is limited by the Heisenberg relation.
- Not every 2D function can be a TF-distribution.

The Heisenberg relation state a fact about the physical structure of a signal, and has in general nothing to do with the techniques that we use to analyze the signal. However, in the case where another signal (a basis) is used to analyze a signal $x(t)$, the final result will be affected by the Heisenberg relation. These techniques (STFT and Wavelet) use an inner-product to measure the similarity between the basis and the signal. Because the basis is limited by the relation, so is the inner-product! The principle of this statement is illustrated in Figure 2.3

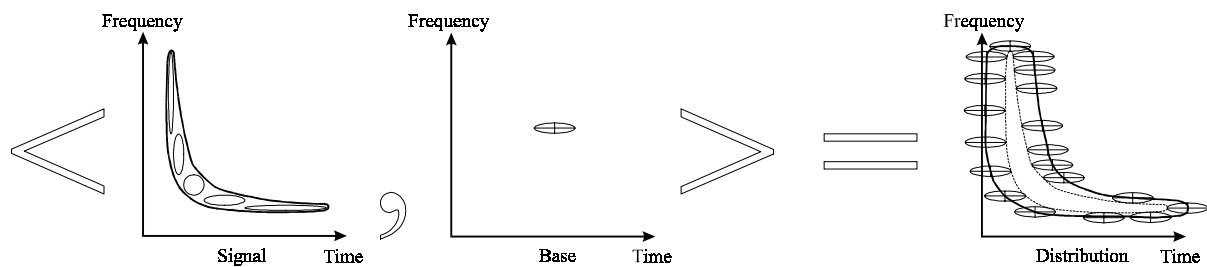


Figure 2.3 Heisenberg's impact on inner-product transformations. These ellipses illustrate the non-zero region, and are therefore larger than the Heisenberg ellipses.

Because the inner-product is equal in both time and frequency:

$$STFT(t, \omega) = \langle x, h_{t, \omega} \rangle = \langle X, H_{t, \omega} \rangle \quad (2.9)$$

the result of the inner-product is only non-zero when the TF structure of the signal and basis is overlapping. Because no function (its densities) can be optimally concentrated in both time and frequency, a trade off between time and frequency resolution exists. An optimal distribution would therefore be reached with the STFT, if it was possible to use a basis with no time-frequency extend (a point in the time-frequency plan) - but unfortunately, such basis does not exist. This phenomenon is known in signal processing as window distortion. In the same figure, the signal has been used to illustrate the fact that not all 2D functions can be a true TF distribution. No area of the TF-distribution can occupy an area smaller than a Heisenberg ellipse.

The energy distribution can be obtained from the STFT by squaring the modulus, and is called the *Fourier Spectrogram* (FS).

$$FS_x(t, \omega) = \left| \int x(\tau) h^*(t-\tau) e^{-j\omega\tau} d\tau \right|^2 \quad (2.10)$$

The FS is the most frequently used technique for performing JTFA. The reasons for this are numerous. Some of them are given in the following list:

- easy to interpret
- positive by definition
- contains no visible cross-terms
- can be calculated fast by means of the Fast Fourier Transformation.

It is often argued that the FS has no cross-terms. But in fact - cross-terms do exist in the FS - they have to because the FS is a non-linear transformation[Williams 92b][Boudreux 92]. This can be seen by the following example:

$$\begin{aligned}
 x(t) &= g(t) + h(t) \\
 STFT_x(t, \omega) &= STFT_g(t, \omega) + STFT_h(t, \omega) \\
 FS_x(t, \omega) &= |STFT_x(t, \omega)|^2 = STFT_x(t, \omega) STFT_x^*(t, \omega) \\
 &= \underbrace{|STFT_g(t, \omega)|^2 + |STFT_h(t, \omega)|^2}_{\text{Auto-terms}} + \underbrace{2 \cdot \operatorname{Re} \{ STFT_g(t, \omega) STFT_h^*(t, \omega) \}}_{\text{Cross-terms}}
 \end{aligned} \tag{2.11}$$

It is obvious that the FS contains cross-terms like in the WVD, but these terms are well-placed, because they are placed at the location of the auto-terms. The following list states a couple of facts regarding cross-terms in the FS.

- If two signal components have non overlapping time-frequency support, they will not generate cross-terms.
- The FS of an n-component signal will contain between zero and $\frac{n(n-1)}{2}$ cross-terms, depending on the amount of overlap.
- The cross-terms in the FS occur at the intersection between two STFT auto-terms, whereas they always occur midway between the WVD auto-terms in the WVD.
- The cross-terms in the FS may have a maximum amplitude as large as twice the amplitude of the FS of a single signal component.
- The cross-terms are real, but can be negative. The negative values are compensated by the positive values in the auto-terms, resulting in non-negative values in the FS.

The FS is in fact not a single distribution, but an infinite number of FS exist, each with a specific window type and length. The FS with a short window length is advantageous when analysing transient and non-stationary signals, but will only give a poor frequency resolution. If a long window is used, a good frequency resolution is obtained for the signal inside the window length, but it will not be possible to see the variation of the frequency inside the window. These two cases are named the *Wideband Fourier Spectrogram* (WFS) and the *Narrowband Fourier Spectrogram* (NFS). Each contains important information about the signal, but it is not possible to obtain a FS which contain both good temporal and spectral resolution, which is why, both the WFS and NFS are often used in signal analysis to compensate each other. An example of this is illustrated in Figure 2.4 for a speech¹ signal containing the utterance “spectrogram”.

1. It should be noted that the speech signal has been preemphasised (high pass filtered) in order to make the spectrum more white.

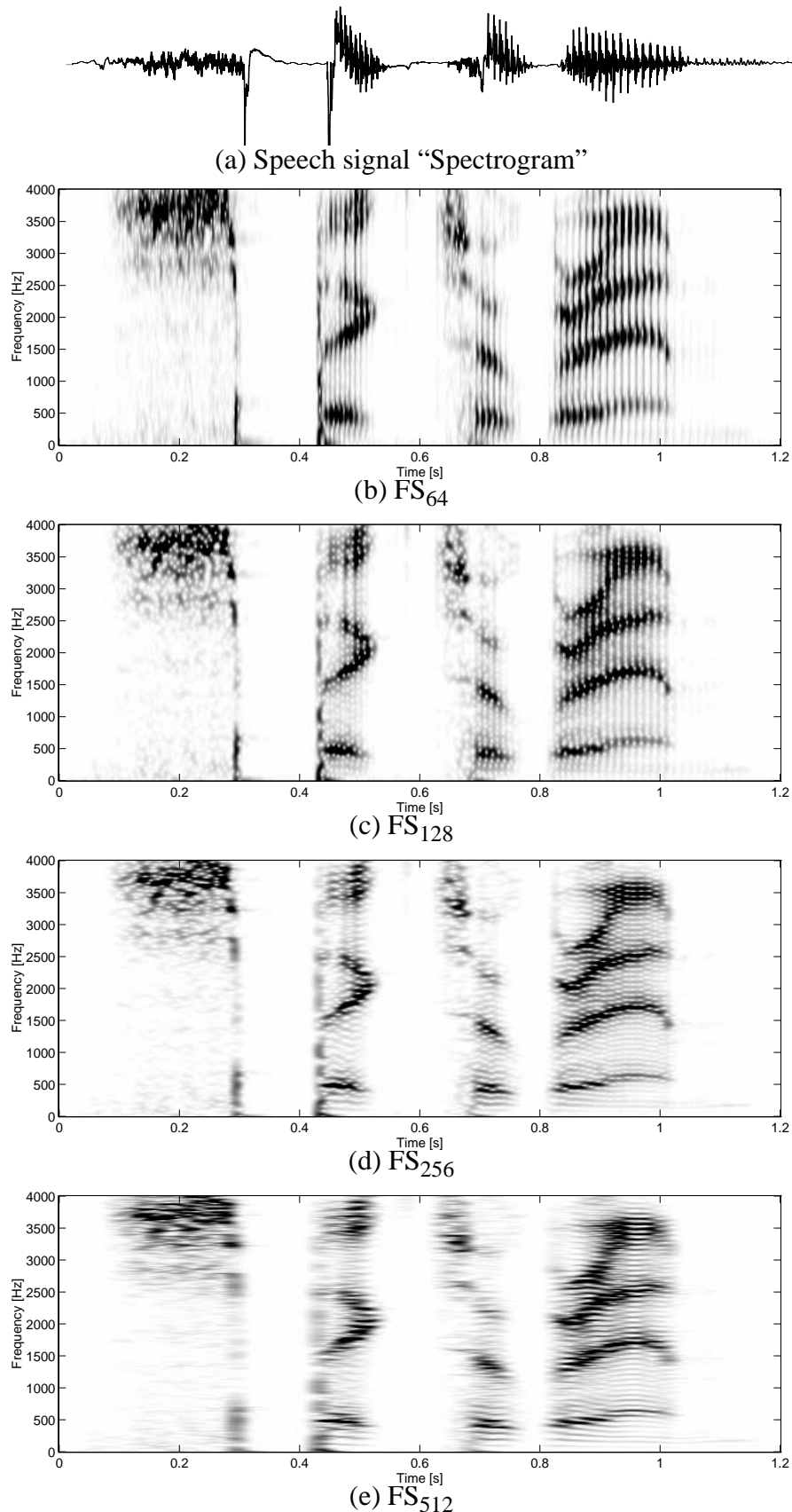


Figure 2.4 The Fourier Spectrogram of the speech signal *spectrogram*.

2.2 Wigner-Ville distribution

The WVD is next to the Fourier Spectrogram the most important distribution in JTFA. The reason will become clear during this chapter. The WVD is defined as the Fourier transformation of $x(t + \tau/2)x^*(t - \tau/2)$ or inverse of Fourier transformation of a frequency domain representation of the signal, $X(\omega + \theta/2)X^*(\omega - \theta/2)$:

$$\begin{aligned} WVD_x(t, \omega) &= \int x(t + \tau/2)x^*(t - \tau/2)e^{-j\omega\tau}d\tau \\ &= \frac{1}{2\pi} \int X(\omega + \theta/2)X^*(\omega - \theta/2)e^{j\theta t}d\theta \end{aligned} \quad (2.12)$$

The WVD is superior to the FS in every sense, except one. The WVD can go negative. In fact, it will go negative for all signals except for a Gaussian function. The non-positive property prohibits an energy interpretation of the WVD, which is one of the reasons for the reduced practical interest in the WVD compared to the FS. Another reason is a drawback of the quadratic nature of the WVD. When analysing a multicomponent signal, the quadratic transformation will cause a non-linear effect. The WVD of a signal containing only two components, $g(t)$ and $h(t)$, will give the following terms.

$$\begin{aligned} x(t) &= g(t) + h(t) \\ WVD_x(t, \omega) &= WVD_g(t, \omega) + WVD_h(t, \omega) + WVD_{g,h}(t, \omega) + WVD_{h,g}(t, \omega) \\ &= \underbrace{WVD_g(t, \omega) + WVD_h(t, \omega)}_{\text{Auto-terms}} + 2 \cdot \underbrace{\text{Re}\{WVD_{g,h}(t, \omega)\}}_{\text{Cross-terms}} \end{aligned} \quad (2.13)$$

At this point, the cross WVD is introduced as:

$$WVD_{x,y}(t, \omega) = \int x(t + \tau/2)y^*(t - \tau/2)e^{-j\omega\tau}d\tau \quad (2.14)$$

The cross WVD is normally complex, but because the indexes can be interchanged (if the distribution is conjugated), the two complex cross WVDs can be compounded into one real cross WVD. The distribution corresponding to each signal component is called *auto-terms*, and the cross distributions are called *cross-terms*¹. This cross-term is a result of the quadratic transformation. A signal containing N component will have N auto-terms and N(N-1) complex cross-terms. The complex cross-terms can be compounded pairwise to 0.5N(N-1) real cross-terms. In order to study the nature of this cross-term, the WVD of a signal containing, first one, and then two Gaussian functions are derived.

$$\begin{aligned} g(t) &= (\pi\sigma^2)^{-0.25} \exp\left(-\frac{t^2}{2\sigma^2}\right) \Rightarrow \\ WVD_g(t, \omega) &= 2 \exp\left(\frac{-t^2}{\sigma^2} - \omega^2\sigma^2\right) = |g(t)|^2 \cdot |G(\omega)|^2 \end{aligned} \quad (2.15)$$

The WVD of a Gaussian function is a 2D Gaussian function. The Gaussian function is the only function for which the WVD is guaranteed to be positive over the whole time-frequency plan, and only in the case of an energy normalized Gaussian function it is possible to write it as the product of the marginals.

1. In the literature this term has many names like interference terms, ghosts, artifacts and cross-terms

If the FS were calculated for an energy normalized Gaussian function (equation (2.15)), and the same function were used as the window function, it would occupy an area in the TF plan **twice** as big as the same function would occupy in the WVD (the true size). This is illustrated in the following example:

Example 2.2 : Calculate the Heisenberg product for the Fourier Spectrogram and Wigner-Ville Distribution using a Gaussian function as input.

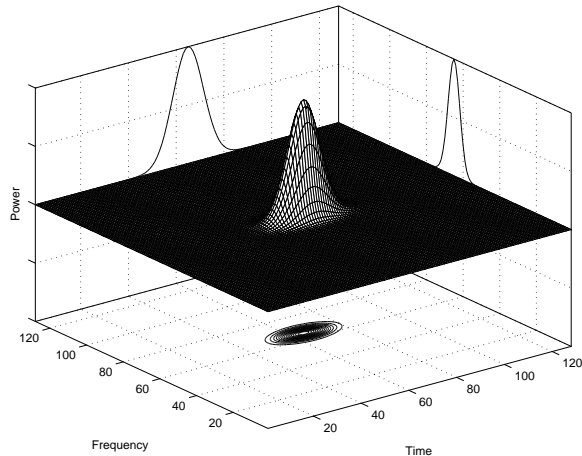
Input function:

$$g(t) = (\pi\sigma^2)^{-0.25} \exp\left(-\frac{t^2}{2\sigma^2}\right) \quad (2.16)$$

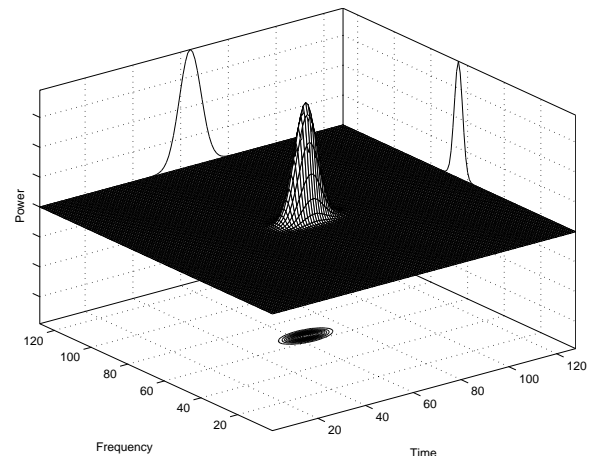
Distributions:

$$WVD_g(t, \omega) = 2 \cdot \exp\left(-\frac{t^2}{\sigma^2} - \frac{\omega^2}{\sigma^2}\right) = 2 \cdot \exp\left(-\frac{t^2}{2\left(\frac{\sigma}{\sqrt{2}}\right)^2} - \frac{\omega^2}{2\left(\frac{1}{\sqrt{2}\sigma}\right)^2}\right) \quad (2.17)$$

$$FS_g(t, \omega) = \exp\left(-\frac{t^2}{2\sigma^2} - \frac{\sigma^2\omega^2}{2}\right) = \exp\left(-\frac{t^2}{2\sigma^2} - \frac{\omega^2}{2\left(\frac{1}{\sigma}\right)^2}\right) \quad (2.18)$$



(a) FS of Gaussian function.



(b) WVD of Gaussian function

Heisenberg product:

$$\text{WVD: } \sigma_t \cdot \sigma_\omega = \frac{\sigma}{\sqrt{2}} \cdot \frac{1}{\sigma\sqrt{2}} = \frac{1}{2} \quad (2.19)$$

$$\text{FS: } \sigma_t \cdot \sigma_\omega = \sigma \cdot \frac{1}{\sigma} = 1 \quad (2.20)$$

The product of the deviations for the WVD reach the same value as the Heisenberg relation because the WVD has correct marginals.

$$\begin{aligned}
\int WVD_g(t, \omega) dt &= |G(\omega)|^2 \\
\frac{1}{2\pi} \int WVD_g(t, \omega) d\omega &= |g(t)|^2 \\
\int FS_g(t, \omega) dt &= |G(\omega)|^2 \otimes |H(\omega)|^2 \\
\frac{1}{2\pi} \int FS_g(t, \omega) d\omega &= |g(t)|^2 \otimes |h(t)|^2
\end{aligned} \tag{2.21}$$

Therefor, this WVD can be considered to be the correct distribution for the Gaussian function. The product for the FS is twice as large because the standard deviation of the density for g is increased under the convolution with the density for the window h [Bracewell 86]:

$$\sigma_{g \otimes h}^2 = \sigma_g^2 + \sigma_h^2 \tag{2.22}$$

Using this relation, the standard deviation for the time marginal of the FS can be found to be:

$$\begin{aligned}
\sigma_t &= \sqrt{\sigma_{g \otimes g}^2} = \sqrt{\sigma_g^2 + \sigma_g^2} = \sqrt{\frac{\sigma^2}{2} + \frac{\sigma^2}{2}} = \sigma \\
\sigma_\omega &= \sqrt{\sigma_{G \otimes G}^2} = \sqrt{\sigma_G^2 + \sigma_G^2} = \sqrt{\frac{1}{2\sigma^2} + \frac{1}{2\sigma^2}} = \frac{1}{\sigma}
\end{aligned} \tag{2.23}$$

The WVD of a signal containing two Gaussian functions gives a more complicated result.

Example 2.3 : Calculate the WVD for a signal containing two TF shifted Gaussian functions.

Input signal:

$$x(t) = g(t - T_1) e^{j\Omega_1 t} + g(t - T_2) e^{j\Omega_2 t} = g_1(t) + g_2(t) \tag{2.24}$$

Distribution:

$$\begin{aligned}
WVD_x(t, \omega) &= WVD_{g_1}(t, \omega) + WVD_{g_2}(t, \omega) + 2 \cdot \operatorname{Re} \{ WVD_{g_1, g_2}(t, \omega) \} \\
&= WVD_g(t - T_1, \omega - \Omega_1) + WVD_g(t - T_2, \omega - \Omega_2) \\
&\quad + 2 WVD_g\left(t - \frac{T_1 + T_2}{2}, \omega - \frac{\Omega_1 + \Omega_2}{2}\right) \cos\left(t(\Omega_1 - \Omega_2) + (T_2 - T_1)\left(\omega - \frac{\Omega_1 + \Omega_2}{2}\right)\right)
\end{aligned} \tag{2.25}$$

This calculation showed the advantage of using the TF shifting property (see Appendix 1.2). By inspection of the cross-term, the following characteristics can be stated:

The cross-term is:

- Placed in the center $\left(\frac{T_1 + T_2}{2}, \frac{\Omega_1 + \Omega_2}{2} \right)$ between the auto-terms.
- 2D Gaussian distributed (only for two Gaussian functions).
- Double the size of the auto-term.
- The oscillation in the time domain $t (\Omega_1 - \Omega_2)$ is proportional to the frequency distance, and the oscillation in the frequency domain $\omega (T_2 - T_1)$ is proportional to the time distance.

The geometric properties of the auto/cross-terms are illustrated in Figure 2.5 [Hlawatsch 84].

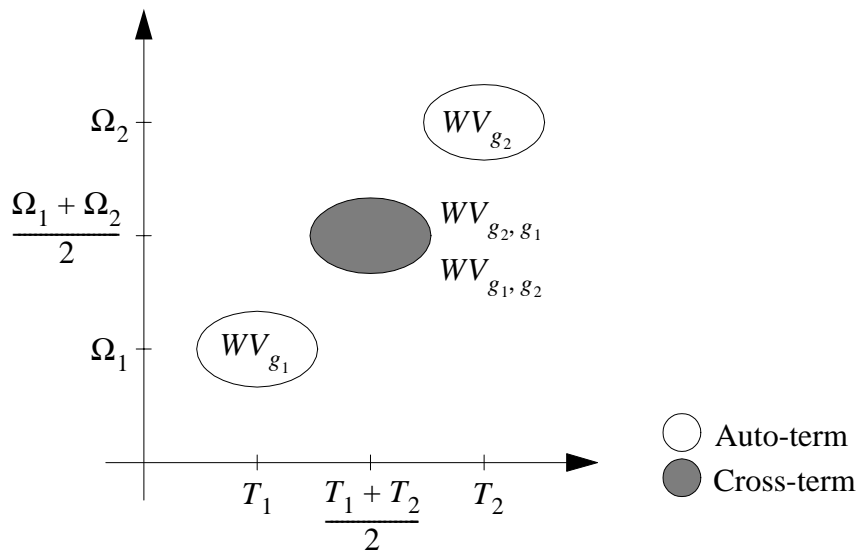


Figure 2.5 Position of auto and cross-terms

Figure 2.6 illustrates how the time-frequency oscillation of the cross-term change depending on the position of the autoterms for two Gaussian functions.

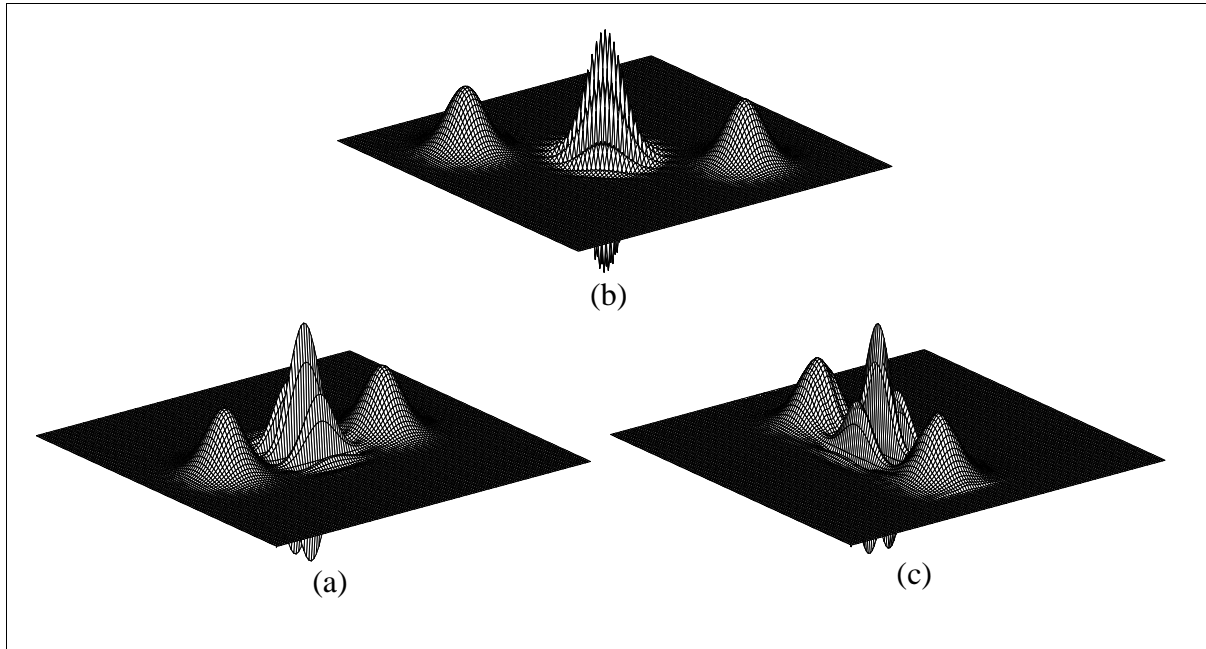


Figure 2.6 The WVD of a multicomponent signal.

- (a) Signal containing two time shifted Gaussian functions.
- (b) Signal containing two time frequency shifted Gaussian functions.
- (c) Signal containing two frequency shifted Gaussian functions.

The existence of cross-terms is the main difficulty of using the WVD. When the signal is a tedious and idealized multicomponent signal with two Gaussian functions (a toy signal), it is possible to identify and remove/ignore the cross-term. But when the signal is a real multicomponent signal, e.g. a speech signal, it is impossible to see what is cross-term and what is auto-term. Time and frequency information provided by the cross-terms is redundant, because it is already given by the auto-terms. However, the removal of the cross-terms in general will spoil two very fundamental properties of the WVD namely both the marginals. This can be seen by the following example:

Example 2.4 : Calculate the marginal distribution of a cross-term deleted WVD.

Input signal:

$$s(t) = s_1(t) + s_2(t) \quad (2.26)$$

Distribution:

$$WVD_s(t, \omega) = WVD_{s_1}(t, \omega) + WVD_{s_2}(t, \omega) + 2 \cdot \operatorname{Re} \{ WVD_{s_1, s_2}(t, \omega) \} \quad (2.27)$$

Time marginal:

$$\frac{1}{2\pi} \int WVD_s(t, \omega) d\omega = |s(t)|^2 = |s_1(t) + s_2(t)|^2 \quad (2.28)$$

Time marginal of a cross-term deleted WVD:

$$\frac{1}{2\pi} \int (WVD_{s_1}(t, \omega) + WVD_{s_2}(t, \omega)) d\omega = |s_1(t)|^2 + |s_2(t)|^2 \neq |s_1(t) + s_2(t)|^2 \quad (2.29)$$

So removing the cross-terms will spoil the time marginal, and the same argument can be found for the frequency marginal. This point is illustrated in Figure 2.7. By itself, the time-shifted Gaussian functions do not contain enough information to construct the marginals. This information is placed in the cross-terms. This makes the cross-terms an important part of the WVD. With this information in mind, it is not desirable to remove the cross-terms, but just move them to the position of the auto-terms.

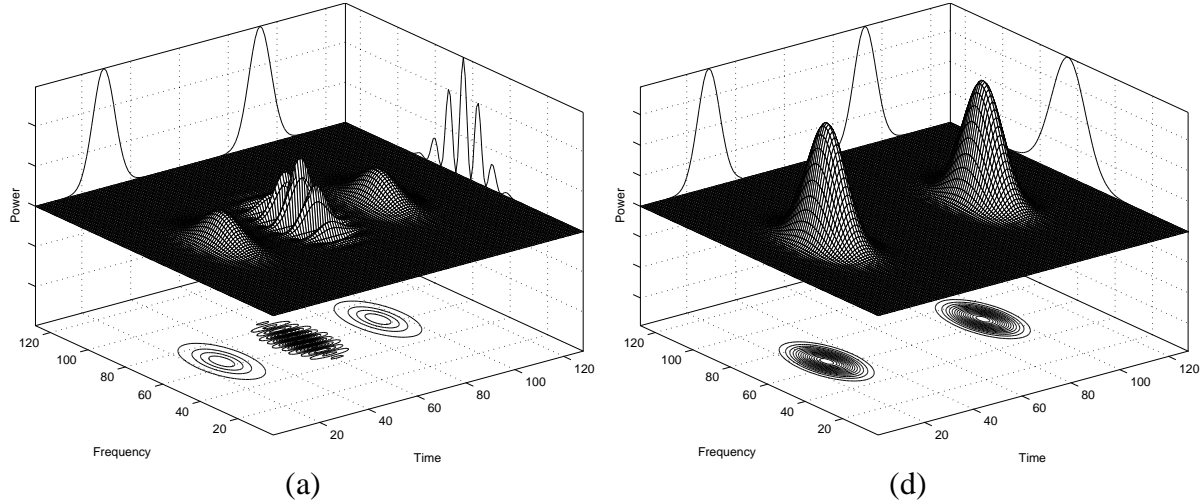


Figure 2.7 (a) The WVD of two time-shifted Gaussian functions and with the corresponding marginals. (b) A modified WVD and the corresponding marginals.

Some useful transformation properties of the WVD have been summarized in Table 2.5 (derived in appendix 1.2.).

Property Name	Property
Addition property	$f(t) = h(t) + g(t)$ $\text{WVD}_f(t, \omega) = \text{WVD}_h + \text{WVD}_g + 2 \cdot \text{re} \{ \text{WVD}_{g,h}(t, \omega) \}$
Product property	$f(t) = h(t) \cdot g(t)$ $\text{WVD}_f(t, \omega) = \text{WVD}_g(t, \omega) \otimes_{\omega} \text{WVD}_h(t, \omega)$
Convolution property	$f(t) = h(t) \otimes g(t)$ $\text{WVD}_f(t, \omega) = \text{WVD}_g(t, \omega) \otimes_t \text{WVD}_h(t, \omega)$

Table 2.5 Some properties of the WVD.

The WVD is defined for continuous signals, and in order to use it on a computer, a discrete version is needed. Many different discrete WVDs have been proposed in the last 10 - 20 years, and the main problem is that the signal has to be oversampled by a factor 2 in order to avoid frequency aliasing. Another way of avoiding aliasing (and oversampling) is to use the analytic signal. The analytic signal can be made from the original signal, by removing the negative part of the spectra, and multiplying the positive frequency plan by 2 to preserve the energy. The problem with the WVD of the analytic signal is that the low frequency portion of the WVD is significantly spread out because the analytic signal is band limited [Qian 96].

A very useful approach was given by Peyrin & Prost [Peyrin 86]. They defined a *Discrete Time WVD (DT-WVD)*, *Discrete Frequency WVD (DF-WVD)* and a *Discrete Time Frequency WVD (DTF-WVD)*. Their idea was to make the signal discrete in both time and frequency, and then

insert this signal into the WVD. A full derivation of the three types can be found in appendix 1.3. and only the DTF-WVD will be used in this section:

$$WVD_{x_{T,NT}}[k, m] = \frac{1}{2NT} \sum_{n=0}^{N-1} x_n x^*_{k-n} e^{-j\frac{m\pi}{N}(2n-k)} \quad (2.30)$$

In order to avoid aliasing in both the frequency and time domain, the signal has to be oversampled by a factor of 2, and zeropadded 100%. The computation load is depending on the signal length N . However, by using a window of length 2^r , a computation with the FFT algorithm will be possible. A side effect to the window version of the DTF-WVD is a reduction/removal of the cross-terms in the time direction. The reason for this is that the WVD will only make cross-terms for signal components inside the window length. Signal components outside the window will not interact and make cross-terms. But by windowing the signal, the resulting WVD will be given by the product property of the WVD:

$$x(t) = g(t) \cdot h(t) \Rightarrow WVD_x(t, \omega) = WVD_g(t, \omega) \otimes_{\omega} WVD_h(t, \omega) \quad (2.31)$$

The reduction of computational load and time cross-terms are obtained at the expense of frequency distortion, which destroys the frequency marginal. Examples of this effect are illustrated in Figure 2.8

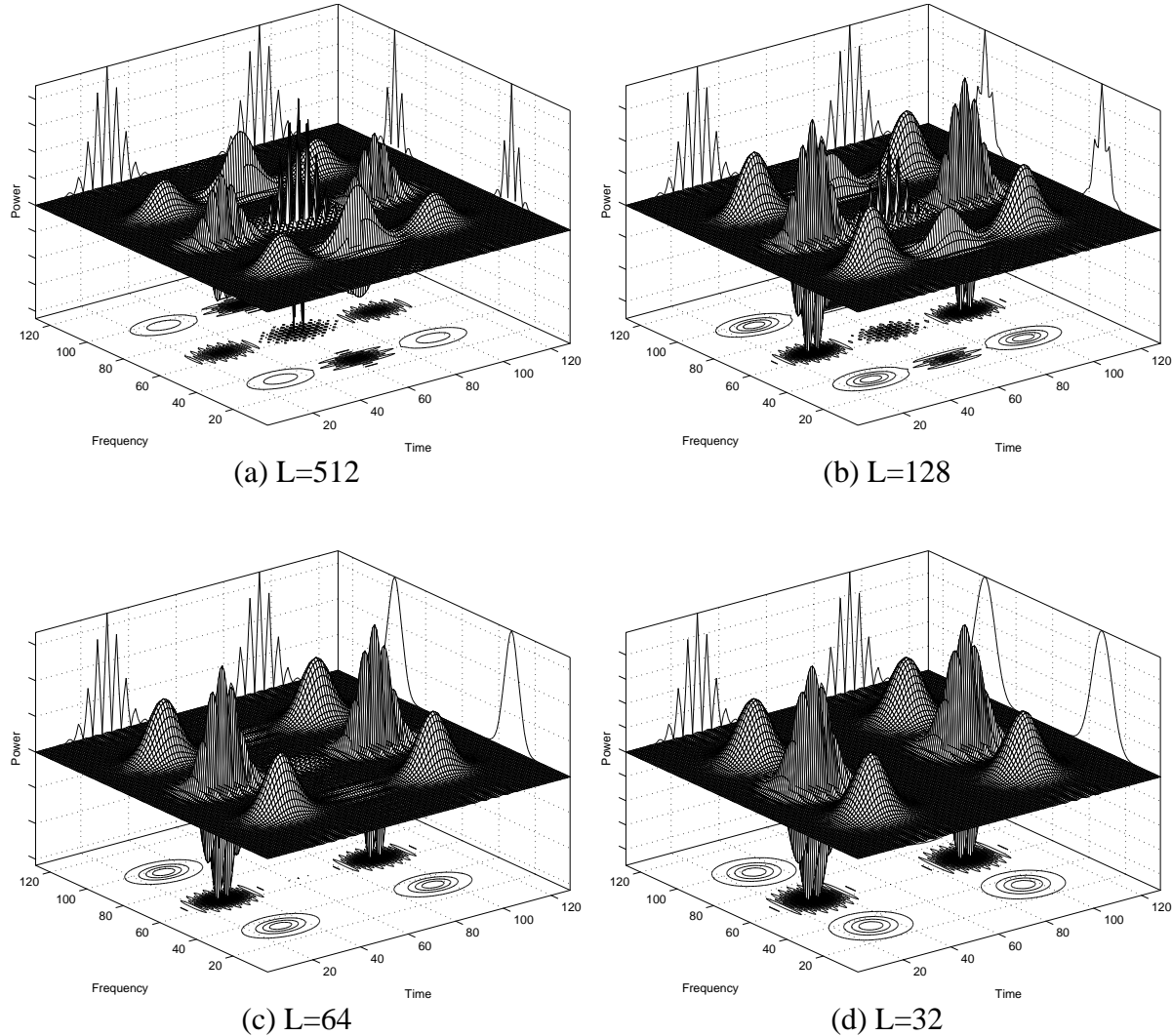


Figure 2.8 The windowed DTF-WVD with different window length L.

The problem with cross-terms in the WVD is very clear when analysing a speech signal. The WVD of the speech signal *spectrogram* is shown in Figure 2.9.

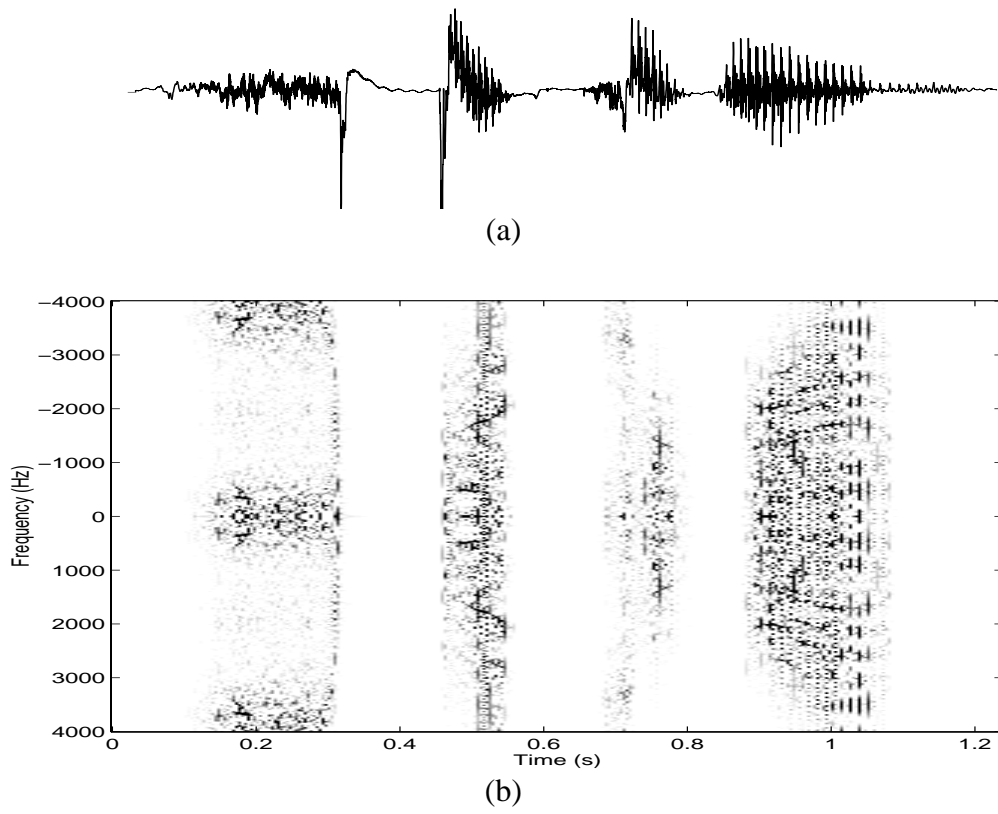


Figure 2.9 DTF-WVD of the speech signal *Spectrogram*.

As the cross-terms have an amplitude larger than the auto-terms, they will dominate the time-frequency picture and make an interpretation difficult.

2.3 The Gabor spectrogram

A very powerfull approach to removes or reduces the CT's in the WV is the *Gabor Spectrogram* (GS). The GS is obtained by inserting a Gabor expansion of the signal into the WVD [Qian 94]. The advantages of this are obtained when only a portion of the expansion is used! Because a fundamental part of the GS is the *Discrete Gabor Expansion (DGE)*, and the spectral/temporary resolution of the GS is depending on the DGE, the Gabor expansion will be described first. The main idea of the Gabor expansion will be given in this section, and a more elaborated version can be found in appendix 2.

The Gabor expansion for a continuous signal is the *Continuous Gabor Expansion (CGE)* and expresses a signal as a double sum:

$$x(t) = \sum_m \sum_n a_{mn} g_{mn}(t) \quad (2.32)$$

$$\text{where } g_{mn}(t) = g(t - mT) \exp(jtn\Omega)$$

The sum contains the Gabor coefficients a_{mn} , and the synthesis function $g(t)$. The indices **m** and **n** are the time and frequency shifting indices. The synthesis function $g(t)$ is by definition a Gaussian function. The reason for this choice is that the Gaussian function is optimally concentrated in the time-frequency plan as it reaches the lower bound of the uncertainty relation. The Gabor coefficients a_{mn} are obtained by sampling the time frequency plan in a certain lattice grid. This grid is illustrated in Figure 2.10. How to calculate the coefficients will be explained later.

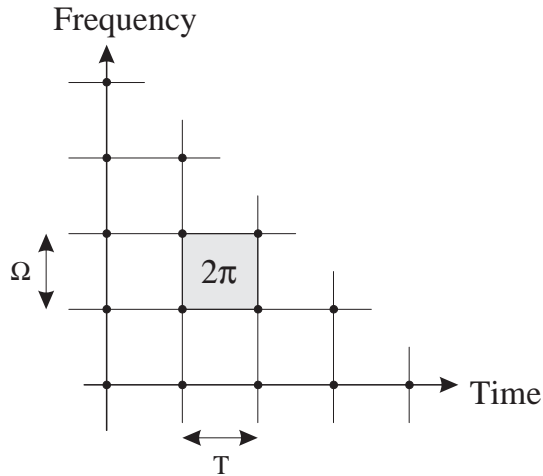


Figure 2.10 Sampling of the time frequency plan.

The time direction is sampled with stepsize T , and the frequency direction is sampled with step-size Ω . A necessary condition for a stable reconstruction is that the area of the sampling lattice/grid is upper limited by $\Omega \cdot T \leq 2\pi$. If the area is larger than 2π , the expansion does not contain enough information about the signal to reconstruct it. An area of 2π is the least necessary area to obtain a correct reconstruction and is called *critical sampling*. If the expansion uses a grid area smaller than 2π , the representation will be redundant, but more robust. This situation is refered to as *oversampling*. The original article by Dennis Gabor [Gabor 45] contained an iterative algorithm for approximation of the coefficients, but it was not until Bastiaans [Bastiaans 80] introduced an auxiliary function $\gamma(t)$ that the Gabor expansion was usable. Bastiaans pro-

posed a technique to calculate the Gabor coefficients by projection of the signal onto an analysis function $\gamma_{mn}(t)$:

$$a_{mn} = \int x(t) \gamma^*(t - mT) e^{-jn\Omega t} dt = \int x(t) \gamma_{mn}^*(t) dt \quad (2.33)$$

where $\gamma_{mn}(t) = \gamma(t - mT) e^{jn\Omega t}$

The remaining part is to determine the analysis function $\gamma(t)$, when the synthesis function $g(t)$ is given. A scheme to find $\gamma(t)$ can be derived by inserting the expression for the Gabor coefficients into the Gabor expansion. The resulting scheme expresses a biorthogonality condition between the analysis function $\gamma(t)$ $g(t)$ and the synthesis function $g(t)$ and is named the *Continuous Biorthogonality Condition (CBC)*.

$$\delta_m \cdot \delta_n = \frac{2\pi}{\Omega T} \int g(\tau) \gamma^* \left(\tau - m \frac{2\pi}{\Omega} \right) e^{-j\tau n \frac{2\pi}{T}} d\tau \quad (2.34)$$

$-\infty < m < \infty \quad -\infty < n < \infty$

The continuous biorthogonality condition has only been solved for very few functions. Bastiaans has solved the closed form for the analysis function, when the synthesis function was a Gaussian function at critical sampling [Bastiaans 81]. The resulting analysis function is either localized in the time or frequency dimension, but the signal can still be reconstructed using the synthesis function. It is important to note that any function can be used as synthesis/analysis function. The corresponding analysis/synthesis function has to be related through the biorthogonality condition. The Gabor expansion is defined by a Gaussian synthesis function.

In order to use the Gabor expansion on a computer, a discrete version of the Gabor expansion has to be found. From the CGE, a discrete version for periodic signal were proposed by [Wexler 90] as a *Periodic Discrete Gabor Expansion (PDGE)* and their approach were extended to non-periodic signals by [Qian 93] and named a *Discrete Gabor Expansion (DGE)*. The details can be found in appendix 2 and we will only be concerned about the DGE as the Gabor spectrogram is based on this expansion. The DGE makes use of the following parameters:

- Δ = Sampling interval for the continuous time signal $x(t)$ [s].
- T = Time step of CGE lattice [s].
- Ω = Frequency step of CGE lattice [rad/s].
- ΔM = Time step of the PDGE lattice - number of grids [integer].
- ΔN = Frequency step of the PDGE lattice - number of grids [integer].
- L_s = Number of samples in the signal $x[k]$ [integer].
- N_1 = Number of grid in the frequency dimension in the DGE
- = Number of grid in the time dimension in the DGE
- L = Number of samples in the analysis/synthesis function.
- M = Number of time steps ΔM in time dimension of the PDGE lattice [integer].
- N = Number of frequency steps ΔN in frequency dimension of PDGE lattice [integer].

and is given by equation (2.35).

$$x[k] = \sum_{m=0}^{M-1} \sum_{n=0}^{N-1} a_{mn} g[k - m \cdot \Delta M] e^{jkn \frac{2\pi}{N}} \quad (2.35)$$

$$a_{mn} = \sum_{k=0}^{L-1} x[k] \gamma^*[k - m \cdot \Delta M] \exp\left(-jkn \frac{2\pi}{N}\right)$$

The analysis function $\gamma[k]$ is found as the solution to the *Discrete Biorthogonality Condition* (DBC):

$$\delta_m \cdot \delta_n = \frac{MN}{N_1} \sum_{k=0}^{N_1-1} \gamma^*[k] g[k + mN] e^{-jkn \frac{2\pi}{\Delta M}} \quad (2.36)$$

$$- \Delta N < m < \Delta N \quad 0 \leq n \leq \Delta M - 1$$

The analysis function $\gamma(t)$ can now be found as the solution to this linear system of equations. The main advantage of this DBC is the independence of the length of the signal. Both the analysis and synthesis functions have a fixed length of L, and can be selected independently of the length of the signal. The solution of the DBC at the DGE is solved using Singular Value Decomposition (SVD). This leaves the DGE with many degrees of freedom. Some possible analysis functions for a *Sampling factor* (SF) of 1, 2 and 4 are illustrated in the following Figure 2.11

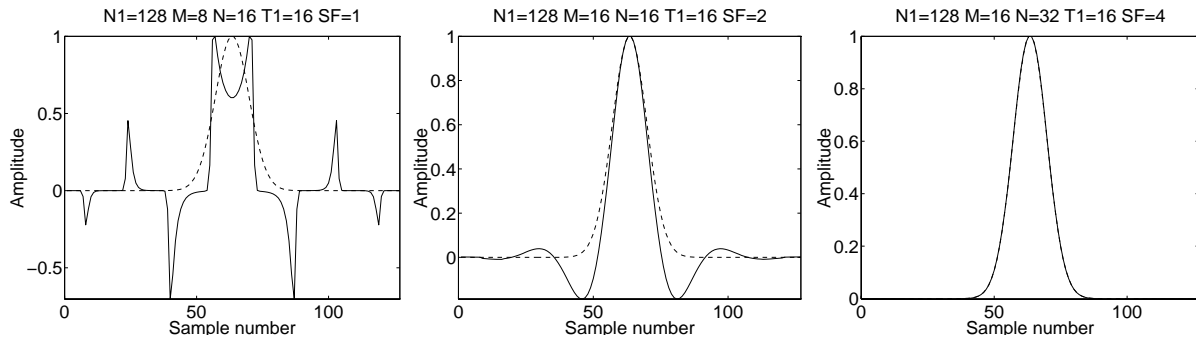


Figure 2.11 Analysis and synthesis functions versus samplings factor.

As the SF is increased, the analysis function is getting more localized in both time and frequency. The Gabor coefficients calculated using the analysing function for a factor of 1-2 will not illustrate the local time and frequency properties of the signal, but they will all reconstruct the signal equally well.

In order to obtain an analysis function that has a Gaussian shape corresponding to the synthesis function, the following error measurement is introduced:

$$\text{error} = \left\| \frac{\gamma}{\|\gamma\|} - g \right\| \quad (2.37)$$

When $g(t)$ and $\gamma(t)$ have the same shape, $g(t)$ is orthogonal to both $\gamma(t)$ and itself. Such a Gabor expansion is called orthogonal-Like Gabor expansion [Qian 93]. It is not easy to obtain such an expansion, but the following three parameter choices have been found and listed in Table 2.6.

Variable\base	base 64	base 128	base 256
$N_1 = L$	64	128	256
SF	4	4	4
M	16	16	8
$N = N_1 \cdot SF/M$	16	32	128
$\Delta M = N_1/M$	4	8	32
$\Delta N = N_1/N$	4	4	2
$T_1 \approx \sqrt{\Delta M \cdot N}$	8	16	64

Table 2.6 Orthogonal-Like Gabor expansion

The GS¹ is obtained by inserting the DGT into the WVD:

$$GS[k, \omega] = WVD\{DGT\{s[k]\}\} \quad (2.38)$$

When the DGT is inserted, the GS can be expressed as four summations:

$$\begin{aligned}
 WVD_s[k, \omega] &= \sum_{m=0}^{M-1} \sum_{n=0}^{N-1} \sum_{m'=0}^{M-1} \sum_{n'=0}^{N-1} a_{mn} a^*_{m'n} WVD_g\left[k - \frac{m+m'}{2} \cdot \Delta M, \omega - \frac{n+n'}{2} \cdot \frac{2\pi}{N}\right) \\
 &\quad \times \exp\left(j\left(k(n-n')\frac{2\pi}{N} + \left(\omega - \frac{n+n'}{2} \cdot \frac{2\pi}{N}\right)\Delta M(m'-m)\right)\right) \\
 &= \sum_{m=0}^{M-1} \sum_{n=0}^{N-1} |a_{mn}|^2 WVD_g\left[k - m \cdot \Delta M, \omega - n \frac{2\pi}{N}\right) \\
 &\quad + \sum_{m=0}^{M-1} \sum_{n=0}^{N-1} \sum_{\substack{m'=0 \\ m \neq m'}}^{M-1} \sum_{\substack{n'=0 \\ n \neq n'}}^{N-1} a_{mn} a^*_{m'n} WVD_g\left[k - \frac{m+m'}{2} \cdot \Delta M, \omega - \frac{n+n'}{2} \cdot \frac{2\pi}{N}\right) \\
 &\quad \times \exp\left(j\left(k(n-n')\frac{2\pi}{N} + \left(\omega - \frac{n+n'}{2} \cdot \frac{2\pi}{N}\right)\Delta M(m'-m)\right)\right) \\
 &= WVD_{CDR}[k, \omega] + WVD_{CR}[k, \omega]
 \end{aligned} \quad (2.39)$$

The WVD_{CDR} is the WVD *Cross-term Deleted Representation* containing the auto-terms. Each auto-term is given by the absolute square of the Gabor coefficients and a 2D Gaussian function centered at the location of the coefficient (m,n). The WVD_{CR} is the WVD *Cross-term Representation* and contain all the cross-terms. The positions of the auto- and cross-terms are

1. The square brackets indicate that k is a discrete parameter, and the parentheses indicate that ω is a continuous parameter.

illustrated in Figure 2.12. There is no advantage of the WVD of the Gabor expansion compared to the WVD calculated from the signal. It will produce the same distribution.

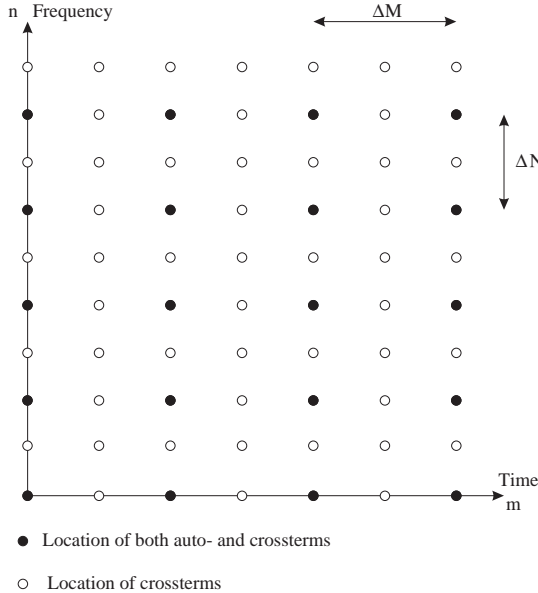


Figure 2.12 Position of auto- and cross-terms.

If the used Gabor expansion is an Orthogonal-Like Gabor expansion, the Gabor coefficients illustrate the time-frequency content of the signal very well (like the STFT). Moreover, the WVD_{CDR} will be a continuous distribution, where the 2D Gaussian function will interpolate the missing values between the Gabor coefficients. This distribution is similar to a FS using a Gaussian window (the analysis function γ). When the WVD_{CR} is added to the WVD_{CDR} , the WVD is obtained which has good time-frequency resolution, but troublesome cross-terms. This makes it very clear that the cross-term contributes with both unwanted and desired properties of the WVD. The golden point in the Gabor Spectrogram is to separate the portion of the cross-terms which contribute to the time-frequency resolution, without going negative between signal component, and add this to the WVD_{CDR} . This is given by :

$$GS_D = WVD_{CDR} + WVD_{CR}^D \quad (2.40)$$

The remaining question is which cross-terms to include. Two complex cross-terms can be compounded to the following real cross-terms:

$$\begin{aligned} & 2Re \{ a_{mn} a_{m'n'}^* \} WVD_g \left[k - \frac{m+m'}{2} \Delta M, \omega - \frac{n+n'}{2} \cdot \frac{2\pi}{N} \right] \\ & \times \cos \left(k(n-n') \frac{2\pi}{N} + \left(\omega - \frac{n+n'}{2} \cdot \frac{2\pi}{N} \right) \Delta M (m'-m) \right) \end{aligned} \quad (2.41)$$

The following three important properties of the cross-terms can be stated:

- Oscillation in the time dimension with the frequency $(n - n') \cdot \frac{2\pi}{N}$
- Oscillation in the frequency dimension with the frequency $(m - m') \cdot \Delta M$
- The energy of a cross contribution is inversely proportional to the distance between a_{mn} and $a_{m'n'}$.

It is clear that cross-terms with high oscillation and low energy are unwanted. This is why cross-

terms corresponding to small time-frequency distance between the indices are added first to the WVD_{CDR} . Letting the variable \mathbf{d} express the sum of the numerical distance between the time indices $|m - m'|$ and the frequency indeces $|n - n'|$, the GS of order \mathbf{D} can be stated as follows:

$$\begin{aligned} GS_D [k, \omega] &= \sum_{d=0}^D P_d [k, \omega] \\ P_d [k, \omega] &= \sum_{A_d} a_{mn} a_{m'n'}^* WVD_g \left[k - \frac{m+m'}{2} \cdot \Delta M, \omega - \frac{n+n'}{2} \cdot \frac{2\pi}{N} \right] \\ &\quad \times \exp \left(j \left(k(n-n') \frac{2\pi}{N} + \left(\omega - \frac{n+n'}{2} \cdot \frac{2\pi}{N} \right) \Delta M (m' - m) \right) \right) \\ A_d &= \{ (m, m'), (n, n') \mid |m - m'| + |n - n'| = d \} \end{aligned} \quad (2.42)$$

Each sub-distribution P_d is constructed by cross-terms from auto-terms with a numerical distance \mathbf{d} . A GS of order D is obtained by summing up sub-distributions from $0 \leq d \leq D$. The GS_0 corresponds to the FS and GS_∞ converging to the WVD. As the order \mathbf{d} (distance) is increased, sub-distributions with decreasing energy contribution, but with increasing oscillation are included.

This process is very time consuming, and certain optimizations can be made because the main part of the summation consists of adding zeros from the boundary of the 2D Gaussian function. Guidance for doing this can be found in appendix 3. An example of the GS is illustrated in Figure 2.13 with a signal containing four Gaussian components. For illustration purposes the four components have been placed very close in time and frequency, and the GS is only calculated in the area of these four. The GS_0 is by definition positive. An increase in temporal/spectral resolution is obtained by adding P_1 which contains negative contributions. The negative contributions are located on the boundary of the auto-terms, and will therefore slice the boundary off. The positive part of the P_1 is located in the area of the auto-terms, and will thereby increase the level of the auto-terms. As the order \mathbf{d} is increased, the positive properties of the GS_d are decreased because it gets more oscillation. How to set the total order \mathbf{D} depends on the signal. If the signal components are located very close (multi component signal like speech signals) the order should not be higher than 3-4. A signal like a Doppler Radar signal can use a much higher order, up to 30 have been used in chapter 3. However, the signal length and size of the order have a non-linear effect on the computation load, and an order up to 3-4 is advisable.

In order to implement a GS, a lot of parameters must be set. Two fundamental choices are which Orthogonal-Like Gabor expansion to choose and how large the order \mathbf{D} can be set. These choices cannot be made without some “a priori” knowledge of the signal. The GS can be viewed as a process of removing the Window effect of a given FS. The FS uses the analysis function γ as window function. So we do in fact have three different FS to choose from (Because we have three Orthogonal-Like Gabor expansions). It is very important to choose the right FS because the improvement will be based/limited by this distribution. The Orthogonal-Like Gabor coefficients which best reveal the time-frequency structure of the signal must be used.

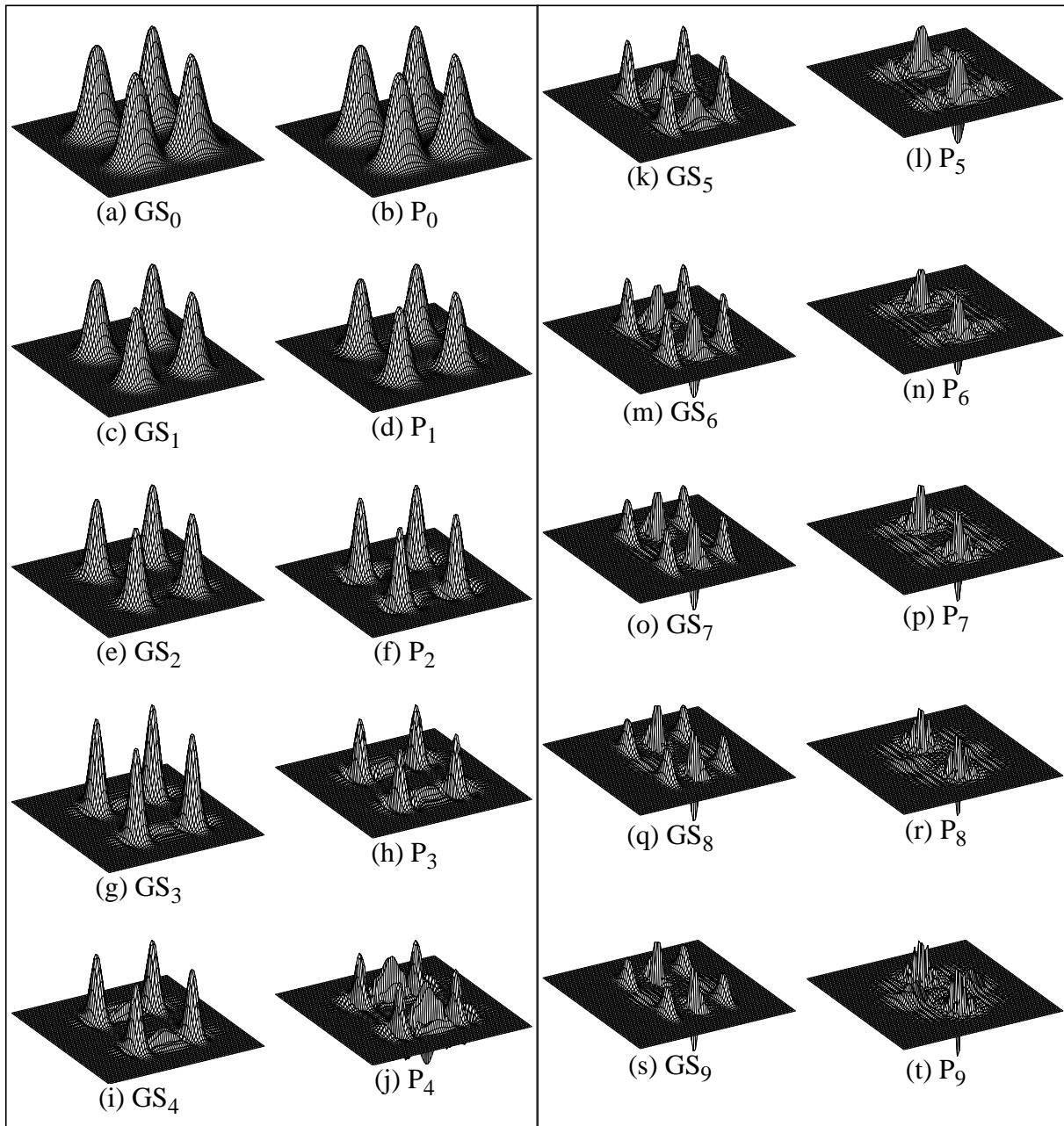


Figure 2.13 Construction of GS.

In Figure 2.14, the GS is calculated for the speech signal *spectrogram*. It is clear, as the order is set to 2 - 3, that the distribution can illustrate both the time variation of the energy from the pitch, and the variation in the spectra as the result of the periodic structure of the voiced sections. This had not been possible to obtain with any FS, and is invisible in the WVD.

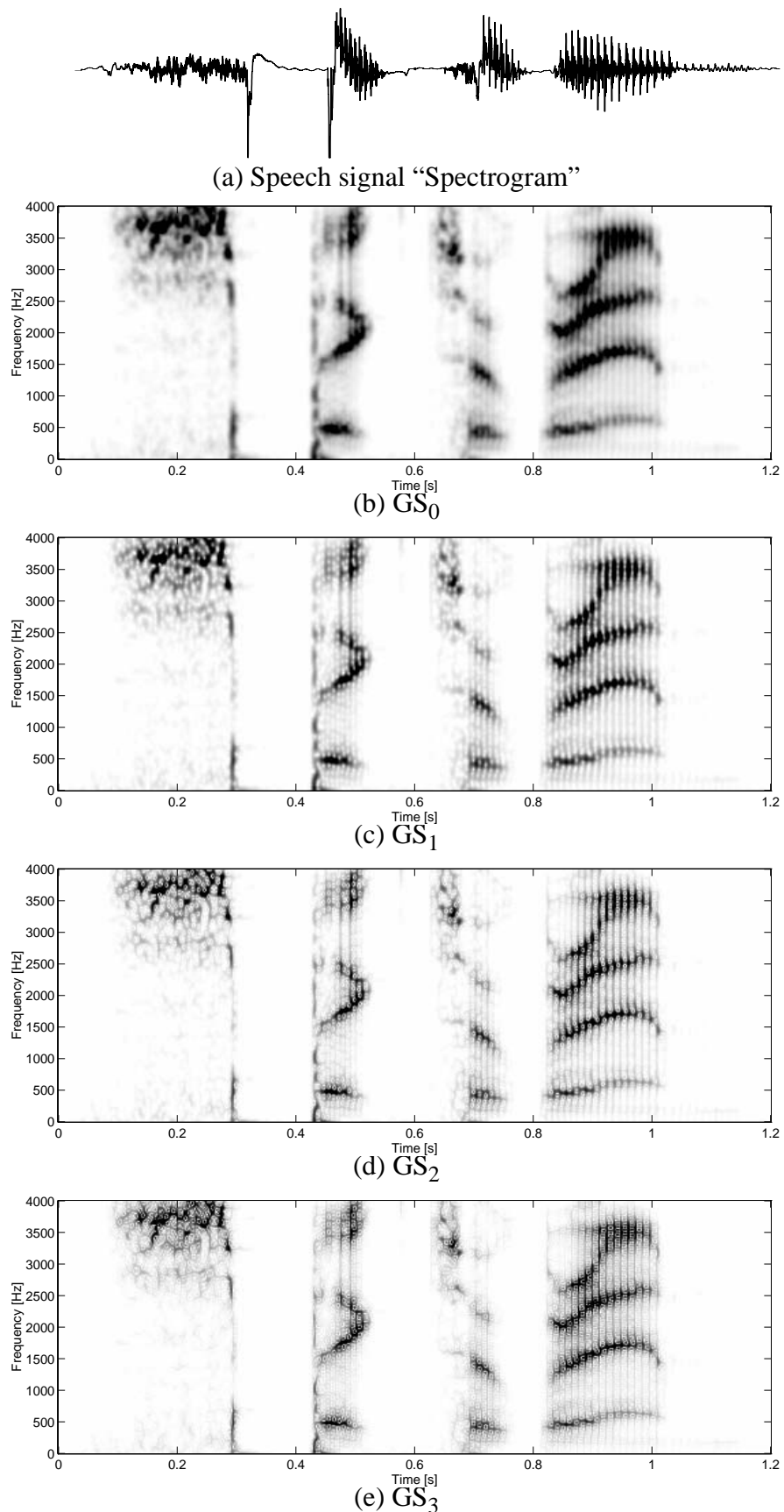


Figure 2.14 The Gabor spectrogram of the speech signal *spectrogram*.

Chapter 3

Application of JTFA in Signal Processing

This chapter introduces three applications where time frequency energy distributions are used. Common for all of them is that the Fourier Spectrogram is used today, and the purpose of this chapter is to evaluate whether any of the distributions described in chapter 2 can offer any improvement. The three applications involve bat echolocation, bird song and doppler radar signals.

3.1 Bat Echolocation

Several bat species use a technique called *echolocation* to maneuver and chase prey in the dark [Møhl 87]. Echolocation is a process in which the bat produces calls and listens to their echoes reflected from surfaces and objects. Because the principle of the sonar sight of bats is analogous to the sonar used by the military; but in this case produced by living organisms rather than by machines; it is often called biosonar.

An echolocating bat registers each outgoing call and compares the originals to returning echoes.

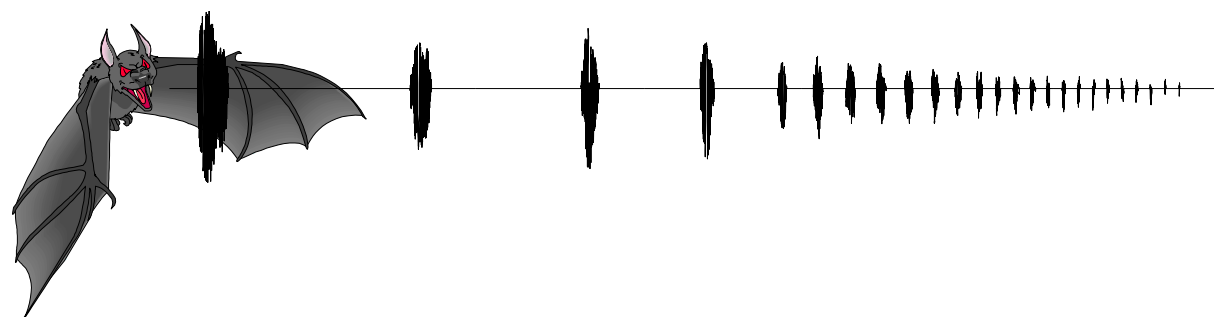


Figure 3.1 An echolocating bat.

The time lapsed between generating the outgoing call and receiving an incoming echo provides an accurate assessment of the target's distance from the bat. Changes in the amplitude (intensity) and frequency (pitch) of the outgoing call provide data about the nature of the target (size, shape, surface structure, velocity, etc.). Most echolocating bats do not produce calls at a *constant frequency (CF)*. Calls usually start at one frequency and sweep down to another (*frequency modulated or FM*, calls). In some cases, bat calls have both a CF and a FM component. The FM portion of a call provides a bat with information on the texture of an insect target, and its position in horizontal and vertical space, while the CF components relay information about the insect's velocity. Harmonics or overtones, which are multiples of the call frequencies used by the bat, further assist in pinpointing the insect's location.

The echolocation is the subject of considerable study by biologists, industry etc., and an important information is the TF structure of the call. In this chapter, a call from the *Pipistrellus pipis-*

trellus (pipistrelle) are processed. The calls were recorded at a sample rate of 250 kHz, at the Institute of Biology, Odense University, Denmark. The signal contain 931 samples and is illustrated in Figure 3.2.

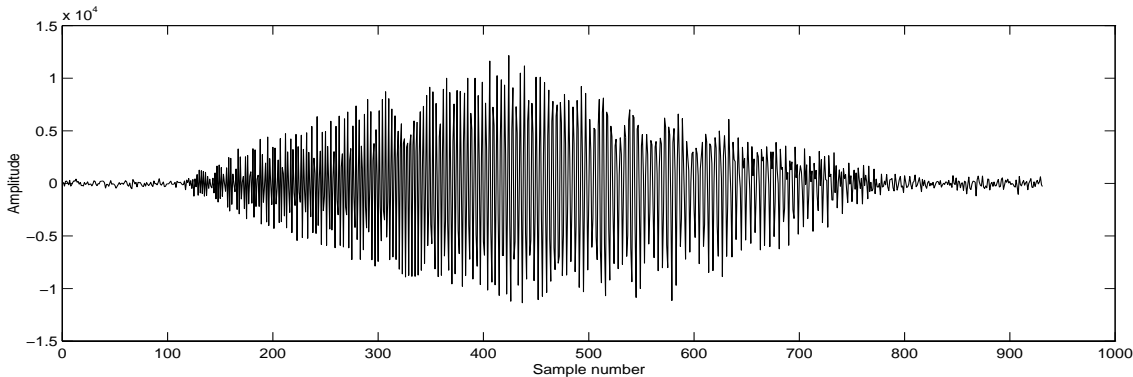


Figure 3.2 The Bat call from a *Pipistrellus pipistrellus*.

The bat signal has traditionally been analysed using the FS. For this reason, the first analysis will be performed by the FS with three different window sizes. For comparability reasons, the analysis function from the Gabor spectrogram will be used. The result¹ is illustrated in Figure 3.3.

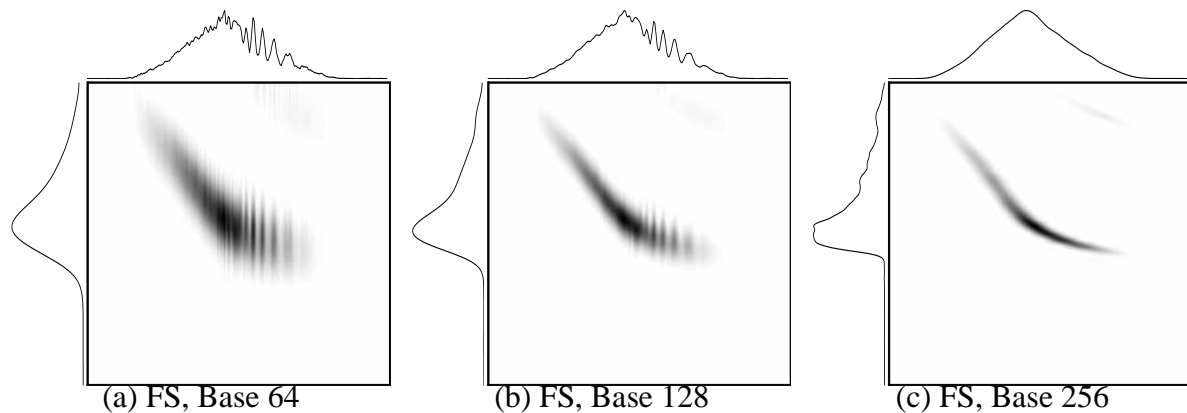


Figure 3.3 Fourier Spectrogram of the Bat Call.

One of the promising distributions from chapter 2 is the Gabor Spectrogram. In order to obtain a satisfactory result, it has been argued that the base which best illustrates the time frequency structure of the signal must be chosen. To illustrate this argument, the Gabor spectrogram has been calculated for all three bases up to an order of 10. The result is illustrated in Figure 3.4 to Figure 3.6.

1. Common for all TF-plans for the bat analysis without axis labels is a time duration of 3,7 ms and a max frequency of 125 kHz.

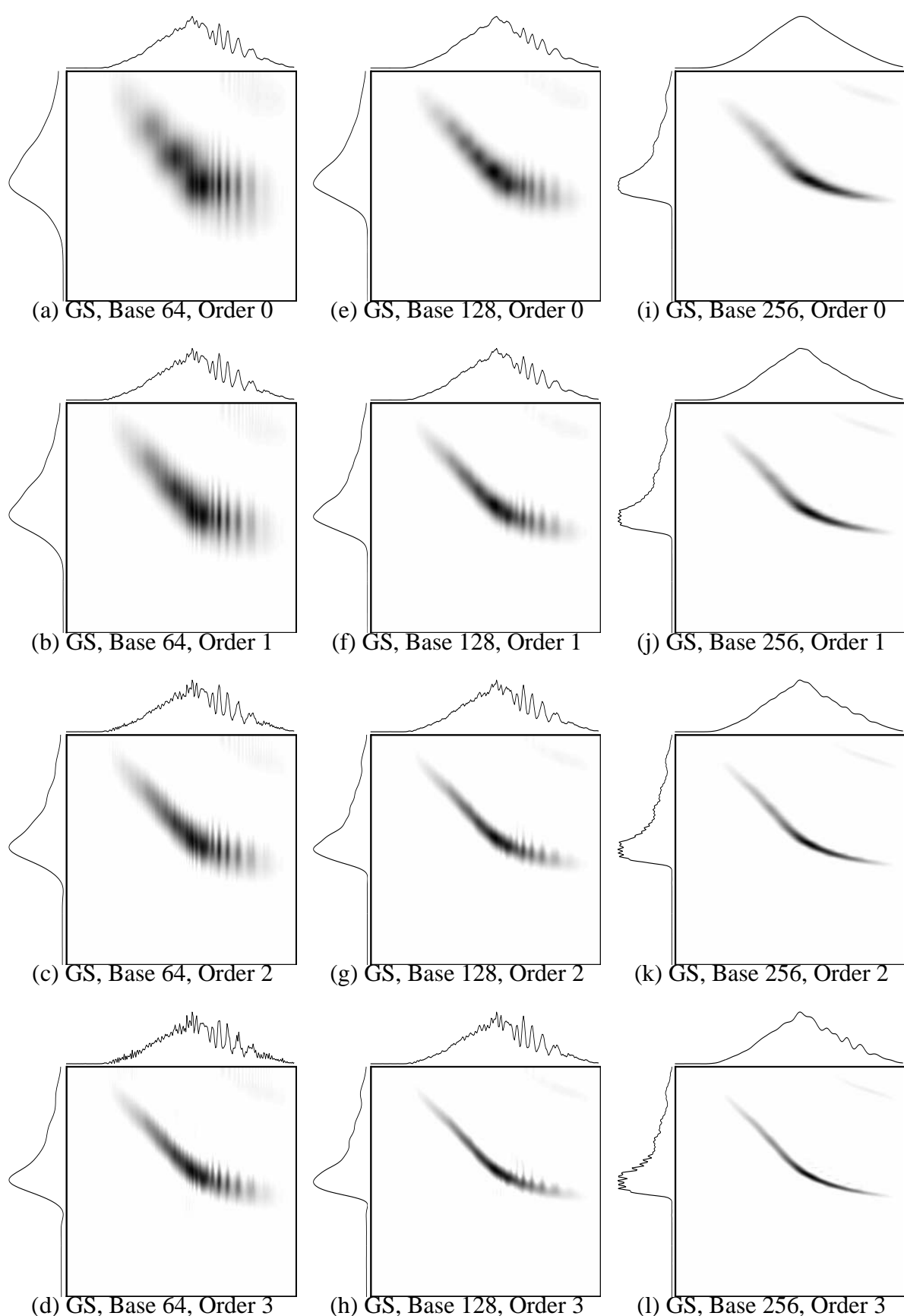


Figure 3.4 Gabor Spectrogram of the Bat Call, Order 0:3.

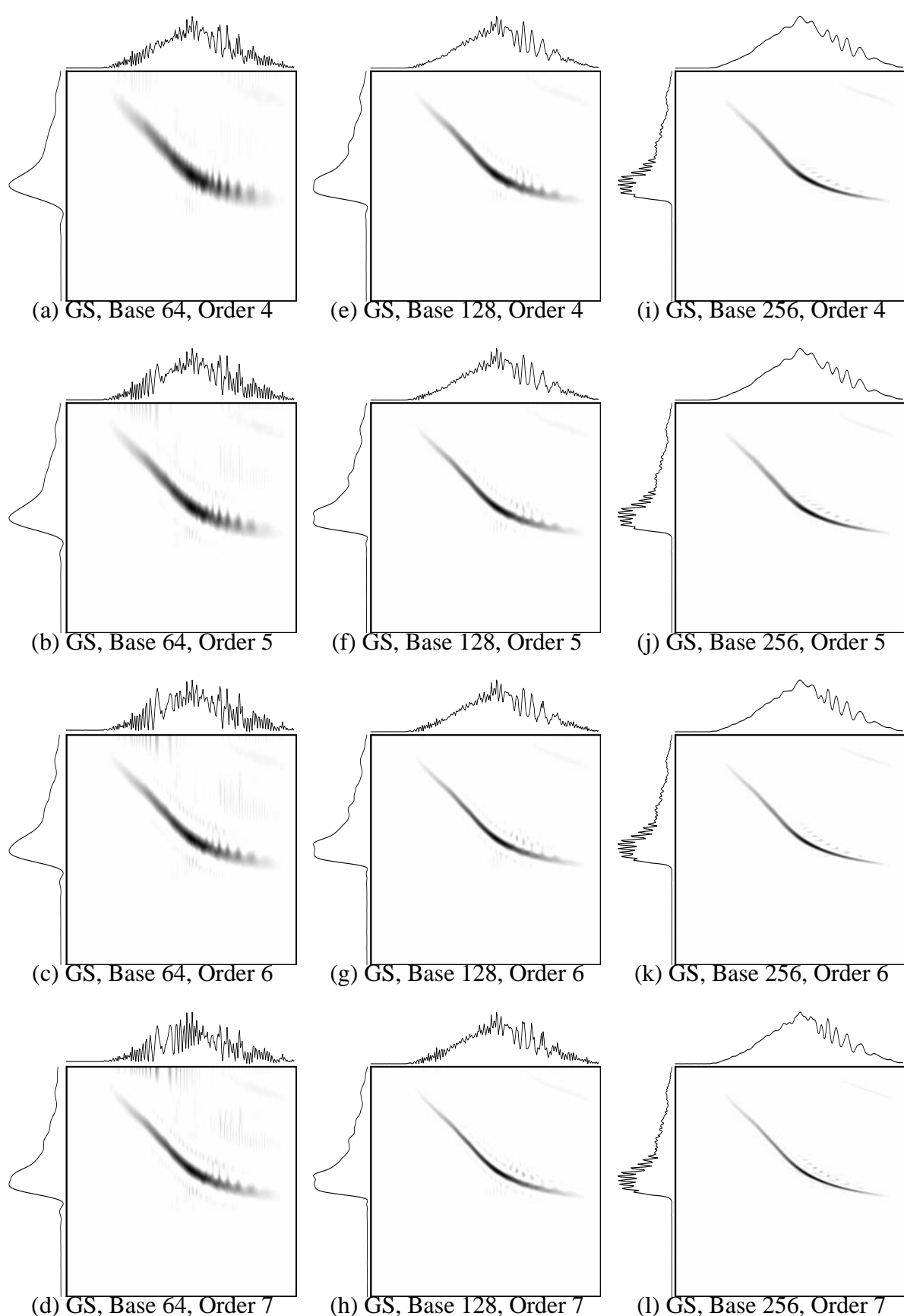


Figure 3.5 Gabor Spectrogram of the Bat Call, Order 4:7.

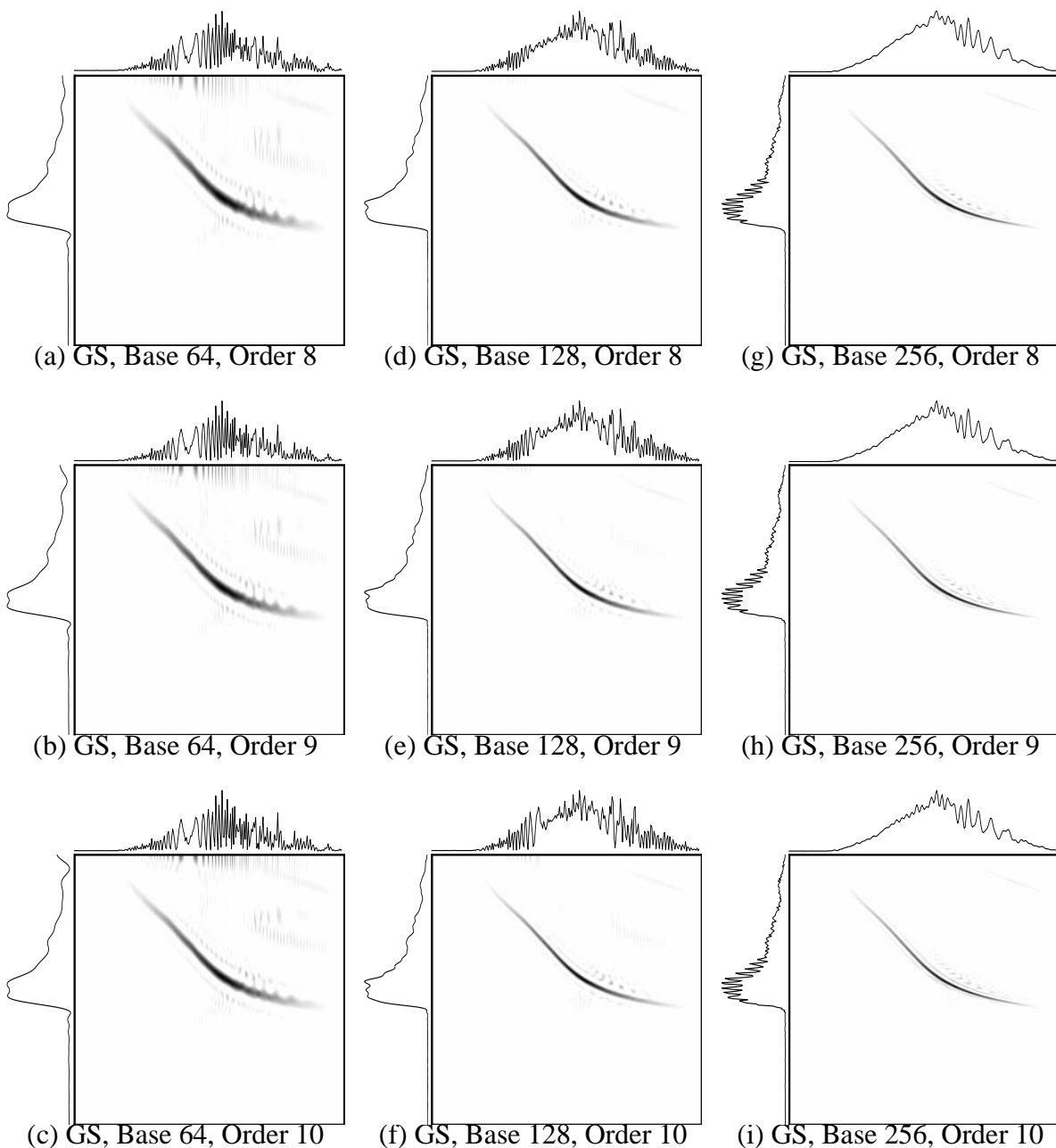


Figure 3.6 Gabor spectrogram of the Bat Call, Order=8:10.

When the Gabor spectrogram is calculated using a base with a small standard deviation, the resulting Gabor coefficients contain very detailed information about the time structure of the signal, while the frequency information is low. When the Gabor Spectrogram is calculated using these coefficients, the spectrogram will inherit this detailed time information. This means that the main improvement will be in the frequency direction. But as the frequency stepsize is high for base 64, the order cannot be increased much before annoying cross-terms appear in the time frequency plan. This can be seen from the GS of the bat call using base 64. The GS in Figure 3.4 (a) is a zero order GS which is simular to a FS. But by comparing the FS using the same analysis function Figure 3.3 (a), it is clear that the resolution of the GS is lower. One should notice the bumps in the time frequency plan of the GS, which are located at the position of the Gabor coefficients. The reasons for these bumps and the lower resolution are that the GS does

not make the correct interpolation of the Gabor coefficients to be a true FS. This point has been explained in note 10. Because the number of coefficients in the frequency direction is $N=16$ for base 64, the distance between the first and second harmonic component of the call is approximately 4. We can therefore expect cross-terms between the harmonics when the order of the GS reach 4. This is verified from Figure 3.5 (a).

If our criterion for an optimal order is that the time frequency plan must not contain cross-terms between the harmonic components, the following orders are optimal for each base:

Order \ Base	Base 64	Base 128	Base 256
Optimal order D	3	8	10>D

Table 3.1 Optimal GS order for a Bat call.

The Gabor spectrogram can be seen as an attempt to remove the window distortion of the FS. The FS is obtained by squaring the modulus of the Fourier coefficients. If these coefficients were instead used as input to the GS, more information about the signal could be extracted! The best improvement which can be made on Figure 3.3(a) is Figure 3.4(d). Figure 5.3(b) can be improved to Figure 3.6(d), and Figure 3.3(c) can improved to Figure 3.6(i). It is clear that the Fourier spectrogram using base 128 has the best simultaneous resolution in time and frequency for this particular signal, and this base will therefore be best for a GS of a bat call.

The last analysis has been made using the WVD. It can be seen from Figure 3.7, that the WVD is not completely aliasing free. This indicate that the preprocessing has not been capable of removing the overlapping images in the discrete implementation .

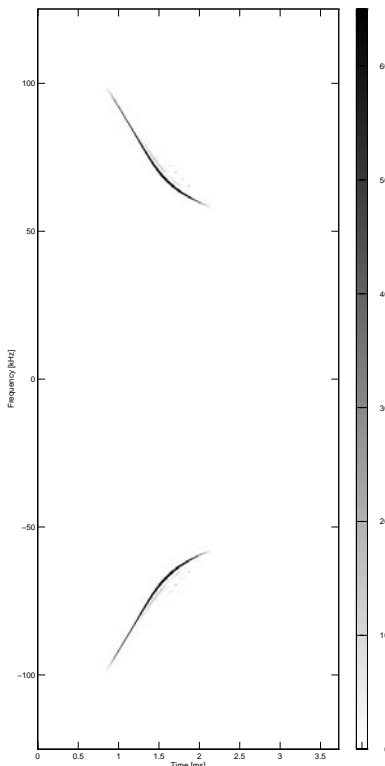


Figure 3.7 Windowed(512) Wigner-Ville distribution of the Bat Call.

3.2 Blackbird

Another interesting research area is the analysis of bird songs. This example has been inspired by a book of Poul Bondesen [Bondesen 86], which contains a detailed description of 150 european birds with spectrograms of their songs. Now, these spectrograms are in fact sonograms which are predecessors of the Fourier spectrogram. They are made by a mechanical equipment, and the resolution is much lower than the FS. So it has been an enormous task to make the 150 sonograms that the book contains.

The purpose of this little example is to demonstrate the improvement which can be reached using the Gabor Spectrogram in analysing bird songs. The example will use a song sequence from a blackbird. The sequence contains 23000 samples and is sampled at 11 kHz. The data have been obtained from the CD enclosed in the book[Génsbøl 96], and are illustrated in Figure 3.8.

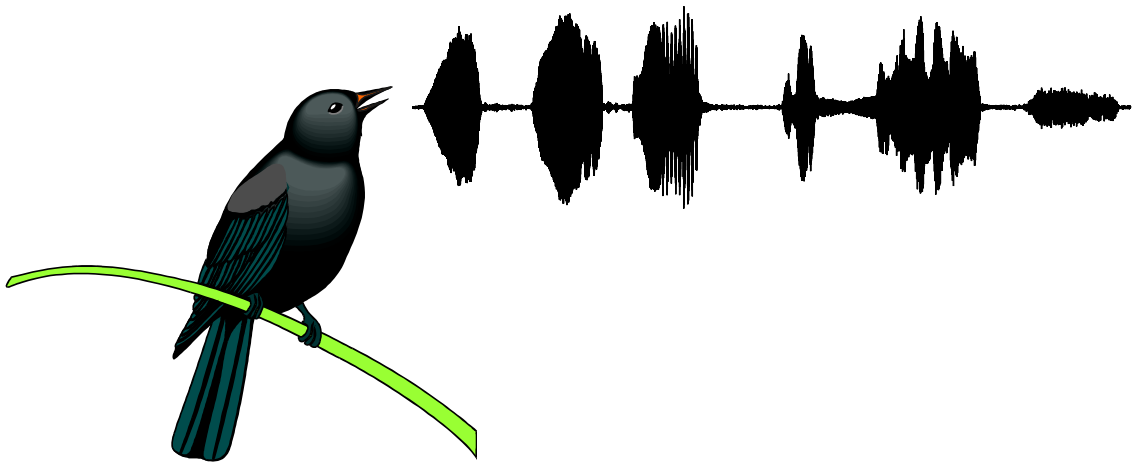


Figure 3.8 A blackbird producing Data.

The Gabor coefficients are calculated using base 256, and the Gabor Spectrogram has been calculated for an order up to 6. The result is illustrated in Figure 3.9 and Figure 3.10.

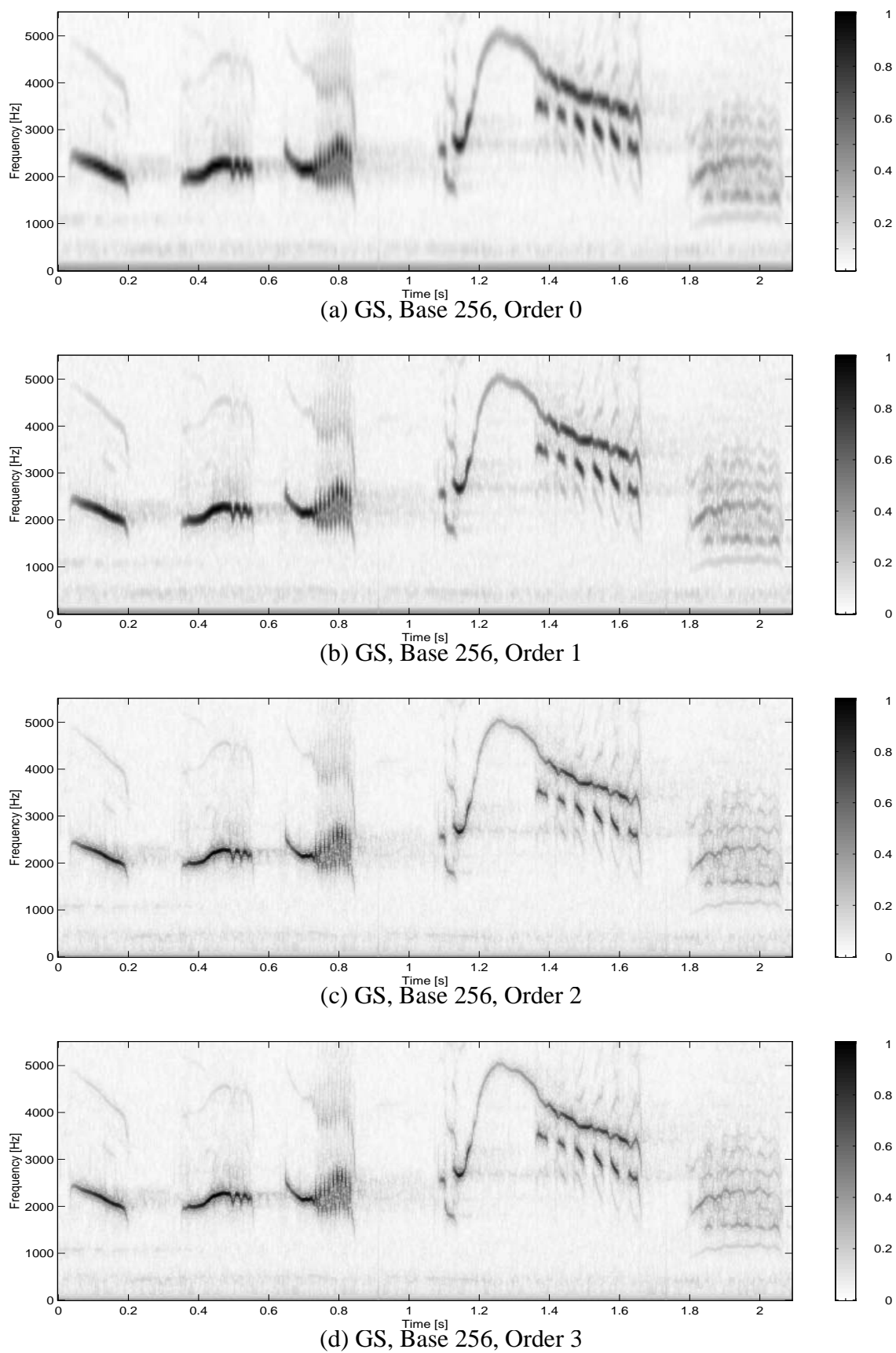


Figure 3.9 Gabor spectrogram of the blackbird signal, order=0:3

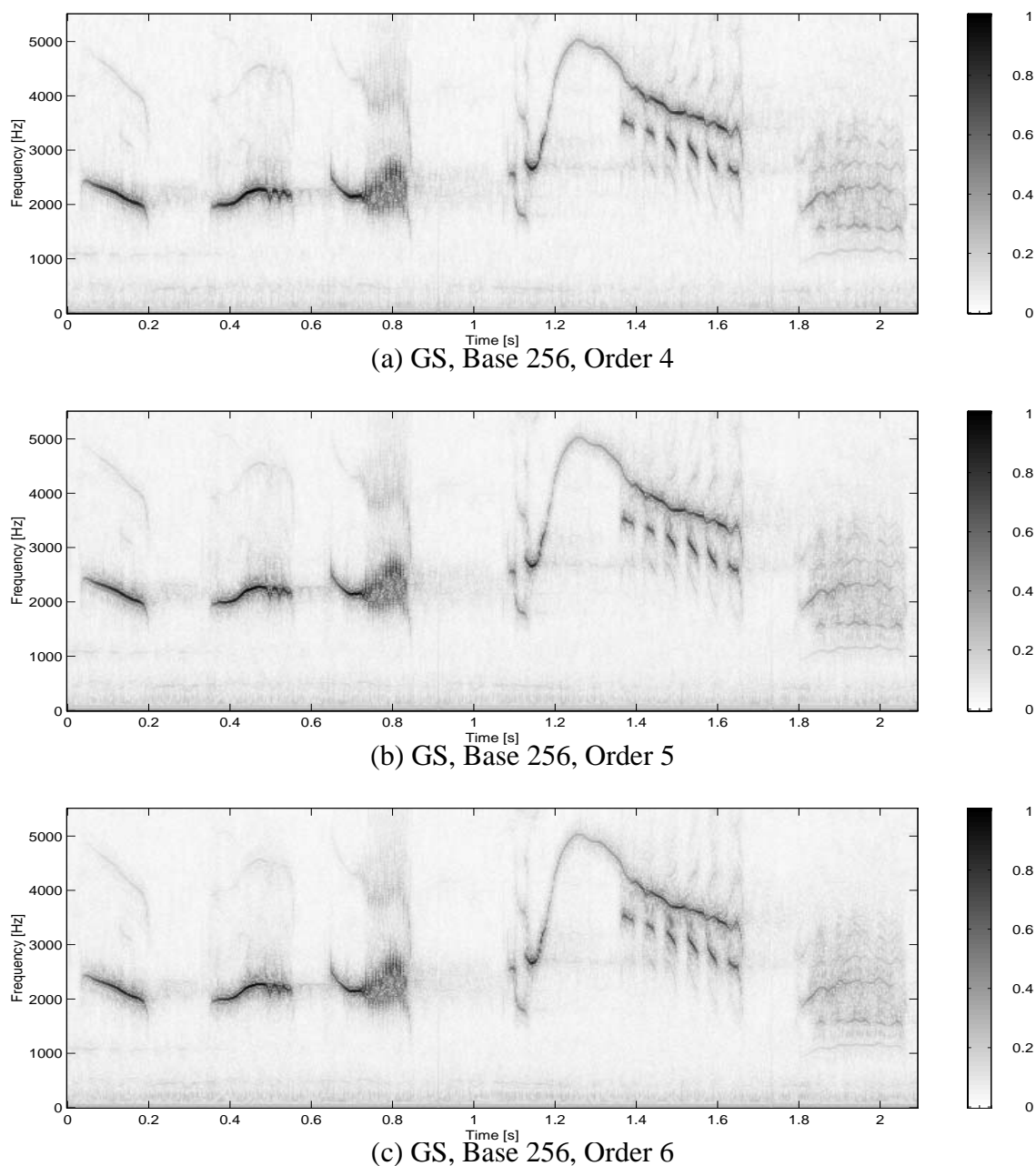


Figure 3.10 Gabor spectrogram of the blackbird signal, order=4:6

An optimal order for the GS analysing a song from a blackbird can e.g. be found by inspecting the area in the plan $(t, \omega) = (0.5\text{s}, 2000\text{Hz})$. This area has the best resolution, when the order is 3.

The last example is different from the previous two examples, because it is a man-made signal.

3.3 In-bore Doppler Radar System

An In-Bore velocity Analyzing System is a radar system capable of measuring the velocity and/or displacement of a projectile inside the gun barrel, and possibly a few meters after the muzzle exit [TERMA 92].

The microwave radiation from the antenna transmitting unit is focussed onto a mirror placed on the bore axis. The radiation is reflected down into the barrel. Some of the radiation is reflected back along the same path to the antenna receiving unit. When the projectile starts moving, the reflected radiation will contain a Doppler frequency shift proportional to the projectile velocity. The measurement continues until the projectile hits the mirror. The measurement setup is illustrated in Figure 3.11.

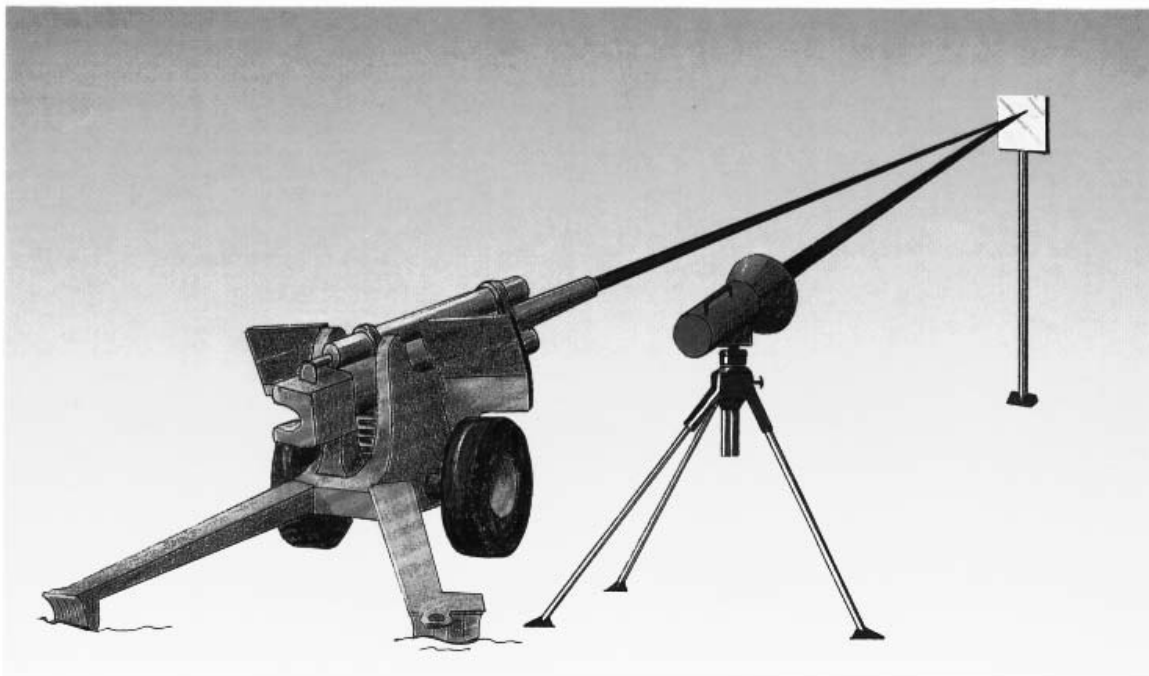


Figure 3.11 Measurement setup.

The velocity measurement can be integrated to give the displacement versus time, or differentiated to give the acceleration versus time. The instantaneous Doppler frequency f_d , and the projectile velocity v is related by means of the formula:

$$v = f_d \cdot \frac{c}{2f_{Tx}} \cdot M_c \quad (3.1)$$

where c is the speed of light ($2,997e8\text{ m/s}$), f_{Tx} is the frequency of the Doppler radar antenna and M_c is a Mode correction factor. This factor is used in order to take into account the difference between the radar wave length inside the barrel and the free-space wave length. It can be found by:

$$M_c = \frac{\lambda_{In-Bore}}{\lambda_{free-space}} = \frac{1}{\sqrt{1 - \left(\frac{1,841 \cdot c}{\pi \cdot d \cdot f_{Tx}}\right)^2}} \quad (3.2)$$

where d is the bore calibre (mm).

The Doppler signal used in this example has been provided by TERMA Elektronik AS, Aarhus, Denmark. The signal contains 15k samples and is sampled with 242,13 kHz. The radar frequency f_{Tx} is 35 GHz and the bore calibre is 115 mm. The corresponding correcting factor M_c can be found from equation (3.2) to 1,000. The final formula to calculate the velocity from the Doppler frequency is:

$$v = f_d \cdot \frac{2,997e8}{2 \cdot 35e9} \cdot 1,000 = f_d \cdot 4,281e-3 \quad (3.3)$$

The signal is illustrated in Figure 3.12

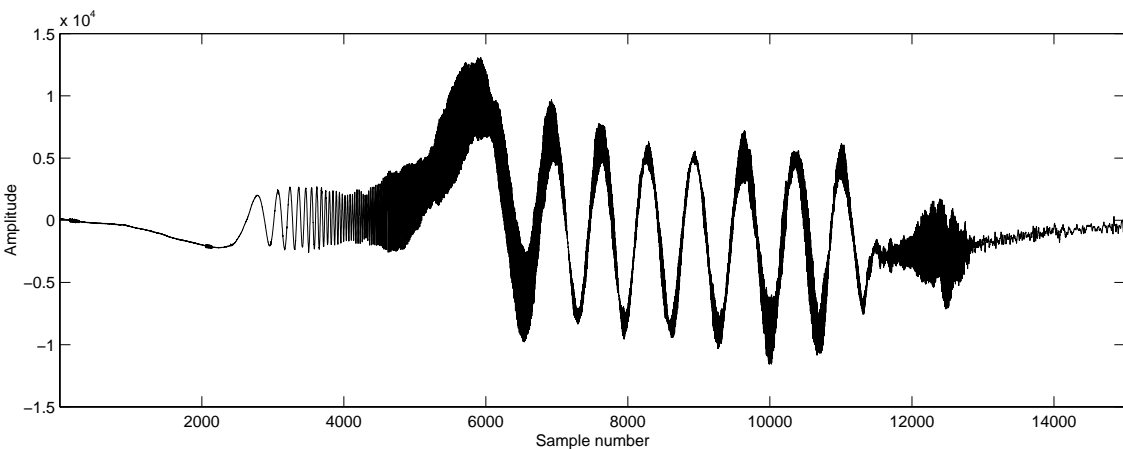


Figure 3.12 Radar signal.

The signal shows the acceleration of the projectile in the barrel until it hits the mirror. The low frequency modulation of the signal is caused by the gun recoil. From this, information about the gun recoil velocity and recoil displacement can be found. The “noise” component about $n = 12000$ is the reflection from the pulverized mirror.

The Gabor spectrogram is calculated using base 256. The signal has been divided into two parts, in order to do the calculation in parallel. Unfortunately, no common overlap were used, which has caused a small error in the intersection ($t=31$ ms).

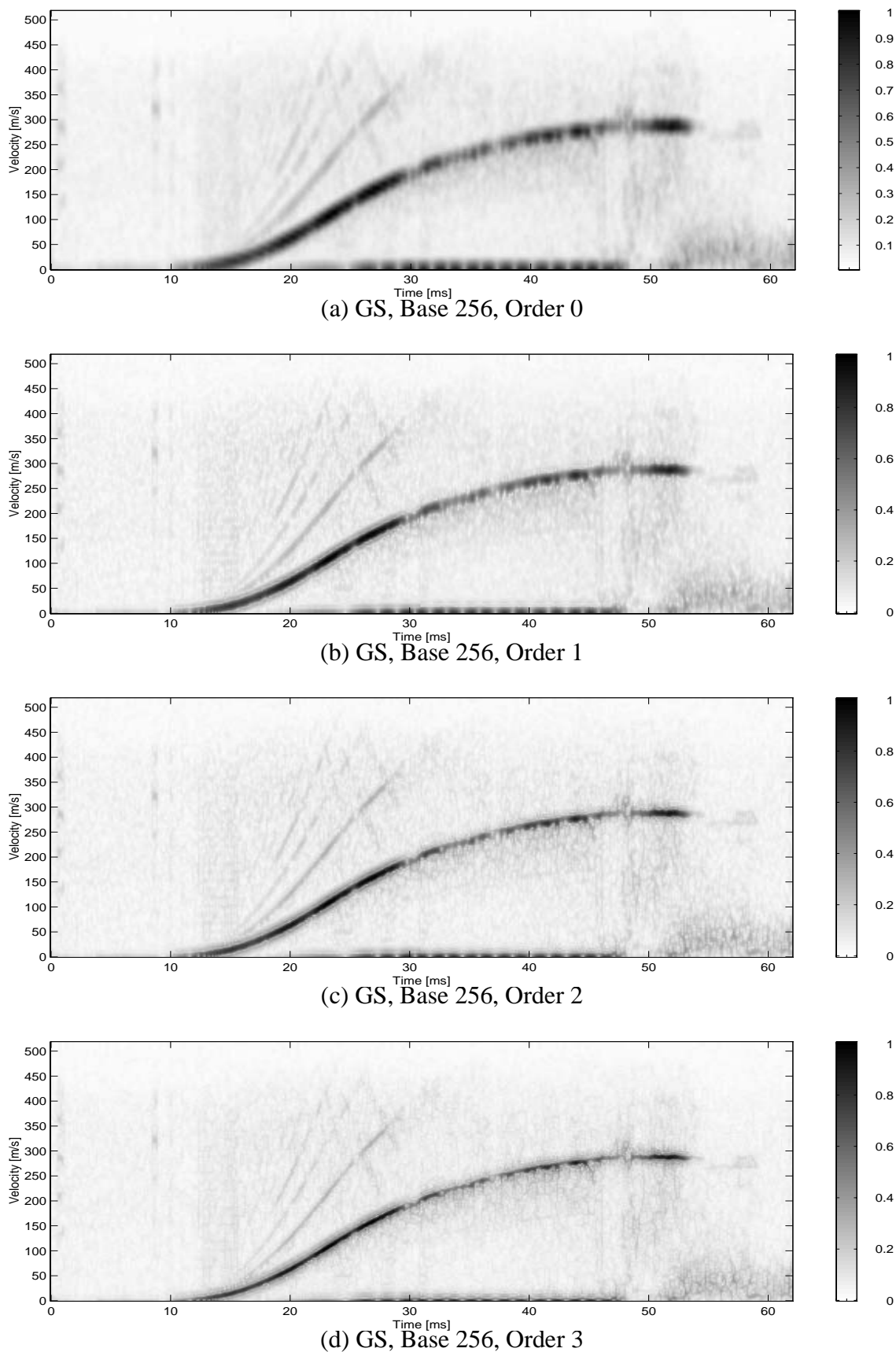


Figure 3.13 Gabor Spectrogram of Radar signal, Order 0:3

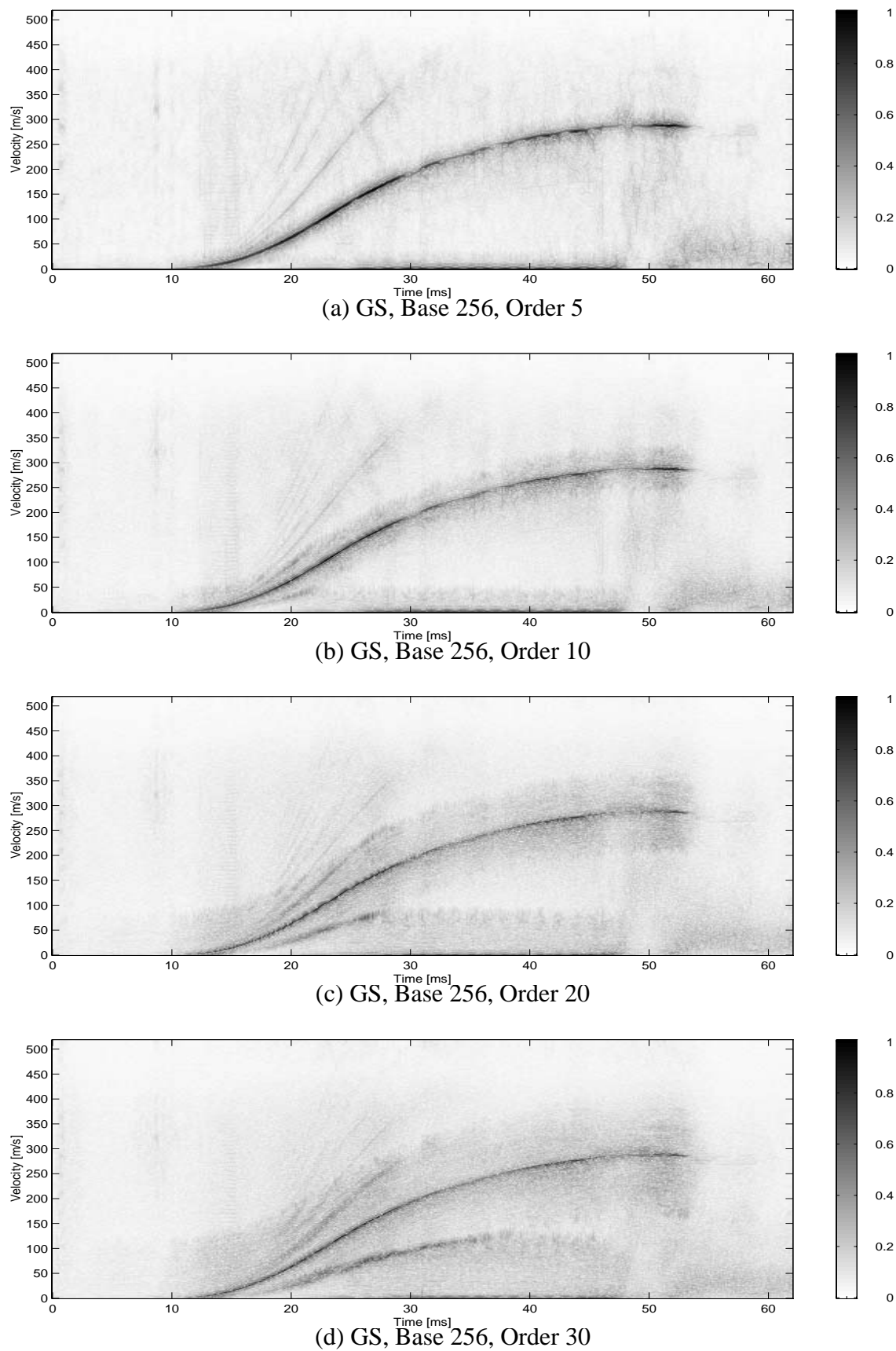


Figure 3.14 Gabor Spectrogram of Radar signal, Order 5,10,20 and 30.

It is clearly shown that an improvement can also be obtained in analyzing Doppler signals. But another problem is whether the GS can be calculated fast enough for this application. As the signal structure is well known (not like different birds), it might be possible to develop a more special tool for this particular signal, instead of using a very general tool like GS or FS.

$$X(\omega) = \int x(\tau) e^{-j\omega\tau} d\tau$$



Appendix

Appendix 1

The Wigner-Ville Distribution

1.1 Derivation of the Wigner-Ville distribution

The following derivation of the Wigner-Ville distributions is based on the original article of J. Ville [Ville 48]. It is the purpose of the derivations, to specify a normalized energy distribution $p(t, f)$ of a continuous signal. It is desirable that this energy distribution has the same properties as a probability distribution. The only connection between the distribution and the signal are the marginal distributions given by:

$$x^*(t) x(t) = \int p(t, f) df \quad X^*(f) X(f) = \int p(t, f) dt \quad (\text{A1.1})$$

The functions $x(t)$ and $X(f)$ are dependent through the Fourier transform. Instead of expressing the distribution directly, it is suitable to express it through the characteristic function for $p(t, f)$, which is defined as the expectation of $e^{j(ut + vf)}$:

$$F(u, v) = \iint_{t, f} e^{j(ut + vf)} p(t, f) df dt \quad (\text{A1.2})$$

To get the unknown distribution $p(t, f)$ substituted with one of the marginal distributions, the exponential function is expressed as a power series

$$\begin{aligned} F(u, v) &= \iint \sum_{n=0}^{\infty} \frac{j^n}{n!} (ut + vf)^n p(t, f) df dt \\ &= \sum_{n=0}^{\infty} \frac{j^n}{n!} \sum_{\{(a, b) | a+b=n\}} u^a v^b \iint t^a f^b p(t, f) dt df \end{aligned} \quad (\text{A1.3})$$

where the second sum is the set of positive power for **a** and **b**. The characteristic function is now expressed as a double sum of the following terms:

$$\iint t^a f^b p(t, f) dt df \quad (\text{A1.4})$$

Either **t** or **f** can now be chosen to be evaluated together with the distribution $p(t, f)$. If the variable **f** is chosen, the following expression has to be solved in order to include the marginal distribution.

$$\int f^b p(t, f) df \quad (\text{A1.5})$$

This may be done by a generalisation of the Parseval theory.

$$\begin{aligned}
\int X^*(f) f^b X(f) df &= \iint x^*(-t_1) e^{-j2\pi ft_1} dt_1 \int \left(\frac{1}{j2\pi} \cdot \frac{\partial}{\partial t_2} \right)^b x(t_2) e^{-j2\pi ft_2} dt_2 df \\
&= \iint x^*(t_1) \left(\frac{1}{j2\pi} \cdot \frac{\partial}{\partial t_2} \right)^b x(t_2) \int e^{j2\pi f(t_1 - t_2)} df dt_2 dt_1 \\
&= \iint x^*(t_1) \left(\frac{1}{j2\pi} \cdot \frac{\partial}{\partial t_2} \right)^b x(t_2) \delta(t_1 - t_2) dt_2 dt_1 \\
&= \int x^*(t) \left(\frac{1}{j2\pi} \cdot \frac{\partial}{\partial t} \right)^b x(t) dt
\end{aligned} \tag{A1.6}$$

Using this result, it will be possible to include the marginal distribution:

$$\begin{aligned}
\iint f^b p(t, f) df dt &= \int X(f) f^b X^*(f) df = \int x^*(t) \left(\frac{1}{j2\pi} \cdot \frac{\partial}{\partial t} \right)^b x(t) dt \Leftrightarrow \\
\int f^b p(t, f) df &= x^*(t) \left(\frac{1}{j2\pi} \cdot \frac{\partial}{\partial t} \right)^b x(t)
\end{aligned} \tag{A1.7}$$

Then the variable f in the power series has to be substituted for the differential operator.

$$\begin{aligned}
F(u, v) &= \sum_{n=0}^{\infty} \frac{1}{n!} \sum_{\{(a, b) | a+b=n\}} u^a v^b \int t^a \int f^b p(t, f) df dt \\
&= \sum_{n=0}^{\infty} \frac{1}{n!} \sum_{\{(a, b) | a+b=n\}} u^a v^b \int t^a x^*(t) \left(\frac{1}{j2\pi} \cdot \frac{\partial}{\partial t} \right)^b x(t) dt \\
&= \int x^*(t) \sum_{n=0}^{\infty} \frac{1}{n!} \sum_{\{(a, b) | a+b=n\}} (ut)^a \left(\frac{v}{j2\pi} \cdot \frac{\partial}{\partial t} \right)^b x(t) dt \\
&= \int x^*(t) e^{j\left(ut + \frac{v}{j2\pi} \cdot \frac{\partial}{\partial t}\right)} x(t) dt
\end{aligned} \tag{A1.8}$$

In order to examine the properties of the exponential operator, a more general example will be analysed. An operator **f** contains two operators **A** and **B**:

$$f(x) = e^{Ax} e^{Bx} \tag{A1.9}$$

The derivation of **f** with respect to the usual parameter **x** will be

$$\begin{aligned}
f'(x) &= Ae^{Ax} e^{Bx} + e^{Ax} Be^{Bx} \\
&= Ae^{Ax} e^{Bx} + e^{Ax} Be^{-Ax} e^{Ax} e^{Bx} \\
&= (A + e^{Ax} Be^{-Ax}) f(x)
\end{aligned} \tag{A1.10}$$

The next step is to express the term $e^{Ax} Be^{-Ax}$. This can be done by the cummulator between the last two operators:

$$[B, e^{-Ax}] = Be^{-Ax} - e^{-Ax} B \Rightarrow Be^{-Ax} = [B, e^{-Ax}] + e^{-Ax} I \tag{A1.11}$$

The cummulator can be expressed as:

$$\begin{aligned}
[B, e^{-Ax}] &= \left[B, \sum_{n=0}^{\infty} \frac{1}{n!} (-Ax)^n \right] \\
&= \sum_{n=0}^{\infty} \frac{1}{n!} (-x)^n [B, A^n] \\
&= \sum_{n=0}^{\infty} \frac{1}{n!} (-x)^n nA^{n-1} [B, A] \\
&= - \sum_{n=0}^{\infty} \left(\frac{1}{(n-1)!} (-x)^{n-1} A^{n-1} \right) x [B, A] \\
&= -\exp(-Ax) [B, A] x
\end{aligned} \tag{A1.12}$$

This is based on the assumption that $[A^N, [A, B]] = 0$ for all N . Now it is possible to use the following conversion $[B, A^N] = NA^{N-1} [B, A]$. This can be seen by the following derivations:

$$\begin{aligned}
[A^N, [A, B]] &= 0 \Leftrightarrow \\
[A^N, [A, B]] &= A^N (AB - BA) - (AB - BA) A^N \\
&= A^{N+1} B - A^N BA - ABA^N + BA^{N+1} = 0 \\
&\Leftrightarrow \\
BA^{N+1} &= A^N BA + ABA^N - A^{N+1} B
\end{aligned} \tag{A1.13}$$

Using this identity, the conversion can be made:

$$\begin{aligned}
[B, A^N] &= \underline{BA^N} - A^N B \\
&= (A^{N-1} \underline{BA} + \underline{ABA^{N-1}} - A^N B) - A^N B \\
&= A^{N-1} BA + A (A^{N-2} \underline{BA} + \underline{ABA^{N-2}} - A^{N-1} B) - 2A^N B \\
&= \dots \dots \dots \\
&= NA^{N-1} BA - NA^{N-1} AB \\
&= NA^{N-1} [B, A]
\end{aligned} \tag{A1.14}$$

The underlined terms is substituted for the parenthesis in subsequent line.
It is now possible to express the term $e^{Ax} B e^{-Ax}$:

$$\begin{aligned}
e^{Ax} B e^{-Ax} &= e^{Ax} [B, e^{-Ax}] + e^{Ax} e^{-Ax} B \\
&= e^{Ax} (-e^{-Ax} [B, A]) + B \\
&= B - [B, A] x
\end{aligned} \tag{A1.15}$$

This result can be used to simplify the derivation of $f(x)$:

$$\begin{aligned} f'(t) &= (A + e^{Ax} Be^{-Ax})f(x) \\ &= (A + B - [B, A]x)f(x) \end{aligned} \quad (\text{A1.16})$$

This differential equation can be solved by the following steps:

$$\begin{aligned} \frac{f'(x)}{f(x)} &= A + B - [B, A]x \Leftrightarrow \\ \int \frac{f'(x)}{f(x)} dx &= \ln(f(x)) = \int ((A + B) - [B, A]x) dx \\ &= (A + B)x - [B, A]\frac{x^2}{2} \\ &\Leftrightarrow \\ f(x) &= e^{(A+B)x} \cdot e^{-\frac{1}{2}[B,A]x^2} = e^{Ax} e^{Bx} \\ f(1) &= e^{A+B} \cdot e^{-\frac{1}{2}[B,A]} = e^A e^B \\ &\Leftrightarrow \\ e^{A+B} &= e^A e^B e^{-\frac{1}{2}[B,A]} \end{aligned} \quad (\text{A1.17})$$

This result is the same as the one obtained by Wilcox [Wilcox 67, formel 4.15] following a different approach. This derivation has shown us that an exponential function containing two operators can be divided into two exponential functions multiplied by an exponential function of the cummulator of the two operators. How this might be used in the derivation of the Wigner-Ville distribution is the topic for the rest of this appendix. Inserting the expression for the A and B operator, we get:

$$\begin{aligned} A &= jut \quad B = j\frac{v}{j2\pi} \cdot \frac{\partial}{\partial t} \\ [B, A]x(t) &= (BA - AB)x(t) = j\frac{v}{j2\pi} \cdot \frac{\partial}{\partial t} jut \cdot x(t) - jut j\frac{v}{j2\pi} \cdot \frac{\partial}{\partial t} x(t) \\ &= -\frac{vu}{j2\pi}(x(t) + tx'(t)) + \frac{vu}{j2\pi}tx'(t) \\ &= -\frac{vu}{j2\pi}x(t) \\ &\Leftrightarrow \\ e^{j\left(ut + \frac{v}{j2\pi} \cdot \frac{\partial}{\partial t}\right)} &= e^{jut} \cdot e^{j\frac{v}{j2\pi} \cdot \frac{\partial}{\partial t}} \cdot e^{-\frac{vu}{j4\pi}} \end{aligned} \quad (\text{A1.18})$$

As this exponential operator is applied on $x(t)$, we are able to find the following result:

$$\begin{aligned}
e^{jut} \cdot e^{j\frac{v}{j2\pi} \cdot \frac{\partial}{\partial t}} \cdot e^{-\frac{vu}{j4\pi}} x(t) &= e^{ju\left(t + \frac{v}{4\pi}\right)} \cdot \int X(f) \sum_{n=0}^{\infty} \frac{1}{n!} \left(\frac{v}{j2\pi} \cdot \frac{\partial}{\partial t}\right)^n e^{jf2\pi t} df \\
&= e^{ju\left(t + \frac{v}{4\pi}\right)} \cdot \int X(f) \sum_{n=0}^{\infty} \frac{1}{n!} \left(\frac{v}{j2\pi} \cdot jf2\pi\right)^n e^{jf2\pi t} df \quad (\text{A1.19}) \\
&= e^{ju\left(t + \frac{v}{4\pi}\right)} \cdot \int X(f) \exp\left(jf2\pi\left(t + \frac{v}{2\pi}\right)\right) df \\
&= e^{ju\left(t + \frac{v}{4\pi}\right)} x\left(t + \frac{v}{2\pi}\right)
\end{aligned}$$

This can be substituted in the formula for the characteristic function:

$$\begin{aligned}
F(u, v) &= \int x^*(t) e^{j\left(ut + \frac{v}{j2\pi} \cdot \frac{\partial}{\partial t}\right)} x(t) dt \\
&= \int x^*(t) e^{jut} \cdot e^{j\frac{v}{j2\pi} \cdot \frac{\partial}{\partial t}} \cdot e^{-\frac{vu}{j4\pi}} x(t) dt \\
&= \int x^*(t) e^{ju\left(t + \frac{v}{4\pi}\right)} x\left(t + \frac{v}{2\pi}\right) dt \\
&= \int x^*\left(t - \frac{v}{4\pi}\right) x\left(t + \frac{v}{4\pi}\right) e^{jut} dt \quad (\text{A1.20})
\end{aligned}$$

The characteristic function is a simple function of the signal $x(t)$, and the energy distribution can now be recovered by a 2D Fourier transformation of $F(u, v)$:

$$\begin{aligned}
F(u, v) &= \iint e^{j(ut + vf)} p(t, f) df dt = \int x^*\left(t - \frac{v}{4\pi}\right) x\left(t + \frac{v}{4\pi}\right) e^{jut} dt \\
p(t, f) &= \iint F(u, v) e^{-j(ut + vf)} du dv \\
&= \iiint x^*\left(t - \frac{v}{4\pi}\right) x\left(t + \frac{v}{4\pi}\right) e^{jut} dt e^{-j(ut + vf)} du dv \\
&= \int x^*\left(t - \frac{v}{4\pi}\right) x\left(t + \frac{v}{4\pi}\right) e^{-jvf} dv \\
&= \int x^*\left(t - \frac{v}{2}\right) x\left(t + \frac{v}{2}\right) e^{-jvf2\pi} dv \\
&\Leftrightarrow \\
WVD(t, \omega) &= \int x^*\left(t - \frac{\tau}{2}\right) x\left(t + \frac{\tau}{2}\right) e^{-j\tau\omega} d\tau
\end{aligned} \quad (\text{A1.21})$$

1.2 Properties of the Wigner Ville Distribution

In this section, some fundamental properties of the Wigner-Ville distribution will be derived. Others can be found in three articles from T.A.C.M Claasen and W.F.G.Mecklenbrauker [Claasen 80a-c].

Shifting property.

The shifting property indicates the result of a time or frequency shift of the signal. A time shift of the signal will give an equivalent of the WVD:

$$\begin{aligned} x(t) &= y(t+T) \\ \text{WVD}_x(t, \omega) &= \int x(t+\tau/2) x^*(t-\tau/2) e^{-j\omega\tau} d\tau \\ &= \int y(t+T+\tau/2) y^*(t+T-\tau/2) e^{-j\omega\tau} d\tau \\ &= \text{WVD}_y(t+T, \omega) \end{aligned} \quad (\text{A1.22})$$

The same is valid for the frequency dimension:

$$\begin{aligned} x(t) &= y(t) e^{j\Omega t} \\ \text{WVD}_x(t, \omega) &= \int x(t+\tau/2) x^*(t-\tau/2) e^{-j\omega\tau} d\tau \\ &= \int y(t+\tau/2) e^{j\Omega(t+\tau/2)} y^*(t-\tau/2) e^{-j\Omega(t-\tau/2)} e^{-j\omega\tau} d\tau \\ &= \int y(t+\tau/2) y^*(t-\tau/2) e^{-j\tau(\omega-\Omega)} d\tau \\ &= \text{WVD}_y(t, \omega-\Omega) \end{aligned} \quad (\text{A1.23})$$

Marginal distribution for the Wigner-Ville distribution.

The time marginal distribution can be found by integrating Dirac the WVD over the frequency axis:

$$\begin{aligned} \frac{1}{2\pi} \int \text{WVD}_{x,y}(t, \omega) d\omega &= \frac{1}{2\pi} \int \int x(t+\tau/2) y^*(t-\tau/2) e^{-j\omega\tau} d\omega d\tau \\ &= \int x(t+\tau/2) y^*(t-\tau/2) \frac{1}{2\pi} \int e^{-j\omega\tau} d\omega d\tau \\ &= \int x(t+\tau/2) y^*(t-\tau/2) \delta(\tau) d\tau \\ &= x(t) y^*(t) \end{aligned} \quad (\text{A1.24})$$

where the Dirac function [Dirac 30] came from the Fourier transform of the Dirac function:

$$\int \delta(t) e^{-j\omega t} dt = 1 \Leftrightarrow \delta(t) = \frac{1}{2\pi} \int e^{j\omega t} d\omega \quad (\text{A1.25})$$

The inversion formula is correctly applied in solution of many problems, regardless it is not easy to accept the validity of the inversion formula, because the integral has no meaning [Papoulis 62, pp5]. The same relation exists in the frequency domain:

$$\frac{1}{2\pi} \int \delta(\omega) e^{j\omega t} d\omega = 1 \Leftrightarrow \delta(\omega) = \int e^{-j\omega t} dt \quad (\text{A1.26})$$

When the two signals $x(t)$ and $y(t)$ are equal, the marginal energy is:

$$\frac{1}{2\pi} \int WVD_x(t, \omega) d\omega = x(t)x^*(t) = |x(t)|^2 \quad (\text{A1.27})$$

The frequency marginal distribution can be found by integrating the WVD over the time axis:

$$\begin{aligned} \int WVD_{X,Y}(t, \omega) dt &= \frac{1}{2\pi} \iint X(\omega + \tau/2) Y^*(\omega - \tau/2) e^{j\tau t} d\tau dt \\ &= \int X(\omega + \tau/2) Y^*(\omega - \tau/2) \frac{1}{2\pi} \int e^{j\tau t} dt d\tau \\ &= \int X(\omega + \tau/2) Y^*(\omega - \tau/2) \delta(\tau) d\tau \\ &= X(\omega) Y^*(\omega) \end{aligned} \quad (\text{A1.28})$$

When the two signals $x(t)$ and $y(t)$ are equal, the marginal energy is:

$$\int WVD_X(t, \omega) dt = X(\omega) X^*(\omega) = |X(\omega)|^2 \quad (\text{A1.29})$$

Fourier approach

The WVD is defined from the time signal, but an analogous definition can be made from the Fourier transform of the signal.

$$\begin{aligned} WVD_x(t, \omega) &= \int x(t + \tau/2) x^*(t - \tau/2) e^{-j\omega\tau} d\tau \\ &= \int e^{-j\omega\tau} \frac{1}{2\pi} \int X(\omega_1) e^{j(t + \tau/2)\omega_1} d\omega_1 \frac{1}{2\pi} \int X^*(\omega_2) e^{-j(t - \tau/2)\omega_2} d\omega_2 d\tau \\ &= \frac{1}{2\pi} \iint X(\omega_1) X^*(\omega_2) e^{jt(\omega_1 - \omega_2)} \frac{1}{2\pi} \int e^{j\tau \left(\frac{\omega_1 + \omega_2}{2} - \omega \right)} d\tau d\omega_1 d\omega_2 \\ &= \frac{1}{2\pi} \iint X(\omega_1) X^*(\omega_2) e^{jt(\omega_1 - \omega_2)} \delta \left(\frac{\omega_1 + \omega_2}{2} - \omega \right) d\omega_1 d\omega_2 \\ &= \frac{1}{2\pi} \int X(\omega_1) X^*(2\omega - \omega_1) e^{jt(2\omega_1 - 2\omega)} d\omega_1 \quad , \omega_1 = \frac{\tau}{2} + \omega \\ &= \frac{1}{2\pi} \int X(\omega + \tau/2) X^*(\omega - \tau/2) e^{j\tau t} d\tau \end{aligned} \quad (\text{A1.30})$$

Addition, product and convolution property

The WVD representation of a signal x containing the addition of two signals g and h is found by the following derivation:

$$\begin{aligned} WVD_x(t, \omega) &= \int x(t + \tau/2) x^*(t - \tau/2) e^{-j\omega\tau} d\tau \\ &= \int (g(t + \tau/2) + h(t + \tau/2)) (g^*(t - \tau/2) + h^*(t - \tau/2)) e^{-j\omega\tau} d\tau \\ &= \int (g(t + \tau/2) g^*(t - \tau/2) + g(t + \tau/2) h^*(t - \tau/2) \\ &\quad + h(t + \tau/2) g^*(t - \tau/2) + h(t + \tau/2) h^*(t - \tau/2)) e^{-j\omega\tau} d\tau \\ &= WVD_g(t, \omega) + WVD_h(t, \omega) + WVD_{g,h}(t, \omega) + WVD_{h,g}(t, \omega) \end{aligned} \quad (\text{A1.31})$$

The variables in the cross Wigner-Ville can be exchanged:

$$\begin{aligned}
WVD_{h,g}(t, \omega) &= \int h(t + \tau/2) g^*(t - \tau/2) e^{-j\omega\tau} d\tau \\
&= \left(\int h^*(t + \tau/2) g(t - \tau/2) e^{j\omega\tau} d\tau \right)^* \\
&= \left(\int h^*(t - \tau/2) g(t + \tau/2) e^{-j\omega\tau} d\tau \right)^* \\
&= WVD_{g,h}^*(t, \omega)
\end{aligned} \tag{A1.32}$$

Using this property, two cross-terms can be compounded into one real cross-term:

$$WVD_x(t, \omega) = WVD_g(t, \omega) + WVD_h(t, \omega) + 2 \cdot \operatorname{Re} \{ WVD_{g,h}(t, \omega) \} \tag{A1.33}$$

The properties express the dependencies between the WVD of two signals that are multiplied together in time.

$$\begin{aligned}
x(t) &= h(t) \cdot g(t) \quad \Leftrightarrow \\
WVD_x(t, \omega) &= \int x(t + \tau/2) x^*(t - \tau/2) e^{-j\omega\tau} d\tau \\
&= \int h(t + \tau/2) g(t + \tau/2) h^*(t - \tau/2) g^*(t - \tau/2) e^{-j\omega\tau} d\tau \\
&= \int h(t + \tau/2) h^*(t - \tau/2) g(t + \tau/2) g^*(t - \tau/2) e^{-j\omega\tau} d\tau \\
&\quad g(t + \tau/2) g^*(t - \tau/2) = \frac{1}{2\pi} \int WV_g(t, \omega) e^{j\omega\tau} d\omega \\
&= \int h(t + \tau/2) h^*(t - \tau/2) \frac{1}{2\pi} \int WV_g(t, \omega') e^{j\omega'\tau} d\omega' e^{-j\omega\tau} d\tau \\
&= \frac{1}{2\pi} \int WVD_g(t, \omega') \int h(t + \tau/2) h^*(t - \tau/2) e^{-j\tau(\omega - \omega')} d\tau d\omega' \\
&= \frac{1}{2\pi} \int WVD_g(t, \omega') WVD_h(t, \omega - \omega') d\omega' \\
&= WVD_g(t, \omega) \otimes_\omega WVD_h(t, \omega)
\end{aligned} \tag{A1.34}$$

In this derivation, the following property is used. The time marginal distribution can be seen to be a special case of this.

$$\begin{aligned}
\frac{1}{2\pi} \int WVD_x(t, \omega) e^{j\omega\tau_1} d\omega &= \frac{1}{2\pi} \int \int x(t + \tau/2) x^*(t - \tau/2) e^{-j\omega\tau} d\tau e^{j\omega\tau_1} d\omega \\
&= \int x(t + \tau/2) x^*(t - \tau/2) \frac{1}{2\pi} \int e^{j\omega(\tau_1 - \tau)} d\omega d\tau \\
&= \int x(t + \tau/2) x^*(t - \tau/2) \delta(\tau_1 - \tau) d\tau \\
&= x(t + \tau_1/2) x^*(t - \tau_1/2)
\end{aligned} \tag{A1.35}$$

When two signals are convoluted in time, the relation between them in the WVD space can be found from the Fourier definition of WVD:

$$\begin{aligned}
x(t) &= h(t) \otimes g(t) \Rightarrow X(\omega) = H(\omega) G(\omega) \quad \Leftrightarrow \\
WVD_X(t, \omega) &= \frac{1}{2\pi} \int X(\omega + \tau/2) X(\omega - \tau/2) e^{j t \tau} d\tau \\
&= \frac{1}{2\pi} \int H(\omega + \tau/2) G(\omega + \tau/2) H^*(\omega - \tau/2) G^*(\omega - \tau/2) e^{j t \tau} d\tau \\
&= \frac{1}{2\pi} \int H(\omega + \tau/2) H^*(\omega - \tau/2) G(\omega + \tau/2) G^*(\omega - \tau/2) e^{j t \tau} d\tau \\
G(\omega + \tau/2) G^*(\omega - \tau/2) &= \int WVD_g(t', \omega) e^{-j t' \tau} dt' \quad (\text{A1.36}) \\
&= \frac{1}{2\pi} \int H(\omega + \tau/2) H^*(\omega - \tau/2) \int WVD_g(t', \omega) e^{-j t' \tau} dt' e^{j t \tau} d\tau \\
&= \int WVD_g(t', \omega) \frac{1}{2\pi} \int H(\omega + \tau/2) H^*(\omega - \tau/2) e^{j \tau(t-t')} d\tau dt' \\
&= \int WVD_g(t', \omega) WVD_h(t - t', \omega) dt' \\
&= WVD_g(t, \omega) \otimes_t WVD_h(t, \omega)
\end{aligned}$$

In this derivation, the following property is used:

$$\begin{aligned}
\int WVD_g(t, \omega) e^{-j t \tau'} dt &= \int \frac{1}{2\pi} \int G(\omega + \tau/2) G^*(\omega - \tau/2) e^{j t \tau} d\tau e^{-j t \tau'} dt \\
&= \int G(\omega + \tau/2) G^*(\omega - \tau/2) \frac{1}{2\pi} \int e^{j t(\tau - \tau')} d\tau dt \quad (\text{A1.37}) \\
&= \int G(\omega + \tau/2) G^*(\omega - \tau/2) \delta(\tau - \tau') d\tau \\
&= G(\omega + \tau'/2) G^*(\omega - \tau'/2)
\end{aligned}$$

The frequency marginal distribution can be seen to be a special case of this.

Instantaneous frequency from the Wigner-Ville distribution.

The mean conditional frequency of the Wigner-Ville gives the derivation of the phase of the Fourier transform of the signal. This is the definition of the instantaneous frequency (IF) when the analytic signal is used. The IF is defined as:

$$\Omega_x = \frac{\frac{1}{2\pi} \int \omega WVD_x(t, \omega) d\omega}{\frac{1}{2\pi} \int WVD_x(t, \omega) d\omega} \quad (\text{A1.38})$$

This expression will be derived by calculating the denominator and nominator separately. The denominator expresses the marginal energy of the signal and is earlier found to be:

$$\frac{1}{2\pi} \int WVD_x(t, \omega) d\omega = x(t) x^*(t) = |x(t)|^2 \quad (\text{A1.39})$$

The nominator can be found to be:

$$\begin{aligned} \frac{1}{2\pi} \int \omega WVD_{x,y}(t, \omega) d\omega &= \frac{1}{2\pi} \int \omega \int e^{-j\omega\tau} x(t + \tau/2) y^*(t - \tau/2) d\tau d\omega \\ &= -\frac{1}{j} \frac{1}{2\pi} \int \int \frac{\partial}{\partial \tau} \{e^{-j\omega\tau}\} x(t + \tau/2) y^*(t - \tau/2) d\tau d\omega \end{aligned} \quad (\text{A1.40})$$

because $\delta e^{-j\omega\tau} = -\frac{1}{j} \frac{\partial}{\partial \tau} \{e^{-j\omega\tau}\}$. The τ integration can be done by partial integration.

$$\begin{aligned} \frac{1}{2\pi} \int \omega WVD_{x,y}(t, \omega) d\omega &= -\frac{1}{j} \frac{1}{2\pi} \int [e^{-j\omega\tau} x(t + \tau/2) y^*(t - \tau/2)]_{\tau=-\infty}^{\tau=\infty} d\omega \\ &\quad + \frac{1}{j} \frac{1}{2\pi} \int \int e^{-j\omega\tau} \frac{\partial}{\partial \tau} \{x(t + \tau/2) y^*(t - \tau/2)\} d\omega d\tau \\ &= -\frac{1}{j} [\delta(\tau) x(t + \tau/2) y^*(t - \tau/2)]_{\tau=-\infty}^{\tau=\infty} \\ &\quad + \frac{1}{j} \int \left(\frac{1}{2\pi} \int e^{-j\omega\tau} d\omega \right) \frac{\partial}{\partial \tau} \{x(t + \tau/2) y^*(t - \tau/2)\} d\tau \quad (\text{A1.41}) \\ &= \frac{1}{j} \int \delta(\tau) \left(\frac{dx(t + \tau/2)}{d(t + \tau/2)} \cdot \frac{\partial(t + \tau/2)}{\partial \tau} \cdot y^*(t - \tau/2) \right. \\ &\quad \left. + \frac{dy^*(t - \tau/2)}{d(t - \tau/2)} \cdot \frac{\partial(t - \tau/2)}{\partial \tau} \cdot x(t + \tau/2) \right) d\tau \\ &= \frac{1}{j2} (x'(t) y^*(t) - x(t) y'^*(t)) \end{aligned}$$

The derivation was initially with respect to τ , but as τ is set to zero, the derivation is now with respect to t . When the two signals $x(t)$ and $y(t)$ are equal, the mean value can be found to be:

$$\begin{aligned} \frac{1}{\pi} \int \omega WVD_x(t, \omega) d\omega &= \frac{1}{j2} ((x'(t) x^*(t) - x(t) x'^*(t))) \\ &= \frac{1}{j2} ((x'(t) x^*(t) - (x'(t) x^*(t))^*)) \\ &= \frac{1}{j2} (j2 \cdot \text{Im} \{ (x'(t) x^*(t)) \}) \\ &= \text{Im} \{ x'(t) x^*(t) \} \end{aligned} \quad (\text{A1.42})$$

An expression for the instantaneous frequency can now be stated:

$$\omega_x = \frac{\text{Im} \{ x'(t) x^*(t) \}}{|x(t)|^2} = \text{Im} \left\{ \frac{x'(t)}{x(t)} \right\}. \quad (\text{A1.43})$$

To see how the instantaneous frequency can be found from the Wigner-Ville distribution, the following test signal is used $x(t) = A(t) e^{j\Phi(t)}$:

$$\begin{aligned} \omega_x &= \text{Im} \left\{ \frac{x'(t)}{x(t)} \right\} = \text{Im} \left\{ \frac{A'(t) e^{j\Phi(t)} + A(t) j e^{j\Phi(t)} \Phi'(t)}{A(t) e^{j\Phi(t)}} \right\} \\ &= \text{Im} \left\{ \frac{A'(t)}{A(t)} + j \Phi'(t) \right\} = \Phi'(t) \end{aligned} \quad (\text{A1.44})$$

Lag constraint

In order to determine some constraints on the lags in the Wigner-Ville distributions, the following special Wigner-Ville distributions are used:

$$WVD_x(t, \omega) = \int x(t + a(\tau)) x^*(t + b(\tau)) e^{-j\omega c(\tau)} d\tau \quad (\text{A1.45})$$

The functions $a(\tau)$, $b(\tau)$ and $c(\tau)$ are assumed to be linear functions of τ . One wanted property of the Wigner-Ville distribution of a stationary signal is that the expected value of the distribution yields the power spectrum.

$$\begin{aligned} E\{WVD_x(t, \omega)\} &= \int E\{x(t + a(\tau)) x^*(t + b(\tau))\} e^{-j\omega c(\tau)} d\tau \\ &= \int E\{x(t) x^*(t + b(\tau) - a(\tau))\} e^{-j\omega c(\tau)} d\tau \\ &= \int R(a(\tau) - b(\tau)) e^{-j\omega c(\tau)} d\tau \end{aligned} \quad (\text{A1.46})$$

In order to get the power spectrum, the following constraint is valid for the functions:

$$|a(\tau) - b(\tau)| = c(\tau) \quad (\text{A1.47})$$

The function $c(\tau)$ can further be specified by considering the derivation of the exponential function in the IF properties.

$$\begin{aligned} -\frac{1}{j} \frac{\partial}{\partial \tau} \{e^{-j\omega c(\tau)}\} &= \frac{1}{j} \omega c'(\tau) e^{-j\omega c(\tau)} = \frac{1}{j} \omega e^{-j\omega c(\tau)} \\ &\Leftrightarrow \\ c'(\tau) &= 1 \\ &\Leftrightarrow \\ c(\tau) &= \tau + \text{const} \end{aligned} \quad (\text{A1.48})$$

The constant is set equal to zero, which is verified later.

For the special Wigner-Ville distribution with $\tau(\tau) = \tau$, the IF can be found from the derivations of the IF to be:

$$\begin{aligned} \Omega_f &= \frac{\frac{1}{j} \int \delta(\tau) \frac{dx^*(t + b(\tau))}{d(t + b(\tau))} \cdot \frac{\partial(t + b(\tau))}{\partial \tau} \cdot x(t + a(\tau))}{\int f(t + a(\tau)) f^*(t + b(\tau)) \delta(\tau) d\tau} \\ &+ \frac{\frac{1}{j} \int \delta(\tau) \frac{dx(t + a(\tau))}{d(t + a(\tau))} \cdot \frac{\partial(t + a(\tau))}{\partial \tau} \cdot x^*(t + b(\tau))}{\int f(t + a(\tau)) f^*(t + b(\tau)) \delta(\tau) d\tau} \\ &= \frac{1}{j} \cdot \frac{x'(t + a(0)) a'(0) x^*(t + b(0)) + x'^*(t + b(0)) b'(0) f(t + a(0))}{x(t + a(0)) x^*(t + b(0))} \end{aligned} \quad (\text{A1.49})$$

The constraint for $a(0)$ and $b(0)$ can be found by inserting the polar expression for $f(t)$:

$$\begin{aligned}
\Omega_x &= \frac{(A'(t+a(0))e^{j\Phi(t+a(0))} + A(t+a(0))e^{j\Phi(t+a(0))}j\Phi'(t+a(0)))}{jA(t+a(0))e^{j\Phi(t+a(0))}A(t+b(0))e^{-j\Phi(t+b(0))}} \\
&\quad \cdot a'(0)A(t+b(0))e^{-j\Phi(t+b(0))} \\
&+ \frac{(A'(t+b(0))e^{-j\Phi(t+b(0))} - A(t+b(0))e^{-j\Phi(t+b(0))}j\Phi'(t+b(0)))}{jA(t+a(0))e^{j\Phi(t+a(0))}A(t+b(0))e^{-j\Phi(t+b(0))}} \\
&\quad \cdot b'(0)A(t+a(0))e^{j\Phi(t+a(0))} \\
&= \frac{a'(0)A'(t+a(0))A(t+b(0))e^{j\Phi(t+a(0))-j\Phi(t+b(0))}}{jA(t+a(0))A(t+b(0))e^{j\Phi(t+a(0))-j\Phi(t+b(0))}} \\
&+ \frac{a'(0)A(t+a(0))A(t+b(0))e^{j\Phi(t+a(0))-j\Phi(t+b(0))}j\Phi'(t+a(0))}{jA(t+a(0))A(t+b(0))e^{j\Phi(t+a(0))-j\Phi(t+b(0))}} \quad (\text{A1.50}) \\
&+ \frac{b'(0)A'(t+b(0))A(t+a(0))e^{j\Phi(t+a(0))-j\Phi(t+b(0))}}{jA(t+a(0))A(t+b(0))e^{j\Phi(t+a(0))-j\Phi(t+b(0))}} \\
&- \frac{b'(0)A(t+b(0))A(t+a(0))e^{j\Phi(t+a(0))-j\Phi(t+b(0))}j\Phi'(t+b(0))}{jA(t+a(0))A(t+b(0))e^{j\Phi(t+a(0))-j\Phi(t+b(0))}} \\
&= \frac{1}{j} \cdot \left(\frac{a'(0)A'(t+a(0))}{A(t+a(0))} + \frac{b'(0)A'(t+b(0))}{A(t+b(0))} \right) \\
&\quad + (a'(0)\Phi'(t+a(0)) - b'(0)\Phi'(t+b(0)))
\end{aligned}$$

Because the IF by definition is a real variable, the imaginary part must be cancelled out. The function $a(\tau)$ and $b(\tau)$ are linear functions of the form $a(\tau) = \alpha \cdot \tau + \beta$. In order to satisfy the IF, the constant β has to be equal to zero. This reduces the expression for the IF to:

$$\Omega_f = \frac{1}{j} \cdot (a'(0) + b'(0)) \cdot \frac{A'(t)}{A(t)} + (a'(0) - b'(0))\Phi'(t) \quad (\text{A1.51})$$

This set the constraints on $a(\tau)$ and $b(\tau)$ to be:

$$\begin{aligned}
'a(0) + b'(0) &= 0 & a(\tau) + b(\tau) &= 0 \\
'a(0) - b'(0) &= 1 & a(\tau) - b(\tau) &=
\end{aligned} \quad (\text{A1.52})$$

The first constraint is called *the centering constraint* in the literature because it centers the correlation term $c(t+a(\tau))x^*(t+b(\tau))$ around t . The second constraint is called *the lag constraint* because it limits the symmetry of the correlation term.

1.3 Discrete Wigner-Ville distribution

This section derivates the Discrete Time-, Discrete Frequency- and Discrete Time Frequency Wigner-Ville distribution. The derivation follows the procedure proposed by [Peyrin 86].

Discrete Time Wigner-Ville distribution DT-WVD

The sampled signal $x_T(t)$ is defined by the following notation:

$$x_T(t) = x(t) \cdot s_T(t) = x(t) \sum_n \delta(t - nT) = \sum_n x(nT) \delta(t - nT) \quad (\text{A1.53})$$

The subscript T indicates that the signal is non-zero in time intervals of T. This signal is inserted in the continuous distribution:

$$\begin{aligned} WVD_{x_T}(t, \omega) &= \int x_T(t + \tau/2) x_T^*(t - \tau/2) e^{-j\omega\tau} d\tau \\ &= \int \sum_k x(kT) \delta(t + \tau/2 - kT) \sum_n x^*(nT) \delta(t - \tau/2 - nT) e^{-j\omega\tau} d\tau \\ &= \sum_k \sum_n x(kT) x^*(nT) \int \delta(t + \tau/2 - kT) \delta(t - \tau/2 - nT) e^{-j\omega\tau} d\tau \\ &\quad t + \tau/2 - kT = 0 \Rightarrow \tau = 2(kT - t) \\ &= \sum_k \sum_n x(kT) x^*(nT) \delta(t - 2(kT - t)/2 - nT) e^{-j\omega 2(kT - t)} \\ &= \sum_k \sum_n x(kT) x^*(nT) \delta(2t - (k+n)T) e^{-j\omega 2(kT - t)} \quad (\text{A1.54}) \\ &= \sum_k \sum_n x(kT) x^*(nT) \frac{1}{2} \delta\left(t - (k+n)\frac{T}{2}\right) e^{-j\omega 2(kT - t)} \\ &= \sum_k \sum_n x(kT) x^*(nT) \frac{1}{2} \delta\left(t - (k+n)\frac{T}{2}\right) e^{-j\omega 2\left(kT - (k+n)\frac{T}{2}\right)} \\ &= \sum_k \sum_n x(kT) x^*(nT) \frac{1}{2} \delta\left(t - (k+n)\frac{T}{2}\right) e^{-j\omega(k-n)\frac{T}{2}} \\ &= \sum_n \underbrace{\frac{1}{2} \sum_k x(kT) x^*((n-k)T)}_{\text{DT-WVD}} e^{-j\omega(2k-n)\frac{T}{2}} \delta\left(t - n\frac{T}{2}\right) \end{aligned}$$

From the Wigner-Ville distribution of the sampled signal, the DT-WVD can be identified:

$$WVD_{x_T}[n, \omega] = \frac{1}{2} \sum_k x[k] x^*[n-k] \exp(-j\omega(2k-n)T) \quad (\text{A1.55})$$

, where $x[k] = x(kT)$. The relation between the DT-WVD and the continuous Wigner-Ville distribution of the sampled signal can be seen to be:

$$WVD_{x_T}(t, u) = \sum_n WVD_{x_T}[n, u] \delta(t - nT/2) \quad (\text{A1.56})$$

To find the relation between the DT-WVD and the WVD of the continuous signal, the properties that express a multiplication between two signals can be used.

$$\begin{aligned} x_T(t) &= x(t) \cdot s_T(t) \\ &\Leftrightarrow \\ WVD_{x_T}(t, \omega) &= WVD_x(t, \omega) \otimes_{\omega} WVD_{S_T}(t, \omega) \end{aligned} \quad (\text{A1.57})$$

The WVD for the sampled signal can be expressed as a convolution in the frequency dimension between the WVD for the signal $WVD_x(t, \omega)$, and the WVD for the sampling function $WVD_{S_T}(t, \omega)$. The WVD for the sampling function $s_T(t)$ can be found from the $WVD_{x_T}(t, \omega)$ for the sampled signal $x_T(t)$, when $x_T(t)$ is substituted for $s_T(t)$. This is shown in the following equation.

$$\begin{aligned} WVD_{s_T}(t, \omega) &= \sum_k \frac{1}{2} \sum_n s_T(kT) s_T^*(((n-k)T) e^{-j\omega(2k-n)T} \delta(t - nT/2) \\ &= \frac{1}{2} \sum_k \sum_n 1 \cdot 1 \delta(t - nT/2) e^{-j\omega(2k-n)T} \\ &= \frac{1}{2} \sum_n e^{j\omega n T} \sum_k e^{-j\omega k 2T} \delta(t - nT/2) \\ &= \frac{1}{2} \sum_n e^{j\omega n T} \frac{2\pi}{2T} \sum_l \delta\left(\omega - l \cdot \frac{2\pi}{2T}\right) \delta\left(t - n \cdot \frac{T}{2}\right), \omega = l \cdot \frac{\pi}{T} \\ &= \frac{2\pi}{4T} \sum_n \sum_l e^{j\pi ln} \delta\left(\omega - l \cdot \frac{2\pi}{2T}\right) \delta\left(t - n \cdot \frac{T}{2}\right) \\ &= \frac{2\pi}{4T} \sum_n \sum_l (-1)^{nl} \delta\left(\omega - l \cdot \frac{2\pi}{2T}\right) \delta\left(t - n \cdot \frac{T}{2}\right) \end{aligned} \quad (\text{A1.58})$$

The conversion from exponential to Dirac is done with the Poisson formula [Haykin 83]:

$$\begin{aligned} \sum_m e^{-j\omega m T} &= \frac{2\pi}{T} \sum_m \delta\left(\omega + m \frac{2\pi}{T}\right) \Leftrightarrow \\ \sum_k e^{-j\omega k 2T} &= \frac{2\pi}{2T} \sum_k \delta\left(\omega + k \frac{2\pi}{2T}\right) \end{aligned} \quad (\text{A1.59})$$

The sign of the summation index in the dirac function does not matter because the sum runs from minus infinity to plus infinity. The relation between the continuous WVD and the WVD for the sampling function can now be stated as:

$$\begin{aligned}
 WVD_{x_T}(t, \omega) &= WVD_x(t, \omega) \otimes_{\omega} \frac{2\pi}{4T} \sum_n \sum_l (-1)^{nl} \delta\left(\omega - l \cdot \frac{2\pi}{2T}\right) \delta\left(t - n \cdot \frac{T}{2}\right) \\
 &= \frac{2\pi}{4T} \sum_n \sum_l WVD_x\left(t, \omega - l \cdot \frac{2\pi}{2T}\right) (-1)^{nl} \delta\left(t - n \cdot \frac{T}{2}\right)
 \end{aligned} \tag{A1.60}$$

From this equation, two important observations can be made. The $WVD_x(t, \omega)$ is sampled at a rate of $\frac{T}{2}$, and $WVD_{x_T}(t, \omega)$ contain a mirror images of $WVD_x(t, \omega)$ every $\frac{1}{2} \cdot \frac{2\pi}{T}$. In order to avoid aliasing, the signal $x(t)$ has to be oversampled at least by a factor 2.

Discrete Frequency Wigner-Ville distribution DF-WVD

In order to obtain a discrete spectrum, the time signal has to be periodic. This is equally obtained by sampling the continuous frequency spectrum.

$$X_\Omega(\omega) = X(\omega) \cdot S_\Omega(\omega) = X(\omega) \sum_n \delta(\omega - n\Omega) = \sum_n X(n\Omega) \delta(\omega - n\Omega) \quad (\text{A1.61})$$

This signal is inserted in the Wigner-Ville distribution defined by the Fourier transformed of the signal.

$$\begin{aligned} WVD_{X_\Omega}(t, \omega) &= \frac{1}{2\pi} \int X_\Omega(\omega + \tau/2) X_\Omega^*(\omega - \tau/2) e^{j t \tau} d\tau \\ &= \frac{1}{2\pi} \int \sum_k X(k\Omega) \delta(\omega + \tau/2 - k\Omega) \sum_n X(n\Omega) \delta(\omega - \tau/2 - n\Omega) e^{j t \tau} d\tau \\ &= \frac{1}{2\pi} \sum_k \sum_n X(k\Omega) X^*(n\Omega) \int \delta(\omega + \tau/2 - k\Omega) \delta(\omega - \tau/2 - n\Omega) e^{j t \tau} d\tau \\ &\quad \omega + \tau/2 - k\Omega = 0 \Rightarrow \tau = 2(k\Omega - \omega) \\ &= \frac{1}{2\pi} \sum_k \sum_n X(k\Omega) X^*(n\Omega) \delta(\omega - 2(k\Omega - \omega)/2 - n\Omega) e^{j t 2(k\Omega - \omega)} \\ &= \frac{1}{2\pi} \sum_k \sum_n X(k\Omega) X^*(n\Omega) \delta(2\omega - (k+n)\Omega) e^{j t 2(k\Omega - \omega)} \\ &= \frac{1}{2\pi} \sum_k \sum_n X(k\Omega) X^*(n\Omega) \frac{1}{2} \delta\left(\omega - (k+n)\frac{\Omega}{2}\right) e^{j t 2(k\Omega - \omega)} \\ &= \frac{1}{2\pi} \sum_k \sum_n X(k\Omega) X^*(n\Omega) \frac{1}{2} \delta\left(\omega - (k+n)\frac{\Omega}{2}\right) e^{j t 2\left(k\Omega - (k+n)\frac{\Omega}{2}\right)} \\ &= \frac{1}{4\pi} \sum_k \sum_n X(k\Omega) X^*(n\Omega) \delta\left(\omega - (k+n)\frac{\Omega}{2}\right) e^{j t (k-n)\frac{\Omega}{2}} \\ &= \sum_n \underbrace{\frac{1}{4\pi} \sum_k X(k\Omega) X^*((n-k)\Omega)}_{\text{DF-WVD}} e^{j t (2k-n)\frac{\Omega}{2}} \delta\left(\omega - n\frac{\Omega}{2}\right) \end{aligned} \quad (\text{A1.62})$$

From the Wigner-Ville distribution of the sampled spectrum, the DF-WVD can be identified:

$$WVD_{X_\Omega}(t, n) = \frac{1}{4\pi} \sum_k X[k] X^*[n-k] \exp(jt(2k-n)\Omega) \quad (\text{A1.63})$$

, where $X[k] = X(k\Omega)$. The relation between the DF-WVD and the WVD of the sampled signal can be seen to be:

$$WVD_{X_\Omega}(t, \omega) = \sum_n WVD_{X_\Omega}(t, n) \delta\left(\omega - n\frac{\Omega}{2}\right) \quad (\text{A1.64})$$

The relation between the DF-WVD and the WVD of the continuous signal can be found from the time-convolution between the $WVD_X(t, \omega)$ and the sampling function $WVD_{S_\Omega}(t, \omega)$ to be:

$$WVD_{X_\Omega}(t, \omega) = WVD_X(t, \omega) \otimes {}_t WVD_{S_\Omega}(t, \omega) \quad (\text{A1.65})$$

For this purpose, the WVD for the sampling function $S_\Omega(\omega)$ in the frequency domain has to be derived. This can be done with the WVD of the sampled spectrum $WVD_{X_\Omega}(t, \omega)$, when X_Ω is substituted for S_Ω .

$$\begin{aligned} WVD_{S_\Omega}(t, \omega) &= \frac{1}{4\pi} \sum_k \sum_n S_\Omega(k\Omega) S_\Omega^*((n-k)\Omega) \delta(\omega - n\Omega/2) e^{jt(2k-n)\Omega} \\ &= \frac{1}{4\pi} \sum_k \sum_n 1 \cdot 1 \delta(\omega - n\Omega/2) e^{jt(2k-n)\Omega} \\ &= \frac{1}{4\pi} \sum_n e^{-jtn\Omega} \sum_k e^{jt2k\Omega} \delta\left(\omega - \frac{n\Omega}{2}\right) \\ &= \frac{1}{4\pi} \sum_n e^{-jtn\Omega} \sum_k e^{\frac{j2\pi tk}{2\Omega}} \delta\left(\omega - \frac{n\Omega}{2}\right) \\ &= \frac{1}{4\pi} \sum_n e^{-jtn\Omega} \frac{2\pi}{2\Omega} \sum_l \delta\left(t - l \cdot \frac{2\pi}{2\Omega}\right) \delta\left(\omega - \frac{n\Omega}{2}\right) \\ &= \sum_n \sum_l e^{-jl\frac{2\pi}{2\Omega}n\Omega} \frac{1}{4\Omega} \delta\left(t - l \cdot \frac{2\pi}{2\Omega}\right) \delta\left(\omega - \frac{n\Omega}{2}\right) \\ &= \frac{1}{4\Omega} \sum_n \sum_l (-1)^{nl} \delta\left(t - l \cdot \frac{2\pi}{2\Omega}\right) \delta\left(\omega - \frac{n\Omega}{2}\right) \end{aligned} \quad (\text{A1.66})$$

The relation can now be stated as:

$$\begin{aligned} WVD_{X_\Omega}(t, \omega) &= WVD_X(t, \omega) \otimes {}_t WVD_{S_\Omega}(t, \omega) \\ &= WVD_X(t, \omega) \otimes \frac{1}{4\Omega} \sum_n \sum_l (-1)^{nl} \delta\left(t - l \cdot \frac{2\pi}{2\Omega}\right) \delta\left(\omega - \frac{n\Omega}{2}\right) \\ &= \frac{1}{4\Omega} \sum_n \sum_l (-1)^{nl} WVD_X\left(t - l \cdot \frac{2\pi}{2\Omega}, \omega\right) \delta\left(\omega - \frac{n\Omega}{2}\right) \end{aligned} \quad (\text{A1.67})$$

The WVD of the sampled spectrum X_Ω is sampled in the frequency dimension with a rate of $\frac{\Omega}{2}$, and contains a mirror of WVD_X in the time dimension every $\frac{12\pi}{2\Omega}$.

Discrete Time Frequency Wigner-Ville distribution DTF-WVD

The signal is defined as a sampling (T) of the extend (NT) of the signal, and then periodised with the period NT.

The signal representation is defined by the following notation:

$$x_{T,NT}(t) = x_T(t) \otimes s_{NT}(t) = \sum_{n=0}^{N-1} x(nT) \delta(t-nT) \otimes \sum_m \delta(t-m \cdot NT) \quad (\text{A1.68})$$

The Wigner-Ville distribution for this signal can be stated to:

$$WVD_{x_{T,NT}}(t, \omega) = WVD_{x_T}(t, \omega) \otimes_t WVD_{s_{NT}}(t, \omega) \quad (\text{A1.69})$$

The Wigner-Ville distribution $WVD_{x_T}(t, \omega)$ and $WVD_{s_{NT}}(t, \omega)$ has to be calculated.

$$\begin{aligned} WVD_{x_T}(t, \omega) &= \int x_T(t + \tau/2) x_T^*(t - \tau/2) e^{-j\omega\tau} d\tau, x_n = x(nT) \\ &= \int \sum_{n=0}^{N-1} x_n \delta(t + \tau/2 - nT) \sum_{k=0}^{N-1} x_k^* \delta(t - \tau/2 - kT) e^{-j\omega\tau} d\tau \\ &= \sum_{n=0}^{N-1} \sum_{k=0}^{N-1} x_n x_k^* \int \delta(t + \tau/2 - nT) \delta(t - \tau/2 - kT) e^{-j\omega\tau} d\tau \\ &\quad t + \tau/2 - nT = 0 \Rightarrow \tau = 2(nT - t) \\ &= \sum_{n=0}^{N-1} \sum_{k=0}^{N-1} x_n x_k^* \delta(t - 2(nT - t)/2 - kT) e^{-j\omega 2(nT - t)} \\ &= \sum_{n=0}^{N-1} \sum_{k=0}^{N-1} x_n x_k^* \frac{1}{2} \delta\left(t - (n+k)\frac{T}{2}\right) e^{-j\omega 2(nT - t)} \\ &= \sum_{n=0}^{N-1} \sum_{k=0}^{N-1} x_n x_k^* \frac{1}{2} \delta\left(t - (n+k)\frac{T}{2}\right) e^{-j\omega 2\left(nT - (n+k)\frac{T}{2}\right)} \\ &= \sum_{n=0}^{N-1} \sum_{k=0}^{N-1} x_n x_k^* \frac{1}{2} \delta\left(t - (n+k)\frac{T}{2}\right) e^{-j\omega(n-k)T} \\ &= \sum_{k=0}^{N-1} \frac{1}{2} \sum_{n=0}^{N-1} x_n x_{k-n}^* e^{-j\omega(2n-k)T} \delta\left(t - k\frac{T}{2}\right) \end{aligned} \quad (\text{A1.70})$$

The WVD for the sampling function can be found from an earlier derivation to be:

$$WVD_{S_{NT}}(t, \omega) = \frac{2\pi}{4NT} \sum_m \sum_{m'} (-1)^{mm'} \delta\left(\omega - m \cdot \frac{2\pi}{2NT}\right) \delta\left(t - \frac{m'NT}{2}\right) \quad (\text{A1.71})$$

The $WVD_{x_{T,NT}}$ distribution for the signal $x_{T,NT}$ can be found to be:

$$\begin{aligned}
WVD_{x_{T,NT}}(t, \omega) &= \int WVD_{x_T}(p, \omega) WVD_{S_{NT}}(t-p, \omega) dp \\
&= \int \frac{1}{2} \sum_{n=0}^{N-1} \sum_{k=0}^{N-1} x_n x^*_{k-n} \delta\left(p - \frac{kT}{2}\right) e^{-j\omega(2n-k)T} \\
&\quad \cdot \frac{2\pi}{4NT} \sum_{m=m'} \sum_{m'=m} (-1)^{mm'} \delta\left(\omega - m \cdot \frac{2\pi}{2NT}\right) \delta\left(t-p - \frac{m'NT}{2}\right) dp \\
&= \frac{\pi}{4NT} \sum_{n=0}^{N-1} \sum_{k=0}^{N-1} x_n x^*_{k-n} e^{-j\omega(2n-k)T} \\
&\quad \cdot \sum_{m=m'} \sum_{m'=m} (-1)^{mm'} \delta\left(\omega - m \cdot \frac{2\pi}{2NT}\right) \int \delta\left(p - \frac{kT}{2}\right) \delta\left(t-p - \frac{m'NT}{2}\right) dp \\
&= \frac{\pi}{4NT} \sum_{n=0}^{N-1} \sum_{k=0}^{N-1} x_n x^*_{k-n} e^{-j\omega(2n-k)T} \\
&\quad \cdot \sum_{m=m'} \sum_{m'=m} (-1)^{mm'} \delta\left(\omega - m \cdot \frac{2\pi}{2NT}\right) \delta\left(t - \frac{kT}{2} - \frac{m'NT}{2}\right) \\
&= \frac{\pi}{4NT} \sum_{n=0}^{N-1} \sum_{k=0}^{N-1} x_n x^*_{k-n} e^{-j\omega(2n-k)T} \\
&\quad \cdot \sum_m \delta\left(\omega - m \cdot \frac{2\pi}{2NT}\right) \sum_{m'} (-1)^{mm'} \delta\left(t - \frac{kT}{2} - \frac{m'NT}{2}\right) \\
&\quad \omega - m \cdot \frac{2\pi}{2NT} = 0 \Rightarrow \omega = \frac{m}{2NT} \cdot 2\pi = \frac{m\pi}{NT} \\
&= \frac{\pi}{4NT} \sum_{n=0}^{N-1} \sum_{k=0}^{N-1} \sum_m x_n x^*_{k-n} e^{-j\frac{m\pi}{NT}(2n-k)T} \\
&\quad \cdot \delta\left(\omega - m \cdot \frac{2\pi}{2NT}\right) \sum_{m'} (-1)^{mm'} \delta\left(t - \frac{kT}{2} - \frac{m'NT}{2}\right)
\end{aligned} \tag{A1.72}$$

If time t is restricted to be in the first period $0 \leq t < (NT)/2$, it will be acceptable to set m' equal to zero in order to obtain a simple formulation.

$$\begin{aligned}
WVD_{x_{T,NT}}(t, \omega) &= \frac{\pi}{4NT} \sum_{n=0}^{N-1} \sum_{k=-\infty}^{\infty} \sum_{m=-\infty}^{\infty} x_n x^*_{k-n} e^{-j\frac{m\pi}{N}(2n-k)} \delta\left(\omega - m \cdot \frac{2\pi}{2NT}\right) \delta\left(t - \frac{kT}{2}\right) \\
&= \sum_{k=-\infty}^{\infty} \sum_{m=-\infty}^{\infty} \left[\frac{\pi}{4NT} \sum_{n=0}^{N-1} x_n x^*_{k-n} e^{-j\frac{m\pi}{N}(2n-k)} \right] \delta\left(\omega - m \cdot \frac{2\pi}{2NT}\right) \delta\left(t - \frac{kT}{2}\right)
\end{aligned} \tag{A1.73}$$

From this the DTF-WVD can be derived:

$$WVD_{x_{T,NT}}[k, m] = \frac{\pi}{4NT} \sum_{n=0}^{N-1} x_n x^*_{k-n} e^{-j\frac{m\pi}{N}(2n-k)} \quad (\text{A1.74})$$

The constant $\frac{\pi}{4NT}$ will be ignored in the comming implementation. The relation between the DTF-WVD and the WVD of the continuous signal can be found from the following identify:

$$x_{T,NT} = x_T \otimes S_{NT} \Rightarrow WVD_{x_{T,NT}} = WVD_{x_T} \otimes_t WVD_{S_{NT}} \quad (\text{A1.75})$$

The WVD_{x_T} for the sampled signal can be found to be:

$$\begin{aligned} x_T &= x \otimes s_T \quad \Leftrightarrow \\ WVD_{x_T} &= WVD_x \otimes_u WVD_{S_T} \\ &= WVD_x(t, u) \otimes_u \frac{2\pi}{4T} \sum_{n=0}^{N-1} \sum_{l=0}^{N-1} (-1)^{nl} \delta(\omega - l \cdot \frac{2\pi}{2T}) \delta(t - \frac{nT}{2}) \\ &= \frac{2\pi}{4T} \sum_{n=0}^{N-1} \sum_{l=0}^{N-1} (-1)^{nl} WVD_x\left(t, \omega - l \cdot \frac{2\pi}{2T}\right) \delta\left(t - \frac{nT}{2}\right) \end{aligned} \quad (\text{A1.76})$$

An equation that relates DTF-WVD and the WVD can be found by the following derivation:

$$\begin{aligned} WVD_{x_{T,NT}}(t, \omega) &= WVD_{x_T}(t, \omega) \otimes_t WVD_{S_{NT}}(t, \omega) \\ &= \int \frac{2\pi}{4T} \sum_{n=0}^{N-1} \sum_{l=0}^{N-1} (-1)^{nl} WVD_x\left(p, \omega - l \cdot \frac{2\pi}{2T}\right) \delta\left(p - n \cdot \frac{T}{2}\right) \\ &\quad \cdot \frac{2\pi}{4NT} \sum_{a=-b}^b (-1)^{ab} \delta(\omega - b \cdot \frac{2\pi}{2NT}) \delta\left(t - p - a \cdot \frac{NT}{2}\right) dp \\ &= \frac{\pi^2}{4NT^2} \sum_{n=0}^{N-1} \sum_{l=0}^{N-1} \sum_{a=-b}^b (-1)^{ab+nl} \delta\left(\omega - b \cdot \frac{2\pi}{2NT}\right) \\ &\quad \cdot \int WVD_x\left(p, \omega - l \cdot \frac{2\pi}{2T}\right) \delta\left(p - \frac{nT}{2}\right) \delta\left(t - p - \frac{aNT}{2}\right) dp \\ &= \frac{\pi^2}{4NT^2} \sum_{n=0}^{N-1} \sum_{l=0}^{N-1} \sum_{a=-b}^b (-1)^{ab+nl} \delta\left(\omega - b \cdot \frac{2\pi}{2NT}\right) \\ &\quad \cdot \int WVD_x\left(\frac{nT}{2}, \omega - l \cdot \frac{2\pi}{2T}\right) \delta\left(t - p - \frac{nT}{2} - \frac{aNT}{2}\right) \end{aligned} \quad (\text{A1.77})$$

$$\begin{aligned}
WVD_{x_{T,NT}}(t, \omega) &= \frac{\pi^2}{4NT^2} \sum_{n=0}^{N-1} \sum_{l=0}^{N-1} \sum_{a} \sum_{b} (-1)^{ab+nl} \delta\left(\omega - b \cdot \frac{2\pi}{2NT}\right) \\
&\quad \cdot WVD_x\left(\frac{nT}{2}, \omega - l \cdot \frac{2\pi}{2T}\right) \delta\left(t - \frac{T}{2}(n+aN)\right) dp \quad , n = n - aN \\
&= \frac{\pi^2}{4NT^2} \sum_{n=0}^{N-1} \sum_{l=0}^{N-1} \sum_{a} \sum_{b} (-1)^{ab+nl-laN} WVD_x\left(\frac{(n-aN)T}{2}, \omega - l \cdot \frac{2\pi}{2T}\right) \\
&\quad \cdot \delta\left(\omega - b \cdot \frac{2\pi}{2NT}\right) \delta\left(t - n\frac{T}{2}\right) \\
&= \frac{\pi^2}{4NT^2} \sum_{n=0}^{N-1} \sum_{l=0}^{N-1} \sum_{a} \sum_{b} (-1)^{ab+nl-laN} WVD_x\left(\frac{T(n-aN)}{2}, \frac{2\pi}{2T}\left(\frac{b}{N}-l\right)\right) \\
&\quad \cdot \delta\left(\omega - b \cdot \frac{2\pi}{2NT}\right) \delta\left(t - n\frac{T}{2}\right) \\
&= \frac{\pi^2}{4NT^2} \sum_{n=0}^{N-1} \sum_{l=0}^{N-1} \sum_{a} \sum_{b} (-1)^{ab+nl+laN} WVD_x\left(\frac{T(n-aN)}{2}, \frac{2\pi}{2NT}(b-lN)\right) \\
&\quad \cdot \delta\left(\omega - b \cdot \frac{2\pi}{2NT}\right) \delta\left(t - n\frac{T}{2}\right)
\end{aligned} \tag{A1.78}$$

In order to compare the two formulations for the DTF-WVD, the indexes are renamed to the following:

$$\begin{aligned}
WVD_{x_{T,NT}}(t, \omega) &= \frac{\pi^2}{4NT^2} \sum_a \sum_b \sum_m \sum_n (-1)^{an+bm+abN} WVD_x\left(\frac{T}{2}(m-aN), \frac{2\pi}{2NT}(n-bN)\right) \\
&= \cdot \delta\left(\omega - n \cdot \frac{2\pi}{2NT}\right) \delta\left(t - m \cdot \frac{T}{2}\right)
\end{aligned} \tag{A1.79}$$

The four indexes **a,b,m** and **n** has the following functions:

- **m** is the time sampling of the $WVD_x(t, \omega)$ every $\frac{T}{2}$.
- **n** is the frequency sampling of $WVD_x(t, \omega)$ every $\frac{1}{2} \cdot \frac{2\pi}{NT}$.
- **a** adds time aliasing every $\frac{NT}{2}$.
- **b** adds frequency aliasing every $\frac{1}{2} \cdot \frac{2\pi}{T}$

Because the **m** and **n** indexes control the discretizing of the time and frequency domain, the DTF-WVD can be isolated:

$$WVD_{x_{T,NT}}(t, \omega) = \sum_m \sum_n WVD[m, n] \delta\left(\omega - n \cdot \frac{2\pi}{2NT}\right) \delta\left(t - m \cdot \frac{T}{2}\right) \tag{A1.80}$$

where the DTF-WVD is given by:

$$\begin{aligned}
 WVD[m, n] &= \frac{\pi^2}{4NT^2} \sum_a \sum_b (-1)^{an + bm + abN} WVD_x\left(\frac{T}{2}(m - aN), \frac{2\pi}{2NT}(n - bN)\right) \\
 &= \frac{1}{2NT} \sum_{k=0}^{N-1} x_k x^*_{m-k} e^{-j\frac{n\pi}{N}(2k-m)}
 \end{aligned} \tag{A1.81}$$

where the last equal definition of the DTF-WVD has been derived earlier. In order to study the aliasing of the DTF-WVD, the non-zero support of the $WV_x(t, \omega)$ has to be found.

$$\begin{aligned}
 WVD_x(t, \omega) \neq 0 \text{ for } 0 \leq t < NT \wedge -\frac{\pi}{T} \leq \omega \leq \frac{\pi}{T} \Leftrightarrow \\
 WVD_x(t, \omega) \neq 0 \text{ for } 0 \leq \frac{T}{2}(m - aN) < NT \wedge -\frac{\pi}{T} \leq \frac{2\pi}{2NT}(n - bN) \leq \frac{\pi}{T} \\
 WVD_x(t, \omega) \neq 0 \text{ for } 0 \leq m - aN < 2N \wedge -N \leq n - bN \leq N
 \end{aligned} \tag{A1.82}$$

This sampling of $WVD_x\left(m \cdot \frac{1}{2}T, n \cdot \frac{1}{2}\frac{2\pi}{NT}\right)$ is illustrated in the next figure.

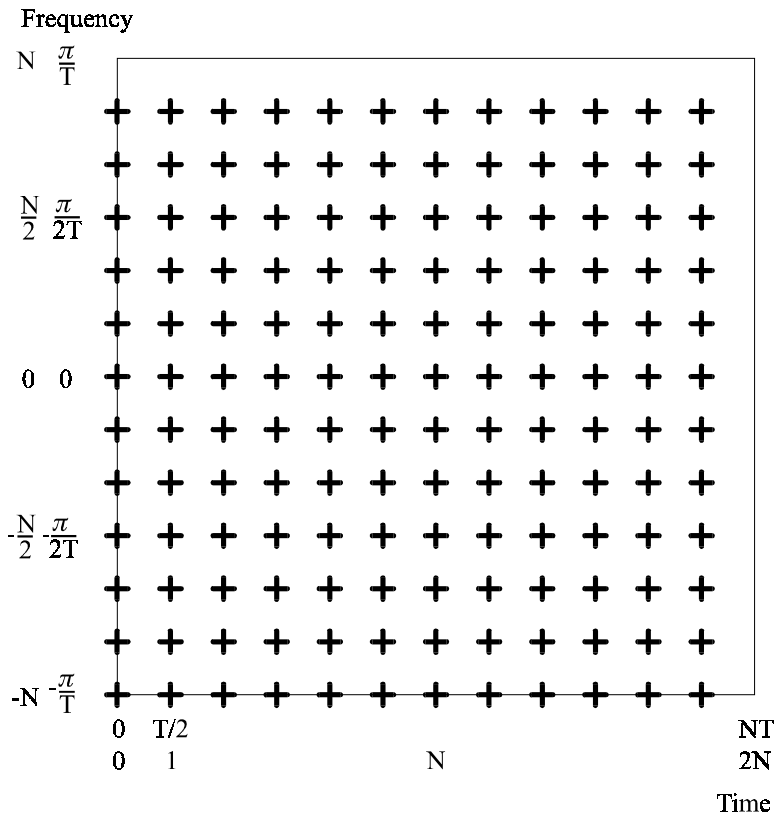


Figure 1.1 Sampling of the continuous WVD.

In order to avoid that the aliasing overlaps in the time domain with $\frac{NT}{2}$, and in the frequency domain with $\frac{1}{2} \cdot \frac{2\pi}{T}$, the signal has to be respectively zeropadded with N and oversampled with

a factor of 2. This is illustrated in figure 3.2.

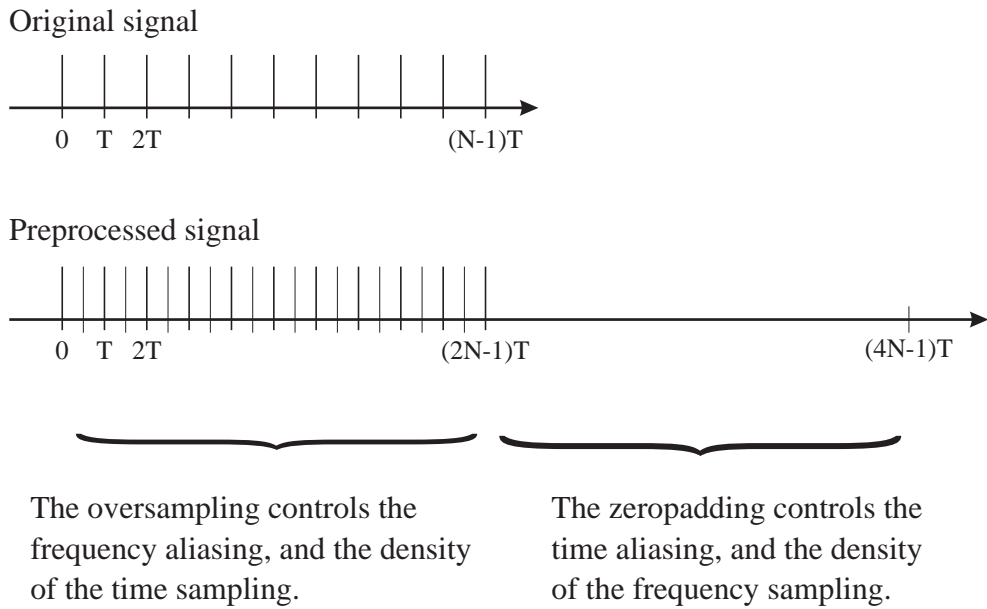


Figure 1.2 Preprocessing of the signal in order to avoid aliasing.

The length of the preprocessed signal will be the new $N!$ When the signal has been preprocessed, the sampling of the continuous distribution will be non-zero in the following area:

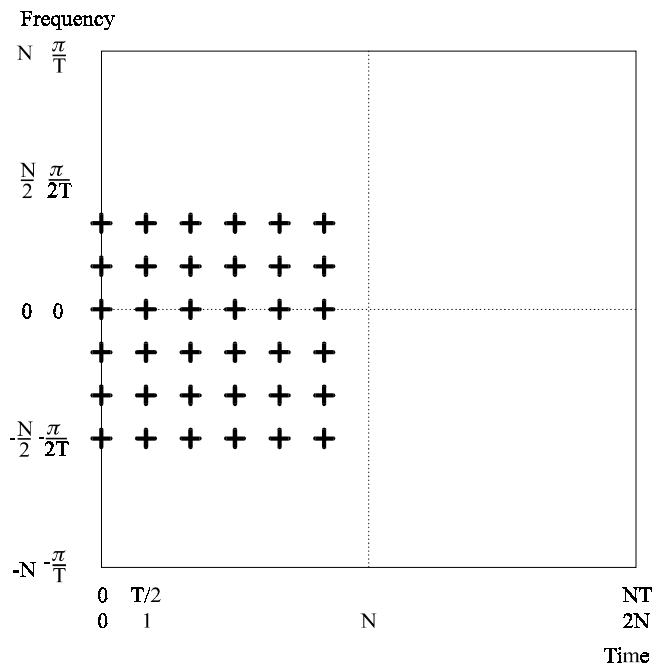


Figure 1.3 Sampling of the continuous distribution with a preprocessed signal.

The DTF-WVD is constructed by time and frequency shifted versions of the sampling of the continuous distribution. Each point of the DTF-WVD has alternating phase depending of the

time-frequency position. This is illustrated in figure 3.4.

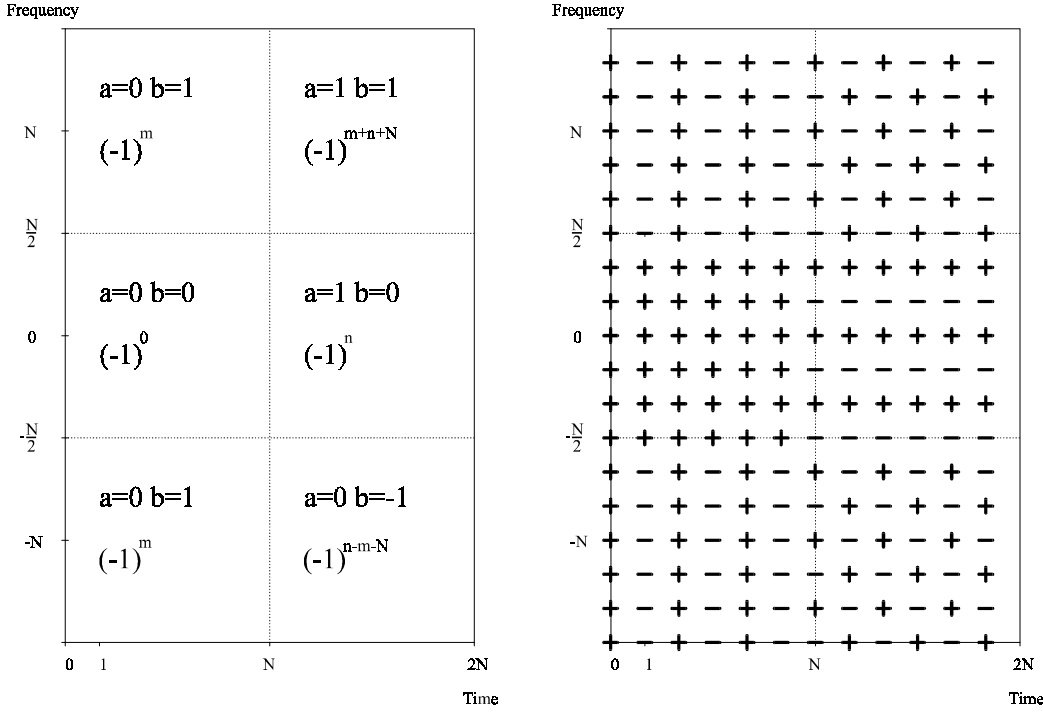


Figure 1.4 The effect of aliasing in the DTF-WVD.

It is sufficient to compute $WVD [m, n]$ for $0 \leq m < N$ and $-\frac{N}{2} \leq n < \frac{N}{2}$. The other values can be obtained from the following relations:

$$\begin{aligned} WVD [m + N, n] &= (-1)^n WVD [m, n] \\ WVD [m, n + N] &= (-1)^m WVD [m, n] \\ WVD [m + N, n + N] &= (-1)^{m+n+N} WVD [m, n] \end{aligned} \quad (\text{A1.83})$$

The final DTF-WVD algorithm can be stated as:

Discrete Time Frequency - Wigner Ville Distribution
Normal Approach

Pre-processing of input signal:

$$x = [\text{interp}(\text{signal}, 2) \text{ zeros}(1, 2*\text{length}(\text{signal}))]; \quad (\text{A1.84})$$

$$N = \text{length}(x); \quad (\text{A1.85})$$

Distribution:

$$WVD [m, n] = \sum_{k=0}^{N-1} x_k x_{m-k}^* e^{-j\frac{n\pi}{N}(2k-m)} \quad (A1.86)$$

$$0 \leq m < N \quad -\frac{N}{2} \leq n < \frac{N}{2}$$

However, if the FFT algorithm has to be used, it is only possible to compute $WVD[m, n]$ for $0 \leq m < N$ and $0 \leq n < N$. The values of the DTF-WVD for $n \geq \frac{N}{2}$ has to be swapped with $(-1)^m$. e.i.

$$WVD[m, n] = \frac{1}{2NT} \underbrace{\left(\sum_{k=0}^{N-1} v_m(k) e^{-jkn\frac{2\pi}{N}} \right)}_{\text{FFT}} e^{j\frac{mn\pi}{N}}, v_m(k) = x_k x^*_{m-k}$$

$$WVD[m, n] = (-1)^m WV[m, n] \quad \text{for } \frac{N}{2} \leq n < N \quad (\text{A1.87})$$

The use and effect of the last equation is illustrated in Figure 1.5. The FFT modified DTF-WVD algorithm is given by:

Discrete Time Frequency - Wigner Ville Distribution FFT Approach

Pre-processing of input signal:

$$x = [\text{interp}(signal, 2) \text{ zeros}(1, 2*\text{length}(signal))]; \quad (\text{A1.88})$$

Distribution:

$$WVD[m, n] = \frac{1}{2NT} \cdot F_m[n] \cdot e^{j\frac{mn\pi}{N}}$$

$$0 \leq m < N \quad 0 \leq n < N \quad (\text{A1.89})$$

$$F_m[n] = \text{FFT}^N \{x_k x^*_{(m-k) \bmod_N}\}$$

Post-processing of distribution:

$$WVD[m, n] = (-1)^m WV[m, n] \quad \text{for } \frac{N}{2} \leq n < N \quad (\text{A1.90})$$

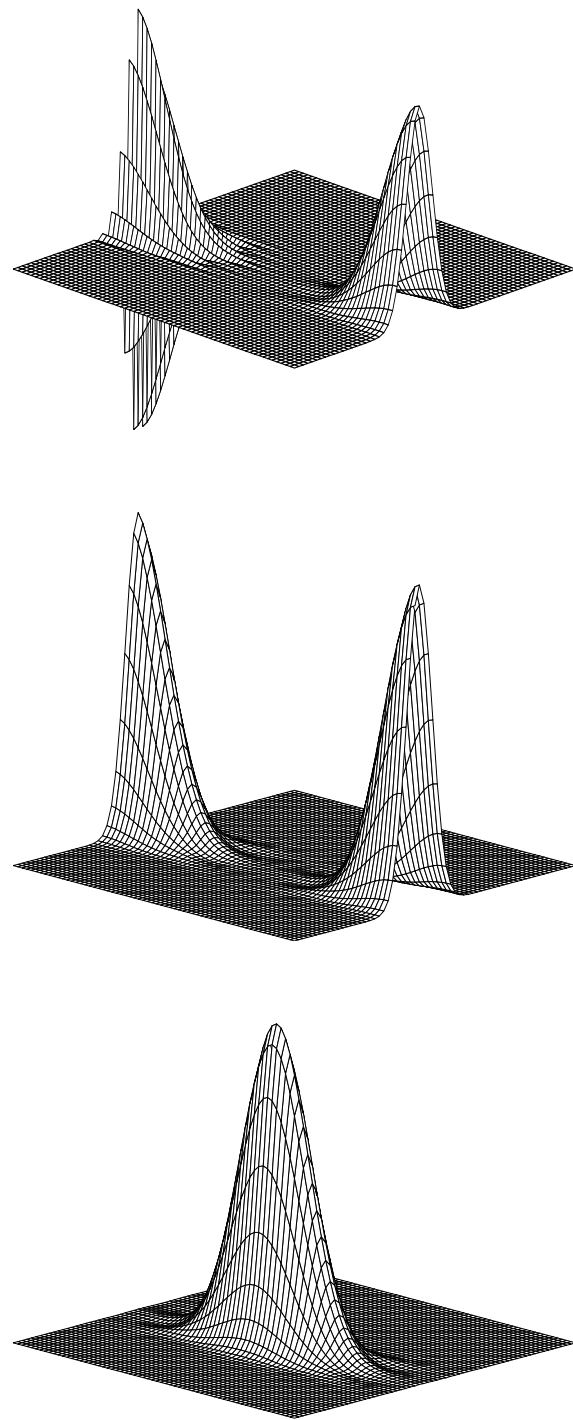


Figure 1.5 Example of shifting and alternating the upper plan elements

First the WVD is calculated using the FFT algorithme where the upper half will have a alternating sign. This is changed with $(-1)^m$, and the final plan is reach by centering the DC.

Appendix 2

Gabor Expansion

The purpose of this appendix is to derive the *Discrete Gabor Expansion* (DGE). The Gabor expansion is obtained when the signal is reconstructed from Fourier coefficients using a minimum of coefficients. The derivation of the Gabor expansion is divided into three sections - the *Continuous Gabor Expansion* (CGE) is valid for continuous functions. The CGE is then made discrete *Periodic Discrete Gabor Expansion* - (PDGE) covering finite periodic discrete signals. Finally, the PDGE is extended to cover infinite non-periodic discrete signals, and this final expansion is the *Discrete Gabor Expansion*.

A2.1 Prologue: The Delta functions

The derivation of the Gabor expansion will demand some confidence with the two delta functions, the *Dirac delta function* and the *Kronecker delta function*. To assist the impending derivation, the definition and some properties of the two function will be given.

Dirac delta function

The *Dirac delta function* is mathematically defined by:

$$\int_{t_1}^{t_2} x(t) \delta(t - T) dt = x(T) \quad t_1 < T < t_2 \quad (\text{A2.1})$$

and possesses the following properties:

$$\delta(0) \rightarrow \infty \quad (\text{A2.2})$$

$$\delta(t) = 0, t \neq 0 \quad (\text{A2.3})$$

$$\int \delta(t) dt = 1 \quad (\text{A2.4})$$

$$\delta(t \cdot N) = \frac{1}{N} \delta(t) \quad (\text{A2.5})$$

Further properties can be obtained , when the Dirac delta function is used together with the Fourier transformation:

$$\int \delta(t) e^{-j\omega t} dt = 1 \Leftrightarrow \delta(t) = \frac{1}{2\pi} \int e^{j\omega t} d\omega \quad (\text{A2.6})$$

The inversion formula is correctly applied in solving of many problems, regardless the fact that it is not easy to accept the validity of the inversion formula, because the integral has no meaning [Papoulis 62, pp5]. The same relation exists in the frequency domain:

$$\frac{1}{2\pi} \int \delta(\omega) e^{j\omega t} d\omega = 1 \Leftrightarrow \delta(\omega) = \int e^{-j\omega t} dt \quad (\text{A2.7})$$

The Dirac delta function is also used in the Poisson's sum formula defined by:

$$\sum_n \delta(t - nT) = \frac{1}{T} \sum_n e^{jtn \frac{2\pi}{T}} \quad (\text{A2.8})$$

and its dual in the frequency domain:

$$\sum_n \delta(\omega + n\Omega) = \frac{1}{\Omega} \sum_n e^{-j\omega n \frac{2\pi}{\Omega}} \quad (\text{A2.9})$$

Kronecker delta function

The *Kronecker delta function* defined as:

$$\delta_{m-n} = \begin{cases} 1, & m = n \\ 0, & m \neq n \end{cases} \quad (\text{A2.10})$$

This function is used in the following discrete Poisson-like sum formula:

$$\sum_{n=0}^{N-1} e^{jn(k-k')\frac{2\pi}{N}} = N \sum_q \delta_{k-k'-qN} \quad (\text{A2.11})$$

A2.2 Continuous Gabor Expansion - CGE

The STFT samples the time-frequency plan by windowing the signal, and then Fourier transforms the windowed sequence. This technique is also called the Sliding-Window representation in the literature [Bastiaans 85]. The purpose is now to investigate how to reconstruct the signal from the STFT coefficients. The STFT for continuous signal is given by:

$$F(t, \omega) = \int x(\tau) \gamma^*(\tau - t) e^{-j\omega\tau} d\tau \quad (\text{A2.12})$$

The window function $\gamma(t)$ (later called the analysis function) has not been time-reversed enabling a more elegant formulation in the derivations. The function is continuous in both time index t and frequency index ω . In order to reconstruct the signal we need not know the entire sliding-window time-frequency plan, but it will be sufficient to know its values at the points of a certain lattice [Bastiaans 85]. This lattice is shown in the Figure A2.1.

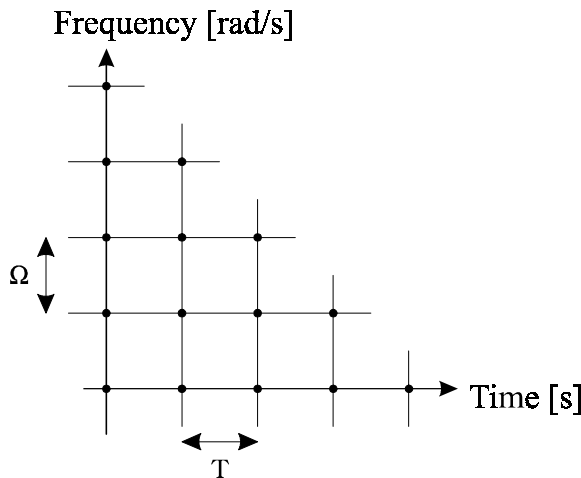


Figure A2.1 The Gabor/Von Neumann lattice

The samples are indexed with \mathbf{m} in the time dimension with the time step T and index with \mathbf{n} in the frequency dimension with frequency step Ω . Each coefficient is given by:

$$a_{mn} = F(mT, n\Omega) = \int x(\tau) \gamma^*(\tau - mT) e^{-jn\Omega\tau} d\tau \quad (\text{A2.13})$$

The task is now to isolate the signal $x(t)$ in equation (A2.13). The first step is to inverse Fourier transform both sides of equation (A2.13) with respect to the frequency index \mathbf{n} , and then Fourier transform both sides with respect to the time index \mathbf{m} .

- Inverse Fourier transforming the frequency index **n**.

$$\begin{aligned}
\sum_n a_{mn} e^{jtn\Omega} &= \sum_n \int x(\tau) \gamma^*(\tau - mT) e^{-j\tau n\Omega} d\tau e^{jtn\Omega} \\
&= \int x(\tau) \gamma^*(\tau - mT) \sum_n e^{jn\Omega(t-\tau)} d\tau \\
&= \int x(\tau) \gamma^*(\tau - mT) \frac{2\pi}{\Omega} \sum_n \delta\left(t - \tau - n\frac{2\pi}{\Omega}\right) d\tau \\
&= \frac{2\pi}{\Omega} \sum_n x\left(t - n\frac{2\pi}{\Omega}\right) \gamma^*\left(t - n\frac{2\pi}{\Omega} - mT\right)
\end{aligned} \tag{A2.14}$$

In equation (A2.14), the following modified Poissons sum formula was used:

$$\begin{aligned}
\frac{1}{T} \sum_n e^{jtn\frac{2\pi}{T}} &= \sum_n \delta(t - nT) \Leftrightarrow \\
\sum_n e^{-jn\Omega(t-\tau)} &= \sum_n e^{-jn(t-\tau)\left(\frac{2\pi}{\Omega}\right)} = \frac{2\pi}{\Omega} \sum_n \delta\left(t - \tau - n\frac{2\pi}{\Omega}\right)
\end{aligned} \tag{A2.15}$$

- Fourier transforming the time index **m**.

$$\begin{aligned}
\sum_m \sum_n a_{mn} e^{jtn\Omega} e^{-j\omega mT} &= \sum_m \frac{2\pi}{\Omega} \sum_n x\left(t - n\frac{2\pi}{\Omega}\right) \gamma^*\left(t - n\frac{2\pi}{\Omega} - mT\right) e^{-j\omega mT} \\
&= \frac{2\pi}{\Omega} \sum_n x\left(t - n\frac{2\pi}{\Omega}\right) \sum_m \gamma^*\left(t - n\frac{2\pi}{\Omega} - mT\right) e^{-j\omega mT} \\
&= \frac{2\pi}{\Omega} \sum_n x\left(t - n\frac{2\pi}{\Omega}\right) \sum_m \gamma^*(t + mT) e^{-j\omega(-m-n\frac{2\pi}{T\Omega})T} \\
&= \frac{2\pi}{\Omega} \sum_n x\left(t - n\frac{2\pi}{\Omega}\right) e^{j\omega n\frac{2\pi}{\Omega}} \sum_m \gamma^*(t + mT) e^{j\omega mT} \\
&= \frac{2\pi}{\Omega} \sum_n x\left(t + n\frac{2\pi}{\Omega}\right) e^{-j\omega n\frac{2\pi}{\Omega}} \sum_m \gamma^*(t + mT) e^{j\omega mT}
\end{aligned} \tag{A2.16}$$

In order to obtain a simple notation, the following three auxiliary functions are introduced:

$$\underbrace{\sum_m \sum_n a_{mn} e^{jtn\Omega} e^{-j\omega mT}}_{\tilde{a}(t, \omega)} = \underbrace{\frac{2\pi}{\Omega} \sum_n x\left(t + n\frac{2\pi}{\Omega}\right) e^{-j\omega n\frac{2\pi}{\Omega}}}_{\tilde{x}(t, \omega)} \underbrace{\sum_m \gamma^*(t + mT) e^{j\omega mT}}_{\gamma^*(t, \omega)} \tag{A2.17}$$

Using these functions, equation (A2.17) will be reduced to:

$$\tilde{a}(t, \omega) = \frac{2\pi}{\Omega} \tilde{x}(t, \omega) \tilde{\gamma}^*(t, \omega) \quad (\text{A2.18})$$

Because the auxiliary function $\tilde{a}(t, \omega)$ is periodic in the variable ω with $\frac{2\pi}{T}$, both of the functions $\tilde{x}(t, \omega)$ and $\tilde{\gamma}(t, \omega)$ must have the same period. But this sets a constraint on Ω and T .

$$\left. \begin{array}{l} \tilde{a}(t, \omega) = \tilde{a}\left(t, \omega + \frac{2\pi}{T}\right) \\ \tilde{x}(t, \omega) = \tilde{x}(t, \omega + \Omega) \\ \tilde{\gamma}(t, \omega) = \tilde{\gamma}\left(t, \omega + \frac{2\pi}{T}\right) \end{array} \right\} \quad \text{Demand } \Omega = \frac{2\pi}{T} \Leftrightarrow \Omega \cdot T = 2\pi \quad (\text{A2.19})$$

The product of Ω and T has to be 2π , which can be regarded as a 2D version of the Nyquist sampling rate. An update version of Figure A2.1 is now Figure A2.2:

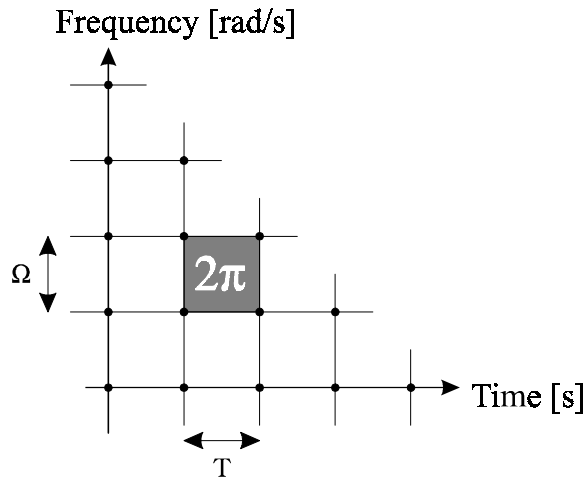


Figure A2.2 The Gabor/Von Neumann lattice constraint

As the goal is to reconstruct the signal x , the function $\tilde{x}(t, \omega)$ has to be isolated. This can be done using a special $\tilde{g}(t, \omega)$ with the property:

$$\tilde{g}(t, \omega) \tilde{\gamma}^*(t, \omega) = \frac{\Omega}{2\pi} \quad (\text{A2.20})$$

The content of this special function will be found later. Multiplying this function on both sides of equation (A2.18) will isolate the signal:

$$\begin{aligned} \tilde{a}(t, \omega) \tilde{g}(t, \omega) &= \frac{2\pi}{\Omega} \tilde{x}(t, \omega) \tilde{\gamma}^*(t, \omega) \tilde{g}(t, \omega) \\ &= \tilde{x}(t, \omega) \end{aligned} \quad (\text{A2.21})$$

The expression for the auxiliary functions is inserted:

$$\begin{aligned}
& \sum_m \sum_n a_{mn} e^{jtn\Omega} e^{-j\omega m T} \sum_{m'} g(t + m'T) e^{-j\omega m' T} = \sum_{n'} x\left(t + n' \frac{2\pi}{\Omega}\right) e^{-j\omega n' \frac{2\pi}{\Omega}} \quad \Leftrightarrow \\
& \int \sum_m \sum_n \sum_{m'} a_{mn} g(t + m'T) e^{jtn\Omega} e^{-j\omega(m' + m)T} d\omega = \int \sum_{n'} x\left(t + n' \frac{2\pi}{\Omega}\right) e^{-j\omega n' \frac{2\pi}{\Omega}} d\omega \quad \Leftrightarrow \\
& \sum_m \sum_n \sum_{m'} a_{mn} g(t + m'T) e^{jtn\Omega} \int e^{-j\omega(m' + m)T} d\omega = \sum_{n'} x\left(t + n' \frac{2\pi}{\Omega}\right) \int e^{-j\omega n' \frac{2\pi}{\Omega}} d\omega \quad (\text{A2.22}) \\
& \sum_m \sum_n \sum_{m'} a_{mn} g(t + m'T) e^{jtn\Omega} \frac{2\pi}{T} \delta(m' + m) = \sum_{n'} x\left(t + n' \frac{2\pi}{\Omega}\right) \Omega \delta(n') \quad \Leftrightarrow \\
& x(t) = \sum_m \sum_n a_{mn} g(t - mT) e^{jtn\Omega} = \sum_m \sum_n a_{mn} g_{mn}(t) \quad \Leftrightarrow
\end{aligned}$$

The equation expresses the signal as a sum of time shifted (T) and frequency shifted (Ω) versions of the special function $g(t)$. As it is used to reconstruct the signal again, we will call it a synthesis function. The amplitude of the synthesis function is given by a_{mn} . These coefficients are sampled values of the sliding-window time-frequency plane, and are obtained in a grid lattice, with a grid area of 2π .

The remaining part of equation (A2.22) is to find the synthesis function $g(t)$. A scheme can be derived by inserting the expression for the Gabor coefficients equation (A2.13) into the Gabor expansion equation (A2.22).

$$\begin{aligned}
x(t) &= \sum_m \sum_n a_{mn} g_{mn}(t) \\
&= \sum_m \sum_n a_{mn} g(t - mT) e^{jtn\Omega} \\
&= \sum_m \sum_n \left(\int x(\tau) \gamma^*(\tau - mT) e^{-j\tau n\Omega} d\tau \right) g(t - mT) e^{jtn\Omega} \\
&= \int x(\tau) \underbrace{\sum_m \gamma^*(\tau - mT) g(t - mT)}_{\delta(t - \tau)} \sum_n e^{jn\Omega(t - \tau)} d\tau \\
\delta(t - \tau) &= \sum_m \gamma^*(\tau - mT) g(t - mT) \sum_n e^{jn\Omega(t - \tau)} \\
&= \sum_m \gamma^*(\tau - mT) g(t - mT) \frac{2\pi}{\Omega} \sum_n \delta\left(t - \tau - n \frac{2\pi}{\Omega}\right) \\
&= \frac{2\pi}{\Omega} \sum_n \delta\left(t - \tau - n \frac{2\pi}{\Omega}\right) \sum_m g(t - mT) \gamma^*\left(t - n \frac{2\pi}{\Omega} - mT\right) \\
&= \frac{2\pi}{\Omega} \sum_n \delta\left(t - \tau - n \frac{2\pi}{\Omega}\right) \sum_m \int g(\tau') \gamma^*\left(\tau' - n \frac{2\pi}{\Omega}\right) \delta(t - mT - \tau') d\tau' \\
&= \frac{2\pi}{\Omega} \sum_n \delta\left(t - \tau - n \frac{2\pi}{\Omega}\right) \int g(\tau') \gamma^*\left(\tau' - n \frac{2\pi}{\Omega}\right) \sum_m \delta(t - mT - \tau') d\tau' \\
&= \frac{2\pi}{\Omega} \sum_n \delta\left(t - \tau - n \frac{2\pi}{\Omega}\right) \int g(\tau') \gamma^*\left(\tau' - n \frac{2\pi}{\Omega}\right) \frac{1}{T} \sum_m e^{j(t - \tau') m \frac{2\pi}{T}} d\tau' \\
&= \sum_n \delta\left(t - \tau - n \frac{2\pi}{\Omega}\right) \sum_m e^{jtm \frac{2\pi}{T}} \underbrace{\frac{2\pi}{\Omega T} \int g(\tau') \gamma^*\left(\tau' - n \frac{2\pi}{\Omega}\right) e^{-j\tau' m \frac{2\pi}{T}} d\tau'}_{\delta_m \delta_n} \quad (A.2.23)
\end{aligned}$$

The resulting scheme expresses a biorthogonality condition between the analysis function $g(t)$ and the synthesis function $\gamma(t)$ and is named the *Continuous Biorthogonality Condition* (CBC):

$$\delta_m \delta_n = \frac{2\pi}{\Omega T} \int g(\tau) \gamma^*\left(\tau - m \frac{2\pi}{\Omega}\right) e^{-j\tau n \frac{2\pi}{T}} d\tau \quad (A.2.24)$$

$-\infty < m < \infty \quad -\infty < n < \infty$

As it is preferred to use **m** to index in time and **n** to index in frequency, and an interchange of **m** and **n** not change the constraints on γ , the **m** and **n** has to be interchanged equation (A.2.24). The δ_m is the Kronecker delta function. An interpretation of this orthogonality condition will be given later.

The continuous biorthogonality condition has only been solved for a very few functions. Bastiaans has solved the closed form for the analysis function, when the synthesis function was a Gaussian function at critical sampling [Bastiaans 81]. But the resulting analysis function is ei-

ther localized in the time or frequency dimension. However, the signal can still be reconstructed using the synthesis function. It is important to note that any function can be used as a synthesis/analysis function. The corresponding analysis/synthesis function has to be related through the bi-orthogonality condition.

When the analysis function is a Gaussian function, the reconstruction formula, equation (A2.22), is known as the Gabor expansion and the corresponding coefficients (Fourier) are called Gabor coefficients. The Gabor framework for continuous functions are constituted by the following three equations:

Continuous Gabor Expansion

Expansion:

$$x(t) = \sum_m \sum_n a_{mn} g_{mn}(t) = \sum_m \sum_n a_{mn} g(t - mT) e^{jn\Omega t} \quad (\text{A2.25})$$

Gabor coefficients:

$$a_{mn} = \int x(\tau) \gamma^*_{mn}(\tau) d\tau = \int x(\tau) \gamma^*(\tau - mT) e^{-jn\Omega\tau} d\tau \quad (\text{A2.26})$$

Biorthogonality condition:

$$\delta_m \delta_n = \frac{2\pi}{\Omega T} \int g(\tau) \gamma^*\left(\tau - m \frac{2\pi}{\Omega}\right) e^{-j\tau n \frac{2\pi}{T}} d\tau \quad (\text{A2.27})$$

$-\infty < m < \infty \quad -\infty < n < \infty$

A necessary condition for a stable reconstruction is that the area of the sampling lattice/grid is upper limited by $T\Omega \leq 2\pi$. If the area is larger than 2π , the expansion does not contain enough information about the signal to reconstruct it. This case is called *under sampling*. An area of 2π is the maximum necessary area to obtain an error free reconstruction and is named *critical sampling*. If the expansion uses a grid area smaller than 2π , the representation will be redundant, but more robust. This situation is called *oversampling*. This will be made clear in this appendix

Because the Gabor coefficients contain all information necessary to reconstruct the signal, the continuous spectrum can be obtained from the sampled values. This is seen by inserting the reconstruction formula into the STFT.

$$\begin{aligned}
F(t, \omega) &= \int x(\tau) \gamma^*(\tau - t) e^{-j\omega\tau} d\tau \\
&= \sum_m \sum_n a_{mn} g(\tau - mT) e^{j\tau n\Omega} \gamma^*(\tau - t) e^{-j\omega\tau} d\tau \\
&= \sum_m \sum_n a_{mn} \int g(\tau - mT) \gamma^*(\tau - t) e^{j\tau(n\Omega - \omega)} d\tau \\
&= \sum_m \sum_n a_{mn} \int g(\tau) \gamma^*(\tau + mT - t) e^{j(\tau + mT)(n\Omega - \omega)} d\tau \quad (\text{A2.28}) \\
&= \sum_m \sum_n a_{mn} e^{-j\omega mT} \int g(\tau) \gamma^*(\tau + mT - t) e^{-j\tau(\omega - n\Omega)} d\tau \\
&= \sum_m \sum_n a_{mn} e^{-j\omega mT} q(t - mT, \omega - n\Omega)
\end{aligned}$$

where $q(t, \omega) = \int g(\tau) \gamma^*(\tau - t) e^{-j\tau\omega} d\tau$

The function $q(t, \omega)$ is an interpolation function, which interpolates the missing values between the grid points in the time-frequency plan. This function is actually an STFT of the synthesis function.

A2.3 Periodic Discrete Gabor Expansion - PDGE

The PDGE is a sampled version of the CGE for periodic sequences of finite extent and was proposed by [Wexler 90]. The initial idea of a discrete Gabor expansion is to make the CGE capable of representing a sampled sequence $x[k]$ for $0 \leq k < N_1$. This can be obtained by constructing a periodic signal $\tilde{x}(t)$ where the non-zero values of each period are samples from the sequence $x[k]$. The following parameters will be used.

- Δ = Sampling interval for the continuous time signal $x(t)$ [s].
- T = Time step of CGE lattice [s].
- Ω = Frequency step of CGE lattice [rad/s].
- ΔM = Time step of the PDGE lattice - number of grids [integer].
- ΔN = Frequency step of the PDGE lattice - number of grids [integer].
- N_1 = Number of samples in the one period of the signal $x[k]$ [integer].
- = Number of grid in the frequency dimensionen in the PDGE
- = Number of grid in the time dimension in the PDGE
- = Number of samples in the analysis/synthesis function.
- M = Number of time steps ΔM in time dimension of the PDGE lattice [integer].
- N = Number of frequency steps ΔN in frequency dimension of PDGE lattice [integer].

These parameters are illustrated in the following Figure A2.3.

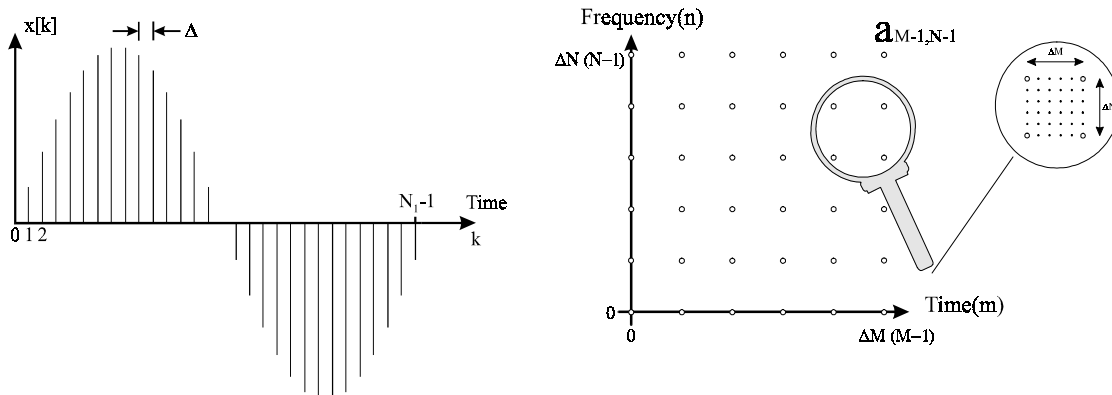


Figure A2.3 Sampling of the signal and sampling of the time-frequency plan.

Observe that the length of the analysis/synthesis function is equal to the number of samples N_1 in one period of the signal. This dependence is a disadvantage, and will be circumvent by the Discrete Gabor Expansion later. The frequency dimension is divided into N_1 grids, but the Gabor coefficients are only calculated every ΔN . The time dimension (one period) is divided into N_1 grid, but the Gabor coefficients are also only calculated every ΔM . Using these definitions, the following relations can be stated:

$$\begin{aligned}
 N \cdot \Delta N &= M \cdot \Delta M = N_1 \\
 T &= \frac{N_1 \cdot \Delta}{M} = \Delta M \cdot \Delta \\
 \Omega &= \frac{\frac{2\pi}{\Delta}}{N} = \Delta N \cdot \frac{\frac{2\pi}{\Delta}}{N_1}
 \end{aligned} \tag{A2.29}$$

In the case of critical sampling, the following relations are valid:

$$\begin{aligned}
 T \cdot \Omega = 2\pi &= \frac{N_1 \cdot \Delta}{M} \cdot \frac{2\pi}{\Delta} = \frac{N_1 \cdot 2\pi}{MN} \Rightarrow N_1 = MN \\
 N &= \frac{N_1}{M} = \frac{M \cdot \Delta M}{M} = \Delta M \\
 M &= \frac{N_1}{N} = \frac{N \cdot \Delta N}{N} = \Delta N \\
 M \cdot N &= \Delta N \cdot \Delta M = N_1
 \end{aligned} \tag{A2.30}$$

The discrete version of $T \cdot \Omega = 2\pi$ is $N_1 = MN$, and gives a lower bound for the number of Gabor coefficients necessary to reconstruct the signal to be the number of samples in the signal.

This illustrates that the Gabor expansion does not constitute any compression of the signal. The sampling factor SF is defined as the relation between the number of Gabor coefficients and the number of samples in the signal N_1

$$SF = \frac{M \cdot N}{N_1} = \frac{N_1}{\Delta M \cdot \Delta N} \tag{A2.31}$$

The continuous periodic signal $\tilde{x}(t)$ is constructed from the N_1 samples $x[k] = x(k \cdot \Delta)$ by first building one period with the non-zero samples, and then obtain a periodic signal $\tilde{x}(t) = \tilde{x}(t + N_1 \cdot \Delta)$ by repeating this:

$$\begin{aligned}
 1 - \text{period} \quad x_1(t) &= \sum_{k=0}^{N_1-1} x[k] \delta(t - k\Delta) \\
 \infty - \text{periods} \quad \tilde{x}(t) &= \sum_l x_1(t - l \cdot N_1 \Delta) = \sum_l \sum_{k=0}^{N_1-1} x[k] \delta(t - (l \cdot N_1 + k) \Delta)
 \end{aligned} \tag{A2.32}$$

When this signal representation is used to calculate the Gabor coefficients, the following equation is obtained:

$$\begin{aligned}
a_{mn} &= \int \tilde{x}(\tau) \gamma_{mn}^*(\tau) d\tau \\
&= \int \left(\sum_l \sum_{k=0}^{N_1-1} x[k] \delta(\tau - (l \cdot N_1 + k) \Delta) \right) (\gamma^*(\tau - mT) e^{-jn\tau\Omega}) d\tau \\
&= \sum_l \sum_{k=0}^{N_1-1} x[k] \int \delta(\tau - (l \cdot N_1 + k) \Delta) \gamma^*(\tau - mT) e^{-jn\tau\Omega} d\tau \\
&= \sum_l \sum_{k=0}^{N_1-1} x[k] \gamma^*((l \cdot N_1 + k) \Delta - mT) e^{-jnl(N_1+k)\Delta\Omega} \\
&= \sum_{k=0}^{N_1-1} x[k] \tilde{\gamma}^*(k\Delta - mT) e^{-jnk\Delta\Omega} \quad \text{where } \tilde{\gamma}(t) = \sum_l \gamma(t + l \cdot N_1 \cdot \Delta)
\end{aligned} \tag{A2.33}$$

The time step Δ can be removed from equation (A2.33), by using the discrete notation:

$$\begin{aligned}
\frac{T}{\Delta} &= \frac{\Delta M \cdot \Delta}{\Delta} = \Delta M \\
\Omega &= \frac{\frac{2\pi}{\Delta}}{N} \Leftrightarrow \Omega \Delta = \frac{2\pi}{N}
\end{aligned} \tag{A2.34}$$

These two conversions are inserted into equation (A2.33):

$$a_{mn} = \sum_{k=0}^{N_1-1} x[k] \tilde{\gamma}^*(k\Delta - mT) e^{-jnk\Delta\Omega} = \sum_{k=0}^{N_1-1} x[k] \tilde{\gamma}^*[k - m \cdot \Delta M] e^{-jkn\frac{2\pi}{N}} \tag{A2.35}$$

The periodic structure of $\tilde{\gamma}_{mn}[k]$ makes the Gabor coefficients periodic. This is illustrated by:

$$\begin{aligned}
a_{(m+M)n} &= \sum_{k=0}^{N_1-1} x[k] \tilde{\gamma}^*[k - (m+M) \cdot \Delta M] e^{-jkn\frac{2\pi}{N}} \\
&= \sum_{k=0}^{N_1-1} x[k] \tilde{\gamma}^*[k - m \cdot \Delta M - N_1] e^{-jkn\frac{2\pi}{N}} = a_{mn} \\
a_{m(n+N)} &= \sum_{k=0}^{N_1-1} x[k] \tilde{\gamma}^*[k - m \cdot \Delta M] e^{-jk(n+N)\frac{2\pi}{N}} \\
&= \sum_{k=0}^{N_1-1} x[k] \tilde{\gamma}^*[k - m \cdot \Delta M] e^{-jk\frac{2\pi}{N} - jk2\pi} = a_{mn}
\end{aligned} \tag{A2.36}$$

This periodic property of the coefficients can be exploited by limiting the indexing of a_{mn} to one period. This is done by dividing the index into two parts, one part controls the position in one period and the other part controls the period number:

$$\begin{aligned}
m &\rightarrow m + l \cdot M & 0 \leq m \leq M - 1 \\
&& l \in \mathbb{Z} \\
n &\rightarrow n + k \cdot N & 0 \leq n \leq N - 1 \\
&& k \in \mathbb{Z}
\end{aligned} \tag{A2.37}$$

The advantage of this separation is clear when used in the Gabor signal representation

$$\begin{aligned}
\tilde{x}(t) &= \sum_m \sum_n a_{mn} g(t - m \cdot T) e^{jtn\Omega} \\
&= \sum_{m=0}^{M-1} \sum_{n=0}^{N-1} \sum_l a_{mn} g(t - (m + l \cdot M) \cdot T) e^{jt(n+k \cdot N)\Omega}
\end{aligned} \tag{A2.38}$$

The next step is to use the conversion $MT = N_1 \cdot \Delta$ and $N \cdot \Omega = 2\pi/\Delta$.

$$\begin{aligned}
\tilde{x}(t) &= \sum_{m=0}^{M-1} \sum_{n=0}^{N-1} a_{mn} \sum_l g(t - m \cdot T - l \cdot N_1 \cdot \Delta) e^{jtn\Omega} \sum_k e^{jtk\frac{2\pi}{\Delta}} \\
&= \sum_{m=0}^{M-1} \sum_{n=0}^{N-1} a_{mn} \sum_l g(t - m \cdot T - l \cdot N_1 \cdot \Delta) e^{jtn\Omega} \Delta \sum_k \delta(t - k\Delta) \\
&\Leftrightarrow \\
\tilde{x}[k] &= \sum_{m=0}^{M-1} \sum_{n=0}^{N-1} a_{mn} \sum_l g(k\Delta - m \cdot T - l \cdot N_1 \cdot \Delta) e^{jk\Delta n\Omega} \\
&= \sum_{m=0}^{M-1} \sum_{n=0}^{N-1} a_{mn} \tilde{g}(k\Delta - m \cdot T) e^{jkn\frac{2\pi}{N}} \\
&= \sum_{m=0}^{M-1} \sum_{n=0}^{N-1} a_{mn} \tilde{g}[k - m \cdot \Delta M] e^{jkn\frac{2\pi}{N}} \\
&= \sum_{m=0}^{M-1} \sum_{n=0}^{N-1} a_{mn} \tilde{g}_{mn}[k]
\end{aligned} \tag{A2.39}$$

The first point in a Gabor representation is the choice of synthesis function $g[n]$. This function defines the first period in the periodic function $\tilde{g}[n]$ given by:

$$\tilde{g}[n] = \sum_{l=-\infty}^{\infty} g[n - lN_1] \tag{A2.40}$$

In order not to have overlapping functions, the extent of $g[n]$ has to be less than N_1 samples. Furthermore, the following two demands are necessary:

$$\sum_{k=0}^{N_1-1} |g[k]|^2 = 1 \quad (A2.41)$$

$$\sum_{k=0}^{N_1-1} \left| \frac{g[k]}{g_{MAX}} \right| = T_1$$

The first demand energy normalizes the synthesis function, and the second demand defines the effective bandwidth T_1 ($T_1 = \sigma\sqrt{2\pi}$). A usable synthesis function is the energy normalized Gaussian function given by:

$$g[n] = \frac{2^{0,25}}{T_1^{0,5}} \exp\left(-\pi\left(\frac{n - \frac{N_1-1}{2}}{T_1}\right)^2\right) \quad 0 \leq n \leq N_1-1 \quad (A2.42)$$

The second point in a Gabor representation is to determine the analysis function. The relation between the analysis function $\gamma[k]$ and synthesis function $g[k]$ is expressed by the *Periodic Discrete Biorthogonality condition* (PDBC). The procedure follows the CBC. The expression for the Gabor coefficients is inserted in the Gabor expansion.

$$\begin{aligned}
x[k] &= \sum_{m=0}^{M-1} \sum_{n=0}^{N-1} a_{mn} \tilde{g}_{mn}[k] \\
&= \sum_{m=0}^{M-1} \sum_{n=0}^{N-1} \left(\sum_{k'=0}^{N_1-1} x[k'] \tilde{\gamma}_{mn}^*[k'] \right) \tilde{g}_{mn}[k] \\
&= \sum_{k'=0}^{N_1-1} x[k'] \underbrace{\sum_{m=0}^{M-1} \sum_{n=0}^{N-1} \tilde{\gamma}_{mn}^*[k'] \tilde{g}_{mn}[k]}_{\delta_{k-k'}} \\
&\quad \delta_{k-k'} \\
\delta_{k-k'} &= \sum_{m=0}^{M-1} \sum_{n=0}^{N-1} \tilde{\gamma}_{mn}^*[k'] \tilde{g}_{mn}[k] \tag{A2.43} \\
&= \sum_{m=0}^{M-1} \sum_{n=0}^{N-1} \tilde{\gamma}^*[k - m \cdot \Delta M] e^{-jk'n \frac{2\pi}{N}} \tilde{g}[k - m \cdot \Delta M] e^{jkn \frac{2\pi}{N}} \\
&= \sum_{n=0}^{N-1} e^{jn(k-k')} \frac{2\pi M-1}{N} \sum_{m=0}^{M-1} \tilde{\gamma}^*[k - m \cdot \Delta M] \tilde{g}[k - m \cdot \Delta M] \\
&= \sum_q \delta_{k-k'-qN} \underbrace{N \sum_{m=0}^{M-1} \tilde{\gamma}^*[k - qN - m \cdot \Delta M] \tilde{g}[k - m \cdot \Delta M]}_{\delta_q}
\end{aligned}$$

$$\begin{aligned}
\delta_q &= N \sum_{m=0}^{M-1} \tilde{\gamma}^* [k - qN - m \cdot \Delta M] \tilde{g} [k - m \cdot \Delta M] \\
&= \frac{1}{\Delta M} \sum_{k_1=0}^{\Delta M-1} \left(\sum_{k=0}^{\Delta M-1} \left(N \sum_{m=0}^{M-1} \tilde{\gamma}^* [k - qN - m \cdot \Delta M] \tilde{g} [k - m \cdot \Delta M] \right) e^{-j k k_1 \frac{2\pi}{\Delta M}} \right) e^{-j k_1 k \frac{2\pi}{\Delta M}} \\
&= \sum_{k_1=0}^{\Delta M-1} \left(\frac{N}{\Delta M} \sum_{k=0}^{N_1-1} \tilde{\gamma}^* [k - qN] e^{-j k k_1 \frac{2\pi}{\Delta M}} \tilde{g} [k] \right) e^{-j k_1 k \frac{2\pi}{\Delta M}} \\
&= \sum_{k_1=0}^{\Delta M-1} \left(\frac{N}{\Delta M} \sum_{k=0}^{N_1-1} \tilde{\gamma}^* [k] e^{-j (k + qN) k_1 \frac{2\pi}{\Delta M}} \tilde{g} [k + qN] \right) e^{-j k_1 k \frac{2\pi}{\Delta M}} \tag{A2.44} \\
&= \sum_{k_1=0}^{\Delta M-1} \left(\frac{N}{\Delta M} \sum_{k=0}^{N_1-1} \tilde{\gamma}^* [k] \tilde{g}_{-q, -k_1} [k] e^{-j q k_1 2\pi \frac{N_1}{\Delta M \Delta N}} \right) e^{-j k_1 k \frac{2\pi}{\Delta M}} \\
&= \sum_{k_1=0}^{\Delta M-1} e^{-j k_1 k \frac{2\pi}{\Delta M}} \underbrace{\frac{N}{\Delta M} \sum_{k=0}^{N_1-1} \tilde{\gamma}^* [k] \tilde{g}_{-q, -k_1} [k]}_{\delta_q \cdot \delta_{k_1}}
\end{aligned}$$

The term $\exp\left(-j q k_1 2\pi \frac{N_1}{\Delta M \Delta N}\right)$ can be dropped under assumption of integer samplings factor.

This last k-sum constitutes the PDBC. Again, it is desirable to use the n-variable to index the frequency domain, and the m-variable to index the time domain. The final PDBC using can be stated as:

$$\delta_m \cdot \delta_n = \frac{MN}{N_1} \sum_{k=0}^{N_1-1} \tilde{\gamma}^* [k] \tilde{g} [k + mN] e^{-j k n \frac{2\pi}{\Delta M}} \tag{A2.45}$$

$$0 \leq m \leq \Delta N - 1 \quad 0 \leq n \leq \Delta M - 1$$

The analysis function $\gamma(t)$ can now be found as the solution of this linear system of equations. The system consists of $\Delta N \cdot \Delta M$ equations with N_1 unknown samples of $\gamma(t)$.

The set of equation for the PDGE is given by:

Periodic Discrete Gabor Expansion

Expansion:

$$\tilde{x}[k] = \sum_{m=0}^{M-1} \sum_{n=0}^{N-1} a_{mn} \tilde{g}_{mn}[k] = \sum_{m=0}^{M-1} \sum_{n=0}^{N-1} a_{mn} \tilde{g}[k - m \cdot \Delta M] e^{jkn \frac{2\pi}{N}} \quad (\text{A2.46})$$

Gabor coefficients:

$$a_{mn} = \sum_{k=0}^{N_1-1} x[k] \tilde{\gamma}_{mn}^*[k] = \sum_{l=0}^{N_1-1} \sum_{k=0}^{N-1} x[k] \tilde{\gamma}_{mn}^*[l \cdot N_1 + k] \quad (\text{A2.47})$$

Biorthogonality condition:

$$\delta_m \cdot \delta_n = \frac{MN}{N_1} \sum_{k=0}^{N_1-1} \tilde{\gamma}^*[k] \tilde{g}[k + mN] e^{-jkn \frac{2\pi}{\Delta M}} \quad (\text{A2.48})$$

$$0 \leq m \leq \Delta N - 1 \quad 0 \leq n \leq \Delta M - 1$$

A2.4 Discrete Gabor Expansion - DGE

The DGT is an extension of the PDGE to handle discrete long non-periodic signals. This approach was proposed by Shie Qian [Qian 93]. The difficulty of the PDGE is the PDBC. At critical sampling, this system of equations contain $\Delta N \cdot \Delta M = N_1$ equations with N_1 unknown. As N_1 is the signal length, the system have to be solved for each new signal, with a different length. Further, in the case of a real signal of maybe 1k-1G sampler, the PDBC is practically unsolvable. The core of the DGE is to make the PDBC independent of the signal length. In the PDGE, the variable N_1 controlled the following four quantities:

- N_1 = Number of samples in the analysis/synthesis function.
- = Number of grid in the frequency dimensionen in the PDGE
- = Number of grid in the time dimension in the PDGE
- = Number of samples in the one periode of the signal $x[k]$ [integer].

In the DGE, the first step is to decouple the length of the signal and the length of the analysis and synthesis functions:

- N_1 = Number of samples in the analysis/synthesis function.
- = Number of grid in the frequency dimensionen in the DGE
- = Number of grid in the time dimension in the DGE
- L_s = Number of samples in the signal $x[k]$ [integer].

In both the PDGE and the DGE, a frame of N_1 samples from the signal (in the case of the PDGE, the whole signal) is represented by $M \cdot N$ Gabor coefficients. The new variable L_s is used in the following new definition of the periodic analysis and systhesis functions (illustrated in Figure A2.4):

$$\begin{aligned} \bar{g}[k + \text{const.} \cdot L_s] &= \begin{cases} g[k] & \text{for } 0 \leq k < N_1 \\ 0 & \text{for } N_1 \leq k < L_s \end{cases} \\ \bar{\gamma}[k + \text{const.} \cdot L_s] &= \begin{cases} \gamma[k] & \text{for } 0 \leq k < N_1 \\ 0 & \text{for } N_1 \leq k < L_s \end{cases} \\ \bar{x}[k + \text{const.} \cdot L_s] &= x[k] \quad \text{for } 0 \leq k < L_s \end{aligned} \quad (\text{A2.49})$$

Now, arbitrary signal length can be used without changing the non-zero part of \bar{g} and $\bar{\gamma}$. The gaussian shaped synthesis function $g[k]$ is defined by:

$$g[k] = \begin{cases} 0 & \text{for } k < 0 \\ \sqrt{\frac{2}{T_1}} \cdot e^{-\pi \cdot \left(\frac{k-0,5(N_1-1)}{T_1} \right)^2} & \text{for } 0 \leq k \leq N_1 - 1 \\ 0 & \text{for } N_1 \leq k \end{cases} \quad (\text{A2.50})$$

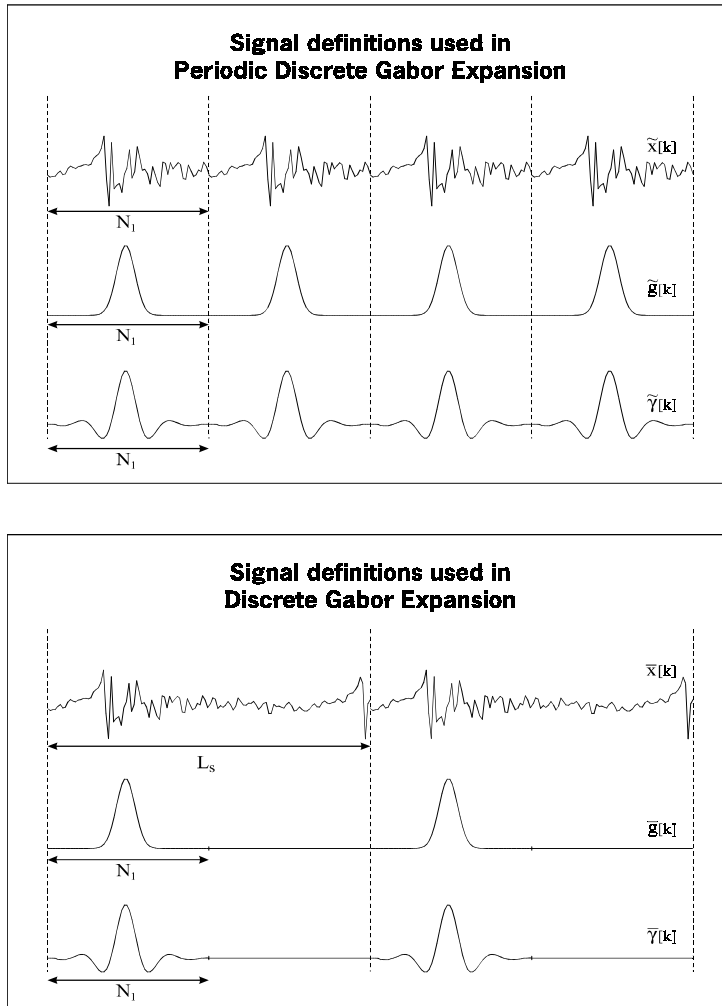


Figure A2.4 The signal definition used in the DGE.

The new signal definitions are now inserted into equation (A2.47):

$$a_{mn} = \sum_{k=0}^{L_s-1} x[k] \tilde{\gamma}^*[k - m \cdot \Delta M] e^{-jkn \frac{2\pi}{N}} \quad (\text{A2.51})$$

The number of Gabor coefficients in the time doamin is no longer M but the number of possible shift of the analysis function inside the signal length - now called M_{total} ¹:

$$M_{Total} = \frac{L_s - N_1}{\Delta M} + 1 \quad (\text{A2.52})$$

The k-summation is dependent on the signal length, but the analysis function is only non-zero in N_1 samples. The summation can therefore be reduced to only including these terms:

1. In the case of a non-integer, the result is round off down to the nearest integer.

$$\begin{aligned}
a_{mn} &= \sum_{k=m \cdot \Delta M}^{m \cdot \Delta M + N_1 - 1} x[k] \gamma^* [k - m \cdot \Delta M] e^{-jkn \frac{2\pi}{N}} \\
&= \sum_{k=0}^{N_1 - 1} x[k + m \cdot \Delta M] \gamma^* [k] e^{-j(k + m \cdot \Delta M)n \frac{2\pi}{N}} \\
&= e^{-jmn\Delta M \frac{2\pi N_1}{N}} \sum_{k=0}^{N_1 - 1} x[k + m \cdot \Delta M] \gamma^* [k] e^{-jkn \frac{2\pi}{N}}
\end{aligned} \tag{A2.53}$$

for
 $0 \leq m \leq M_{Total}$ $0 \leq n < N$

When the new signal definitions are used in equation (A2.46), the discrete signal $x[k]$ can be reconstructed by:

$$\begin{aligned}
x[k] &= \sum_{m=0}^{M_{Total}-1} \sum_{n=0}^{N-1} a_{mn} \bar{g}[k - m \cdot \Delta M] e^{jkn \frac{2\pi}{N}} \\
&= \sum_{m=0}^{M_{Total}-1} \sum_{n=0}^{N-1} a_{mn} g_{mn}[k] \quad \text{for } 0 \leq k < L_s
\end{aligned} \tag{A2.54}$$

as $\bar{g}[k]$ is only indexed inside the non-zero part of $g[k]$ equation (A2.50). The main difference between the PDGE and the DGE is the biorthogonality condition. From the PDGE we had:

$$\delta_m \cdot \delta_n = \frac{MN}{N_1} \sum_{k=0}^{N_1-1} \tilde{\gamma}^*[k] \tilde{g}[k + mN] e^{-jkn \frac{2\pi}{\Delta M}} \tag{A2.55}$$

$0 \leq m \leq \Delta N - 1$ $0 \leq n \leq \Delta M - 1$

The first step to develop a *Discrete Biorthogonality Condition* (DBC) from the PDBC is to insert the new signal definitions:

$$\begin{aligned}
\delta_m \cdot \delta_n &= \frac{MN}{N_1} \sum_{k=0}^{L_s-1} \tilde{\gamma}^*[k] \bar{g}[k + mN] e^{-jkn \frac{2\pi}{\Delta M}} \\
&\quad 0 \leq m \leq \frac{L_s}{N} - 1 \quad 0 \leq n \leq \Delta M - 1
\end{aligned} \tag{A2.56}$$

This system of equations contain $\Delta M \cdot L_s / N$ equations with L_s unknowns. As the length of the signal increases, the number of equations increases, but the number of non-zero equations remains constant. A non-zero equation appears when the analysis and synthesis function are overlapping, and this will only take place at a finite number of time shifts. When $\bar{g}[k]$ is time shifted more than $\pm N_1$ samples, the two functions are not overlapping. As the biorthogonality condition uses a time step N , the overlapping steps will be $-N_1/N < m < N_1/N$. Using only these equations, the total number of equations has now been reduced to:

$$\text{Number of equations} = \left(2 \frac{N_1}{N} - 1 \right) \cdot \Delta M = (2\Delta N - 1) \cdot \Delta M \tag{A2.57}$$

Another modification of equation (A2.56) is to reduce the k-summation to only include the first N_1 terms as the remaining $L_s - N_1$ terms are zero because $\bar{\gamma}[k]$ is zero. These two modifications makes the PDBC independent of the signal length and the result is called the *Discrete Biorthogonality Condition (DBC)* :

$$\delta_m \cdot \delta_n = \frac{MN}{N_1} \sum_{k=0}^{N_1-1} \gamma^*[k] g[k + mN] e^{-jkn\frac{2\pi}{\Delta M}} \quad (A2.58)$$

$-\Delta N < m < \Delta N \quad 0 \leq n \leq \Delta M - 1$

The biorthogonality condition expresses the inner-product between the unknown analysis function $\gamma[k]$, and time and frequency shifted synthesis function $g[k]$. For arbitrary time shift mN and frequency shift $2\pi/\Delta M$, the inner-product has to be zero - the two functions are orthogonal!

The final set of equations for the DGE can now be summarized to:

Discrete Gabor Expansion

Expansion:

$$x[k] = \sum_{m=0}^{M_{Total}-1} \sum_{n=0}^{N-1} a_{mn} g[k - m \cdot \Delta M] e^{jkn\frac{2\pi}{N}} \quad (A2.59)$$

$0 \leq k < L_s$

Gabor coefficients:

$$a_{mn} = e^{-jmn\Delta M\frac{2\pi N_1}{N}} \sum_{k=0}^{N_1-1} x[k + m \cdot \Delta M] \gamma^*[k] e^{-jkn\frac{2\pi}{N}} \quad (A2.60)$$

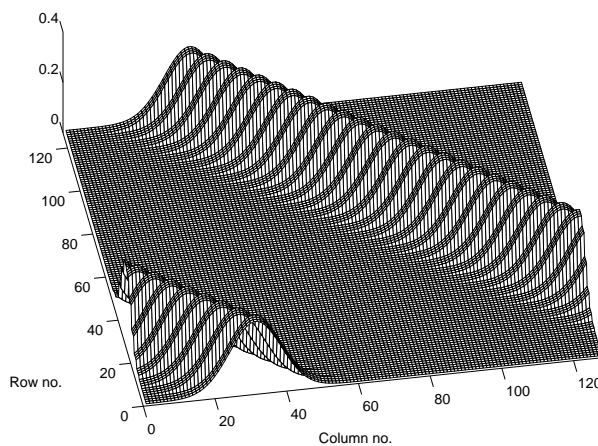
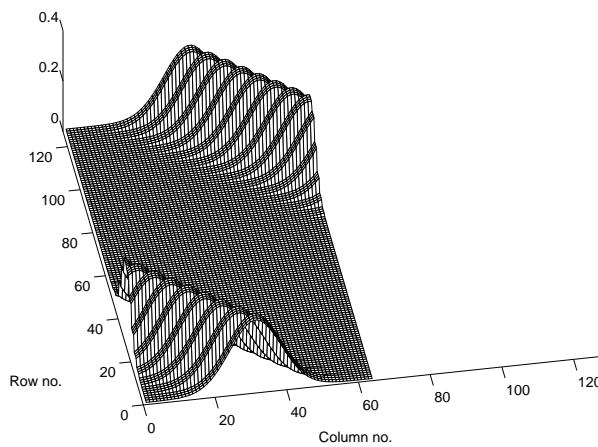
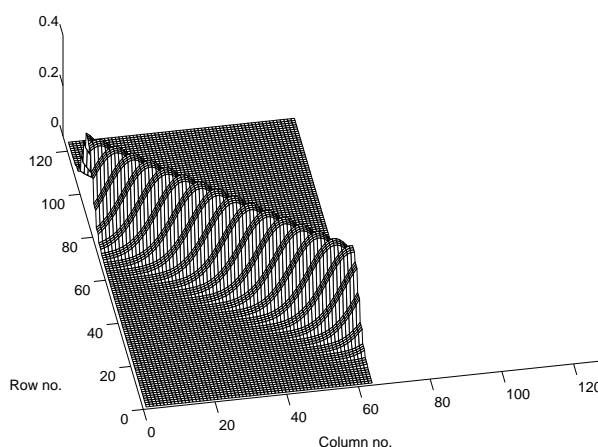
$0 \leq m \leq M_{Total} \quad 0 \leq n < N$

Biorthogonality condition:

$$\delta_m \cdot \delta_n = \frac{MN}{N_1} \sum_{k=0}^{N_1-1} \gamma^*[k] g[k + mN] e^{-jkn\frac{2\pi}{\Delta M}} \quad (A2.61)$$

$-\Delta N < m < \Delta N \quad 0 \leq n \leq \Delta M - 1$

Using matrix notation, equation (A2.61) can be expressed by $H\gamma = \delta_m \cdot \delta_n$. For illustration purpose, the content of the H matrix is illustrated in Figure A2.5 for $N_1=64$ and $L_s=128$ as the two modifications are introduced.

(a) System matrix^a of equation (A2.56)(b) Including only the first N_1 terms of the K-sum of equation (A2.56)

(c) Rearranging of non-zero equations of equation (A2.56)

- four zero equations has been removed from Figure A2.5b.

Figure A2.5 Graphic illustration of system matrices i DBC

a. As the system matrix is complex, only the magnitude is illustrated.

The remaining part of this appendix, the practical implementation of the DGE will be addressed.

Step 1. Implementation of the Biorthogonality condition.

To implement the DGE, the DBC has to be solved. The main advantage of this DBC is its independence of the signal length. Both the analysis and synthesis functions have a fixed length of N_1 , and this can be selected independently of the length of the signal length. The following parameters have to be set:

- T_1 Effective bandwidth of the synthesis function.
- N_1 Length of the analysis/synthesis functions.
- M Number of sampling intervals in the time dimension.
- N Number of sampling intervals in the frequency dimension.

This leaves the DGT with many degrees of freedom. Using matrix notation, equation (A2.61) can be expressed by:

$$H_{(2\Delta N - 1) \times \Delta M \times N_1} \gamma_{N_1 \times 1} = u_{(2\Delta N - 1) \times \Delta M \times 1}$$

where

$$H[n + (m + \Delta N - 1) \cdot \Delta M + 1, k + 1] = g[k + mN] e^{-jkn \frac{2\pi}{\Delta M}}$$

$$0 \leq k \leq N_1 - 1 \quad -(\Delta N - 1) \leq m \leq (\Delta N - 1) \quad 0 \leq n \leq \Delta M - 1$$

and

(A2.62)

$$u[k] = \begin{cases} 0 & \text{for } 1 \leq k \leq (\Delta N - 1) \cdot \Delta M \\ \frac{N_1}{MN} & \text{for } k = (\Delta N - 1) \cdot \Delta M + 1 \\ 0 & \text{for } (\Delta N - 1) \cdot \Delta M + 2 \leq k \leq (2\Delta N - 1) \cdot \Delta M \end{cases}$$

The matrix H and the vector u can be constructed in matlab using the following code:

```
% Initial
N = 16;
M = 16;
N1 = 64;
dM = N1/M;
dN = N1/N;
T1 = 8;
g=(2^0.25)./(T1^0.5)*exp(-pi*(([0:N1-1]-0.5*(N1-1))./T1).^2);

% System matrix
for m=-(dN-1):1:(dN-1),
    for n=0:1:dM-1,
        for k=0:1:N1-1,
            arg=k+m*N;
            if arg>=0,
                if arg<N1,
                    H((m+dN-1)*dM+n+1,k+1)=g(arg+1)*exp(-j*k*n*2*pi/dM);
                ,end
            ,end
        ,end
    ,end
u=zeros((2*dN-1)*dM,1);
u((dN-1)*dM+1,1)=N1/(M*N);
```

The matrix H cannot be expected to be of full-rank, and a H^{-1} does therefore not exist. In the case where the system have an infinity number of solutions, a choise has to be made. The analysis function γ , who has a shape close or identical to g is to be preferred. The Gabor coefficients are very dependent on the γ , and if the coefficients should illustrate information about the signal local time and frequency structure, it is vital that γ is well-behaved and localized in both time and frequency. As the gaussian function like g is the ideal function for this purpose, we prefer a solution vector for γ close to g . When $g(t)$ and $\gamma(t)$ have the same shape, $g(t)$ is orthogonal with both $\gamma(t)$ and itself. Such a Gabor expansion is called orthogonal-Like Gabor expansion [Qian 93]. To evaluate the error between the solution vector γ and the preferred solution vector g , the following error measure is introduced:

$$E = \sum_{k=0}^{N_1-1} \left| \frac{\gamma[k]}{\|\gamma\|} - g[k] \right|^2 \quad (\text{A2.63})$$

This set the constraints on how to select between varius γ . By further rewriting of equation (A2.63), the following fact can be found about the perfered solution vector:

$$\begin{aligned} E &= \sum_{k=0}^{N_1-1} \left| \frac{\gamma[k]}{\|\gamma\|} - g[k] \right|^2 = \sum_{k=0}^{N_1-1} \left(\frac{\gamma[k]^2}{\|\gamma\|^2} - 2 \frac{\gamma[k]}{\|\gamma\|} g[k] + g[k]^2 \right) \\ &= \frac{\sum_{k=0}^{N_1-1} \gamma[k]^2}{\|\gamma\|^2} - \frac{\sum_{k=0}^{N_1-1} \gamma[k] g[k]}{\|\gamma\|} + \sum_{k=0}^{N_1-1} g[k]^2 = \frac{\|\gamma\|^2}{\|\gamma\|^2} - \frac{2 \frac{N_1}{MN}}{\|\gamma\|} + \|g\|^2 \\ &= 2 - 2 \frac{N_1}{MN} \cdot \frac{1}{\|\gamma\|} \geq 0 \Rightarrow \|\gamma\| \geq \frac{N_1}{MN} \end{aligned} \quad (\text{A2.64})$$

So the preferred solution is a minimum length solution. If the null-space of H is empty, a solution could be obtained using least squares, but in the case of a non-zero null-space a minimum length least squares solution $\gamma^+ = H^+ u$ can always be obtained using the pseudo inverse H^+ . The application of pseudo-inverse should be well-known from Linear Algebra, and is illustrated in Figure A2.6 for revision.

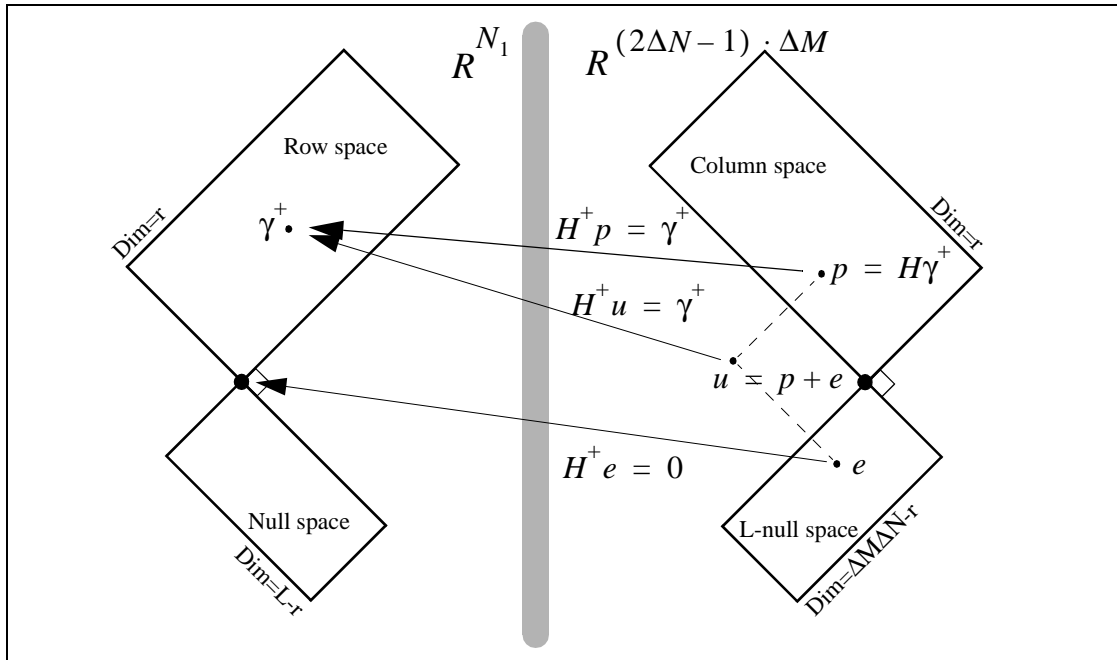


Figure A2.6 H is invertible from row space to column space. H^+ inverts it.

The pseudo inverse is calculated from the Singular Value Decomposition (SVD) diagonalization of H :

$$H_{row \times col} = U_{row \times row} \Sigma_{row \times col} V_{col \times col}^T = [u_1 \ u_2 \ \dots \ u_{row}] \begin{bmatrix} \sigma_1 & 0 & 0 & \dots \\ 0 & \sigma_2 & 0 & \dots \\ \dots & \dots & \dots & \dots \\ 0 & 0 & 0 & \sigma_{col} \\ 0 & 0 & 0 & 0 \end{bmatrix}^T [v_1 \ v_2 \ \dots \ v_{col}]^T \quad (\text{A2.65})$$

where $row = (2\Delta N - 1) \cdot \Delta M$ and $col = N_1$

The pseudo inverse is constructed from the following sum of eigenvectors and singular values:

$$H^+ = \sum_{k=1}^R \frac{v_i u_i^T}{\sigma_i} \quad (\text{A2.66})$$

where the R is the rank of H - equal to the number of $\sigma > 0, 1$. The pseudo inverse solution γ^+ is now calculated by:

$$\gamma^+ = H^+ u \quad (\text{A2.67})$$

The Matlab code for this pseudo inverse solution is:

```
% Pseudo inverse solution of DBC
[U S V]=svd(H);
[m n]=size(H);
H_inv(n,m)=0;
[row_antal,sojle_antal]=size(S);
```

```

for n=1:min([row_antal,sojle_antal]),
    if (S(n,n)>0.1),
        H_inv=H_inv+V(:,n)*U(:,n)'./S(n,n);
    ,end
,end
analysis=real(H_inv*u);

```

The shape of analysis function depend strongly on how the parameters are selected. In the following, some guidelines for this parameter choice are given.

The parameter N_1 is the length of the analysis and synthesis functions. It also indicate that N_1 samples from the signal are represented by $SF \cdot N_1 = M \cdot N$ Gabor coefficients in the DGE. When N_1 , the samplings factor SF and the number of Gabor coefficients in the time dimension have been selected, the remaining parameters are fixed: the number of Gabor coefficients in the Frequency dimension has to be $N = N_1 \cdot SF/M$, the time step is $\Delta M = N_1/M$, the frequency step is $\Delta N = N_1/N$. The effective bandwidth of the synthesisfunction is not fixed, but experimental simulations have shown that a good choice is $T_1 \approx \sqrt{\Delta M \cdot N}$. The following three Orthogonal-Like Gabor has been found:

Variable\base	base 64	base 128	base 256
N_1	64	128	256
SF	4	4	4
M	16	16	8
$N = N_1 \cdot SF/M$	16	32	128
$\Delta M = N_1/M$	4	8	32
$\Delta N = N_1/N$	4	4	2
$T_1 \approx \sqrt{\Delta M \cdot N}$	8	16	64

Table A2.1Orthogonal-Like Gabor expansion

Both analysis and synthesis functions for *base64*, *base128* and *base256* have a gaussian shape. To illustrate the effects of T_1 on the error between the analysis, the error E as a function of T_1 have been calculated for the three orthogonal-like bases from Table A2.1, and placed in Figure A2.7 .

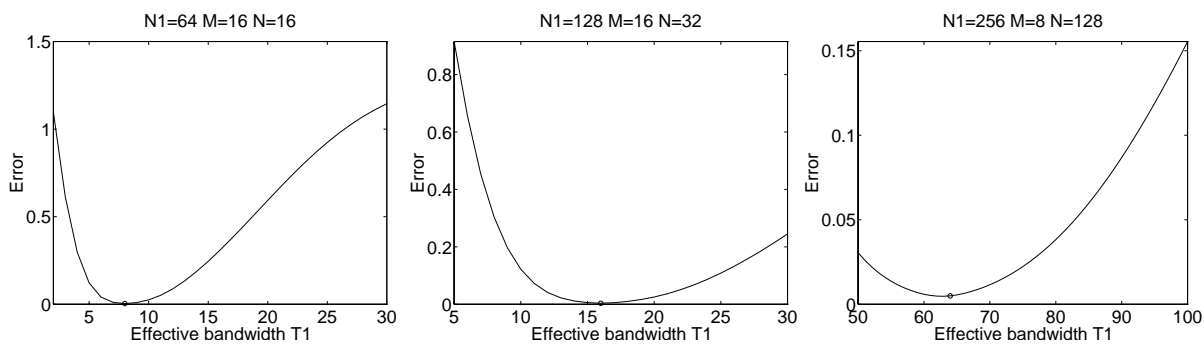


Figure A2.7 The error function $E(T_1)$ versus the effective bandwidth

The proposed value $T_1 \approx \sqrt{\Delta M \cdot N}$ has been indicated with a circle. It is clear that this is an optimal value for a orthogonal-like expansion. The resulting analysis function is also very dependent on the samplings factor. This is illustrated for base128 in Figure A2.8.

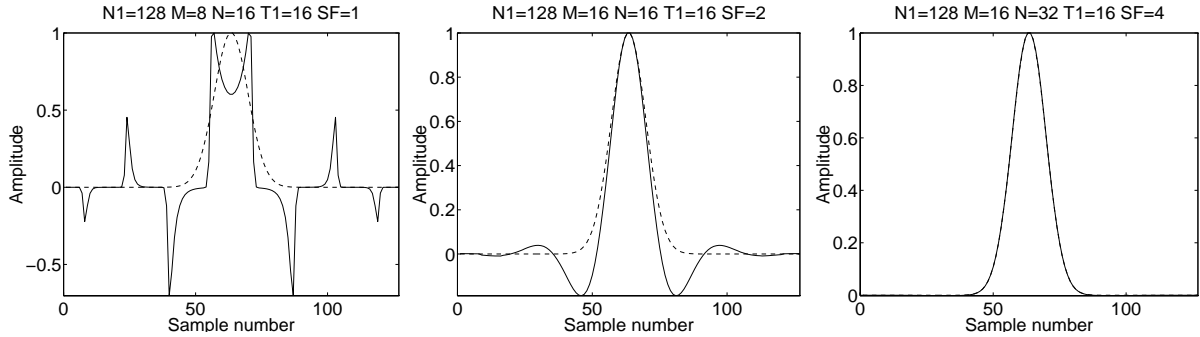


Figure A2.8 Analysis and synthesis functions versus samplings factor.

As the sampling factor is increased, the analysis function is getting more localized in both time and frequency. The Gabor coefficients calculated using the analysing function for a factor of 1-2 will not illustrate the local time and frequency properties of the signal, but they will all reconstruct the signal equally well.

The coefficients can be calculated with the FFT algorithm when the following modification is done:

$$\begin{aligned}
 a_{mn} &= e^{-jmn\Delta M \frac{2\pi}{N}} \sum_{k=0}^{2\pi N_1 - 1} x[k + m \cdot \Delta M] \gamma^*[k] e^{-jkn \frac{2\pi}{N}} \\
 &= e^{-jmn\Delta M \frac{2\pi}{N}} \sum_{b=0}^{N_1 - 1} \sum_{a=0}^{N-1} x[a + bN + m \cdot \Delta M] \gamma^*[a + bN] e^{-j(a + bN)n \frac{2\pi}{N}} \\
 &= e^{-jmn\Delta M \frac{2\pi}{N}} \sum_{b=0}^{N-1} \underbrace{\sum_{a=0}^{N-1} x[a + bN + m \cdot \Delta M] \gamma^*[a + bN] e^{-jan \frac{2\pi}{N}}}_{\text{FFT}}
 \end{aligned} \quad (\text{A2.68})$$

For each time step m , all N Gabor coefficients can be calculated by adding ΔN FFT vectors

followed by a phase shift $e^{-jmn\Delta M \frac{2\pi}{N}}$.

The following matlab code will calculate the Gabor coefficients for a vector called *signal*:

```
% Gabor transformation
x=zeros(1,0.5*N1) signal zeros(1,0.5*N1);
L_s=length(x);
M_total=fix( (L_s-N1)/dM )+1;

for m=0:M_total-1,
    a(N,m+1)=0;
    for b=0:dN-1,
        s=x(b*N+[0:N-1]+m*dM+1).'*analysis([0:N-1]+1+b*N);
        F=fft(s);
        a(:,m+1)=a(:,m+1)+F;
    ,end
    a(:,m+1)=a(:,m+1).*exp(-j*[0:N-1]'*m*dM*2*pi/N);
,end
```

When the coefficients are calculated, it is possible to reestablish the signal with the following formula:

$$x[k] = \sum_{m=0}^{M_{total}-1} \sum_{n=0}^{N-1} a_{mn} g \underbrace{[k - m \cdot \Delta M]}_{\text{Include only the contributions of the sum, in which the argument is in the interval 0 to } L-1} \exp\left(jkn \frac{2\pi}{N}\right) \quad (\text{A2.69})$$

Include only the contributions of the sum, in which
the argument is in the interval 0 to $L-1$

The reconstruction is important, because it tests the validity of the Gabor coefficients. When the original signal was a real signal, the number of summation can be reduced by exploring the symmetry of the coefficients:

$$x[k] = \sum_{m=0}^{M_{total}-1} \sum_{n=0}^{N-1} a_{mn} g [k - m \cdot \Delta M] \exp\left(jkn \frac{2\pi}{N}\right) = \sum_{m=0}^{M_{total}-1} g [k - m \cdot \Delta M] \cdot \begin{cases} \sum_{n=1}^{\frac{N}{2}-1} 2|a_{mn}| \cos\left(kn \frac{2\pi}{N} + \angle a_{mn}\right) + \operatorname{Re}\{a_{mn}\} + \operatorname{Re}\{a_{mn}\} \cos(k\pi) \\ \end{cases} \quad (\text{A2.70})$$

A possible Matlab implementation of the reconstruction formula is the following code:

```
% Reconstruction
k=[0:1:(M_total-1)*dM-1+N1];
s=zeros(1,length(k));
for m=0:M_total-1,
    for n=1:0.5*N-1,
        s(m*dM+1:m*dM+N1)=s(m*dM+1:m*dM+N1)+abs(a(n+1,m+1))...
        *g.*2.*cos(angle(a(n+1,m+1))+n*(m*dM:m*dM+N1-1)*2*pi./N);
    ,end
    s(m*dM+1:m*dM+N1)=s(m*dM+1:m*dM+N1)+real(a(0+1,m+1))...
    .*g+real(a(0.5*N+1,m+1)).*g.*cos((m*dM:m*dM+N1-1)*pi);
,end
x_r=s(0.5*N1+1:0.5*N1+(M_total-1)*dM);
```

Appendix 3

Gabor spectrogram

This appendix derive the decomposition of the Wigner-Ville distribution by a Gabor transformation of the signal. It follows the pioneering work of Qian et al. [Qian 94], and is extended by an implementation approach.

A discrete signal can be represented by the following Gabor expansion:

$$x[k] = \sum_{m=0}^{M-1} \sum_{n=0}^{N-1} a_{mn} g[k - m \cdot \Delta M] e^{jkn \frac{2\pi}{N}} \quad (\text{A3.1})$$

When the Gabor coefficients contain sufficient information to reconstruct the discrete signal, it will be possible to reconstruct the continuous signal likewise:

$$\begin{aligned} x(k\Delta) &= \sum_{m=0}^{M-1} \sum_{n=0}^{N-1} a_{mn} g(k\Delta - m \cdot \Delta M \cdot \Delta) e^{jk\Delta n \frac{2\pi}{N\Delta}} \\ &\Leftrightarrow \\ x(t) &= \sum_{m=0}^{M-1} \sum_{n=0}^{N-1} a_{mn} g(t - m \cdot T) e^{jtn\Omega} \end{aligned} \quad (\text{A3.2})$$

The continuous signal representation can be inserted into the Wigner-Ville distribution. Because the signal is continuous, no preprocessing like oversampling will be necessary:

$$\begin{aligned} WVD_x(t, \omega) &= \int x(t + \tau/2) x^*(t - \tau/2) e^{-j\omega\tau} d\tau \\ &= \int \sum_{m=0}^{M-1} \sum_{n=0}^{N-1} a_{mn} g(t + \tau/2 - m \cdot T) e^{j(t + \tau/2)n\Omega} \\ &\quad \cdot \sum_{m'=0}^{M-1} \sum_{n'=0}^{N-1} a_{m'n}^* g^*(t - \tau/2 - m' \cdot T) e^{-j(t - \tau/2)n'\Omega} e^{-j\omega\tau} d\tau \quad (\text{A3.3}) \\ &= \sum_{m=0}^{M-1} \sum_{n=0}^{N-1} \sum_{m'=0}^{M-1} \sum_{n'=0}^{N-1} a_{mn} a_{m'n}^* e^{jt\Omega(n-n')} \\ &\quad \cdot \int g(t + \tau/2 - m \cdot T) g^*(t - \tau/2 - m' \cdot T) e^{-j\tau\left(\omega - \frac{n'+n}{2}\Omega\right)} d\tau \end{aligned}$$

The integration index τ is shifted by $\tau = \tau + mT - m'T$, in order to change the structure of the

integral to the same structure of a Wigner-Ville distribution.

$$\begin{aligned}
 WVD_x(t, \omega) &= \sum_{m=0}^{M-1} \sum_{n=0}^{N-1} \sum_{m'=0}^{M-1} \sum_{n'=0}^{N-1} a_{mn} a_{m'n'}^* e^{j t \Omega (n-n')} e^{-j(m-m')} T\left(\omega - \frac{n'+n}{2} \Omega\right) \\
 &\quad \cdot \int g\left(t - \frac{m'+m}{2} T + \tau/2\right) g^*\left(t - \frac{m'+m}{2} T - \tau/2\right) e^{-j\tau\left(\omega - \frac{n'+n}{2} \Omega\right)} d\tau \\
 &= \sum_{m=0}^{M-1} \sum_{n=0}^{N-1} \sum_{m'=0}^{M-1} \sum_{n'=0}^{N-1} a_{mn} a_{m'n'}^* WV_g\left(t - \frac{m'+m}{2} T, \omega - \frac{n'+n}{2} \Omega\right) \\
 &\quad \cdot e^{j\left(t(n-n')\Omega + \left(\omega - \frac{n'+n}{2} \Omega\right)(m'-m)T\right)}
 \end{aligned} \tag{A3.4}$$

This Wigner-Ville distribution is continuous in both indices. The indices are now made discrete with a time step size of Δ and a frequency step size of $\frac{2\pi}{N_1 \cdot \Delta}$. The total number of time and frequency steps will be equal to N_1 .

$$\begin{aligned}
 WVD_x\left(k \cdot \Delta, v \cdot \frac{2\pi}{N_1 \cdot \Delta}\right) &= WVD_x[k, v] = \\
 &\sum_{m=0}^{M-1} \sum_{n=0}^{N-1} \sum_{m'=0}^{M-1} \sum_{n'=0}^{N-1} a_{mn} a_{m'n'}^* WVD_g\left(k \cdot \Delta - \frac{m'+m}{2} T, v \cdot \frac{2\pi}{N_1 \cdot \Delta} - \frac{n'+n}{2} \Omega\right) \\
 &\quad \cdot e^{j\left(k \cdot \Delta (n-n') \Omega + \left(v \cdot \frac{2\pi}{N_1 \cdot \Delta} - \frac{n'+n}{2} \Omega\right) (m'-m) T\right)}
 \end{aligned} \tag{A3.5}$$

The indexing of the Wigner-Ville distribution of the synthesis function $g(t)$ can also be made discrete by:

$$\begin{aligned}
 k \cdot \Delta - \frac{m'+m}{2} T &= \left(k - \frac{m'+m}{2} \cdot \frac{T}{\Delta}\right) \cdot \Delta = \left(k - \frac{m'+m}{2} \cdot \Delta M\right) \cdot \Delta \\
 v \cdot \frac{2\pi}{N_1 \cdot \Delta} - \frac{n'+n}{2} \Omega &= v \cdot \frac{2\pi}{N_1 \cdot \Delta} - \frac{n'+n}{2} \cdot \Delta N \cdot \frac{2\pi}{N_1 \cdot \Delta} = \left(v - \frac{n'+n}{2} \cdot \Delta N\right) \cdot \frac{2\pi}{N_1 \cdot \Delta}
 \end{aligned} \tag{A3.6}$$

This is used to make the WV_g discrete in both indices:

$$\begin{aligned}
 WVD_x[k, v] &= \sum_{m=0}^{M-1} \sum_{n=0}^{N-1} \sum_{m'=0}^{M-1} \sum_{n'=0}^{N-1} a_{mn} a_{m'n'}^* WV_g\left[k - \frac{m'+m}{2} \cdot \Delta M, v - \frac{n'+n}{2} \cdot \Delta N\right] \\
 &\quad \cdot e^{j\left(k \cdot \Delta (n-n') \Omega + \left(v \cdot \frac{\Omega_s}{N_1} - \frac{n'+n}{2} \Omega\right) (m'-m) T\right)}
 \end{aligned} \tag{A3.7}$$

The argument to the exponential function can be changed likewise:

$$\begin{aligned}
& k \cdot \Delta (n - n') \Omega + \left(v \cdot \frac{2\pi}{N_1 \cdot \Delta} - \frac{n' + n}{2} \cdot \Omega \right) (m' - m) T = \\
& k \cdot \Delta (n - n') \Delta N \cdot \frac{2\pi}{N_1 \cdot \Delta} + \left(v \cdot \frac{2\pi}{N_1 \cdot \Delta} - \frac{n' + n}{2} \cdot \Delta N \cdot \frac{2\pi}{N_1 \cdot \Delta} \right) (m' - m) \Delta M \cdot \Delta \quad \text{(A3.8)} \\
& \left(k (n - n') \cdot \Delta N + \left(v - \frac{n' + n}{2} \cdot \Delta N \right) (m' - m) \Delta M \right) \cdot \frac{2\pi}{N_1}
\end{aligned}$$

This change is inserted in equation (3.7).

$$\begin{aligned}
WVD_x[k, v] &= \sum_{m=0}^{M-1} \sum_{n=0}^{N-1} \sum_{m'=0}^{M-1} \sum_{n'=0}^{N-1} a_{mn} a_{m'n'}^* WVD_g \left[k - \frac{m' + m}{2} \cdot \Delta M, v - \frac{n' + n}{2} \cdot \Delta N \right] \\
&\quad \cdot e^{j \left(k (n - n') \cdot \Delta N + \left(v - \frac{n' + n}{2} \cdot \Delta N \right) (m' - m) \Delta M \right) \cdot \frac{2\pi}{N_1}} \quad \text{(A3.9)}
\end{aligned}$$

The discrete version of the WVD_g is given by:

$$\begin{aligned}
WVD_g[k, v] &= WVD_g \left(k \cdot \Delta, v \cdot \frac{2\pi}{N_1 \cdot \Delta} \right) = 2 \cdot \exp \left(-\frac{(k \cdot \Delta)^2}{\sigma^2} - \left(v \cdot \frac{2\pi}{N_1 \cdot \Delta} \right)^2 \cdot \sigma^2 \right) \\
&= 2 \cdot \exp \left(-\frac{k^2}{2 \left(\frac{\sigma}{\Delta \sqrt{2}} \right)^2} - \frac{v^2}{2 \left(\frac{\Delta \cdot N_1}{\sqrt{2} \sigma 2\pi} \right)^2} \right) \\
&= 2 \cdot \exp \left(-\frac{k^2}{2\sigma_k^2} - \frac{v^2}{2\sigma_v^2} \right) \quad \text{(A3.10)}
\end{aligned}$$

$$\text{where } \sigma_k = \frac{\sigma}{\Delta \sqrt{2}} \quad \sigma_v = \frac{\Delta \cdot N_1}{\sqrt{8} \sigma \pi}$$

It is clear that the area of this WVD is still 0.5, i.e. :

$$(\sigma_k \cdot \Delta) \cdot \left(\sigma_v \cdot \frac{2\pi}{N_1 \cdot \Delta} \right) = \sigma_k \cdot \sigma_v \cdot \frac{2\pi}{N_1} = \frac{\sigma}{\Delta \sqrt{2}} \cdot \frac{\Delta \cdot N_1}{\sqrt{8} \sigma \pi} \cdot \frac{2\pi}{N_1} = \frac{1}{2} \quad \text{(A3.11)}$$

In the remaining of this appendix, the samplings step Δ will be normalized. The spreading of the synthesis function is given by the effective bandwidth $T_1 = \sigma \sqrt{2\pi}$. This T_1 is incorporated in σ_k and σ_v :

$$\begin{aligned}
\sigma_k &= \frac{1}{\sqrt{2}} \cdot \frac{T_1}{\sqrt{2\pi}} = \frac{T_1}{2\sqrt{\pi}} \\
\sigma_v &= \frac{N_1}{\sqrt{8}\pi} \cdot \frac{\sqrt{2\pi}}{T_1} = \frac{N_1}{T_1 2\sqrt{\pi}} \quad \text{(A3.12)}
\end{aligned}$$

The Wigner-Ville distribution is expresses in equation (3.9) as a sum of Wigner-Ville distributions (2D Gaussian functions), where each distribution is scaled by the product of two coefficients. The location of these WVD are illustrated in Figure 3.1. Because the Gabor expansion is a multicomponent signal, the WVD will contain a cross-term between every pair of

components.

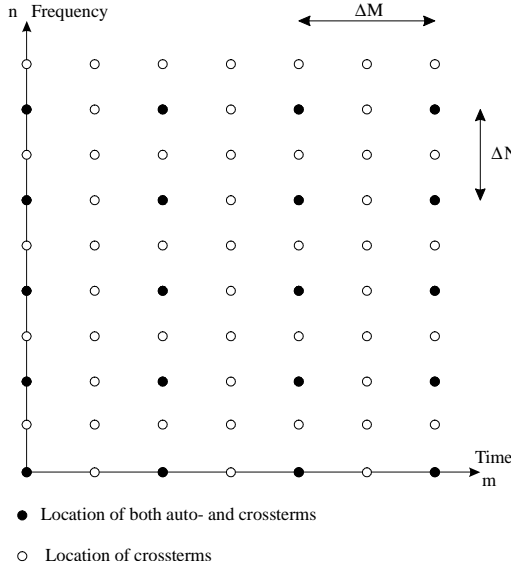


Figure A3.1 Position of WVD_g .

Because the Gabor expansion is a well defined multicomponent representation of the signal, it is possible to isolate the auto- and crossterms in equation (3.9). This has been done in

$$\begin{aligned}
 WVD_x[k, v] &= \sum_{m=0}^{M-1} \sum_{n=0}^{N-1} \sum_{m'=0}^{M-1} \sum_{n'=0}^{N-1} a_{mn} a_{m'n'}^* WVD_g \left[k - \frac{m'+m}{2} \cdot \Delta M, v - \frac{n'+n}{2} \cdot \Delta N \right] \\
 &\quad \cdot e^{j\left(\left(k(n-n')\cdot \Delta N + \left(v - \frac{n'+n}{2} \cdot \Delta N\right)(m'-m)\Delta M\right) \cdot \frac{2\pi}{N_1}\right)} \\
 &= \sum_{m=0}^{M-1} \sum_{n=0}^{N-1} |a_{mn}|^2 WVD_g [k - m \cdot \Delta M, v - n \cdot \Delta N] \\
 &\quad + \sum_{m=0}^{M-1} \sum_{n=0}^{N-1} \sum_{m'=0}^{M-1} \sum_{n'=0}^{N-1} a_{mn} a_{m'n'}^* WVD_g \left[k - \frac{m'+m}{2} \cdot \Delta M, v - \frac{n'+n}{2} \cdot \Delta N \right] \\
 &\quad \cdot e^{j\left(\left(k(n-n')\cdot \Delta N + \left(v - \frac{n'+n}{2} \cdot \Delta N\right)(m'-m)\Delta M\right) \cdot \frac{2\pi}{N_1}\right)}
 \end{aligned} \tag{A3.13}$$

The first sum is called *Cross-term Deleted Representation* WVD_{CDR} and the second sum is called *Cross-term Representation* WVD_{CR} . Whether the Gabor expansion is done with critical or with oversampling, the resulting WVD_x will be the Wigner-Ville distribution of the signal. But the advantage of using the *orthogonal-like Gabor expansion* (analysis and synthesis function are both Gaussian function $\gamma = \text{const} \cdot g$) will be prominent when only part of the expansion is used. If only the WVD_{CDR} is used, the resulting distribution will be an interpolation of the Gabor coefficients calculated by the STFT with a Gaussian window, which is similar to the Fourier Spectrogram. If all terms are used, the resulting distribution will be the Wigner-Ville distribution. This means that the WVD_{CR} contain both the high resolution and the cross-terms.

The next step will be only to include those terms of the WVD_{CR} which will increase the resolution. The purpose will be to use an adjustable part (parameter D) of the WVD_{CR} :

$$GS^D = WVD_{CDR} + WVD_{CR}^D \quad (\text{A3.14})$$

In order to conclude which cross-terms to use, it is noted that two complex cross-terms can be combined to one real cross-term:

$$\begin{aligned} & a_{mn} a_{m'n'}^* WVD_{g_{mn}, g_{m'n'}}[k, v] + a_{m'n'} a_{mn}^* WVD_{g_{m'n'}, g_{mn}}[k, v] \\ &= 2\operatorname{Re} \{a_{mn} a_{m'n'}^*\} WVD_g \left[k - \frac{m+m'}{2} \Delta M, v - \frac{n+n'}{2} \cdot \Delta N \right] \quad (\text{A3.15}) \\ & \times \cos \left(\left(k(n-n') \cdot \Delta N + \left(v - \frac{n'+n}{2} \cdot \Delta N \right) (m'-m) \Delta M \right) \cdot \frac{2\pi}{N_1} \right) \end{aligned}$$

By inspection, it is seen that the cross-terms are:

- Oscillating in the time dimension with the frequency $(n-n') \frac{2\pi}{N}$
- Oscillation in the frequency dimension with the frequency $\Delta M (m'-m)$

The energy can be found by 2D integration:

$$\begin{aligned} E &= \iint a_{mn} a_{m'n'}^* WVD_{g_{mn}, g_{m'n'}}(t, \omega) dt d\omega \\ &= 2|a_{mn} a_{m'n'}^*|^2 \cdot e^{-\frac{\left(\frac{m-m'}{2} \Delta M\right)^2}{\sigma^2} - \sigma^2 \left(\frac{n-n'}{2} \cdot \frac{2\pi}{N}\right)^2} \quad (\text{A3.16}) \end{aligned}$$

- The energy of a cross term is inversely proportional to the distance between g_{mn} and $g_{m'n'}$.

It is clear that the desired properties like high resolution and positive energy are obtained by us-

ing local cross-terms. This is also illustrated in Figure 3.2.

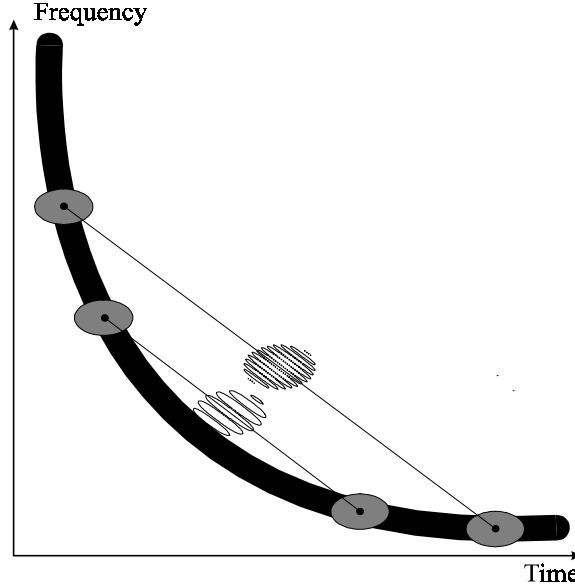


Figure A3.2 Local cross-terms are desired.

The local cross-terms will contribute to constructing the distribution of the hyperbolic chirp signal in Figure 3.2, whereas the global cross-terms will spoil the distribution.

The Gabor spectrogram is defined as the Wigner-Ville distribution of the Gabor expansion, when only a limited part of the expansion is used. The *Gabor Spectrogram (GS)* is given by:

$$\begin{aligned}
 GS_D [k, v] &= \sum_{d=0}^D P_d [k, v] \\
 P_d [k, v] &= \sum_{A_d} a_{mn} a_{m'n'}^* W V_g \left[k - \frac{m+m'}{2} \cdot \Delta M, v - \frac{n+n'}{2} \cdot \Delta N \right] \\
 &\quad \cdot e^{j \left(k(n-n') \cdot \Delta N + \left(v - \frac{n'+n}{2} \cdot \Delta N \right) (m'-m) \Delta M \right) \cdot \frac{2\pi}{N_1}}
 \end{aligned} \tag{A3.17}$$

$$A_d = \{ (m, m'), (n, n') \mid |m - m'| + |n - n'| = d \}$$

The order D is the Manhattan distance between the coefficients. This means that GS_0 is the Fourier spectrogram using a Gaussian window and GS_∞ corresponds to a Wigner-Ville distribution.

The Gabor coefficients are calculated for $n=0:N-1$, because this enables the FFT algorithm. However, when constructing a TF distribution we will prefer to have the mirror of the spectrum below DC (with negative frequency) instead of a mirror above the half samplings frequency. This can be obtained when the N Gabor coefficients are indexed with modulus N by $-N/2 \leq n \leq N/2 - 1$

In order to make an implementation of GS, the WVD_g will be represented by an exponential function. The final Gabor spectrogram can be given by the following equation:

$$\begin{aligned}
GS_D[k, v] &= \sum_{d=0}^D P_d[k, v] \\
P_d[k, v] &= \sum_{A_d} 2 \cdot a_{mn} a^{*}_{m'n'} \cdot e^{-\frac{\left(k - \frac{m+m'}{2} \cdot \Delta M\right)^2}{2\sigma_k^2} - \frac{\left(v - \frac{n+n'}{2} \cdot \Delta N\right)^2}{2\sigma_v^2}} \\
&\quad \cdot e^{j\left(k(n-n')\Delta N + \left(v - \frac{n+n'}{2} \cdot \Delta N\right)\Delta M(m'-m)\right)\frac{2\pi}{N_1}} \\
A_d &= \{(m, m'), (n, n') \mid |m - m'| + |n - n'| = d\} \\
0 \leq m \leq M_{total} - 1 &\quad -\frac{N}{2} \leq n \leq \frac{N}{2} - 1 \\
0 \leq m' \leq M_{total} - 1 &\quad -\frac{N}{2} \leq n' \leq \frac{N}{2} - 1 \\
0 \leq k < \text{signal length} &\quad N_1/2 \leq v < N_1/2 - 1
\end{aligned} \tag{A3.18}$$

In the rest of this appendix some practical consideration will be addressed. A pure implementation of equation (3.18) may not be practical because of the size of the summation, and the number of point in the TF plane. The following steps can be used to obtain a reasonable efficient matlab code for the Gabor spectrogram:

Step 1. Wigner-Ville Tabel

The summation terms have the following structure:

$$\begin{aligned}
&2 \cdot a_{mn} a^{*}_{m'n'} \cdot WV_g\left[k - \frac{m+m'}{2} \cdot \Delta M, v - \frac{n+n'}{2} \cdot \Delta N\right] \\
&\quad \cdot e^{j\left(k(n-n')\Delta N + \left(v - \frac{n+n'}{2} \cdot \Delta N\right)\Delta M(m'-m)\right)\frac{2\pi}{N_1}}
\end{aligned} \tag{A3.19}$$

As the WVD has a 2D gaussian shape, the summation terms will only give a non-zero contribution in the area around the center of the WVD - $(t, \omega) = \left(\frac{m+m'}{2} \cdot \Delta M, \frac{n+n'}{2} \cdot \Delta N\right)$. It will therefore be sufficient to calculate this non-zero contribution. The main contribution from the 2D gaussian function will be in the intervals $-4 \cdot \sigma_k \leq k \leq 4 \cdot \sigma_k$ and $-4 \cdot \sigma_v \leq v \leq 4 \cdot \sigma_v$. This WVD is signal independent and can be calculated and placed in a tabel for further use. The following matlab code will generate a matrix containing the WVD:

```

sigma_k = T1/(2*sqrt(pi));
sigma_v = N1/(T1*2*sqrt(pi));
WV_v_min = -floor(4*sigma_v);
WV_v_max = floor(4*sigma_v);
WV_k_min = -floor(4*sigma_k);
WV_k_max = floor(4*sigma_k);
WV = 2*exp(-([WV_v_min:WV_v_max]).^2/(2*sigma_v^2))...
*exp(-([WV_k_min:WV_k_max]).^2/(2*sigma_k^2));

```

An example of this WVD tabel is illustrated in the following Figure 3.3

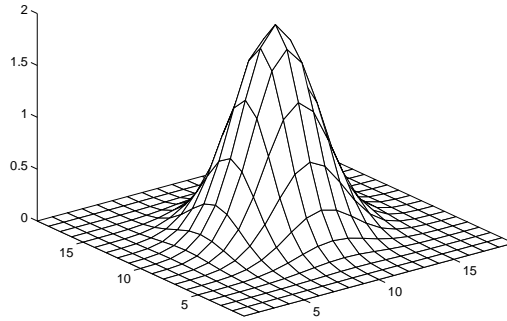


Figure A3.3 Content of the WVD tabel for base64.

For a zero-order Gabor spectrogram, this WVD will be placed on the Gabor grid lattices. This is illustrated in the following Figure 3.4:

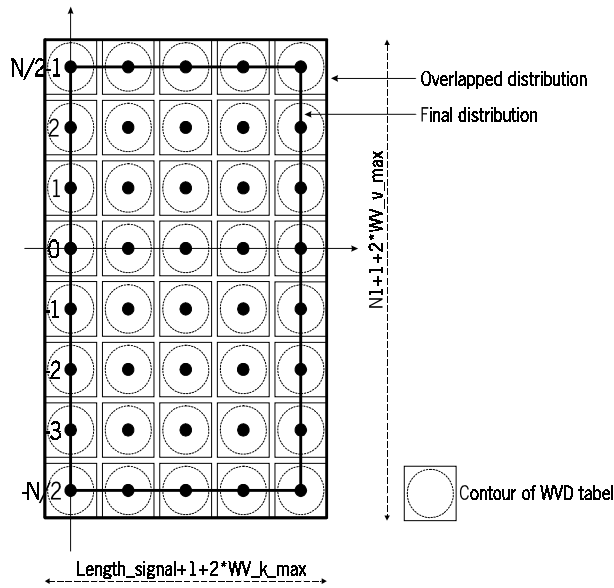


Figure A3.4 Position of the Gaussian tabel for a zero-order GS.

Some of the WVD tabels will overlap with the final border of the TF plan. This problem can be solved by either checking each grid and take action if an overlap arises or just allowing the overlap, and cut out the true plan when the computation is finish. The last approach will be used in the following. The matrix containing the GS is initialized with $1+2*WV_v_max$ extra point in the frequency dimension and with $1+2*WV_k_max$ extra points in the time dimension

```
dist=zeros(N1+1+2*WV_v_max,Length_signal+2*WV_k_max+1);
```

where the Length_signal is $(M_{total}-1)*dM$.

A zero-order Gabor spectrogram can be calculated by the following Matlab code:

```
%##### Calculation of P(0) #####
d=0
for m=0:M_total-1,
    for n=-0.5*N:N*0.5-1,
        v=(n+0.5*N)*dN:(n+0.5*N)*dN+2*WV_v_max;
        k=m*dM:m*dM+2*WV_k_max;
        dist(v+1,k+1)=dist(v+1,k+1)+abs(a(mod(n,N)+1,m+1))^2*WV;
    ,end
,end
```

Step 2. Manhattan distance

The main implementation difficulty is caused by A_d . Each component in the Gabor expansion will enter into a cross term with another component with a distance of $|m - m'| + |n - n'| = d$. As two complex cross-WVD can be compounded into one real WVD, the number of cross terms in the summation will be reduced by 50%. This compounding of two cross terms is given by:

$$\begin{aligned} WVD_{x+y} &= WVD_{x,x} + WVD_{x,y} + WVD_{y,x} + WVD_{y,y} \\ &= WVD_x + WVD_y + 2 \cdot \operatorname{Re} \{ WVD_{x,y} \} \end{aligned} \quad (\text{A3.20})$$

This affect the points in the Manhattan square, because only half of the points have to be used. Now, only the point above and points to the right of the origin point should be used. This *Reduced Manhattan* is illustrated in Figure 3.5.

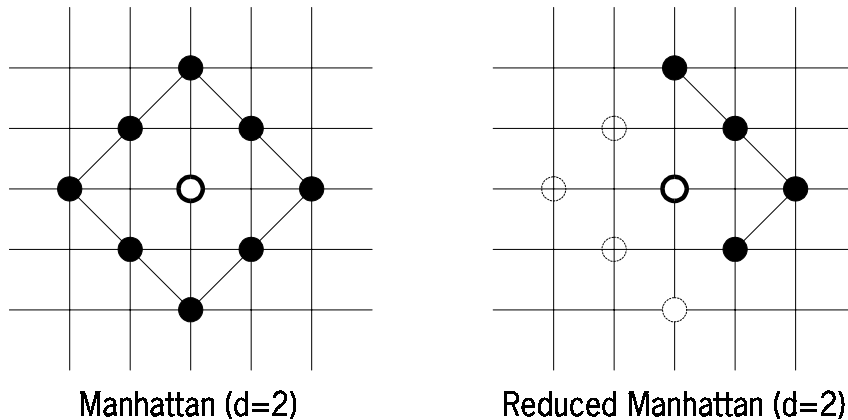


Figure A3.5 Illustration of the Manhattan distance

The Matlab code to generate the offset coordinates is given by (dependent on the order d):

```
%Manhattan distance
Manhat=[];
for k=1:d-1,
    Manhat=[Manhat [k k;(d-abs(k)) -(d-abs(k))]];
,end
Manhat=[[0;d] Manhat [d;0]];
```

The final summation for a D-order Gabor spectrogram can be calculated using the following Matlab code:

```
%##### Calculation of P(d) #####
for d=1:D,
    d
    %Manhattan distance
    Manhat=[];
    for k=1:d-1,
        Manhat=[Manhat [k k;(d-abs(k)) -(d-abs(k))]];
    ,end
    Manhat=[[0;d] Manhat [d;0]];

    % Main summation
    for m1=0:M_total-1,
        for n1=-0.5*N:0.5*N-1,
            l=Manhat+[m1*ones(1,2+2*(d-1));n1*ones(1,2+2*(d-1))];
            OK_index=find((l(1,:)>=0 & l(1,:)<M_total & l(2,:)>=-0.5*N & l(2,:)<0.5*N-1);
            m2_vector=l(1,OK_index);
            n2_vector=l(2,OK_index);
            for k=1:length(m2_vector),
                m2=m2_vector(k);
                n2=n2_vector(k);

cos_matrix=exp(j*2*pi/N1*[WV_v_min:1:WV_v_max]^(m2-m1)*dM)*...
exp(j*2*pi/N1*[0.5*(m1+m2)*dM+WV_k_min:1:0.5*(m1+m2)*dM+WV_k_max] ...
.*(n1-n2)*dN);

v=0.5*(n1+n2+N)*dN+1:(0.5*(n1+n2+N)*dN+2*WV_v_max)+1;
k=0.5*(m1+m2)*dM+1:(0.5*(m1+m2)*dM+2*WV_k_max)+1;

dist(v,k)=dist(v,k)+2*real(a(mod(n1,N)+1,m1+1)*conj(a(mod(n2,N)+1,m2+1))) ...
*WV.*cos_matrix);

,end
,end
,end
,end
```

Step 3. Include only large Gabor coefficients

Considerable speedup can be achieved when only large Gabor coefficients are used in the calculation of the Gabor spectrogram. A good lower limits is:

```
a_minimum = 0.01*max(max(abs(a)));
```

where a is the coefficients matrix

The core of the loop in P(0) should only be calculated when the cofficients are above this minimum. This can be achieved by the following Matlab condition:

```
if abs(a(mod(n,N)+1,m+1))> a_minimum
..core of loop..
,end
```

and in the case of P(D), the same improvement can be achieved by:

```
if min([abs(a(mod(n1,N)+1,m1+1)) abs(a(mod(n2,N)+1,m2+1))])> a_minimum
..core of loop..
,end
```

When the calculation has ended, the final Gabor spectrogram has to be extracted from the *dist* matrix because of the overlap. This is done by:

```
GS=real(dist(WV_v_max+1:WV_v_max+N1,WV_k_max+1:WV_k_max+Length_signal));
```

The last topic in this appendix is to illustrate that the Fourier Spectrogram can be constructed from a Gabor expansion of the signal. This fact can be used to argue that a zero order Gabor spectrogram has a resolution which is a bit lower than the FS.

$$\begin{aligned} FS(t, \omega) &= \left| \int x(\tau) g(t - \tau) e^{-j\omega\tau} d\tau \right|^2 \\ &= \left| \int \sum_m \sum_n a_{mn} g_{mn}(\tau) g(t - \tau) e^{-j\omega\tau} d\tau \right|^2 \\ &= \left| \sum_m \sum_n a_{mn} \int g_{mn}(\tau) g(t - \tau) e^{-j\omega\tau} d\tau \right|^2 \end{aligned} \quad (\text{A3.21})$$

The integral express a short time Fourier transform of a time-frequency shifted syntheses function where the STFT use the same function as a window function. With no TF shift, the integral can be calculted to:

$$\int g(\tau) g(t - \tau) e^{-j\omega\tau} dt = \exp\left(-\frac{t^2}{4\sigma^2} - \frac{\omega^2 \sigma^2}{4} - \frac{jt\omega}{2}\right) = STFT_g(t, \omega) \quad (\text{A3.22})$$

The Gabor interpolated Fourier Spectrogram can now be expressed as:

$$FS(t, \omega) = \left| \sum_m \sum_n a_{mn} STFT_g(t - mT, \omega - n\Omega) \right|^2 \quad (\text{A3.23})$$

The Gabor coefficients are interpolated using the STFT of the synthesis function. To compare, the zero-order Gabor Spectrogram is given by:

$$GS^0(t, \omega) = \sum_{m=0}^{M-1} \sum_{n=0}^{N-1} |a_{mn}|^2 WVD_g(t - mT, \omega - n\Omega) \quad (\text{A3.24})$$

But it will not be possible to make a proper interpolation of the absolut value of the Gabor coefficients, because the phase information is missing. When the number of Gabor coefficients in the frequency direction is low, it will be possible to see that the GS^0 is constructed of 2D Gaussian functions located at the Gabor lattice.

Exercises

The exercises are divide into Matlab(M) and pencil&paper(P) exercises.

Ex: M1

Analysis the speech signal *spec.mat* with a Fourier Spectrogram(FS) in Matlab. Construct the spectrogram using the FFT algorithme, as Matlab's own routine must not be used. Apply a hamming window function with the following length 64, 128, 256 and 512. The frequency axis must contain 256 points, independent of the window length. The Spectrogram's must to be stored (printed or saved), so these results can be compared with the Gabor Spectrogram in MM 5. The speech signal has to be preemphasised.

Ex: M2

Program the *Discrete Time Frequency Wigner-Ville Distribution* in matlab and analysis the four test signals generated by *test_sig.m*. Explain the results.

Ex: M3

- a. Calculate the analysis and synthesis functions for L=64, 128 and 256. (Solve the DBC using SVD in matlab).
- b. Calculate the Gabor coefficients of respectively *test5.mat* and *spec.mat* in matlab using one of the analysis functions.
- c. Reconstruct the original signals from the Gabor coefficients.

Ex: M4

- a. Program the Discrete Gabor Spectrogram in matlab for an order d=0, and analysis test0 to obtain a 2D gaussian function.
- b. Extent the matlab program to compute the Discrete Gabor Spectrogram for an order d=1:5. Analysis test signals test0-test5 and spec.mat and explain the results.

Ex: P1

Determine the marginal distributions for the Fourier Spectrogram.

Ex: P2

Derive the following properties:

$$\text{Addition property } x(t) = g(t) + h(t) \quad (4)$$

$$\text{Product property } x(t) = g(t) \cdot h(t) \quad (5)$$

$$\text{Convolution property } x(t) = g(t) \otimes h(t) \quad (6)$$

for the Fourier transformation, Short Time Fourier Transformation, and the Fourier spectrogram.

Ex: P3

For an inner product defined by:

$$\langle f, g \rangle = \int_{-\infty}^{\infty} f(t) g^*(t) dt \quad (7)$$

prove the following property:

$$\langle f, g \rangle = \langle F, G \rangle \quad (8)$$

where F and G are the Fourier transformed of f and g.

Ex: P4

Given the statistical Gaussian function defined by:

$$N(t) = \frac{1}{\sqrt{2\pi}\sigma} e^{-\frac{t^2}{2\sigma^2}} \quad (9)$$

with the property $\int N(t) dt = 1$, find the coefficient A, so the gaussian function $g(t) = A \cdot N(t)$ has unity energy ($\int |g(t)|^2 dt = 1$).

(Hint: calculate the weight A knowing that $\int e^{-t^2} dt = \sqrt{\pi}$).

Ex: P5

Determine the instantaneous power and the Power spectrum for

$$g(t) = (\pi\sigma^2)^{-0,25} e^{-\frac{t^2}{2\sigma^2}} \quad (10)$$

Ex: P6

Determine analytical the Wigner-Ville distribution of the energy normalised Gaussian function

Ex: P7

Show that the Wigner-Ville distribution for a Gaussian function can be expressed as the product of the instantaneous power and the Power spectrum of the Gaussian function:

$$WV_g(t, \omega) = |g(t)|^2 \cdot |G(\omega)|^2 \quad (11)$$

when

$$g(t) = (\pi\sigma^2)^{-0,25} e^{-\frac{t^2}{2\sigma^2}} \quad (12)$$

Ex: P8

Show how the Fourier Transformed signal can be reconstructed from the Gabor coefficients.

Ex: P9

Show how the Instantaneous Power can be reconstructed from the Gabor coefficients.

Ex: P10

Show how the Power Spectrum signal can be reconstructed from the Gabor coefficients.

Ex: P11

Insert the Gabor expansion into the Wigner-Ville distribution, and calculate the frequency marginal. Compare the result with exercise P10.

References

- [Bastiaans 80] **Gabor's Expansion of a Signal into Gaussian Elementary Signals**, by Martin J. Bastiaans, Proceedings of the IEEE, Vol. 68, No. 4, April 1980, pp. 538-539
- [Bastiaans 81] **Signal Description by Mean of a Local Frequency Spectrum**, by Martin J. Bastiaans, SPIE Vol. 373, Transformations in Optical Signal Processing (1981), pp. 49-62.
- [Bastiaans 85] **On the Sliding-Window Representation in Digital Signal Processing**, by Martin J. Bastiaans, IEEE Trans. on ASSP, Vol ASSP-33, No. 4, August 1985, pp. 868-873.
- [Battle 88] **Heisenberg Proof of the Balian-Low Theorem**, by Guy Battle, Letters in Mathematical Physics 15(1988), pp. 175-177
- [Boudreux 92] **A Comparison of the Existence of "Cross Terms" in the Wigner Distribution and the Squared Magnitude of the Wavelet Transform and the Short Time Fourier Transform**, by Shubha Kadambé and Gloria Faye Boudreux-Bartels, IEEE Trans. on SP, Vol. 40, No. 10, October 1992, pp. 2498-2517.
- [Bracewell 86] **The Fourier Transform And Its Applications**, Ronald N. Bracewell 1986 (1965), pp 146.
- [Claasen 80a] **The Wigner Distribution - A Tool for Time-Frequency Signal Analysis, Part I: Continuous-Time Signals**, by T.A.C.M Claasen and W.F.G.Mecklenbrauker, Philips Journal of Research, Vol. 35, No. 3, 1980, pp. 217-250
- [Claasen 80b] **The Wigner Distribution - A Tool for Time-Frequency Signal Analysis, Part II: Discrete-Time Signals**, by T.A.C.M Claasen and W.F.G.Mecklenbrauker, Philips Journal of Research, Vol. 35, No. 4/5, 1980, pp. 276-300
- [Claasen 80c] **The Wigner Distribution - A Tool for Time-Frequency Signal Analysis, Part III: Relations With Other Time-Frequency Signal Transformations**, by T.A.C.M Claasen and W.F.G.Mecklenbrauker, Philips Journal of Research, Vol. 35, No. 6, 1980, pp. 372-389
- [Cohen 66] **Generalized Phase-Space Distribution Functions**, by Leon Cohen, Journal Of mathematical Physics, Vol. 7, No. 5, May 1966, pp. 781-786.
- [Cohen 76] **Quantization problem and variational principle in the phasespace formulation of quantum mechanics**, by Leon Cohen, Journal of Mathematical Physics, Vol. 17, No. 10, October 1976, pp 1863-1866
- [Cohen 85] **Positive Time-Frequency Distribution functions**, by Leon Cohen and Theodore E. Posch, IEEE Trans. on ASSP, Vol. ASSP-33, No. 1, February 1985, pp. 31-38.
- [Cohen 95] **Time-Frequency Analysis**, by Leon Cohen, Prentice Hall 1995, ISBN 0-13-594532-1
- [Dirac 30] **Principles of Quantum Mechanics**, by P. A. M. Dirac, (First published 1930), Fourth editon 1987, ISBN 0-19-852011-5, pp 58.
- [Feichtinger 98] **Gabor Analysis and Algorithms - Theory and Applications**, Ed. by Hans G. Feichtinger, Thomas Strohmer, Birkhauser 1998, ISBN 0-8176-3959-4.
- [Gabor 45] **Theory Of Communication**, by Dennis Gabor, Journal of the Institute of Electrical Engineers, Vol 93, 1945, pp. 429-457.
- [Gram 89] **Simultaneous Time And Frequency Analysis**, by Klaus Gram-Hansen, Erhvervsforskerprojekt EF-232, ATV (Industrial Ph.D. thesis), Denmark 1989
- [Hansen] **Beethoven Sonaten Bd.1.**, by Wilhelm Hansen, Edition nr. 3413, pp. 248.
- [Haykin 83] **Communication Systems**, by Simon Haykin, John Wiley & Sons Inc, 1983, ISBN 0-471-88088-4, pp 79.
- [Hlawatsch 84] **Interference Terms In The Wigner Distribution**, by Franz Hlawatsch, Digital Signal Processing - 84, pp. 363-367.
- [Hlawatsch 92] **Linear And Quadratic Time-Frequency Signal Representations**, by Franz Hlawatsch and Gloria Faye Boudreux-Bartels, IEEE SP Magazine, April 1992, pp. 21-67 (page 34).
- [Hlawatsch 97] **The Wigner Distribution - Theory and Applications in Signal Processing**, Ed. by W. Mecklenbrauker and F. Hlawatsch, Elsevier 1997, ISBN 0-444-88856-X

- [Janse 83] **Time-Frequency Distributions of Loudspeakers: The Application of the Wigner Distribution**, by Cornelis P. Janse and Arie J.M. Kaizer, J. Audio Eng. Soc., Vol 31, No. 4, April 1983, pp. 198-223.
- [Moyal 49] **Quantum Mechanics as a Statistical Theory**, by J. E. Moyal, Proceedings of the Cambridge Philosophical Society, Volume 45, Cambridge At The University Press 1949, pp. 99-124.
- [Papoulis 62] **The Fourier Integral And Its Applications**, Athanasios Papoulis 1962
- [Peyrin 86] **A Unified Definition for the Discrete-Time, Discrete-Frequency, and Discrete-Time/Frequency Wigner Distribution**, by Francoise Peyrin and Remy Prost, IEEE Trans. on ASSP, Vol. ASSP-34, No. 4, August 1986, pp. 858-867.
- [Qian 93] **Discrete Gabor Transform**, by Shie Qian and Dapang Chen, IEEE Trans on Signal Processing. Vol. 41, No. 7, July 1993, pp. 2429-2438.
- [Qian 94] **Decomposition of the Wigner-Ville Distribution and Time-Frequency Distribution Series**, by Shie Qian and Dapang Chen, IEEE Trans. on Signal Processing. Vol. 42, No. 10, Oct. 1994, pp. 2836-2842.
- [Qian 96] **Joint Time-Frequency Analysis - Methods and Applications**, by Shie Qian and Dapang Chen. Prentice Hall 1996, ISBN: 0-13-254384-2.
- [Ville 48] **Theorie Et Applications De La Notation De Signal Analytique**, by J. Ville, Cables et Transmission, Vol. 2, 1948, pp. 61-74
- [Wexler 90] **Discrete Gabor Expansions**, by J. Wexler and S. Ray, Signal Processing, Vol. 21, No. 3, Nov. 1990, pp. 207-221.
- [Wigner 32] **On the Quantum Correction for Thermodynamic Equilibrium**, by Eugene Paul Wigner , Physical Review, Vol. 40, June 1, 1932, pp. 749-759.
- [Wilcox 67] **Exponential Operators and Parameter Differentiation in Quantum Physics**, by R.M. Wilcox, Journal of Mathematical Physics, Vol. 8, Number 4, April 1967, pp. 962-982.
- [Williams 92b] **Mechanism of the Cross-Terms in Spectrograms**, by Jechang Jeong and William J. Williams, IEEE Trans, on SP, Vol. 40, No. 10, October 1992, pp. 2608-2613.

Abbreviation

AT	Auto Terms
CBC	Continuous Biorthogonality Condition
CDR	Cross-term Deleted Representation
CGE	Continuous Gabor Expansion
CR	Cross-term Representation
CT	Cross Terms
DBC	Discrete Biorthogonality Condition
DCT	Decomposed Cross Term
DGE	Discrete Gabor Expansion
DT-WVD	Discrete Time Wigner-Ville Distribution
DF-WVD	Discrete Frequency Wigner-Ville Distribution
DTF-WVD	Discrete Time Frequency Wigner-Wille Distribution
EEG	ElectroEncephaloGram
FS	Fourier Spectrogram
FT	Fourier Transformation
IF	Instantaneous Frequency
IP	Instantaneous Power
GS	Gabor Spectrogram
JTFA	Joint Time Frequency Analysis
NFS	Narrowband Fourier Spectrogram
PDGE	Periodic Discrete Gabor Expansion
PDBC	Periodic Discrete Biorthogonality Condicion
PS	Power Spectrum
SCF	Spectral Correlation Function
SF	Samplings Factor
TF	Time Frequency
WFS	Wideband Fourier Spectrogram
WVD	Wigner-Ville Distribution
WVD _{CDR}	Wigner-Ville DistributionCross-terms Deleted Representation
WVD _{CR}	Wigner-Ville Distribution Cross-terms Representation
1D	One Dimensional
2D	Two Dimensional

Notation

Integration

$$\int x(t) dt = \int_{-\infty}^{\infty} x(t) dt \quad (\text{N1})$$

Summation:

$$\sum_n x_n = \sum_{n=-\infty}^{\infty} x_n \quad (\text{N2})$$

Inner-product:

$$\langle h, g \rangle = \int_{-\infty}^{\infty} h(t) g^*(t) dt \quad (\text{N3})$$

In $x[a, b]$ the square brackets indicate that **a** is a discrete parameter taking integer values and the parentheses indicate that **b** is a continuous parameter

Transparents for lecture no 1.

Course prerequisite/assumption:

Prerequisite

- Fourier transformation and Linear Algebra (mainly SVD)

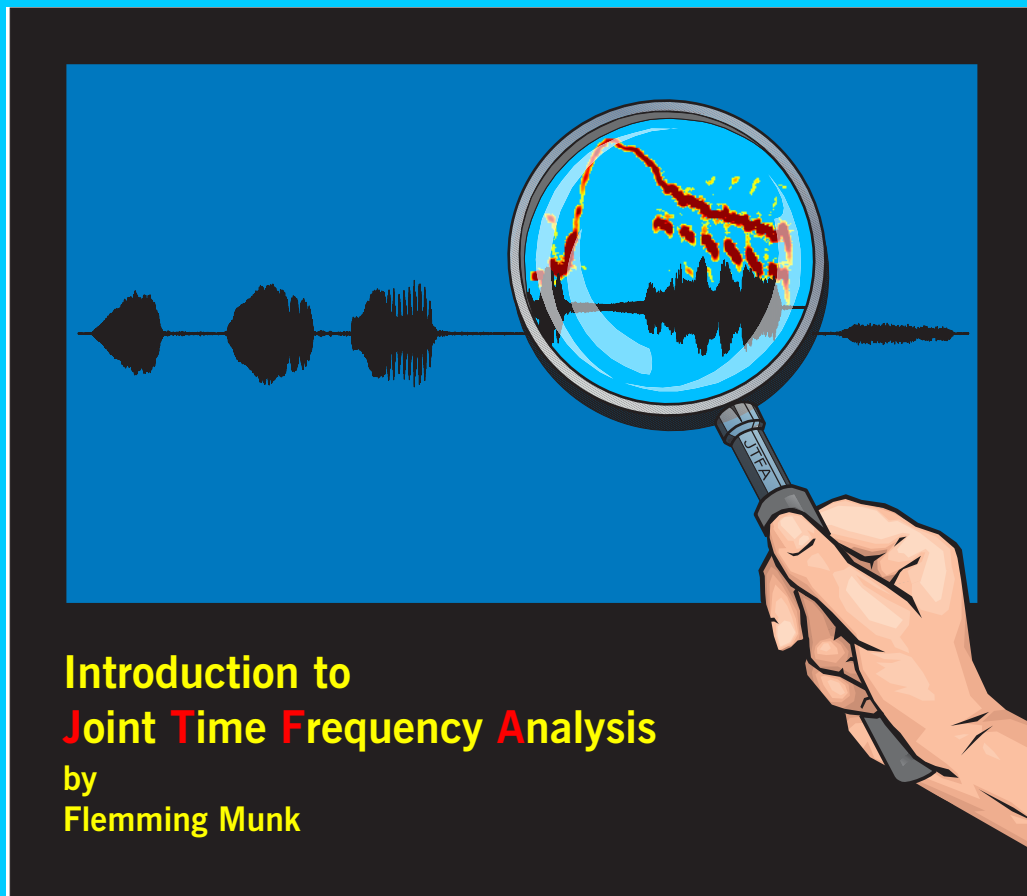
Assumptions:

The lectures are given under the assumption that the student:

- has studied the day's text very careful
- has made some reflections about the exercises
- is reasonably well rested

Under these assumptions, the purpose of each lecture is to give the student a general view of the topic, and elaborate on some selected areas. It is not possible to go through every details.

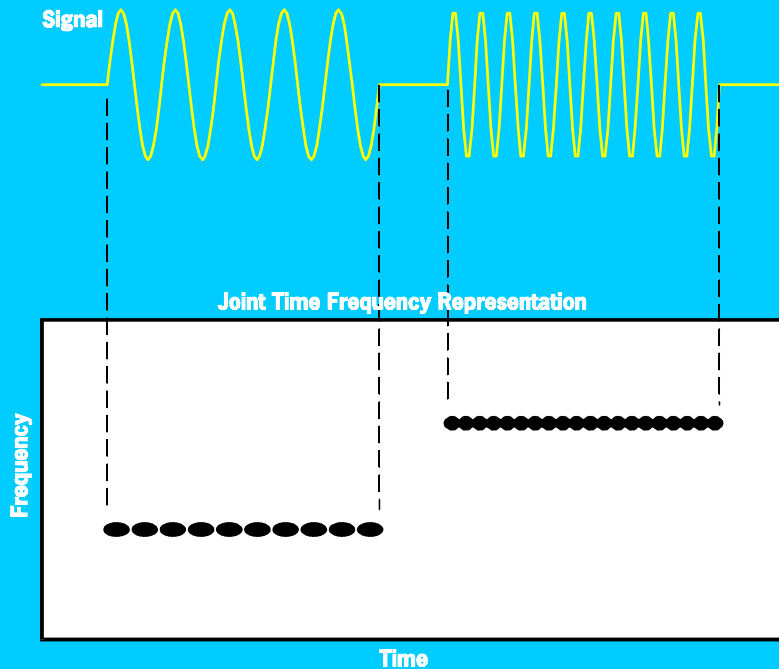
Aalborg University



Aalborg University

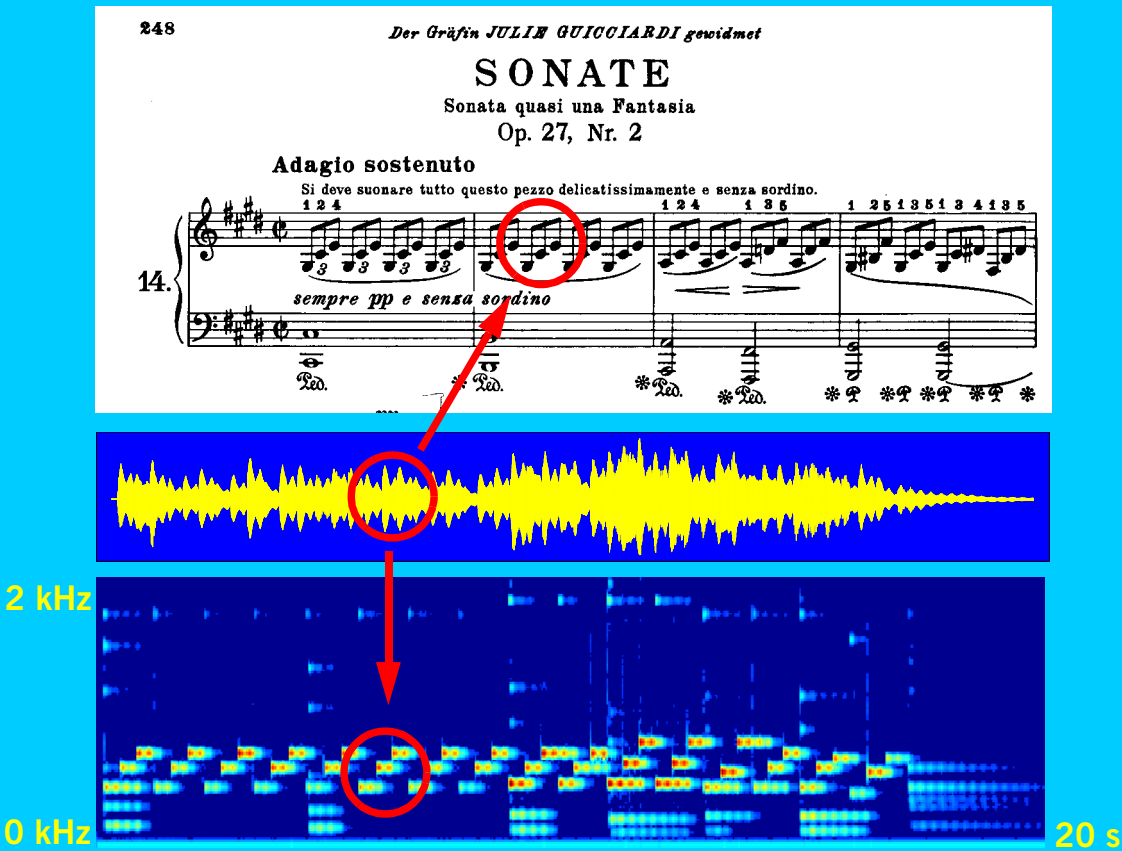
What is Joint Time Frequency Analysis?

The purpose of JTFA is to map a one-dimensional function of time or frequency into a two-dimensional function of time and frequency.



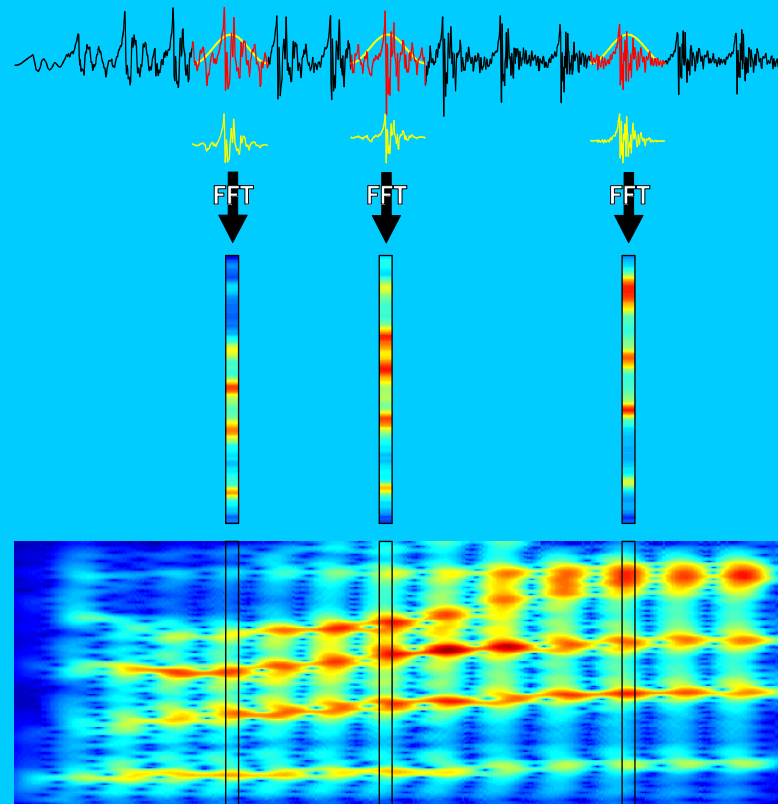
Aalborg University

A historical approach: Musical notes



Aalborg University

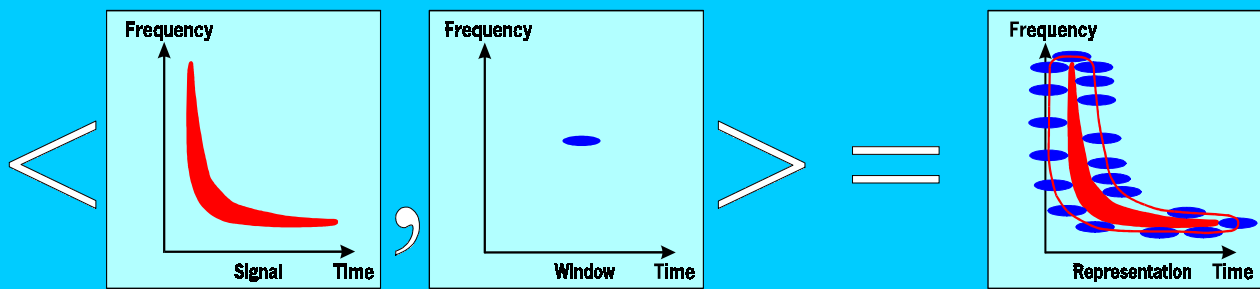
Procedure of Short Time Fourier Transformations



Aalborg University

Short Time Fourier Transformations as Inner-product

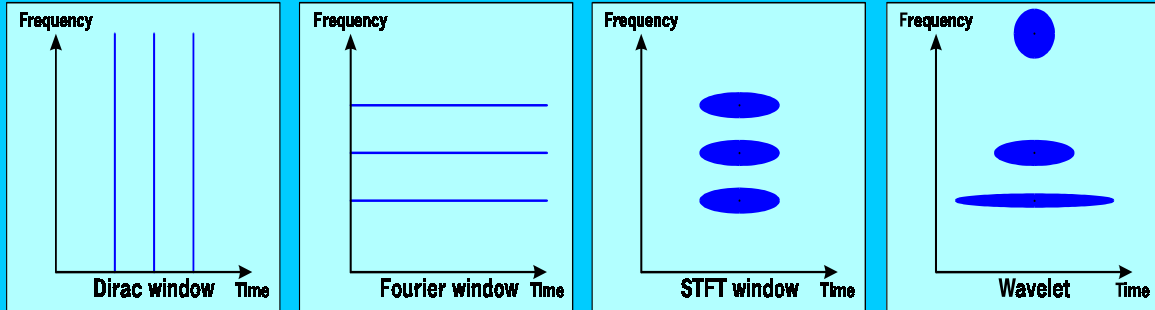
$$\begin{aligned} F_x(t, \omega) &= \int_{-\infty}^{\infty} x(\tau) h^*(t - \tau) e^{-j\tau\omega} d\tau \\ &= \langle x, h_{t, \omega} \rangle = \langle X, H_{t, \omega} \rangle \end{aligned}$$



- The resulting distribution will be very dependent of the selected window function!

Aalborg University

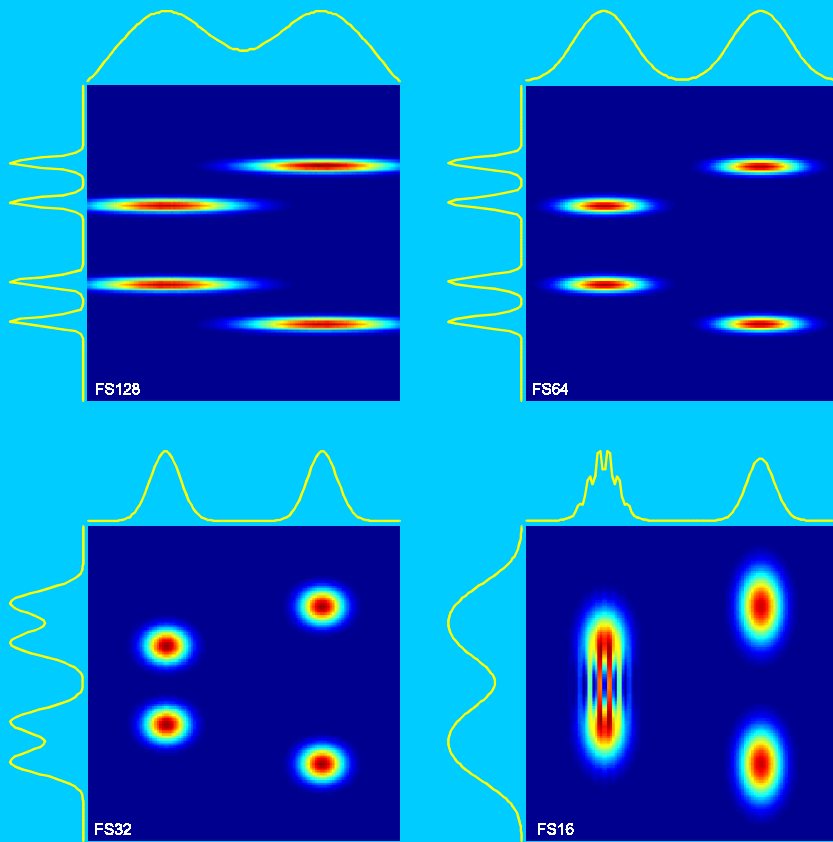
The Four fundamental windows



- An optimal basis would be a point in the TF plan.
- Transformations based on inner-product will always have a limited TF resolution.

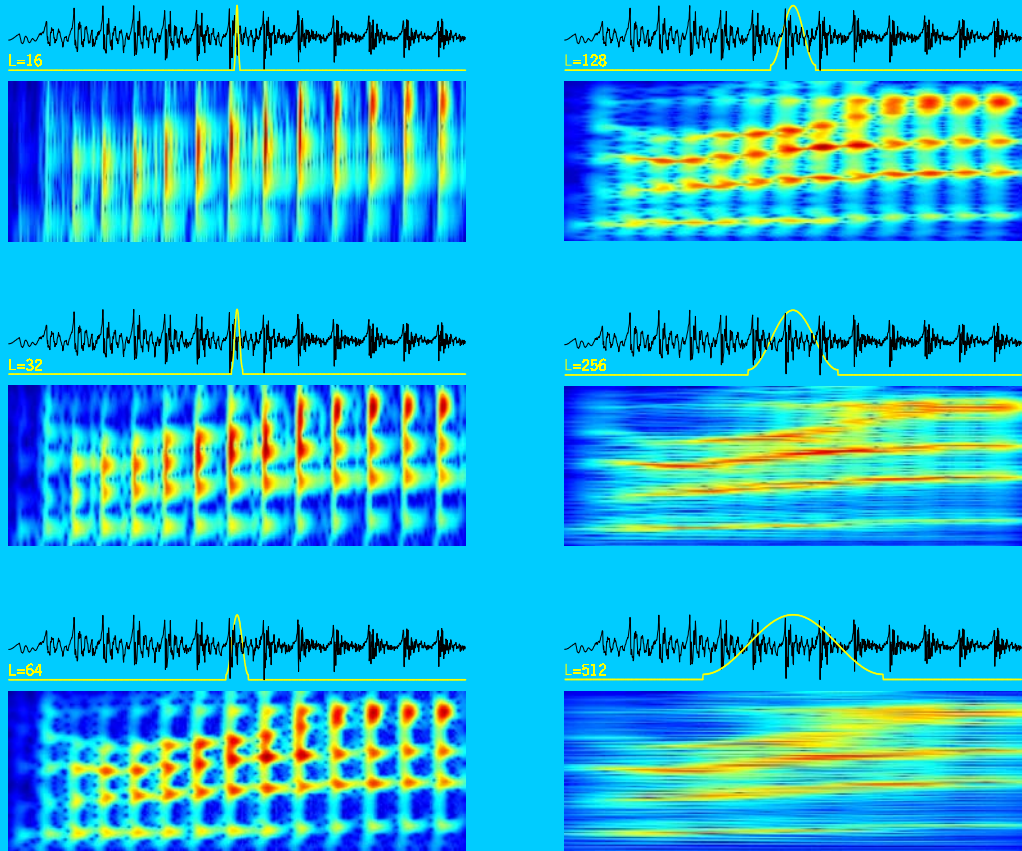
Aalborg University

Examples of window distortion



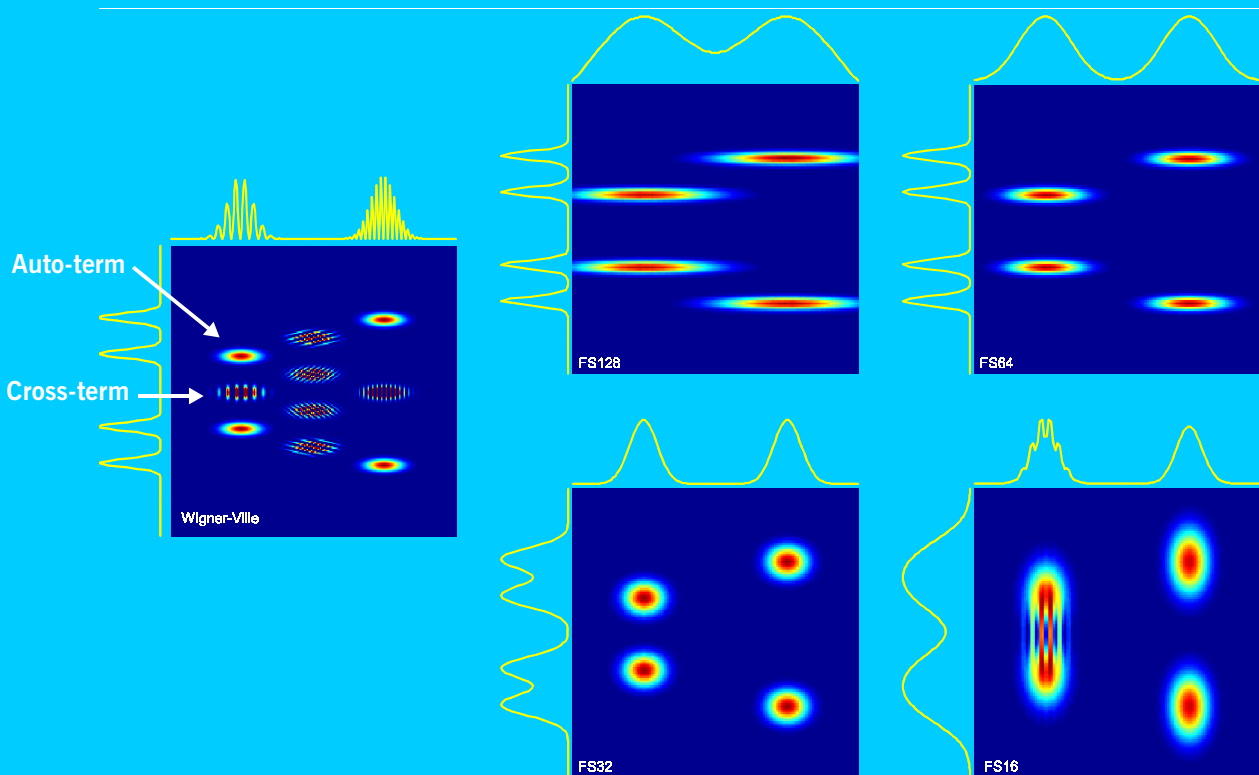
Aalborg University

Examples of window distortion



Aalborg University

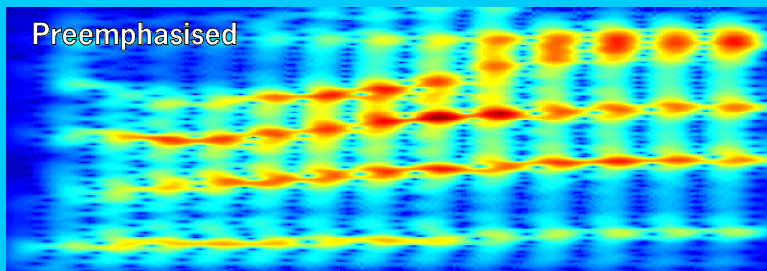
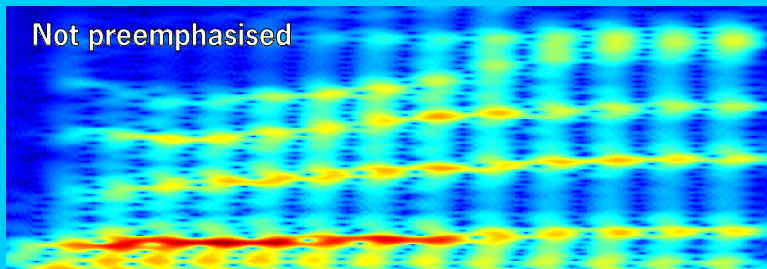
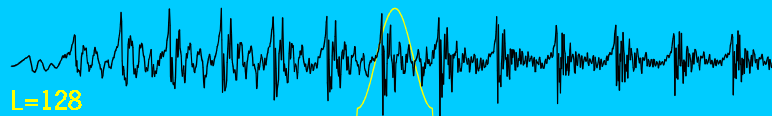
Fourier Spectrogram versus the Wigner-Ville Distribution



Aalborg University

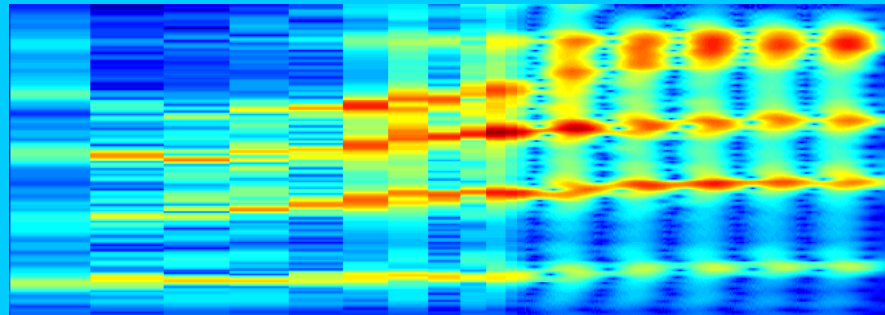
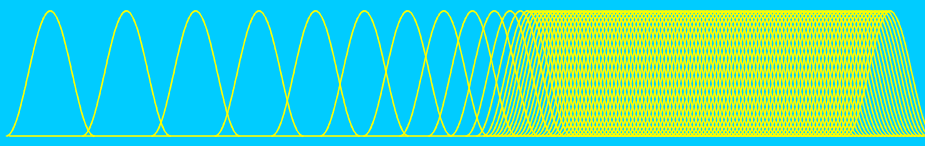
Application of a preemphasing filter for speech signals

$$H(z) = 1 - 0.95z^{-1} \quad \text{Matlab: } x_{\text{pre}}=\text{filter}([1 -0.95],[1 0],x);$$



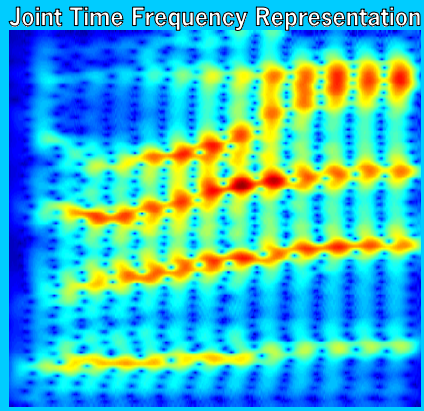
Aalborg University

Effect of overmapping windows in the STFT



Aalborg University

Relation between JTFA and JTFS

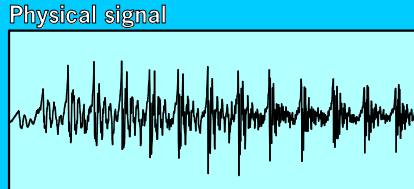


Joint Time Frequency Synthesis

Spectral masking
Specific test signals
Pseudo Spectral compression
....

Joint Time Frequency Analysis

Speech analysis
Feature extraction
Seismic interpretation
Measuring of velocity using radar
....



Aalborg University



How can the window distortion
in
inner-product based techniques
like
the STFT, Wavelets and Fourier Spectrogram
be avoided?

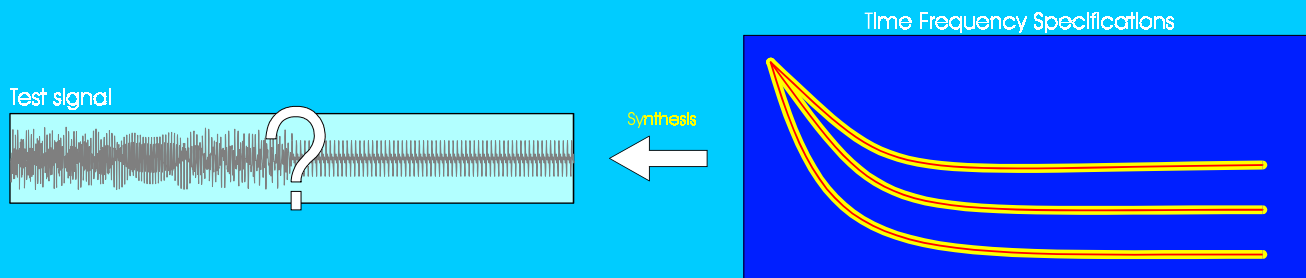
Aalborg University

Inner-product summarize

- Comparing theory and applicability, the Fourier Spectrogram is the best time frequency distribution
- Improved time and frequency resolution can be obtained by using other distributions, but these improvements are only obtained by a considerable increase in theory and algorithm!

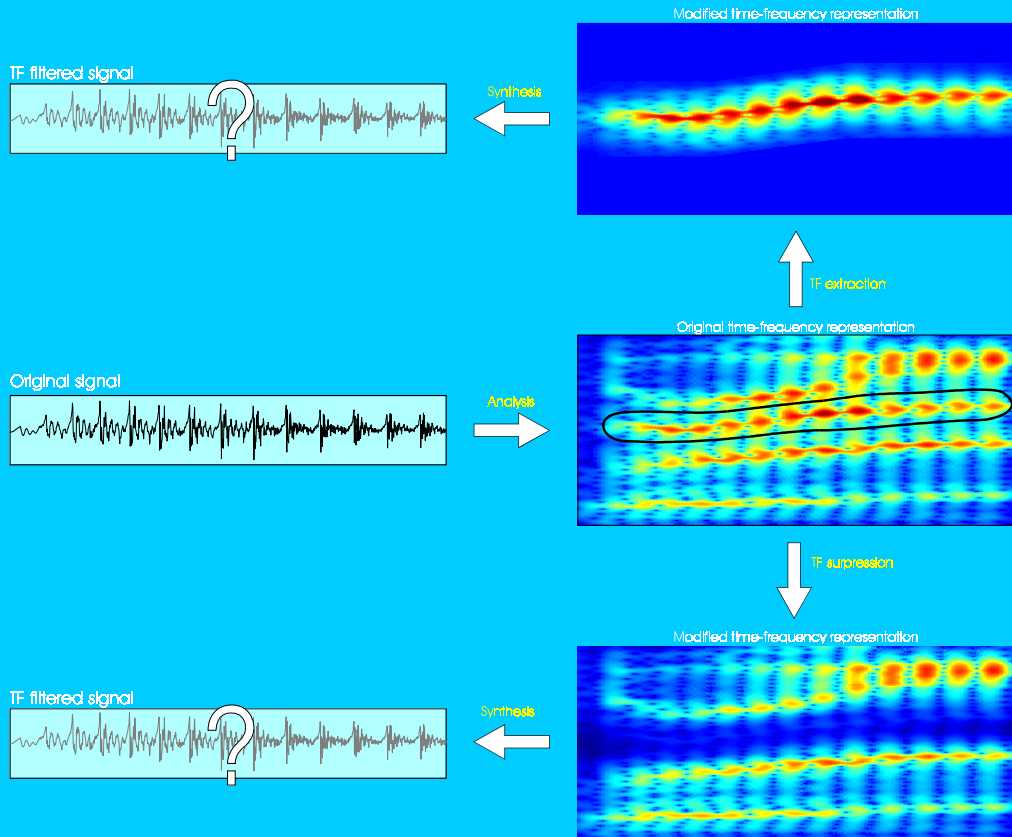
Aalborg University

Joint Time Frequency Synthesis - Signal Design



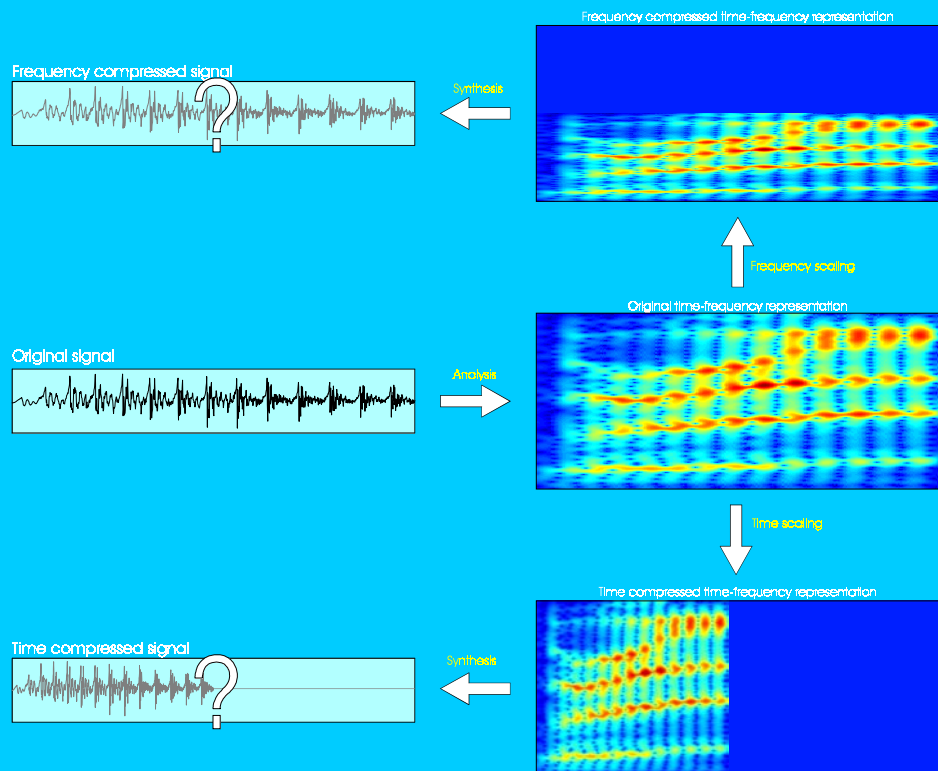
Aalborg University

Joint Time Frequency Filtering



Aalborg University

Joint Time Frequency Scaling



Aalborg University

Transparents for lecture no 2.

Fundamental properties of the Wigner-Ville Distribution

P1. Shifting property

$$x(t) = y(t+T) \Rightarrow WV_x(t, \omega) = WV_y(t+T, \omega)$$

$$x(t) = y(t) e^{jt\Omega} \Rightarrow WV_x(t, \omega) = WV_y(t, \omega + \Omega)$$

P2. Marginal property

$$\int WV_x(t, \omega) dt = |X(\omega)|^2$$

$$\frac{1}{2\pi} \int WV_x(t, \omega) d\omega = |x(t)|^2$$

$$\frac{1}{2\pi} \int \int WV_x(t, \omega) d\omega dt = \|x\|^2$$

P3. Addition property

$$x(t) = x_1(t) + x_2(t)$$

$$WV_x(t, \omega) = WV_{x_1}(t, \omega) + WV_{x_2}(t, \omega) + 2Re \{ WV_{x_1, x_2}(t, \omega) \}$$

Aalborg University

Fundamental properties of the Wigner-Ville Distribution

P4. Product property

$$x(t) = x_1(t) \cdot x_2(t)$$

$$WV_x(t, \omega) = WV_{x_1}(t, \omega) \otimes_{\omega} WV_{x_2}(t, \omega)$$

P5. Convolution property

$$x(t) = x_1(t) \otimes x_2(t)$$

$$WV_x(t, \omega) = WV_{x_1}(t, \omega) \otimes_t WV_{x_2}(t, \omega)$$

Aalborg University

Wigner-Ville distribution

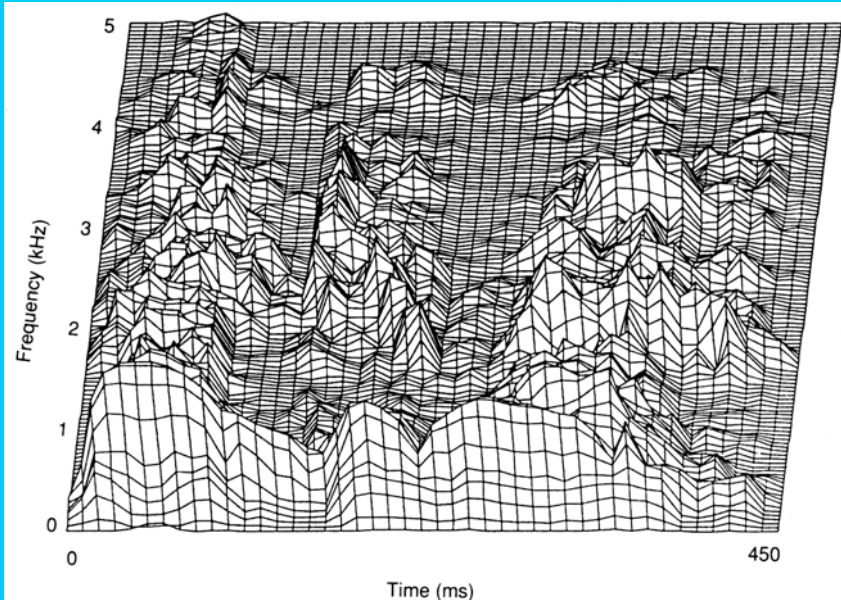
$$WVD_x(t, \omega) = \int_{-\infty}^{\infty} x(t + \tau/2) x(t - \tau/2) e^{-j\omega\tau} d\tau$$

Developed in quantum mechanics by Eugene Paul Wigner in 1932 and introduced in signal processing by Jean Ville in 1948

- Not intuitive
- No window function, no parameter to change
- Quadratic function, cross terms!

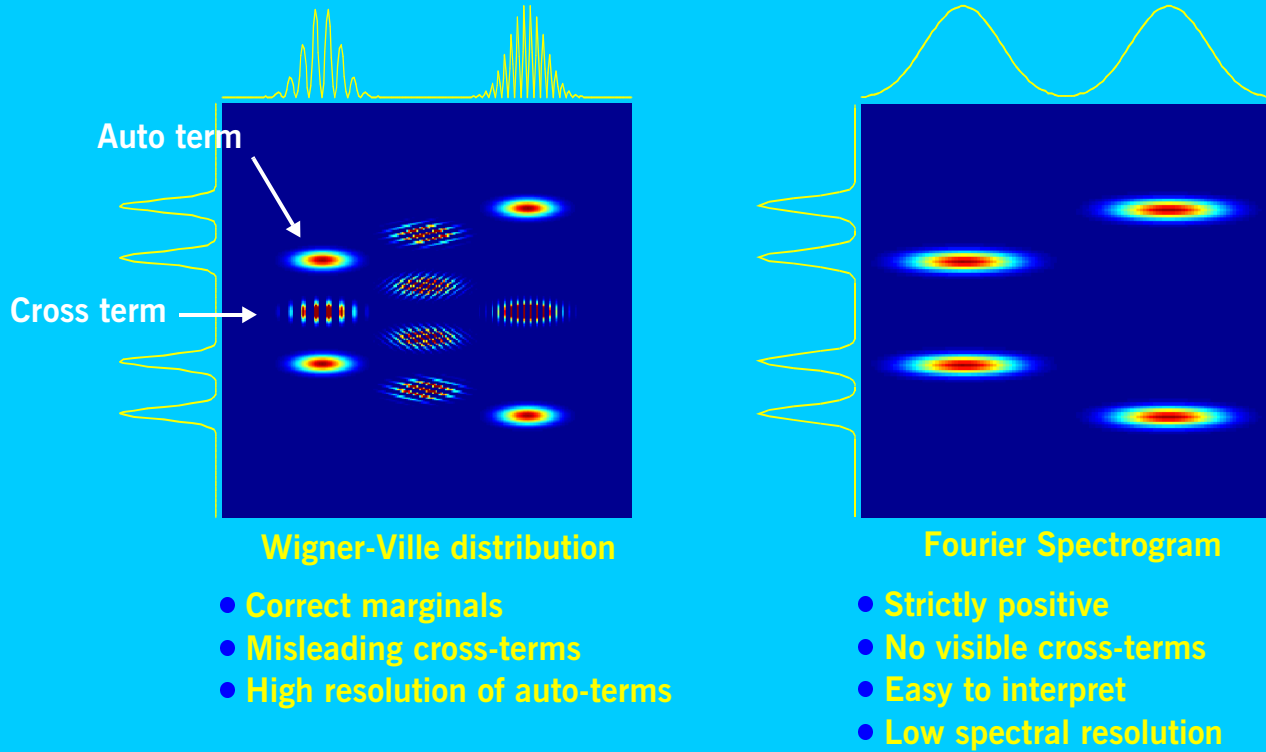
Aalborg University

This is an original Wigner-Ville Distribution



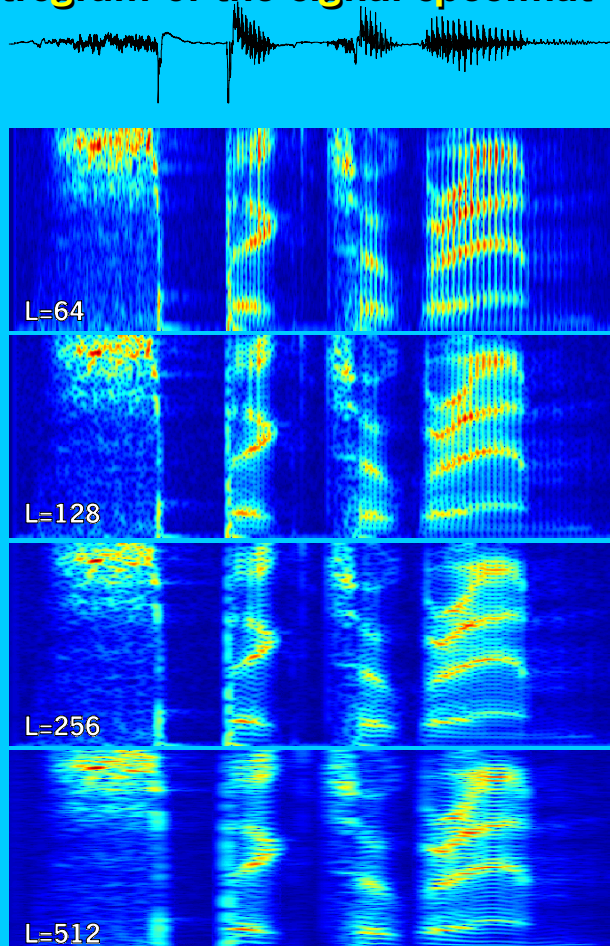
Aalborg University

Wigner-Ville versus the Fourier Spectrogram



Aalborg University

Fourier Spectrogram of the signal spec.mat



Aalborg University

Discrete Time Frequency Wigner-Ville distribution (DTF-WVD)

Peyring&Prost 1986

Discrete Time Frequency - Wigner Ville Distribution

Pre-processing of input signal:

$$x = [\text{interp}(\text{signal}, 2) \text{ zeros}(1, 2 * \text{length}(\text{signal}))]$$

Distribution:

$$\begin{aligned} WVD[m, n] &= \sum_{k=0}^{N-1} x_k x^*_{m-k} e^{-j\frac{n\pi}{N}(2k-m)} \\ 0 \leq m < N \quad -\frac{N}{2} \leq n &< \frac{N}{2} \end{aligned}$$

Aalborg University

Discrete Time Frequency Wigner-Ville distribution (DTF-WVD)

Peyring&Prost 1986

Discrete Time Frequency - Wigner Ville Distribution
FFT-version

Pre-processing of input signal:

$$x = [\text{interp}(\text{signal}, 2) \text{ zeros}(1, 2 * \text{length}(\text{signal}))]$$

Distribution:

$$\begin{aligned} WVD[m, n] &= \frac{1}{2NT} \cdot F_m[n] \cdot e^{j\frac{mn\pi}{N}} \\ 0 \leq m < N \quad 0 \leq n < N \\ F_m[n] &= \text{FFT}^N \{ x_k x^*_{(m-k) \bmod N} \} \end{aligned}$$

Post-processing of distribution:

$$WVD[m, n] = (-1)^m WVD[m, n] \quad \text{for } \frac{N}{2} \leq n < N$$

Aalborg University

Cohens class of bilinear distributions

Developed in quantum mechanic by Leon Cohen in 1966 and introduced in signal processing by himself.

$$C(t, \omega; \varphi) = \frac{1}{2\pi} \int \int e^{j\theta(t-u) - j\tau\omega} \varphi(\theta, \tau) x(u + \tau/2) x(u - \tau/2) d\theta d\tau du$$

Kernel function 2. order

- describes all TF distributions with a second order dependence of the signal
- each distribution is characterized by a kernel function.
- enables a structural way of constructing a distribution with certain properties.

Aalborg University

Properties of Cohens class of bilinear distributions

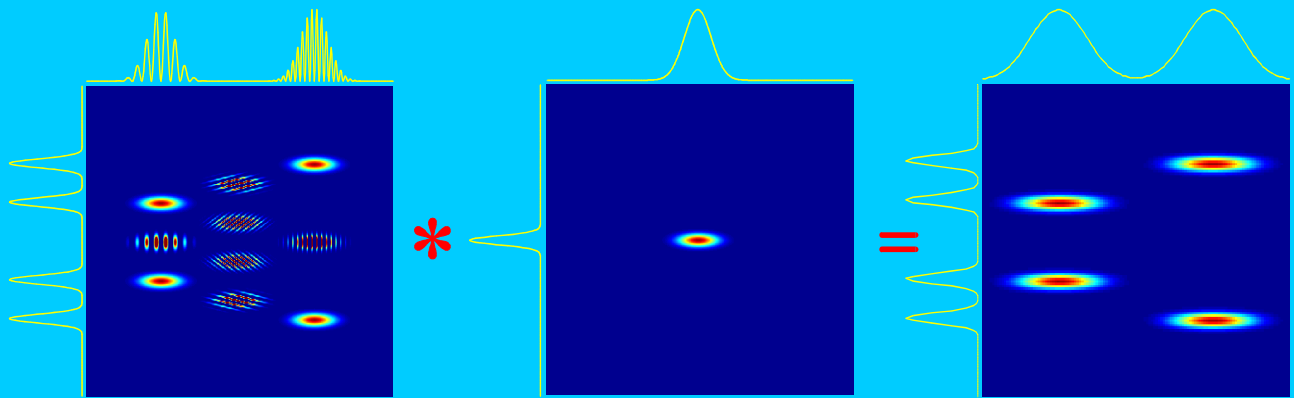
Property Name	Property	Property Constraint
1. Instantaneous energy	$\frac{1}{2\pi} \int C_x(t, \omega; \varphi) d\omega = x(t) ^2$	$\varphi(0, 0) = 1$ for all θ
2. Power Spectrum	$\int C_x(t, \omega; \varphi) dt = X(\omega) ^2$	$\varphi(0, \tau) = 1$ for all τ
3. Shifting in time	$x(t) = y(t-T) \Leftrightarrow C_x(t, \omega; \varphi) = C_y(t-T, \omega; \Phi)$	$\varphi(\theta, \tau)$ independent of t
4. Shifting in frequency	$x(t) = y(t) e^{j\Omega t} \Leftrightarrow C_x(t, \omega; \varphi) = C_y(t, \omega - \Omega; \Phi)$	$\varphi(\theta, \tau)$ independent of ω
5. Real distribution	$C_x(t, \omega; \varphi) = C_x^*(t, \omega; \varphi)$	$\varphi(\theta, \tau) = \varphi^*(-\theta, -\tau)$
6. Time extend	$x(t) = 0$ for $ t > T \Leftrightarrow C_x(t, \omega; \Phi) = 0$ for $ t > T \forall \omega$	$\int e^{j\theta t} \varphi(\theta, \tau) d\theta = 0$ for $2 t > \tau $
7. Frequency extend	$X(\omega) = 0$ for $ \omega > \Omega \Leftrightarrow C_x(t, \omega; \varphi) = 0$ for $ \omega > \Omega \forall t$	$\int e^{-j\tau\omega} \varphi(\theta, \tau) d\tau = 0$ for $2 \omega > \theta $
8. Group delay	$\frac{\int t C_x(t, \omega; \varphi) dt}{\int C_x(t, \omega; \varphi) dt} = t_{delay}(\omega)$	$\left. \frac{\partial \varphi(\theta, \tau)}{\partial \theta} \right _{\theta=0} = 0$ for all τ $\varphi(0, \tau) = 1$ for all θ
9. Instantaneous frequency	$\frac{\int \omega C_x(t, \omega; \varphi) d\omega}{\int C_x(t, \omega; \varphi) d\omega} = \Omega_x(\omega)$	$\left. \frac{\partial \varphi(\theta, \tau)}{\partial \tau} \right _{\tau=0} = 0$ for all θ $\varphi(0, 0) = 1$ for all θ
10. Positive distribution	$C_x(t, \omega; \varphi) \geq 0$ for all t, ω	$\varphi(\theta, \tau) = A F_h(\theta, \tau)$

Aalborg University

Cohens class of bilinear distributions

$$\begin{aligned} C(t, \omega; \varphi) &= \frac{1}{2\pi} \int \int e^{j\theta(t-u) - j\tau\omega} \varphi(\theta, \tau) x(u + \tau/2) x(u - \tau/2) d\theta d\tau du \\ &= WVD_x(t, \omega) \otimes_{t, \omega} \Phi(t, \omega) \end{aligned}$$

Cohens class describes all distributions obtained by filtering the Wigner-Ville distribution.



Aalborg University

Filtering approach

- Describes a group of Wigner-Ville modified distributions.
- The filtering approach modifies both auto- and cross-terms
- Correct marginals and positivity are incompatible.



Another approach

- For a general signal, it is impossible to separate auto- and cross-terms in the Wigner-Ville distribution.
- By making a well-defined decomposition of the signal, it will be possible to separate auto- and cross-terms

Aalborg University

Gabor Spectrogram

Developed by Shie Qian in 1992

Wigner-Ville Distribution

$$WVD_x(t, \omega) = \int_{-\infty}^{\infty} x(t + \tau/2)x(t - \tau/2)e^{-j\omega\tau}d\tau$$

Gabor expansion

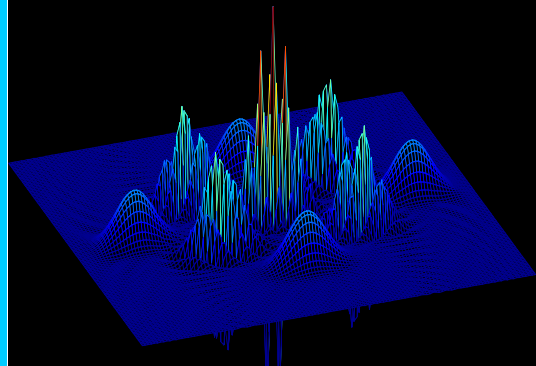
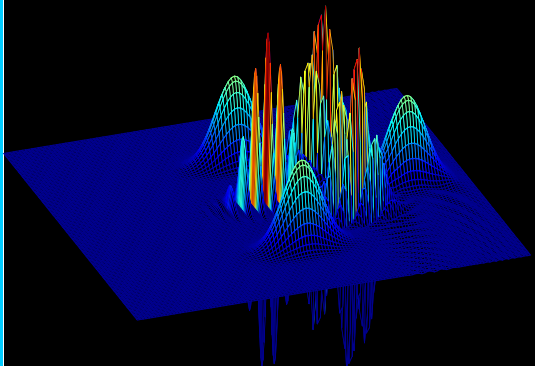
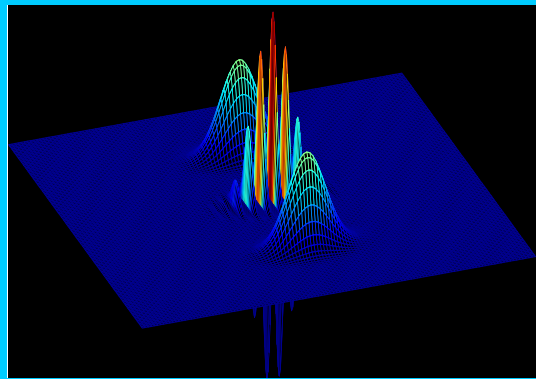
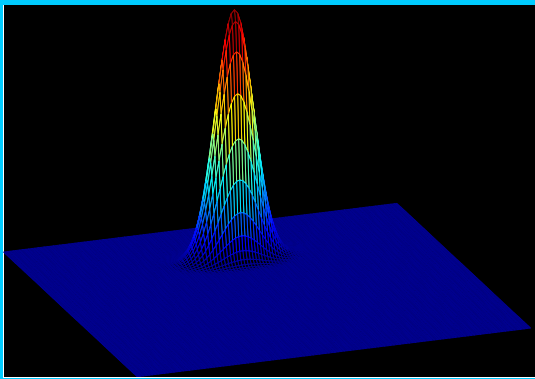
$$x(t) = \sum_m \sum_n a_{mn} g(t - mT) e^{jtn\Omega}$$

The Gabor Spectrogram is based on two well-known signal transformations- the Wigner-Ville distribution and the Gabor expansion.

By using a well-defined multicomponent definition of the signal, auto- and cross-terms can be identified!

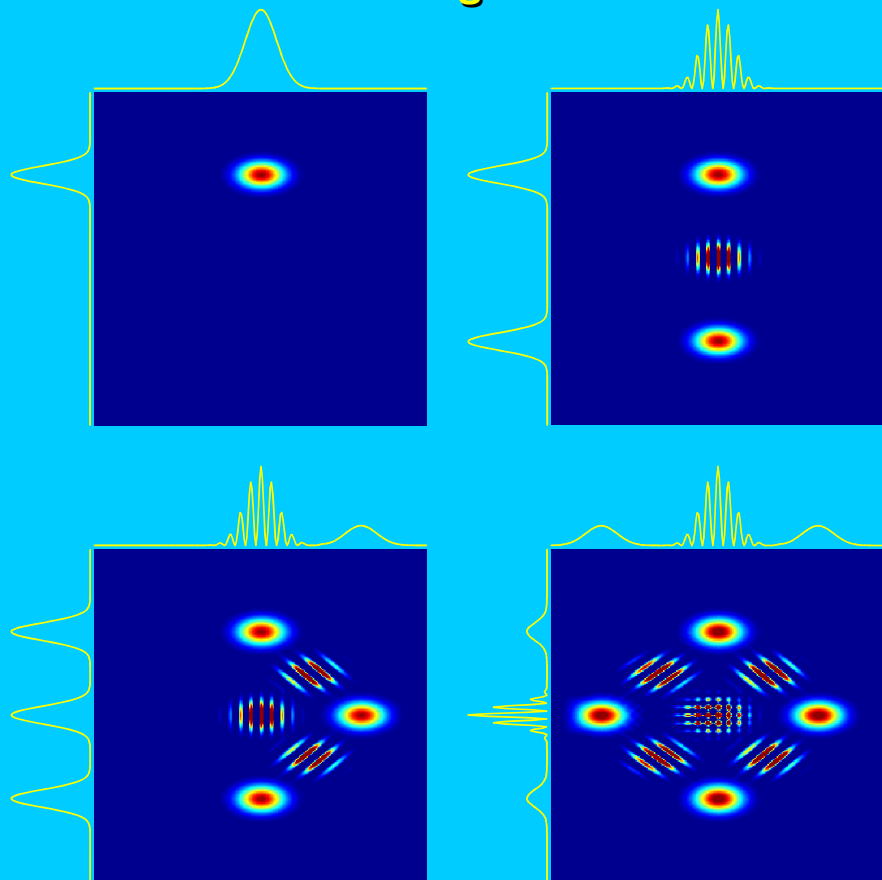
Aalborg University

The Wigner-Ville distribution of 1-4 gaussian function - mesh plot



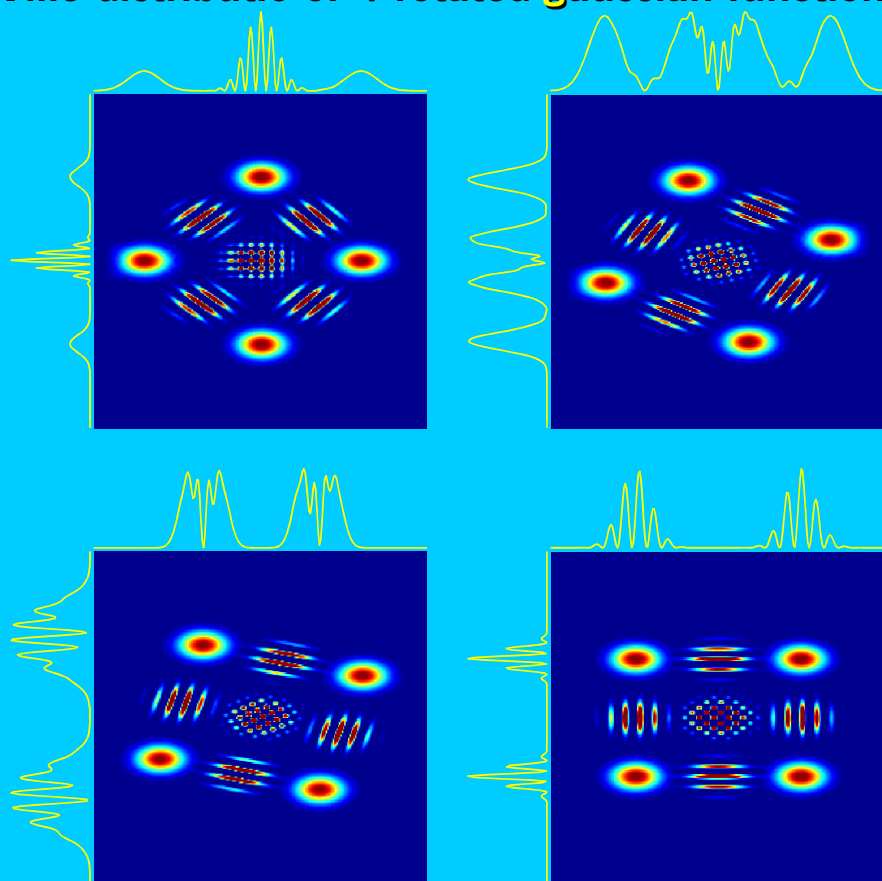
Aalborg University

The Wigner-Ville distribution of 1-4 gaussian functions - image plot



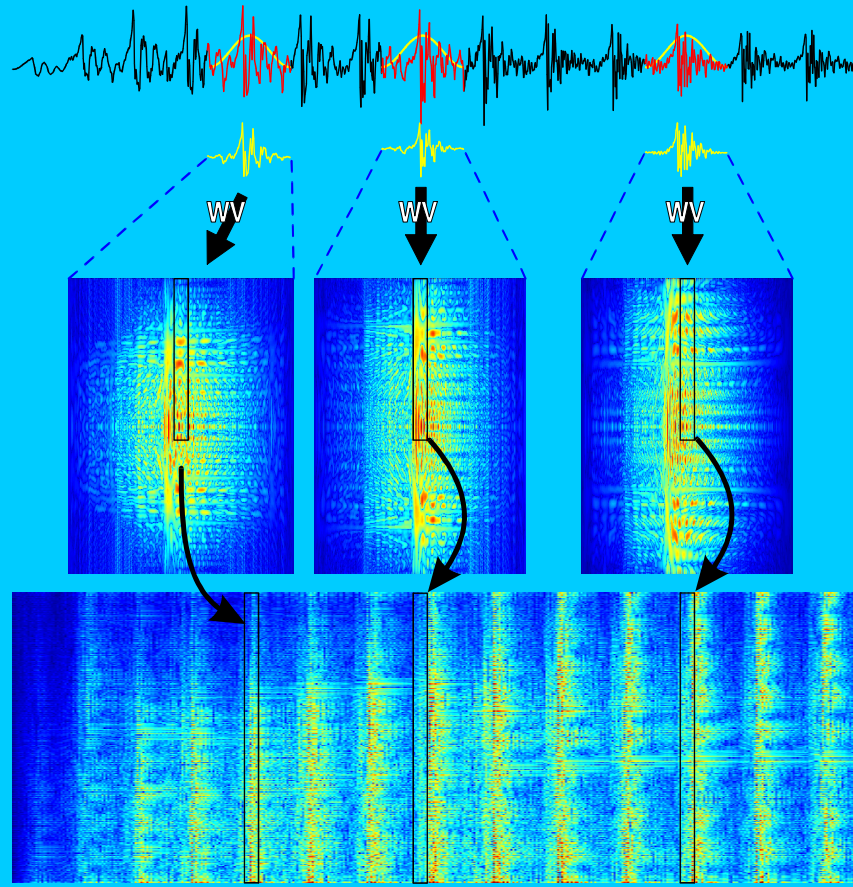
Aalborg University

The Wigner-Ville distribution of 4 rotated gaussian functions



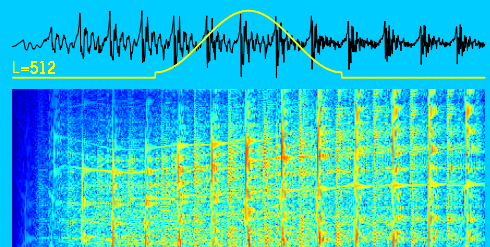
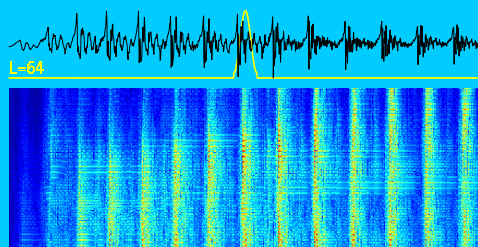
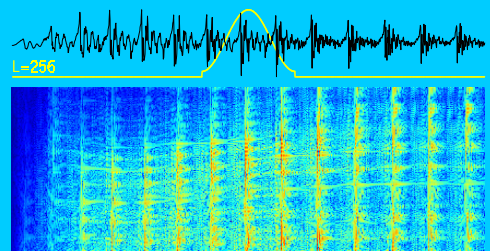
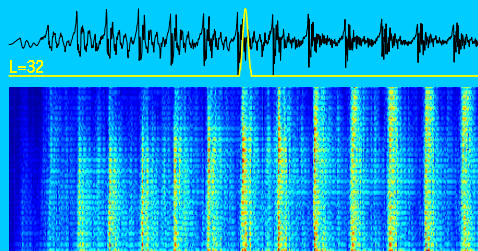
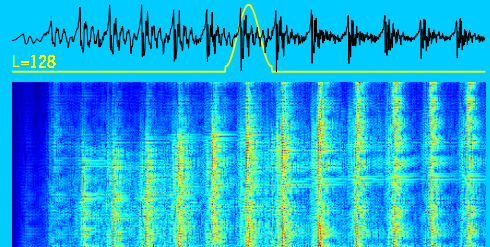
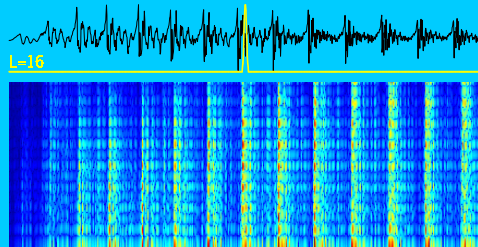
Aalborg University

Procedure of the windowed DTF-WVD



Aalborg University

Examples of window distortion in the windowed DTF-WV



Aalborg University

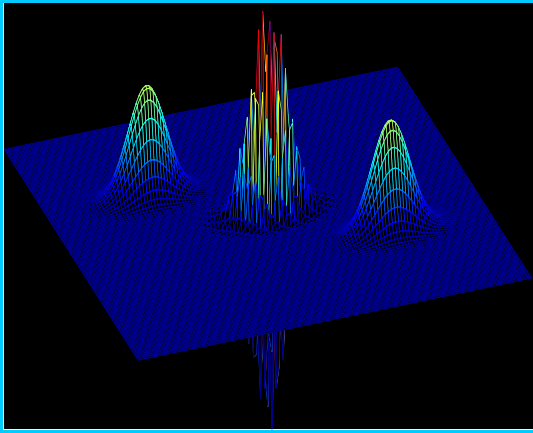
A cross-term deleted Wigner-Ville distribution

$$x(t) = g(t - T_1) e^{jt\Omega_1} + g(t - T_2) e^{jt\Omega_2}$$

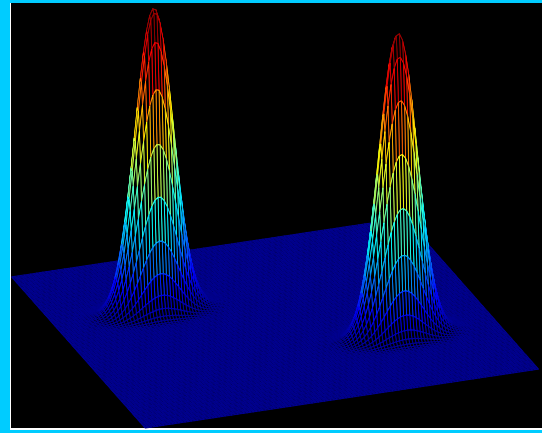
$$WV_x(t, \omega) = WV_g(t - T_1, \omega - \Omega_1) + WV_g(t - T_2, \omega - \Omega_2) + 2Re \{ WV_{g_1, g_2}(t, \omega) \}$$



Original distribution

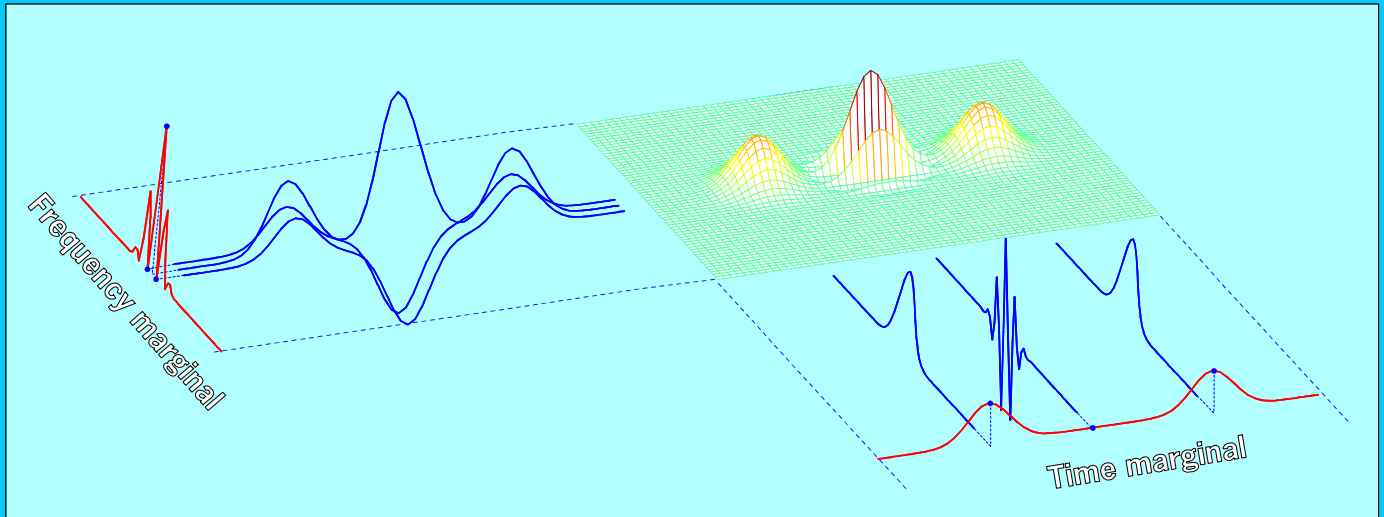


Cross-term deleted distribution



Aalborg University

Correct marginals are dependent on cross-terms !

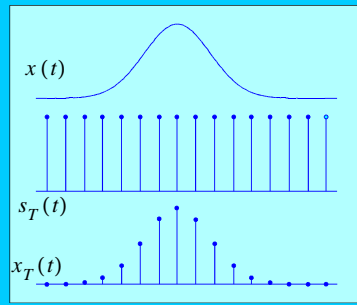


Aalborg University

Discrete Time WVD

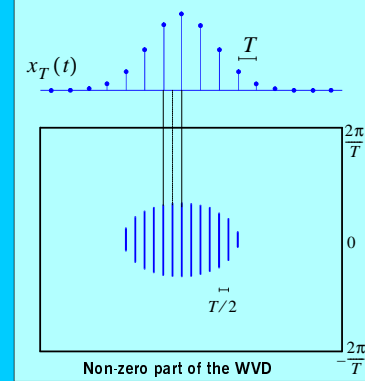
Signal definition:

$$x(t) \\ s_T(t) = \sum_n \delta(t - nT) \\ x_T(t) = x(t) \cdot s_T(t) = \sum_n x(nT) \delta(t - nT)$$



WVD:

$$WVD_{x_T}(t, \omega) = \int x_T(t + \tau/2) x_T^*(t - \tau/2) e^{-j\omega\tau} d\tau \\ = \sum_n \underbrace{\frac{1}{2} \sum_k x(kT) x^*((n-k)T)}_{DT-WVD} e^{-j\omega(2k-n)\frac{T}{2}} \delta\left(t - n\frac{T}{2}\right)$$



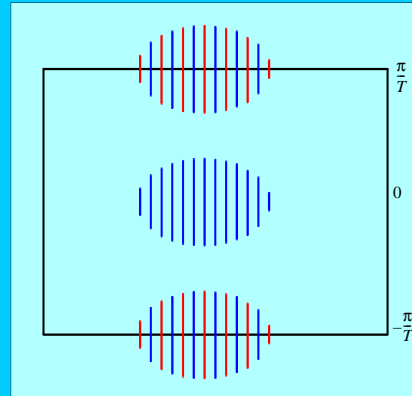
- The WVD of the sampled signal is sampled in time at a rate twice finer $T/2$ than the signal

Aalborg University

Discrete Time WVD - cont.

WVD:

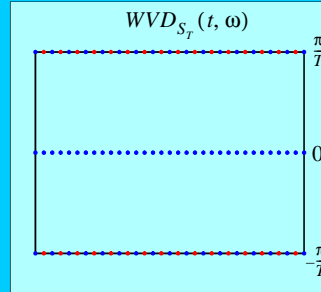
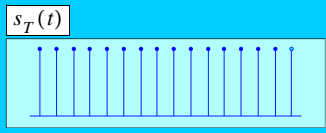
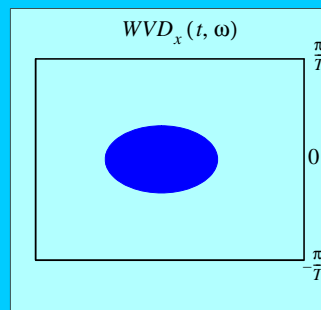
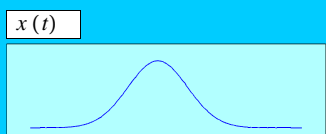
$$WVD_{x \cdot s_T}(t, \omega) = WVD_x(t, \omega) \otimes_{\omega} WVD_{s_T}(t, \omega) \\ = WVD_x(t, \omega) \otimes \frac{2\pi}{4T} \sum_n \sum_l (-1)^{nl} \delta\left(\omega - l \cdot \frac{2\pi}{2T}\right) \delta\left(t - n \cdot \frac{T}{2}\right) \\ = \frac{2\pi}{4T} \sum_n \sum_l WVD_x\left(t, \omega - l \cdot \frac{2\pi}{2T}\right) (-1)^{nl} \delta\left(t - n \cdot \frac{T}{2}\right)$$



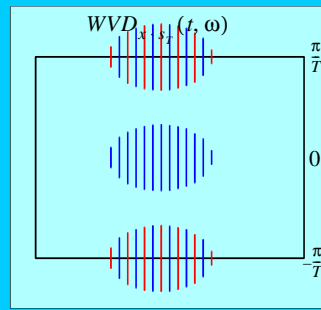
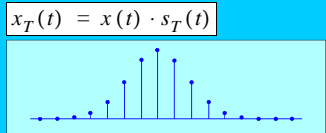
- The WVD is repeated in the frequency with period $\frac{\pi}{T}$ and alternance of sign. Not every $\frac{2\pi}{T}$ like the DFT!
- To avoid frequency aliasing, the signal has to be oversampled with a factor of 2!

Aalborg University

Discrete Time WVD - cont.



$$WVD_{S_T}(t, \omega) = \frac{2\pi}{4T} \sum_n \sum_l (-1)^{nl} \delta(\omega - l \cdot \frac{2\pi}{2T}) \delta(t - n \cdot \frac{T}{2})$$



$$WVD_{x * s_T}(t, \omega) = WVD_x(t, \omega) \otimes_{\omega} WVD_{S_T}(t, \omega)$$

Aalborg

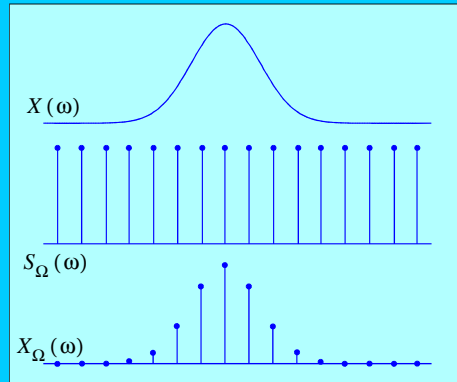
Discrete Frequency WVD

Signal definition:

$$X(\omega)$$

$$S_\Omega(\omega) = \sum_n \delta(\omega - n\Omega)$$

$$X_\Omega(\omega) = X(\omega) \cdot S_\Omega(\omega) = \sum_n X(n\Omega) \delta(\omega - n\Omega)$$



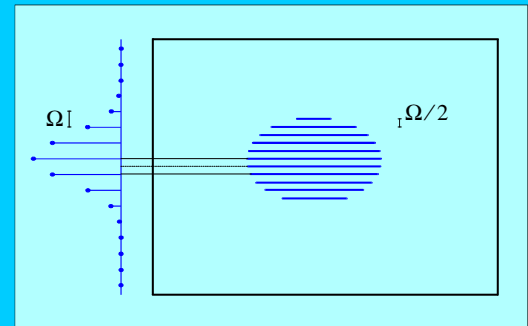
Discrete spectrum \Leftrightarrow Periodic signal

Step size = Ω

$$\text{Period} = \frac{2\pi}{\Omega}$$

WVD:

$$\begin{aligned} WVD_{X_\Omega}(t, \omega) &= \frac{1}{2\pi} \int X_\Omega(\omega + \tau/2) X_\Omega^*(\omega - \tau/2) e^{j\tau t} d\tau \\ &= \sum_n \underbrace{\frac{1}{4\pi} \sum_k X(k\Omega) X^*((n-k)\Omega)}_{\text{DF-WVD}} e^{jt(2k-n)\frac{\Omega}{2}} \delta(\omega - n\frac{\Omega}{2}) \end{aligned}$$

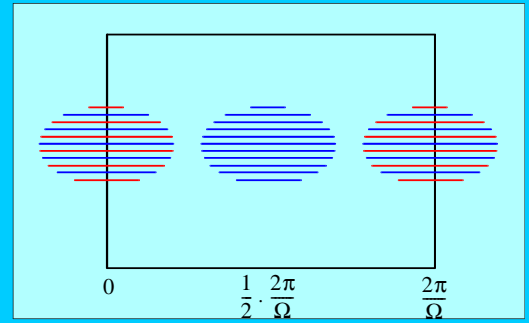


- The WVD of the periodic signal X_Ω is sampled in frequency at a rate twice finer $\Omega/2$ than the spectrum (Ω).

Discrete Frequency WVD - cont.

WVD:

$$\begin{aligned}
 WVD_{X \cdot S_\Omega}(t, \omega) &= WVD_X(t, \omega) \otimes {}_t WVD_{S_\Omega}(t, \omega) \\
 &= WVD_X(t, \omega) \otimes \frac{1}{4\Omega} \sum_n \sum_l (-1)^{nl} \delta\left(t - l \cdot \frac{2\pi}{2\Omega}\right) \delta\left(\omega - \frac{n\Omega}{2}\right) \\
 &= \frac{1}{4\Omega} \sum_n \sum_l (-1)^{nl} WVD_X\left(t - l \cdot \frac{2\pi}{2\Omega}, \omega\right) \delta\left(\omega - \frac{n\Omega}{2}\right)
 \end{aligned}$$



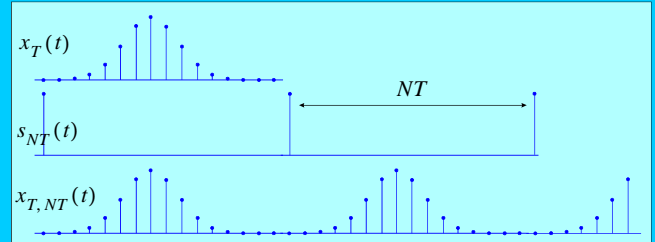
- The WVD is periodic in the time domain with $\frac{1}{2} \cdot \frac{2\pi}{\Omega}$, and an alternance of sign!
- To avoid time aliasing, the signal must be zeropadded to double length!

Aalborg University

Discrete Time Frequency WVD

Signal definition:

$$\begin{aligned}
 x_T(t) &= \sum_{n=0}^{N-1} x(nT) \delta(t - nT) \\
 s_{NT}(t) &= \sum_m \delta(t - m \cdot NT) \\
 x_{T,NT}(t) &= x_T(t) \otimes s_{NT}(t) = \sum_{n=0}^{N-1} x(nT) \delta(t - nT) \otimes \sum_m \delta(t - m \cdot NT)
 \end{aligned}$$



WVD:

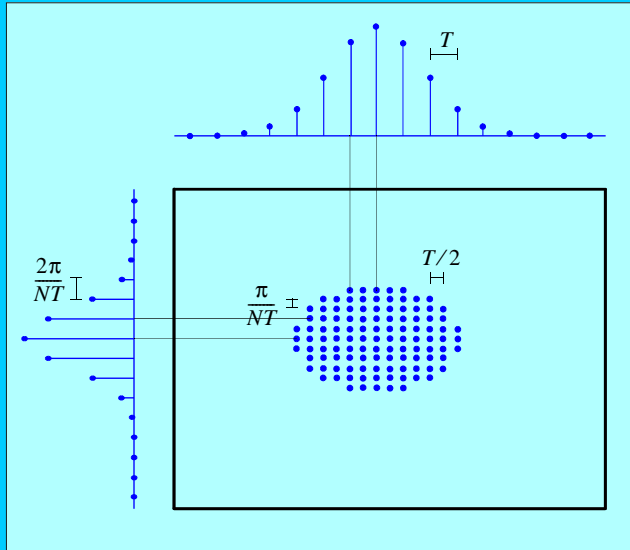
$$WVD_{x_{T,NT}}(t, \omega) = WVD_{x_T}(t, \omega) \otimes {}_t WVD_{s_{NT}}(t, \omega)$$

where

$$\begin{aligned}
 WVD_{x_T}(t, \omega) &= \sum_{k=0}^{N-1} \frac{1}{2} \sum_{n=0}^{N-1} x_n x_{k-n}^* e^{-j\omega(2n-k)T} \delta\left(t - k \frac{T}{2}\right) \\
 WVD_{s_{NT}}(t, \omega) &= \frac{2\pi}{4NT} \sum_m \sum_{m'} (-1)^{mm'} \delta\left(\omega - m \cdot \frac{2\pi}{2NT}\right) \delta\left(t - \frac{m'NT}{2}\right) \\
 WVD_{x_{T,NT}}(t, \omega) &= \int WVD_{x_T}(p, \omega) WVD_{s_{NT}}(t-p, \omega) dp \\
 &= \sum_{k=-\infty}^{\infty} \sum_{m=-\infty}^{\infty} \underbrace{\left[\frac{\pi}{4NT} \sum_{n=0}^{N-1} x_n x_{k-n}^* e^{-j\frac{m\pi}{N}(2n-k)} \right]}_{\text{DTF-WVD}} \delta\left(\omega - m \cdot \frac{2\pi}{2NT}\right) \delta\left(t - \frac{kT}{2}\right)
 \end{aligned}$$

Aalborg University

Discrete Time Frequency WVD cont.



Aalborg University

Discrete Time Frequency WVD - cont.

WVD:

$$WVD_{x_{T,NT}}(t, \omega) = WVD_{x_T}(t, \omega) \otimes_t WVD_{s_{NT}}(t, \omega)$$

where

$$WVD_{x_T}(t, \omega) = \frac{2\pi}{4T} \sum_{n=0}^{N-1} \sum_{l=0}^{N-1} (-1)^{nl} WVD_x\left(t, \omega - l \cdot \frac{2\pi}{2T}\right) \delta\left(t - \frac{nT}{2}\right)$$

$$WVD_{S_{NT}}(t, \omega) = \frac{2\pi}{4NT} \sum_m \sum_{m'} (-1)^{mm'} \delta\left(\omega - m \cdot \frac{2\pi}{2NT}\right) \delta\left(t - \frac{m'NT}{2}\right)$$

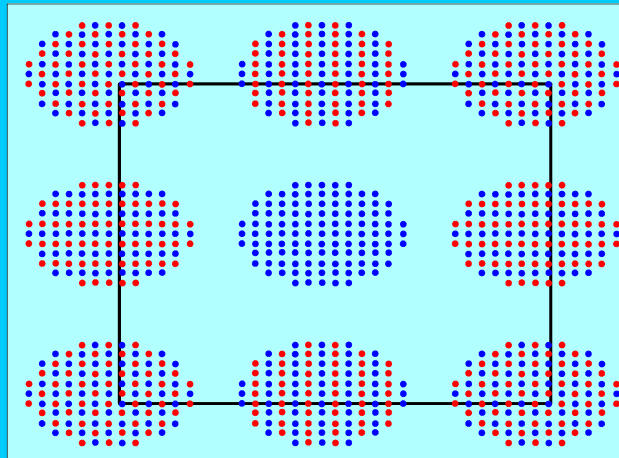
$$\begin{aligned} WVD_{x_{T,NT}}(t, \omega) &= \int WVD_{x_T}(p, \omega) WVD_{S_{NT}}(t-p, \omega) dp \\ &= \frac{\pi^2}{4NT^2} \sum_{n=0}^{N-1} \sum_{l=0}^{N-1} \sum_{a} \sum_{b} (-1)^{ab + nl + laN} WVD_x\left(\frac{T}{2}(n-aN), \frac{2\pi}{2NT}(b-lN)\right) \\ &\quad \cdot \delta\left(\omega - b \cdot \frac{2\pi}{2NT}\right) \delta\left(t - n \frac{T}{2}\right) \end{aligned}$$

↑
Time aliasing ↑
Frequency aliasing

- The WVD contain time aliasing every $\frac{NT}{2}$, and frequency aliasing every $\frac{\pi}{T}$!

Aalborg University

Discrete Time Frequency WVD - cont.

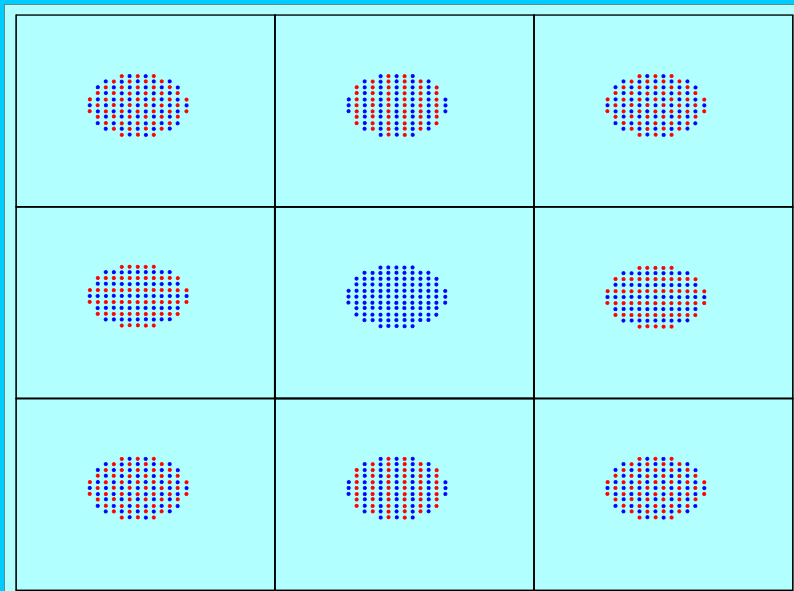


To avoid time and frequency aliasing, the signal must be oversampled and zeropadded to double length!

Aalborg University

Discrete Time Frequency WVD - cont.

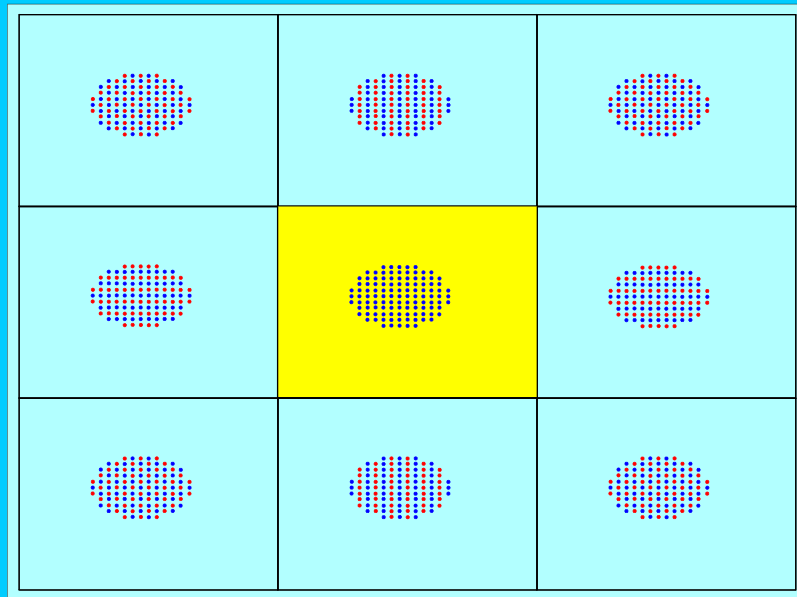
After preprocessing:



Aalborg University

Discrete Time Frequency WVD - cont.

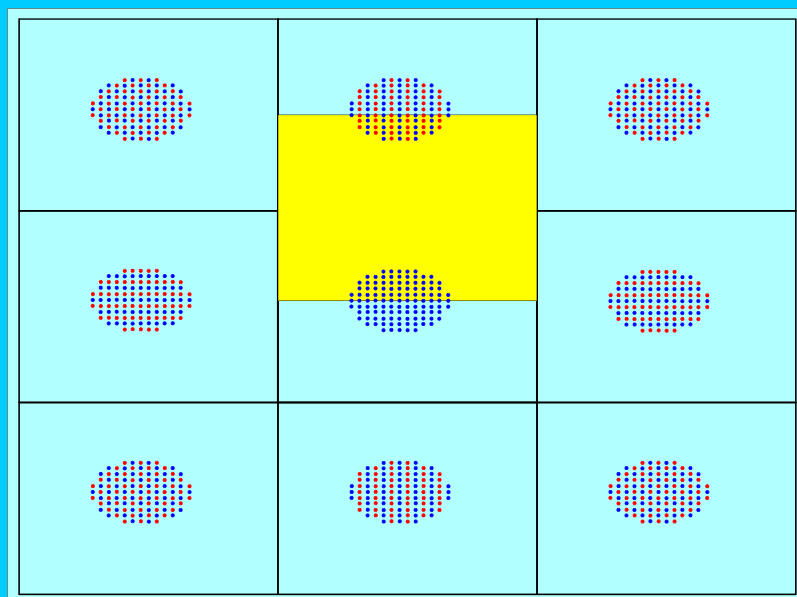
Normal implementation:



Aalborg University

Discrete Time Frequency WVD - cont.

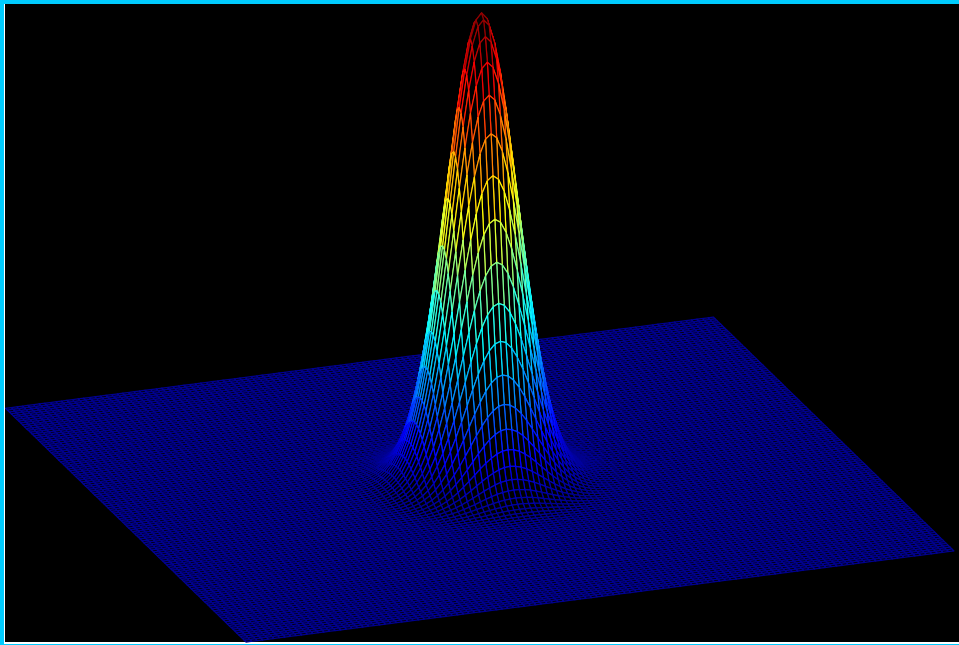
FFT implementation:



Aalborg University

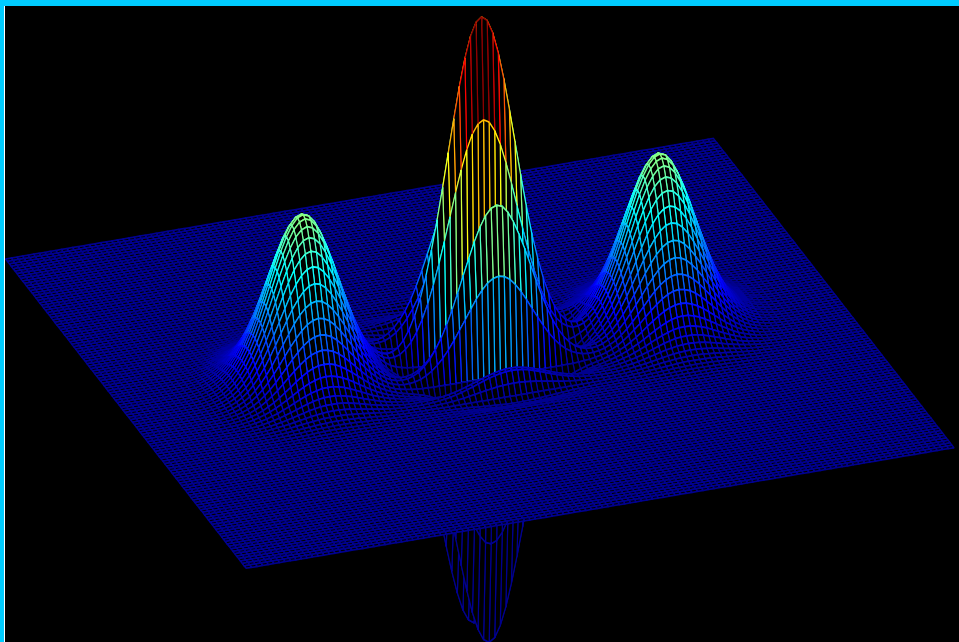
Transparents for lecture no 3.

The Wigner-Ville distribution of a gaussian function



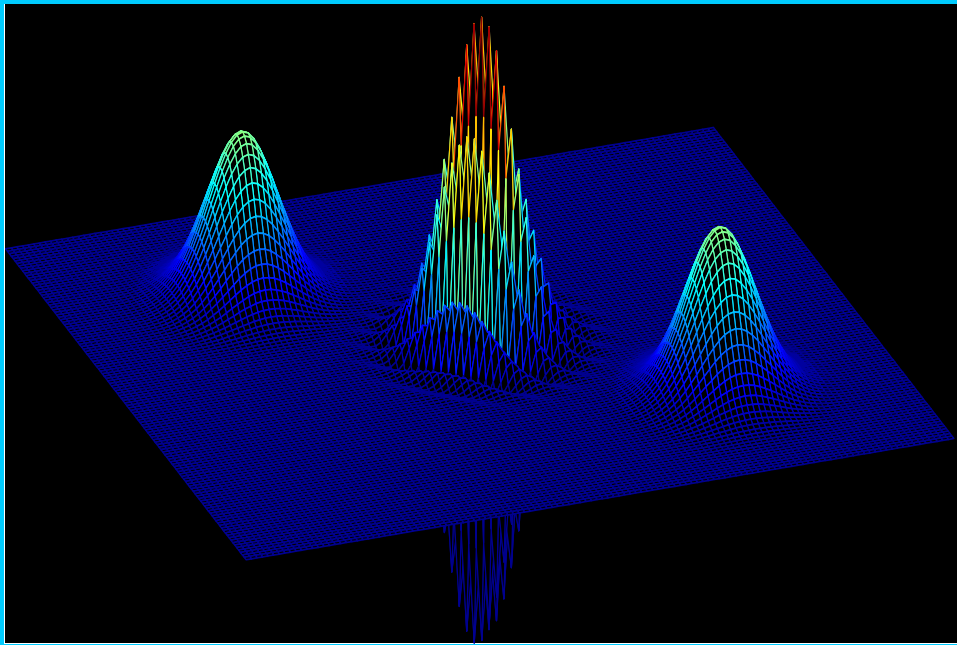
Aalborg University

The Wigner-Ville distribution of two time shifted gaussian functions



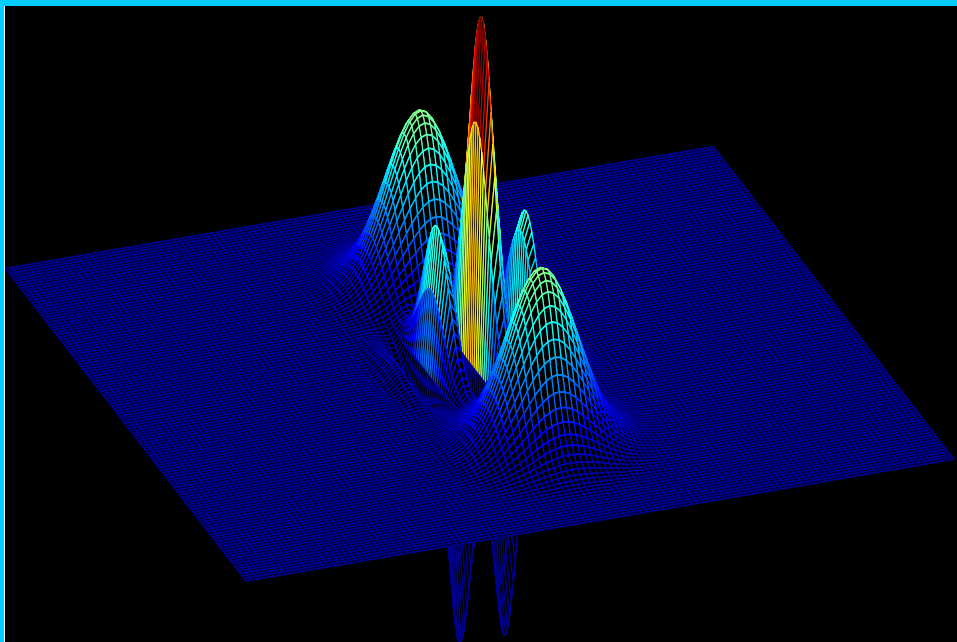
Aalborg University

The Wigner-Ville distribution of two time and frequency shifted gaussian functions



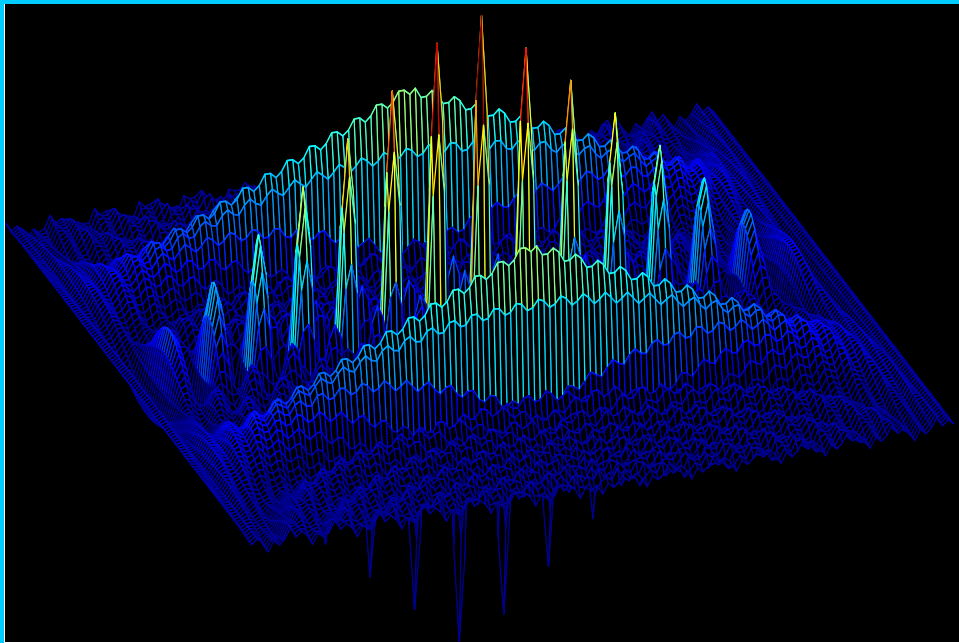
Aalborg University

The Wigner-Ville distribution of two frequency shifted gaussian functions



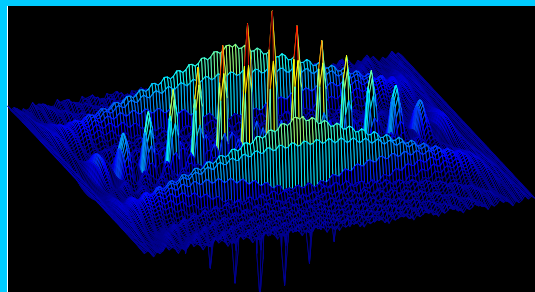
Aalborg University

The Wigner-Ville distribution of a time limited cosinus function

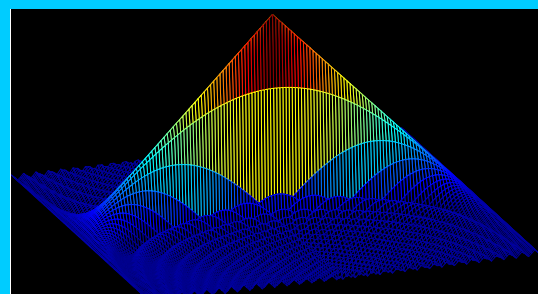
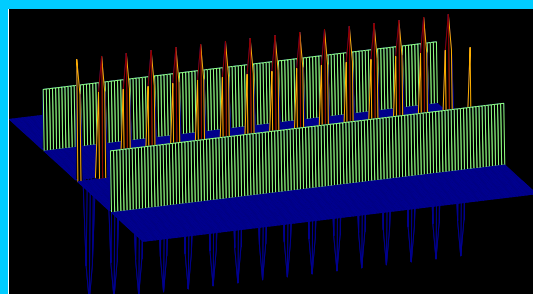


Aalborg University

The Wigner-Ville of a time limited cosinus function



=



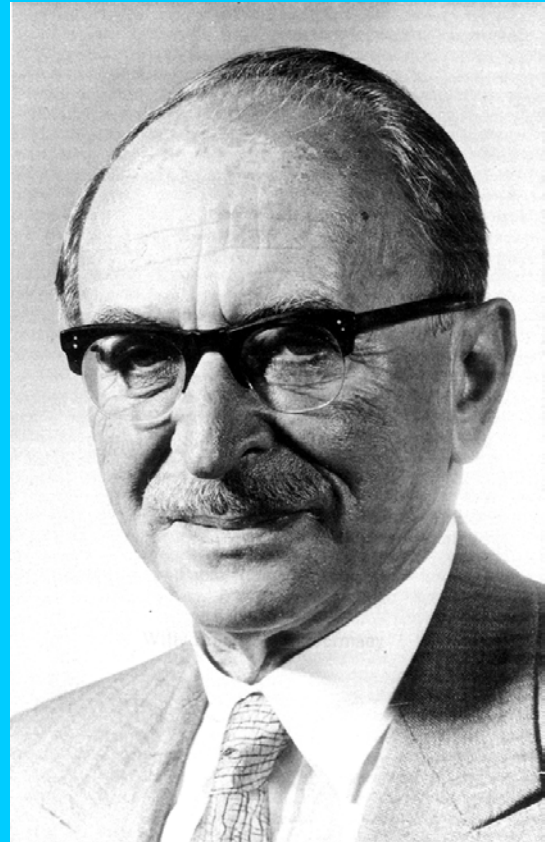
Aalborg University

Dennis Gabor

Born: June 5, 1900 in Budapest, Hungary

Dead: 1979 in London.

- Invented the Gabor expansion in November 1946
- Developed the theory of holography in 1947, which he received the Nobel Prize for in 1971.



Aalborg University

Continuous Gabor Expansion

Expansion:

$$x(t) = \sum_m \sum_n a_{mn} g_{mn}(t) = \sum_m \sum_n a_{mn} g(t - mT) e^{jn\Omega t}$$

Gabor coefficients:

$$a_{mn} = \int x(t) \gamma^*_{mn}(t) dt = \int x(t) \gamma^*(t - mT) e^{-jn\Omega t} dt$$

Biorthogonality condition:

$$\delta_m \cdot \delta_n = \frac{2\pi}{\Omega T} \int g(t) \gamma^*\left(t - m\frac{2\pi}{\Omega}\right) e^{-jtn\frac{2\pi}{T}} dt$$
$$-\infty < m < \infty \quad -\infty < n < \infty$$

Aalborg University

Transparents for lecture no 4.

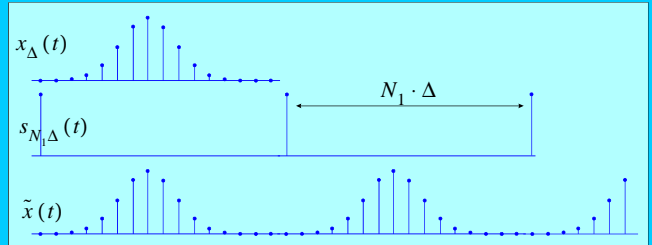
Periodic Discrete Gabor Expansion

Signal definition:

$$x_{\Delta}(t) = \sum_{k=0}^{N_1-1} x[k] \delta(t - k\Delta)$$

$$s_{N_1 \cdot \Delta}(t) = \sum_l \delta(t - l \cdot N_1 \Delta)$$

$$\tilde{x}(t) = x_{\Delta}(t) \otimes s_{N_1 \cdot \Delta}(t) = \sum_l \sum_{k=0}^{N_1-1} x[k] \delta(t - (l \cdot N_1 + k) \Delta)$$

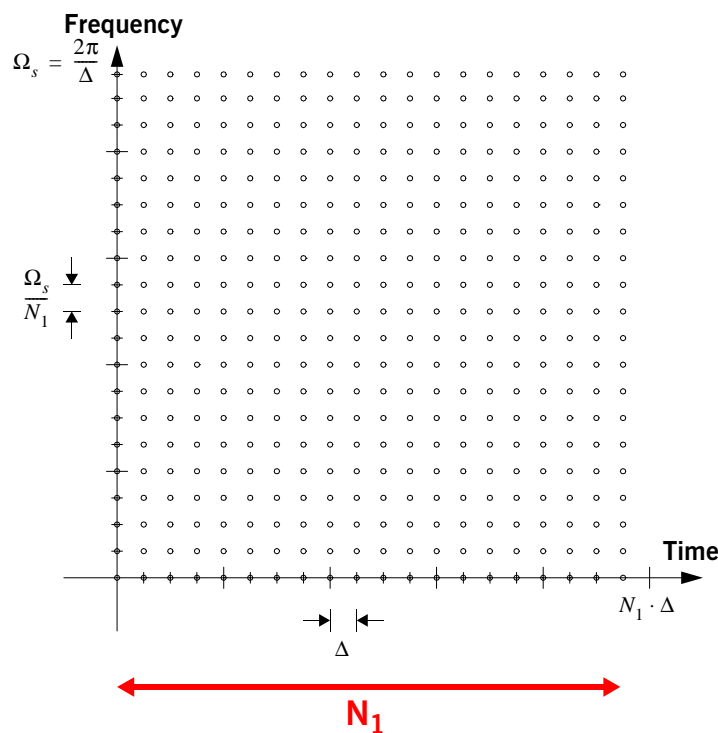


Time discrete Δ \Leftrightarrow Frequency periodic $\frac{2\pi}{\Delta} = \Omega_s$

Time periodic $N_1 \cdot \Delta$ \Leftrightarrow Frequency discrete $\frac{\Omega_s}{N_1}$

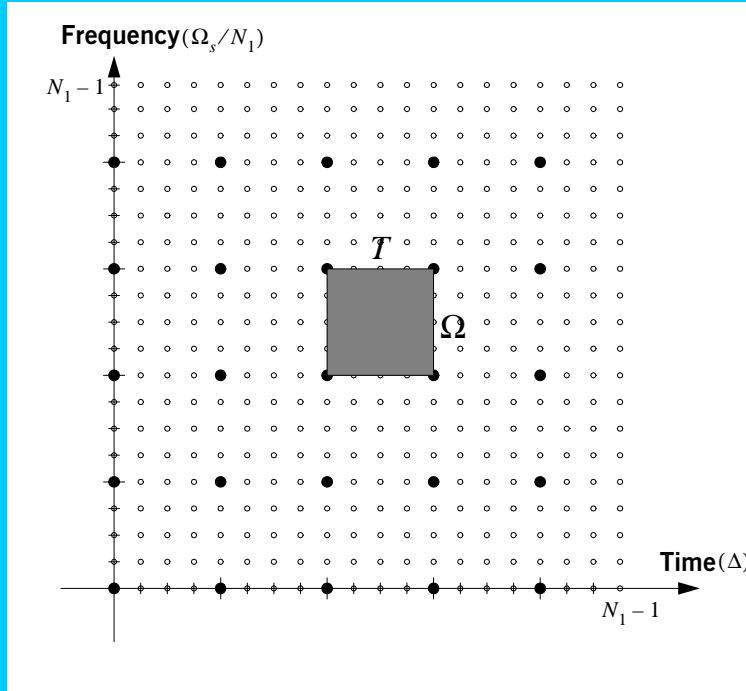
Aalborg University

Non-zero TF plan



Aalborg University

Non-zero TF plan



Aalborg University

From the continuous Gabor expansion:

$$a_{mn} = \int \tilde{x}(t) \gamma^*(t - mT) e^{-jn\Omega t} dt = \sum_{k=0}^{N_1-1} x[k] \tilde{\gamma}^* \left[k - m \cdot \frac{T}{\Delta} \right] e^{-jnk\Delta\Omega}$$

Constant conversion:

$$\frac{T}{\Delta} = \Delta M$$

The number of time steps between the position of the Gabor coefficients

$$\frac{N_1}{\Delta M} = M$$

The number of Gabor coefficients in the time domain

$$\Delta \cdot \Omega = \frac{\Delta}{2\pi} \cdot 2\pi \cdot \Omega = \frac{\Omega}{\Omega_s} \cdot 2\pi = \frac{2\pi}{N} \Rightarrow$$

$$\frac{\Omega_s}{\Omega} = N$$

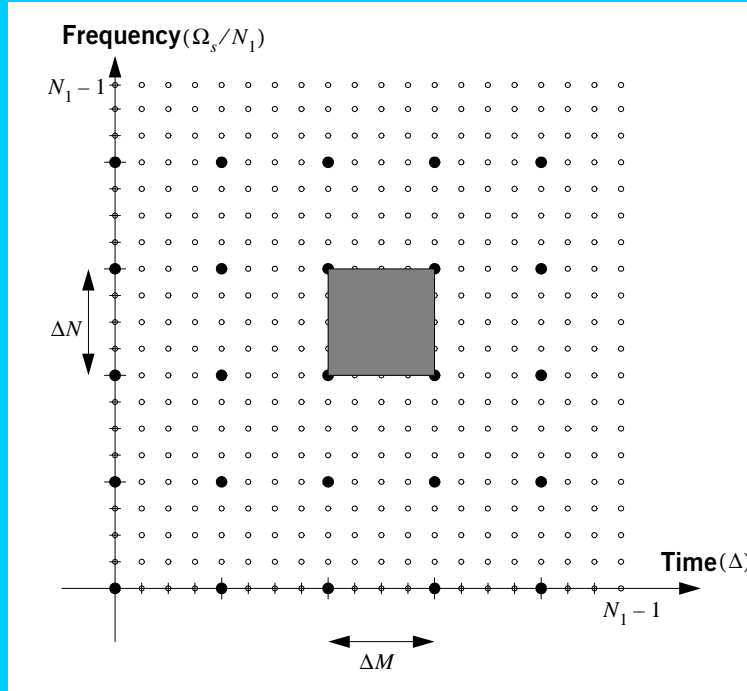
The number of Gabor coefficients in the frequency domain

$$\frac{N_1}{N} = \Delta N$$

The number of frequency steps between the Gabor coefficients.

Aalborg University

Non-zero TF plan



Aalborg University

Constant relation under critical sampling

$$\left. \begin{array}{l} T \cdot \Omega = 2\pi \\ T = \Delta M \cdot \Delta \\ \Omega = \frac{\Omega_s}{N} \end{array} \right\}$$

$$T \cdot \Omega = \Delta M \cdot \Delta \cdot \frac{\left(\frac{2\pi}{\Delta}\right)}{N} = \Delta M \cdot \frac{1}{N} \cdot 2\pi = 2\pi$$

$$\begin{aligned} N_1 &= M \cdot N \\ &= \Delta M \cdot \Delta N \\ N &= \Delta M \\ M &= \Delta N \end{aligned}$$

- N_1 signal samples are transformed into N_1 Gabor coefficients!
- The critical area in the continuous version is $T \cdot \Omega = 2\pi$, and its discrete part is $N_1 = \Delta M \cdot \Delta N$.

Constant relation under oversampling

$$\begin{aligned} N_1 &< M \cdot N \\ N_1 &> \Delta M \cdot \Delta N \\ N &\neq \Delta M \\ M &\neq \Delta N \end{aligned}$$

Aalborg University

The Gabor coefficients are periodic:

$$a_{mn} = a_{m+M, n} = a_{m, n+N}$$

Expansion:

$$\begin{aligned}\tilde{x}(t) &= \sum_m \sum_n a_{mn} g(t - m \cdot T) e^{jtn\Omega} \\ &= \sum_{m=0}^{M-1} \sum_{n=0}^{N-1} \sum_{l,k} a_{mn} g(t - (m + l \cdot M) \cdot T) e^{jt(n+k \cdot N)\Omega} \\ &\Leftrightarrow \\ \tilde{x}[k] &= \sum_{m=0}^{M-1} \sum_{n=0}^{N-1} a_{mn} \tilde{g}[k - m \cdot \Delta M] e^{jkn \frac{2\pi}{N}}\end{aligned}$$

Aalborg University

Status:

$$\begin{aligned}\tilde{x}[k] &= \sum_{m=0}^{M-1} \sum_{n=0}^{N-1} a_{mn} \tilde{g}[k - m \cdot \Delta M] e^{jkn \frac{2\pi}{N}} \\ a_{mn} &= \sum_{k=0}^{N_1-1} x[k] \tilde{\gamma}^*[k - m \cdot \frac{T}{\Delta}] e^{-jnk\Delta\Omega}\end{aligned}$$

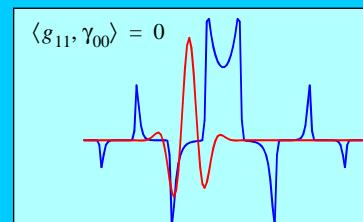
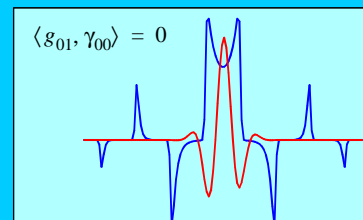
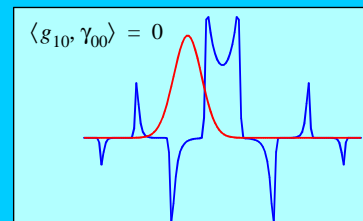
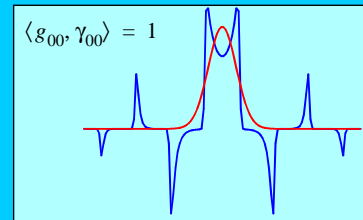
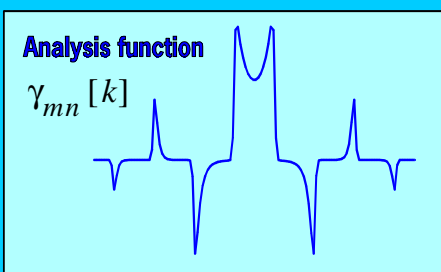
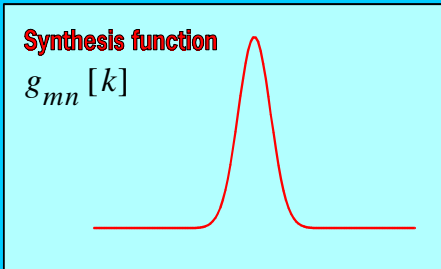
We are missing the synthesis function!

$$\begin{aligned}\delta_m \cdot \delta_n &= \frac{MN}{N_1} \sum_{k=0}^{N_1-1} \tilde{\gamma}^*[k] \tilde{g}[k + mN] e^{-jkn \frac{2\pi}{\Delta M}} \\ 0 \leq m &\leq \Delta N - 1 \quad 0 \leq n \leq \Delta M - 1\end{aligned}$$

This system of equations are signal dependent!!!

Aalborg University

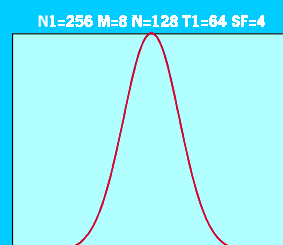
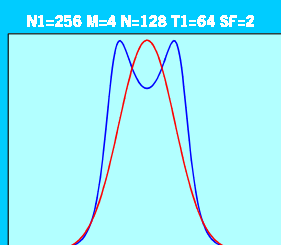
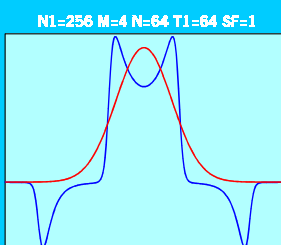
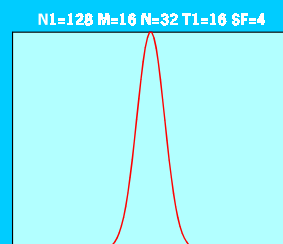
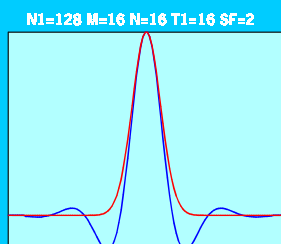
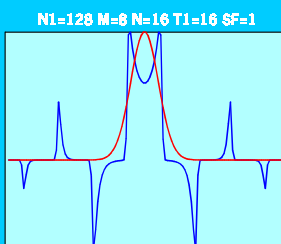
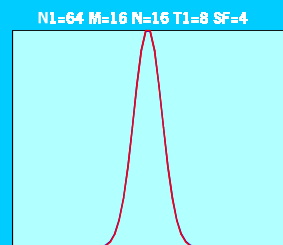
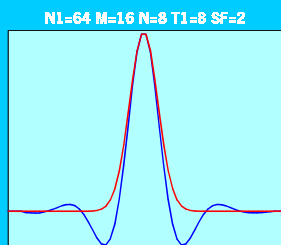
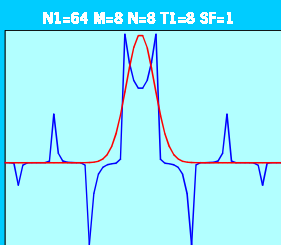
The biorthogonality condition a graphic interpretation



$$\sum_{k=0}^{N_1-1} g^*_{m,n}[k] \gamma_{m',n'}[k] = \delta_{n'-n} \cdot \delta_{m'-m}$$

Aalborg University

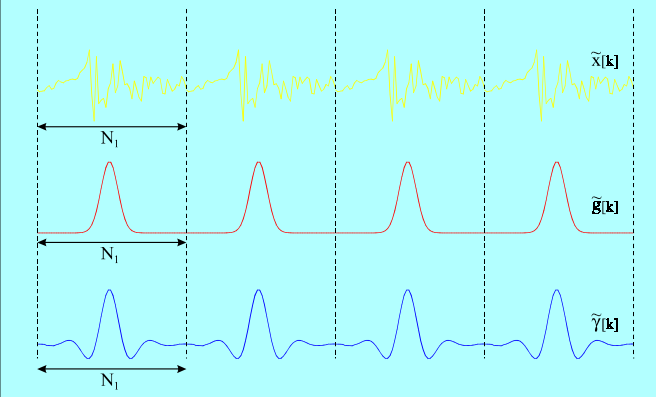
Analysis functions using different Samplings Factors



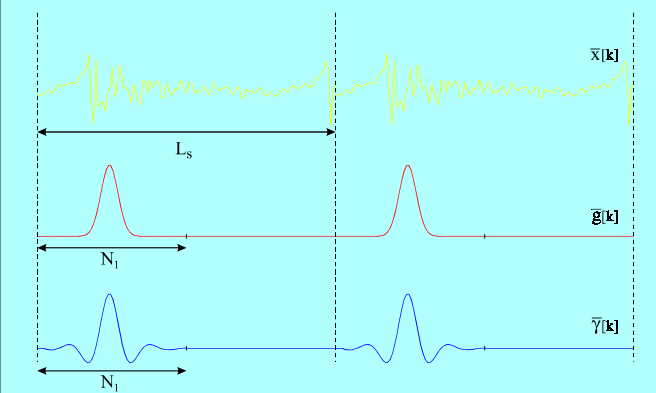
Analysis function
Synthesis function

Aalborg University

**Signal definitions used in
Periodic Discrete Gabor Expansion**

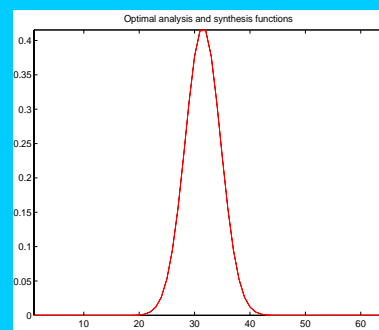
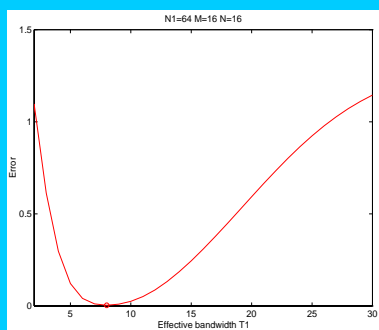
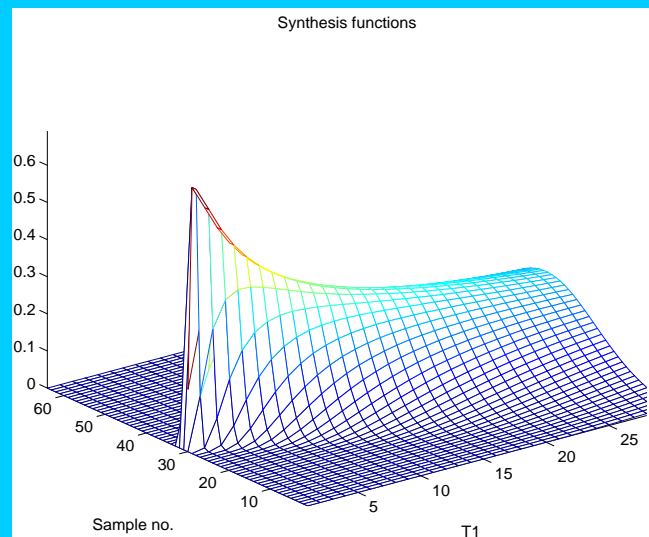
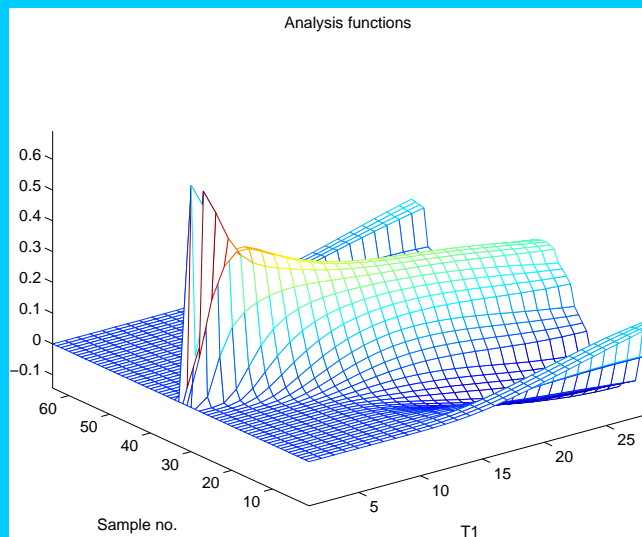


**Signal definitions used in
Discrete Gabor Expansion**



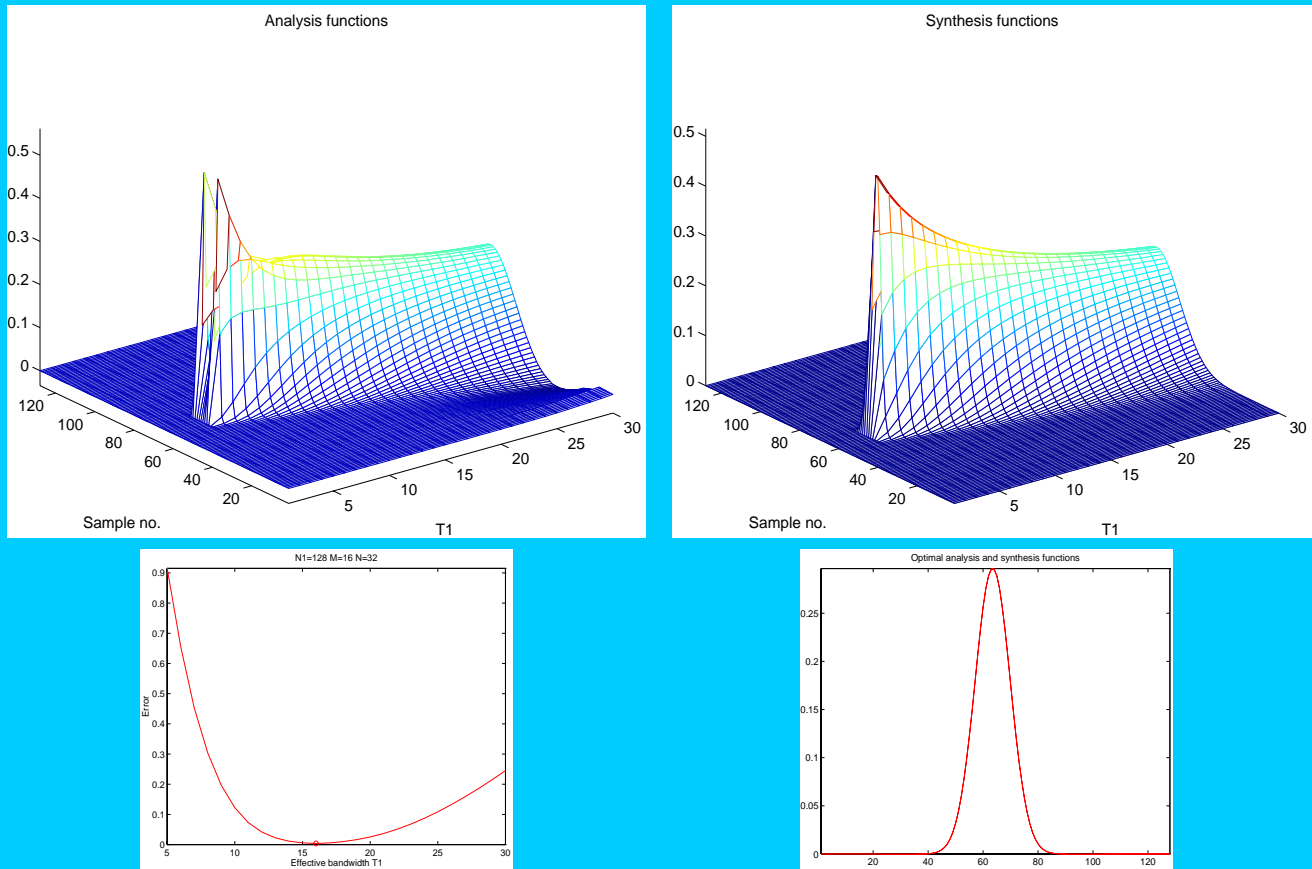
Aalborg University

The SVD solution as a function of T1 ($N_1=64$ $M=16$ $N=16$)



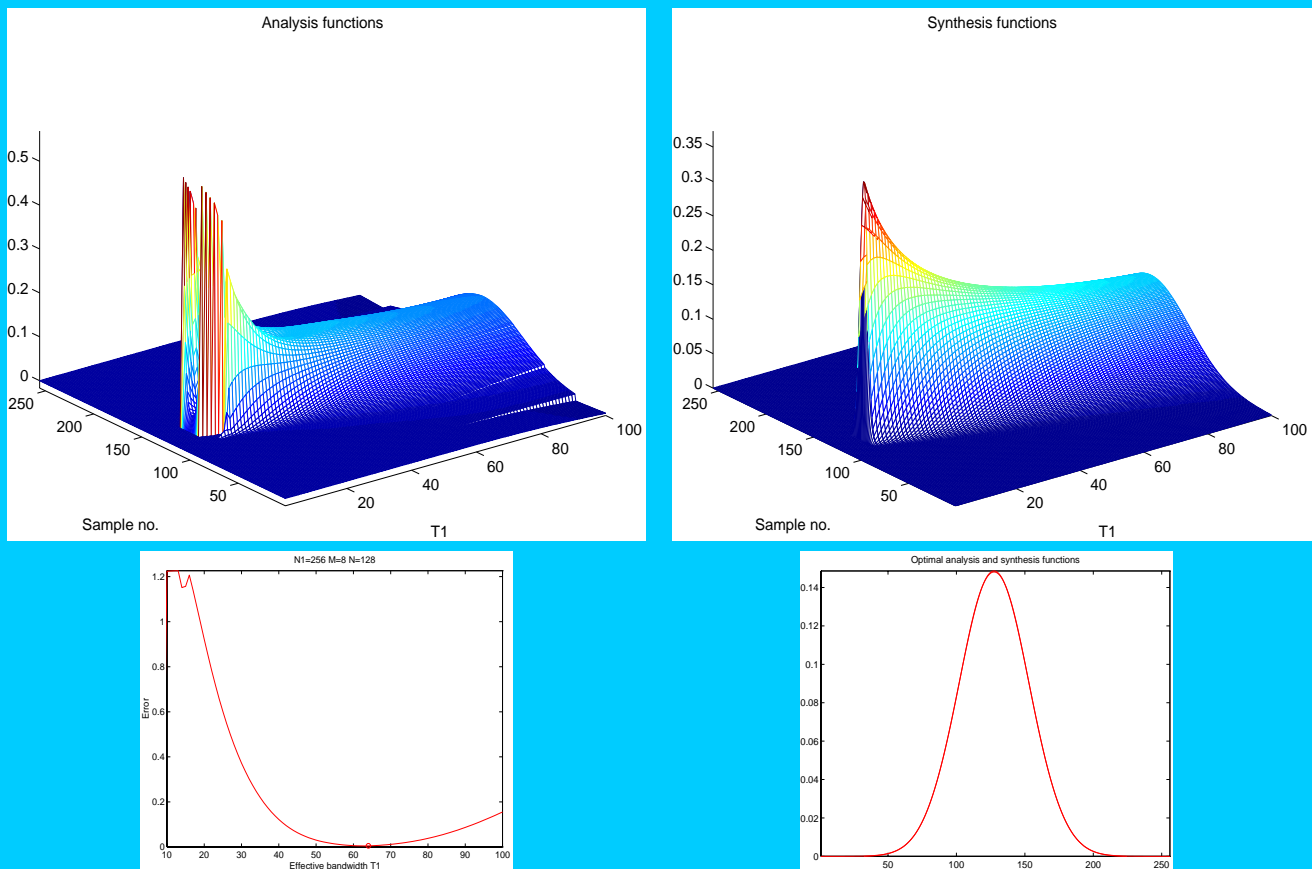
Aalborg University

The SVD solution as a function of T1 (N1=128 M=16 N=32)



Aalborg University

The SVD solution as a function of T1 (N1=256 M=8 N=128)



Aalborg University

Continuous Gabor Expansion

Expansion:

$$x(t) = \sum_m \sum_n a_{mn} g_{mn}(t) = \sum_m \sum_n a_{mn} g(t - mT) e^{jn\Omega t}$$

Gabor coefficients:

$$a_{mn} = \int x(t) \gamma_{mn}^*(t) dt = \int x(t) \gamma^*(t - mT) e^{-jn\Omega t} dt$$

Biorthogonality condition:

$$\delta_m \cdot \delta_n = \frac{2\pi}{\Omega T} \int g(t) \gamma^* \left(t - m \frac{2\pi}{\Omega} \right) e^{-jtn \frac{2\pi}{T}} dt$$

$-\infty < m < \infty \quad -\infty < n < \infty$

Aalborg University

Periodic Discrete Gabor Expansion

Expansion:

$$\tilde{x}[k] = \sum_{m=0}^{M-1} \sum_{n=0}^{N-1} a_{mn} \tilde{g}_{mn}[k] = \sum_{m=0}^{M-1} \sum_{n=0}^{N-1} a_{mn} \tilde{g}[k - m \cdot \Delta M] e^{jk n \frac{2\pi}{N}}$$

Gabor coefficients:

$$a_{mn} = \sum_{k=0}^{N_1-1} x[k] \tilde{\gamma}_{mn}^*[k] = \sum_l \sum_{k=0}^{N_1-1} x[k] \gamma_{mn}^*[l \cdot N_1 + k]$$

Biorthogonality condition:

$$\delta_m \cdot \delta_n = \frac{MN}{N_1} \sum_{k=0}^{N_1-1} \tilde{\gamma}^*[k] \tilde{g}[k + mN] e^{-jk n \frac{2\pi}{\Delta M}}$$

$$0 \leq m \leq \Delta N - 1 \quad 0 \leq n \leq \Delta M - 1$$

Aalborg University

Discrete Gabor Expansion

Expansion:

$$x[k] = \sum_{m=0}^{M_{Total}-1} \sum_{n=0}^{N-1} a_{mn} g[k - m \cdot \Delta M] e^{jkn \frac{2\pi}{N}} \quad 0 \leq k < L_s$$

Gabor coefficients:

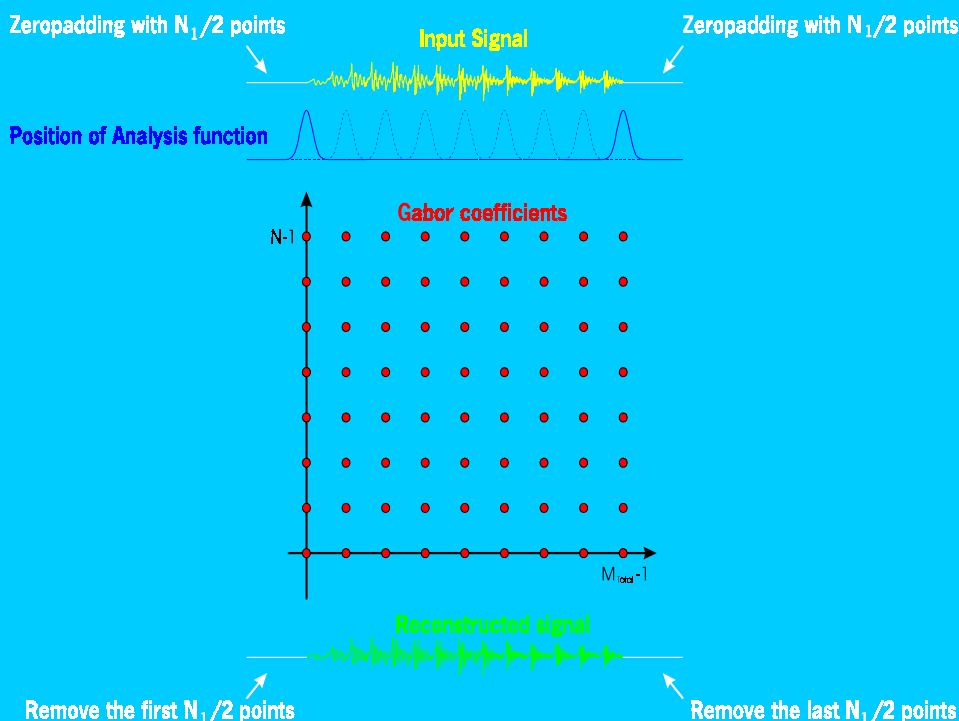
$$a_{mn} = e^{-jmn\Delta M \frac{2\pi}{N}} \sum_{k=0}^{N_1-1} x[k + m \cdot \Delta M] \gamma^*[k] e^{-jkn \frac{2\pi}{N}} \quad 0 \leq m \leq M_{Total} \quad 0 \leq n < N$$

Biorthogonality condition:

$$\delta_m \cdot \delta_n = \frac{MN}{N_1} \sum_{k=0}^{N_1-1} \gamma^*[k] g[k + mN] e^{-jkn \frac{2\pi}{\Delta M}} \quad -\Delta N < m < \Delta N \quad 0 \leq n \leq \Delta M - 1$$

Aalborg University

Procedure of M_{Total} and L_s



The length of the signal L_s must be a multiple of ΔM

Aalborg University

Transparents for lecture no 5.

Gabor Expansion

$$x(t) = \sum_{m=0}^{M-1} \sum_{n=0}^{N-1} a_{mn} g(t - m \cdot T) e^{jkn\Omega}$$

Adaptive Echo Cancellation

IEEE SP Magazine, March 1999

Fourier Spectrogram

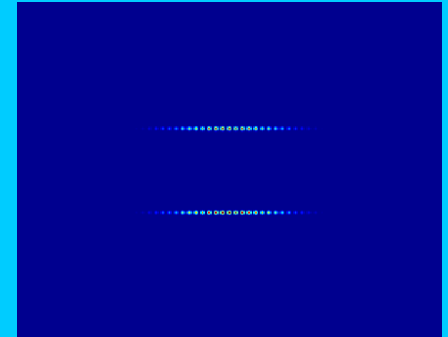
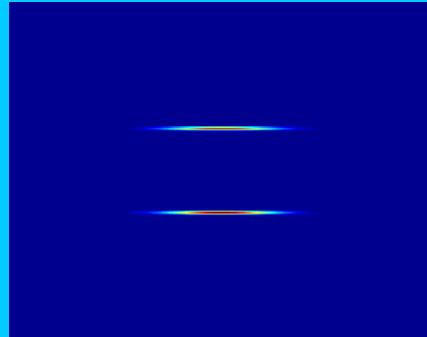
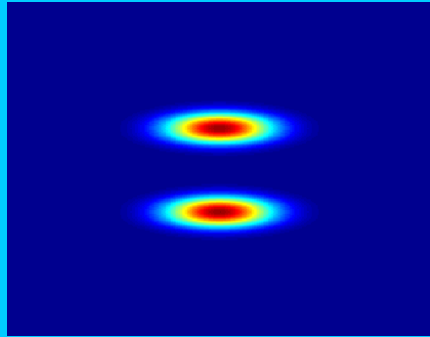
IEEE Trans on ASSP, Aug 1985

Gabor Spectrogram

IEEE Trans on SP , Oct 1994

Positive Gabor Spectrogram

IEEE Trans on SP , Feb 1999

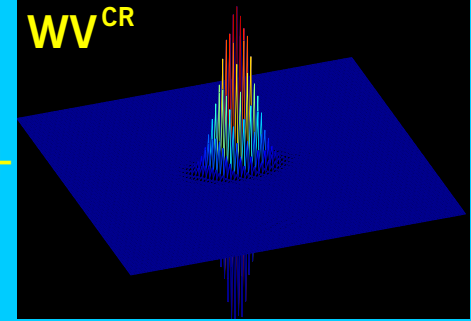
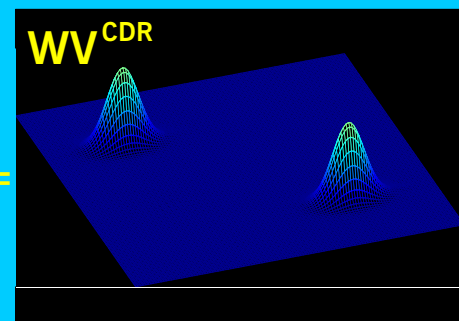
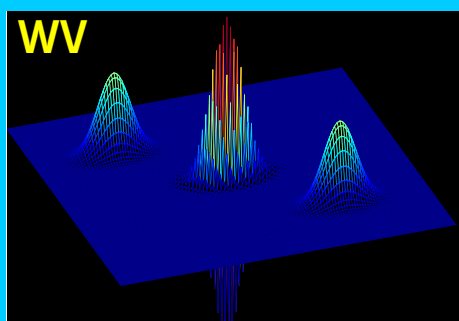


Aalborg University

Separation of auto and cross terms - the initial case

$$x(t) = g_1(t) + g_2(t)$$

$$\begin{aligned} WV_x(t, \omega) &= \underbrace{WV_{g_1}(t, \omega) + WV_{g_2}(t, \omega)}_{WV^{CDR}(t, \omega)} + \underbrace{WV_{g_1, g_2}(t, \omega) + WV_{g_2, g_1}(t, \omega)}_{WV^{CR}(t, \omega)} \\ &= WV^{CDR}(t, \omega) + WV^{CR}(t, \omega) \end{aligned}$$



$$WV^{CDR} = \sum \text{auto terms} \quad (\text{Wigner-Ville Cross-term Deleted Representation})$$

$$WV^{CR} = \sum \text{cross terms} \quad (\text{Wigner-Ville Cross-term Representation})$$

Aalborg University

Separation of auto and cross terms - the general case

$$x(t) = \sum_{m=0}^{M-1} \sum_{n=0}^{N-1} g_{mn}(t) \quad \text{where} \quad g_{mn}(t) = a_{mn} g(t - m \cdot T) e^{jtn\Omega}$$

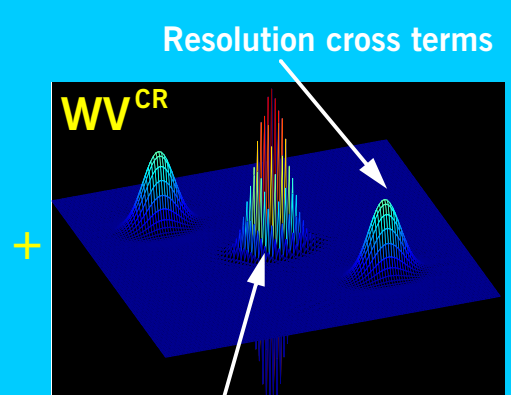
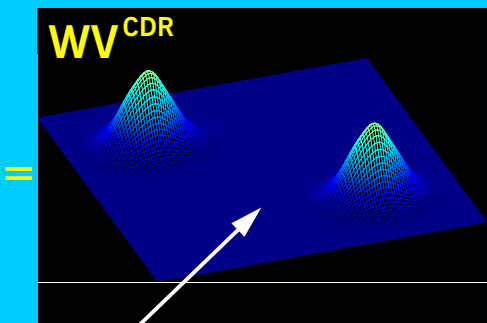
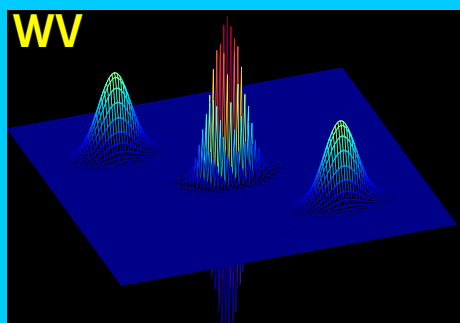
$$\begin{aligned} WVD_x(t, \omega) &= \sum_{m=0}^{M-1} \sum_{n=0}^{N-1} \sum_{m'=0}^{M-1} \sum_{n'=0}^{N-1} WV_{g_{mn}g_{m'n'}}(t, \omega) \\ &= \underbrace{\sum_{m=0}^{M-1} \sum_{n=0}^{N-1} WV_{g_{mn}}(t, \omega)}_{A_0} + \underbrace{\sum_{m=0}^{M-1} \sum_{n=0}^{N-1} WV_{g_{mn}g_{m'n'}}(t, \omega)}_{A_0} \\ &= WV^{CDR}(t, \omega) + WV^{CR}(t, \omega) \end{aligned}$$

where

$$A_0 = \{(m, n), (m', n') \mid |m - m'| + |n - n'| \neq 0\}$$

Aalborg University

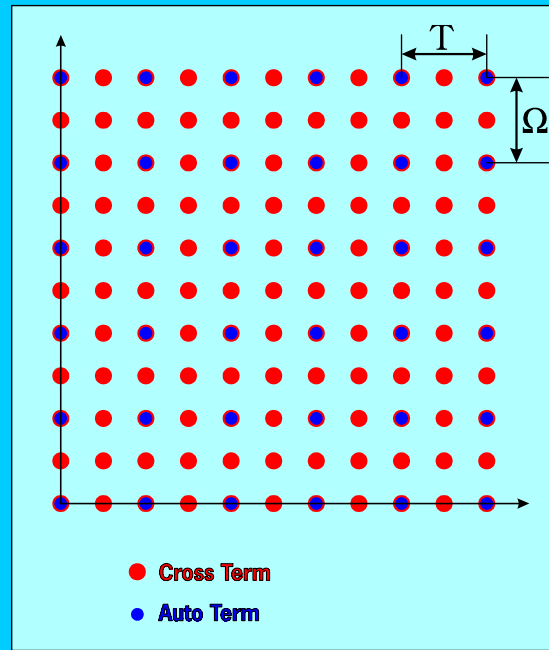
Separation of auto and cross terms - the general case



The initial resolution
Resolution like the Fourier spectrogram
Very dependent on the analysis function

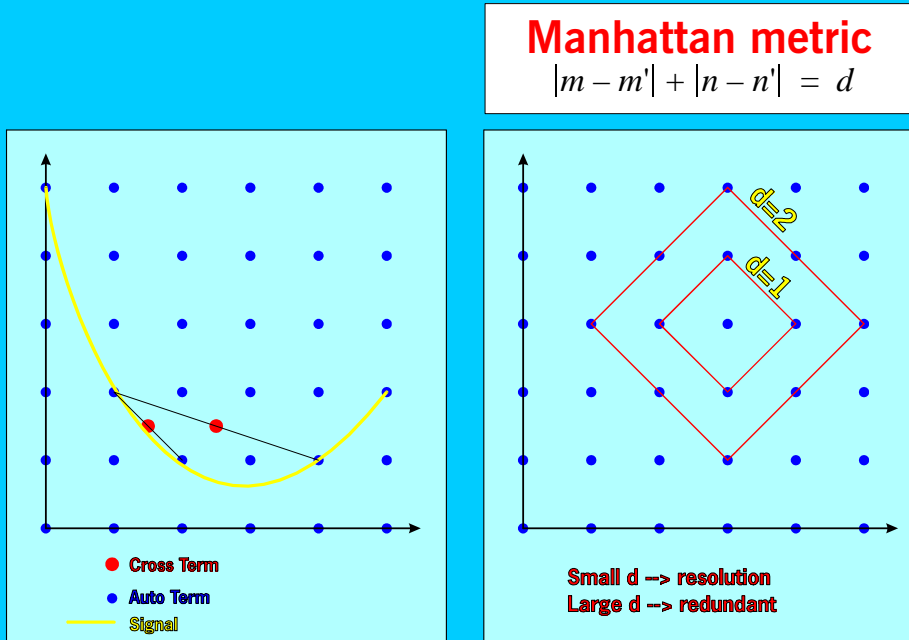
Aalborg University

Where are the auto and cross terms placed ?



Aalborg University

Which cross terms should be included ?



Aalborg University

The Gabor Spectrogram

- introduction of a metric ordering of cross terms

$$GS_D(t, \omega) = \sum_{d=0}^D P_d(t, \omega) \quad 0 \leq D \leq D_{Max}, \quad D_{Max} = N + M_{total} - 2$$

where

$$P_d(t, \omega) = \sum_{A_d} WV_{g_{mn}g_{m'n'}}(t, \omega)$$

$$A_d = \{ (m, n), (m, n) \mid |m - m'| + |n - n'| = d \}$$

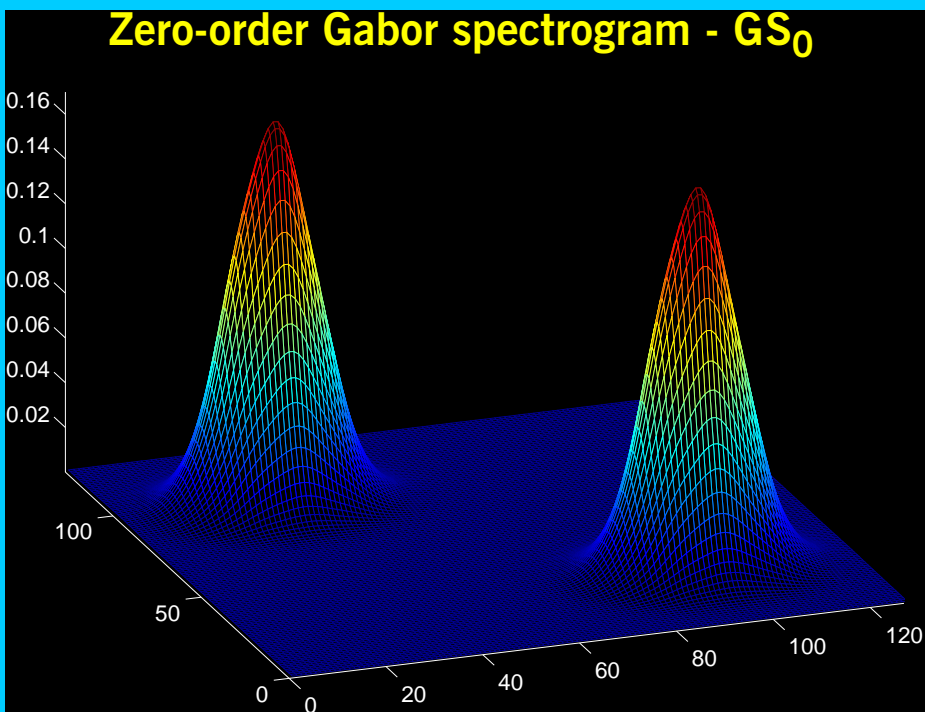
$$\begin{aligned} WV_{g_{mn}g_{m'n'}}(t, \omega) &= a_{mn} a_{m'n'}^* WV_g \left(t - \frac{m' + m}{2} T, \omega - \frac{n' + n}{2} \Omega \right) \\ &\cdot e^{j \left(t(n - n') \Omega + \left(\omega - \frac{n' + n}{2} \Omega \right) (m' - m) T \right)} \end{aligned}$$

$GS_0(t, \omega)$ = Fourier Spectrogram look-a-like representation

$GS_{D_{Max}}(t, \omega)$ = Wigner-Ville distribution

Aalborg University

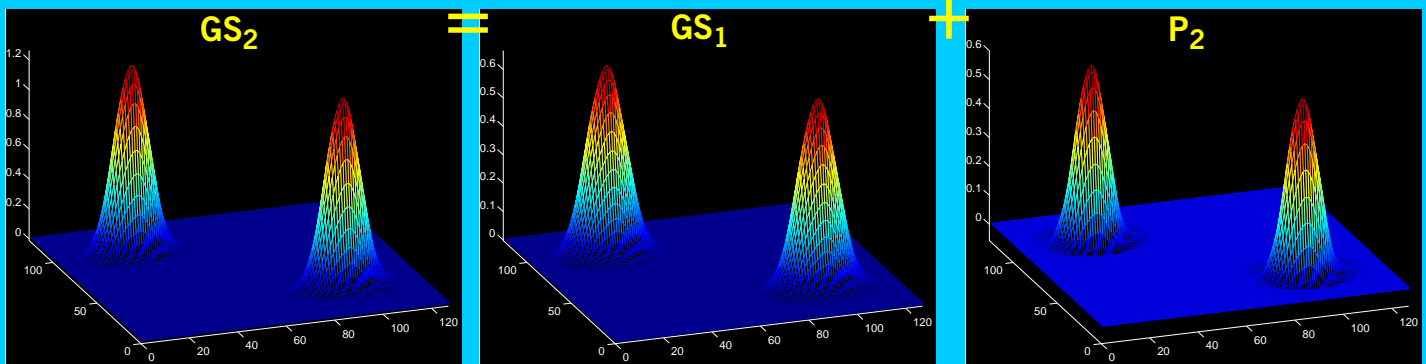
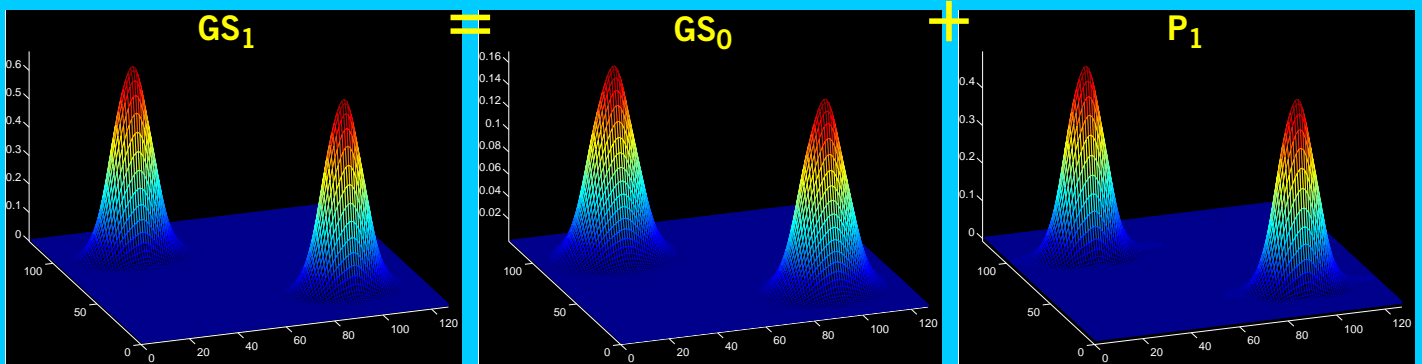
Example: Gabor Spectrogram of two Gaussian functions.



A Fourier Spectrogram look-a-like representation

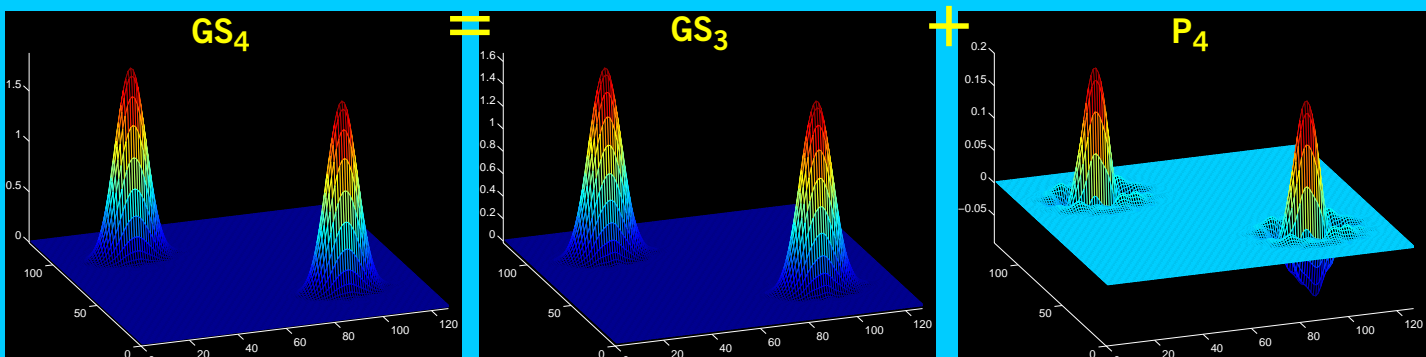
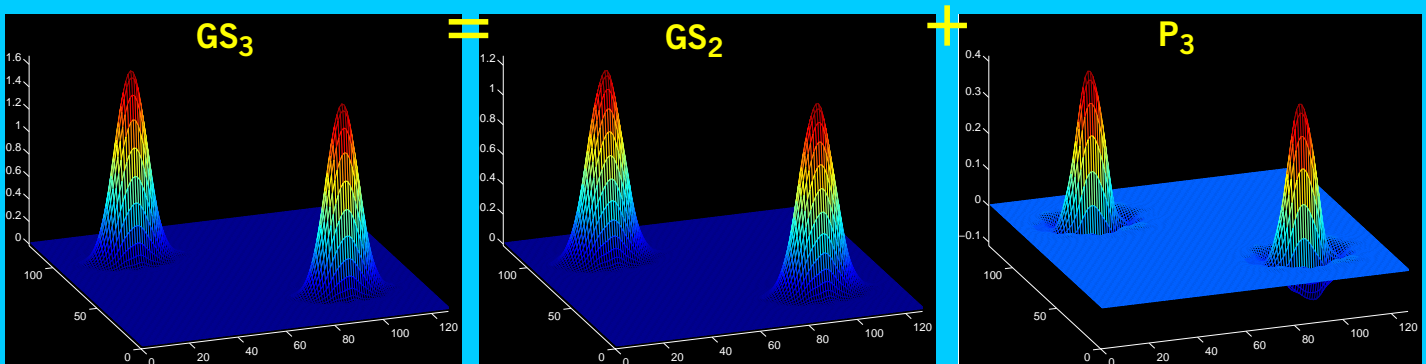
Aalborg University

Example: Gabor Spectrogram of two Gaussian functions.



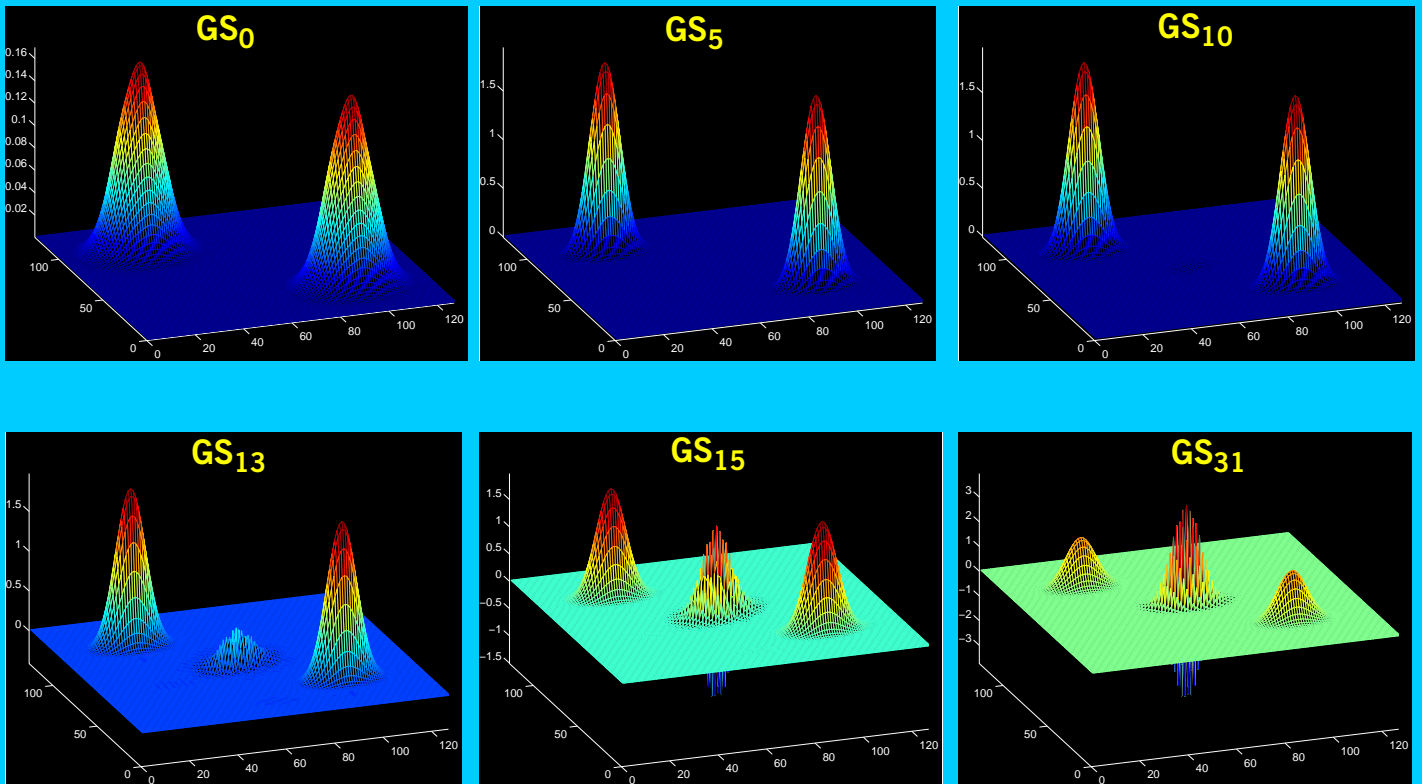
Aalborg University

Example: Gabor Spectrogram of two Gaussian functions.



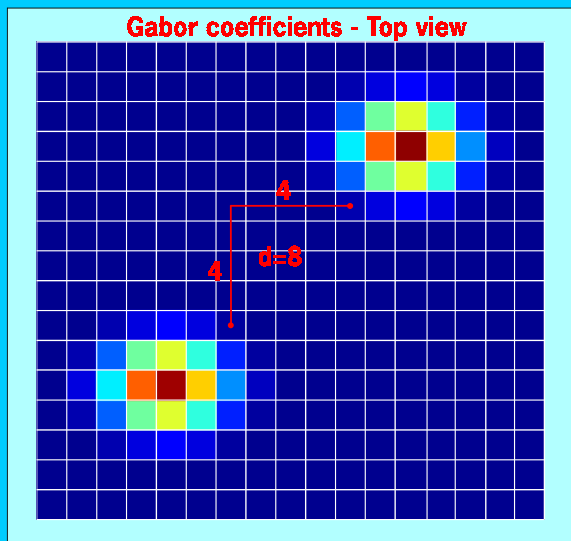
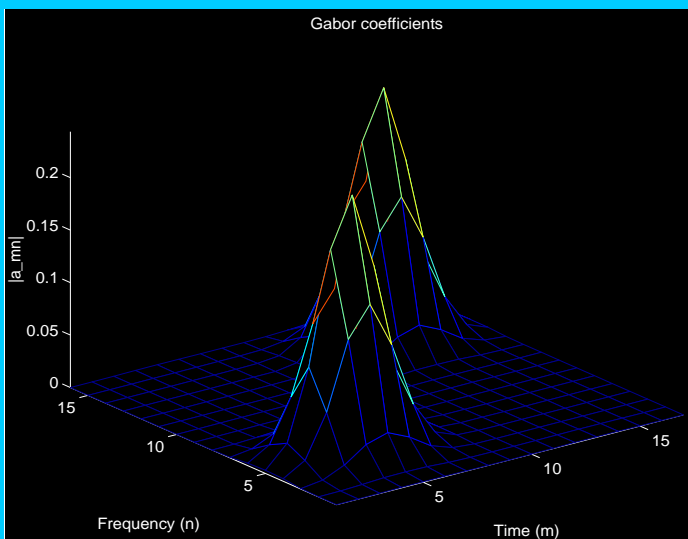
Aalborg University

Example: Gabor Spectrogram of two Gaussian functions.



Aalborg University

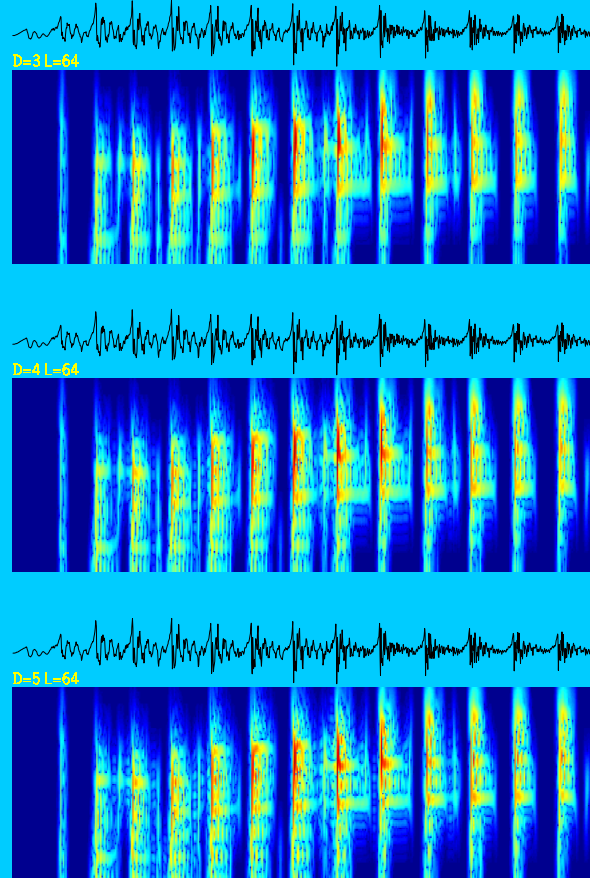
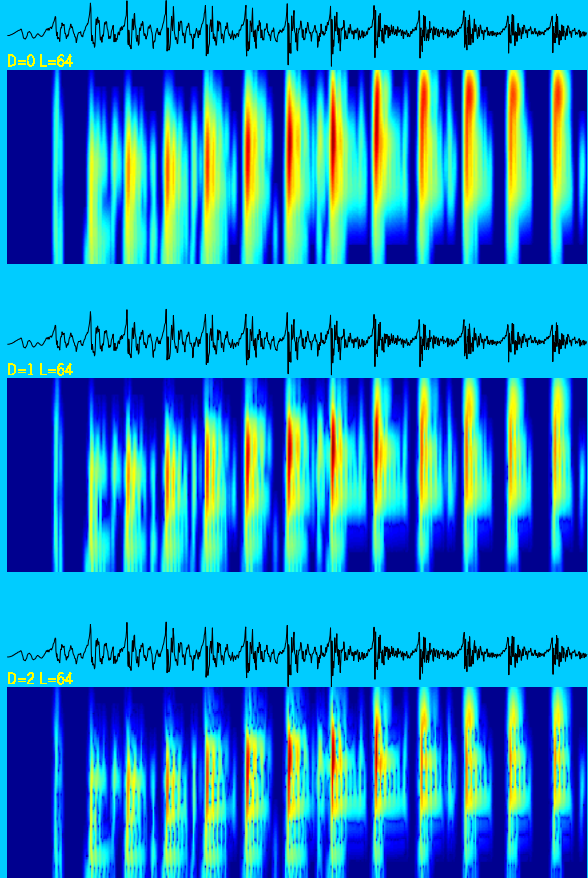
How to select the optimal order D !



The order should be lower than the Manhattan distance between the auto terms !

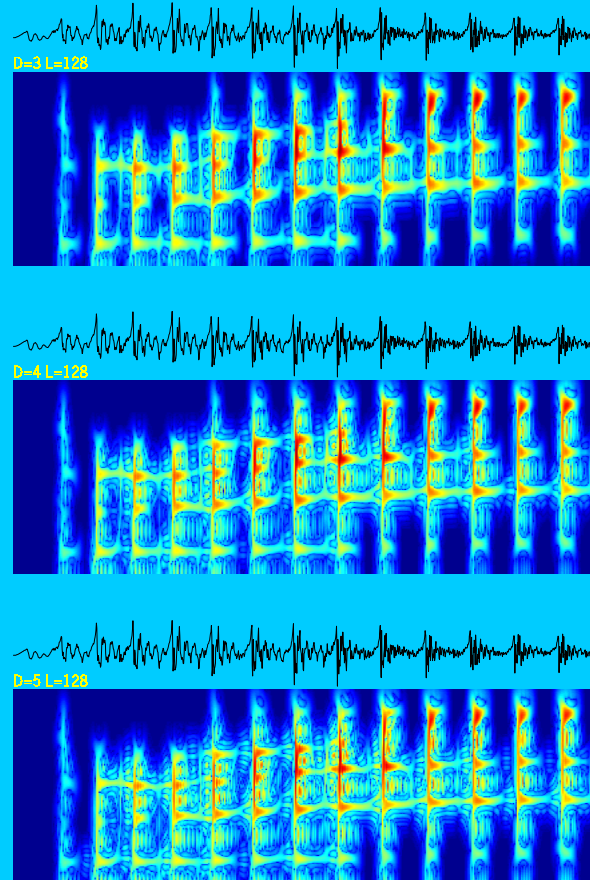
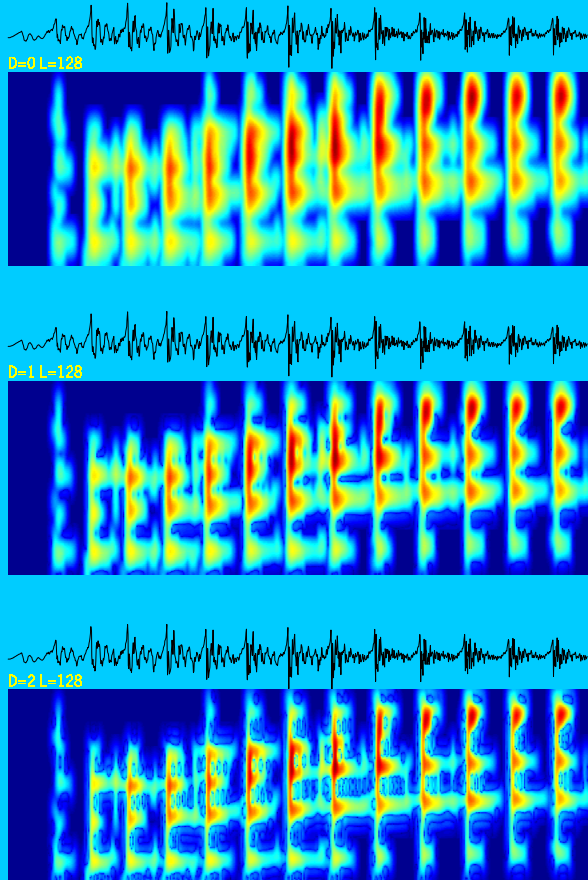
Aalborg University

Gabor Spectrogram of a speech signal - L=64



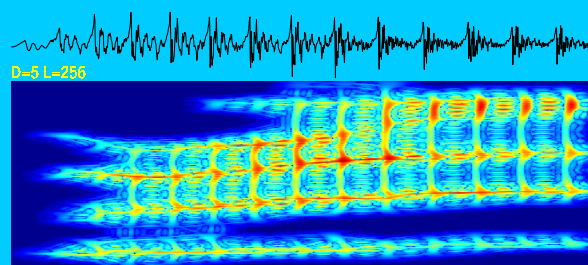
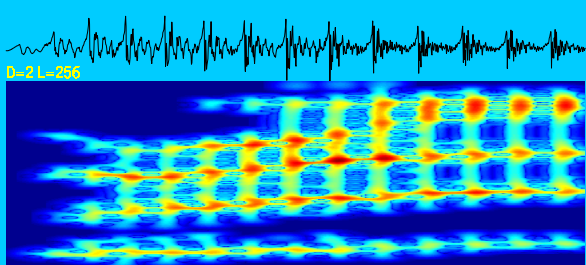
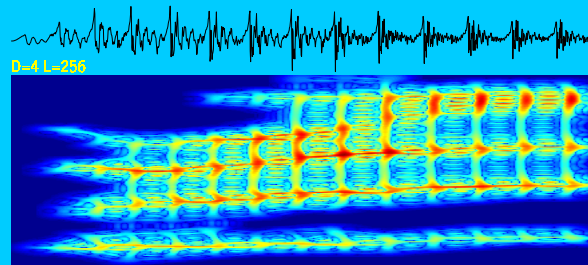
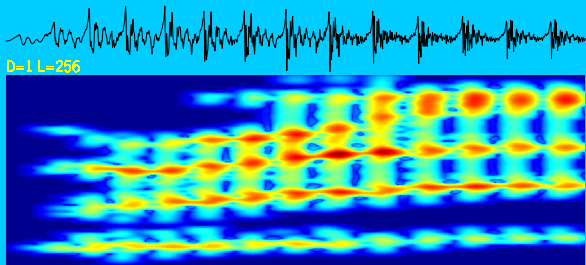
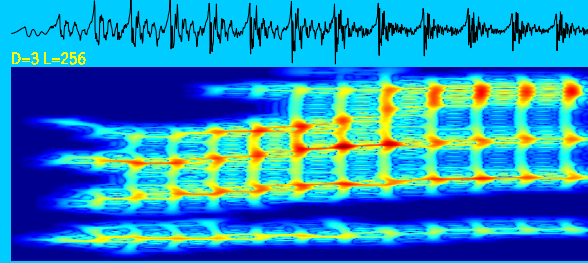
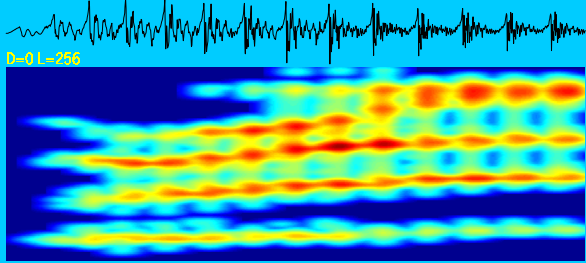
Aalborg University

Gabor Spectrogram of a speech signal - L=128



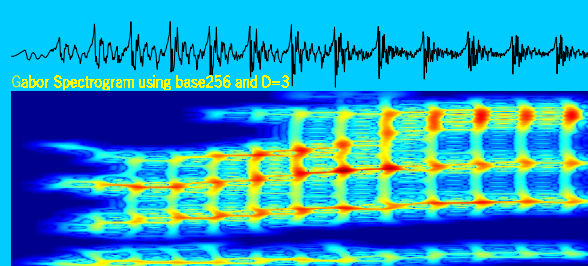
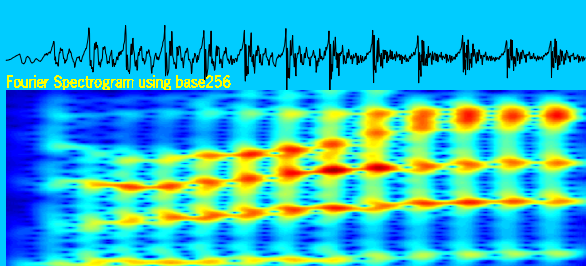
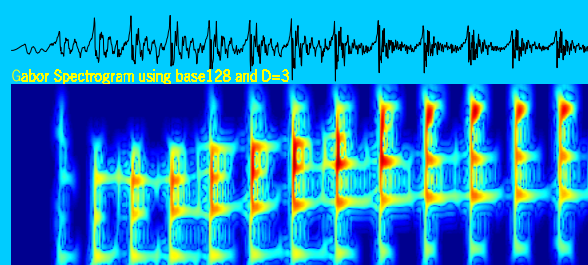
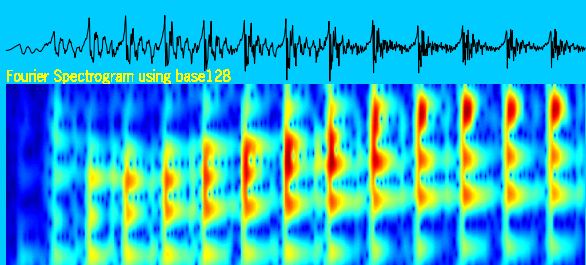
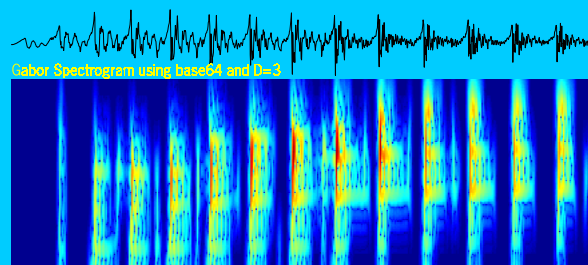
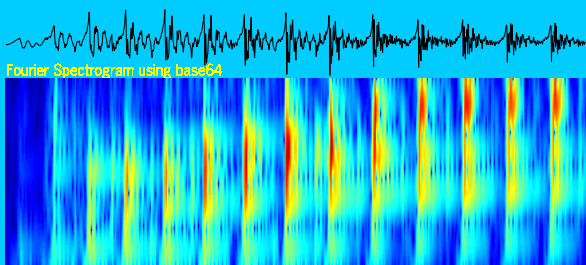
Aalborg University

Gabor Spectrogram of a speech signal - L=256



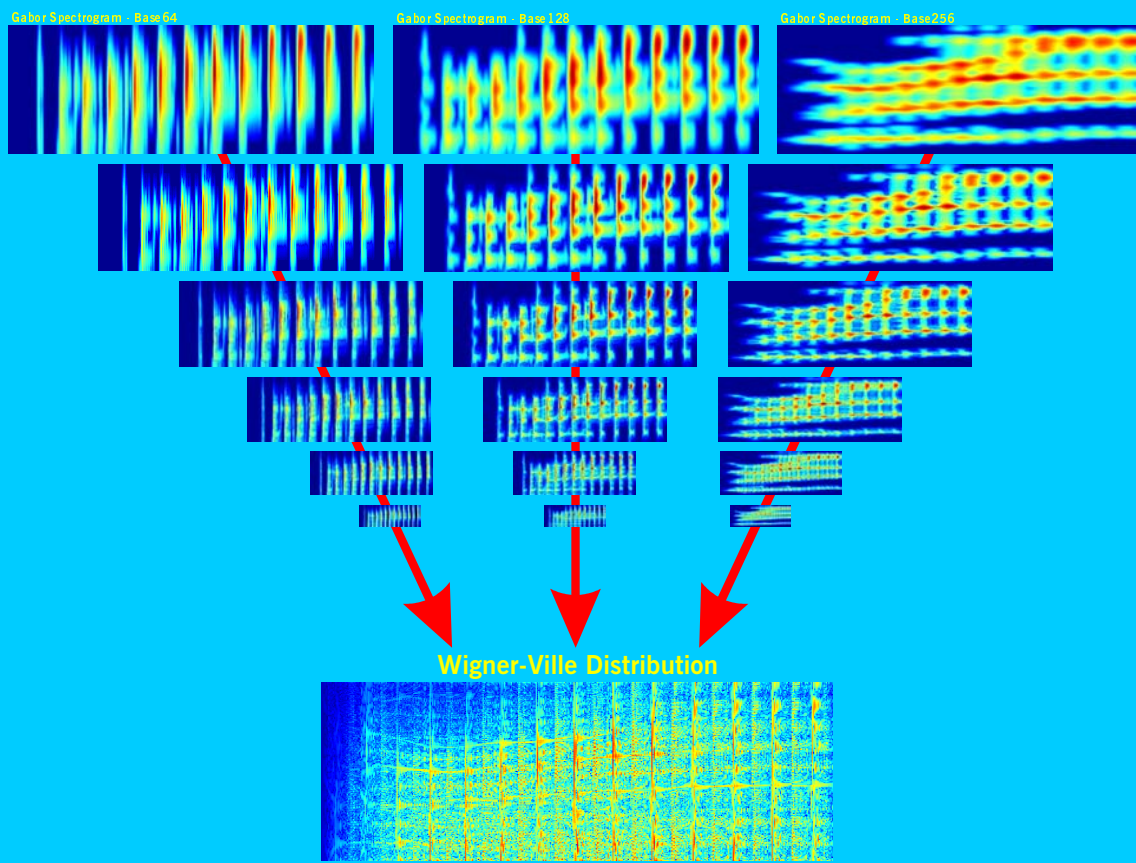
Aalborg University

The Gabor spectrogram versus the Fourier Spectrogram



Aalborg University

The Gabor Spectrogram convergence towards the Wigner-Ville !



Aalborg University

